DOCTOR OF PHILOSOPHY

Variations in the carbon isotope ratio of phytoplankton and dissolved inorganic carbon in the marine environment.

Middleton, Gideon Paul Grevatt

Award date:
1997

Awarding institution:
Bangor University

Variations in the Carbon Isotope Ratio of Phytoplankton and Dissolved Inorganic Carbon in the Marine Environment

A thesis submitted in accordance with the requirements of the University of Wales for the degree of Doctor of Philosophy.

Gideon Paul Grevatt Middleton

University of Wales, Bangor,
School of Ocean Sciences,
Menai Bridge,
Anglesey. LL59 5EY.
UK

March 1997

Abstract

The two main aims of this study were; (i) to determine the equilibrium fractionation effects of the stable isotopes of carbon between dissolved molecular CO_2 ($CO_{2(aq)}$) and bicarbonate (HCO_3^-) ($\epsilon_{b/a}$) and HCO_3^- and carbonate (CO_3^{2-}) ($\epsilon_{c/b}$) in sea water, and (ii) to investigate the relationship between the isotopic composition of phytoplankton ($\delta^{13}C_{POC}$) and their photosynthetic source of inorganic carbon.

To determine $\epsilon_{b/a}$ and $\epsilon_{c/b}$ in sea water (S = ~34) experiments were conducted at different pHs and two temperatures (5°C and 20°C). The measured values of $\epsilon_{b/a}$ (5°C = 11.67 ± 0.34 ‰ and 20°C = 9.48 ± 0.26 ‰) agreed well with previous estimates derived in distilled water indicating $\epsilon_{b/a}$ is not modified by the ionic effects of sea water. The values of $\epsilon_{c/b}$ determined during the same experiments were significantly larger than previous estimates (5°C = -8.1 ± 2.2 ‰ and 20°C = -14.2 ± 2.4 ‰). This may indicate that the measurement made during this study are in error. It is suggested that the error is either due to the relative imprecision associated with the determination of the isotopic composition of the total dissolved inorganic carbon pool or due to incomplete isotopic equilibrium within the experimental system.

The relationship between changes in the $\delta^{13}C_{POC}$ and the dissolved inorganic carbon pool was investigated during temporal studies of phytoplankton blooms in a mesocosm and the Menai Strait, North Wales.

During the mesocosm experiment the isotopic enrichment between the phytoplankton and $CO_{2(aq)}$ ($\epsilon_{POC/a}$) decreased from ~ -10 ‰ to ~ +0 ‰ during the course of the bloom. The observed changes in $\delta^{13}C_{POC}$ are generally consistent with previously published empirical models which assume $CO_{2(aq)}$ is the exclusive source of photosynthetic inorganic carbon. This agreement, and the application of physiological models appeared to confirm that $CO_{2(aq)}$ is the most likely source of photosynthetic inorganic carbon.

The $\delta^{13}C_{POC}$ results obtained during two consecutive phytoplankton blooms in the Menai Strait, North Wales, were corrected for the presence of refractory organic matter to obtain the isotopic signal associated with the phytoplankton, $\delta^{13}C_P$. It was apparent that the relationship between $\delta^{13}C_P$ and $[CO_{2(aq)}]$ differed between the two blooms. During the first bloom (diatomaceous), the observed relationship between $\delta^{13}C_P$ and $[CO_{2(aq)}]$ was consistent with the uptake of $CO_{2(aq)}$. However, the $\delta^{13}C_P$ signal during the second bloom, dominated by *Phaeocystis*, was independent of the $[CO_{2(aq)}]$ and therefore it was concluded that HCO_3^- is the most likely source of inorganic carbon.

Contents

Title
Abstract
Contents i.
Acknowledgements iv.
Declaration v.

***Chapter* 1: Introduction** 1

***Chapter* 2: The Basic Chemistry of the ΣCO_2 System in the Marine Environment From the Viewpoint of Thermodynamics, Kinetics and Transitions State Theory**
2.1 Introduction 6
2.2 The Basic Chemistry of Dissolved Inorganic Carbon 7
2.3 The Analytical Determination of Parameters Associated with the ΣCO_2 system 9
2.4 Activity and pH Scales 11
2.5 A Thermodynamic Approach to the Chemistry of Dissolved Inorganic Carbon 13
2.6 A Kinetic Approach to the Chemistry of Dissolved Inorganic Carbon 20
2.7 The Dissolved Inorganic Carbon System and the Transition State Theory 26
2.8 Summary 29

***Chapter* 3: Isotope Theory**
3.1 Introduction 31
3.2 Definitions 31
3.3 A Thermodynamic Approach to Equilibrium Isotope Effects 33
3.4 A Kinetic Approach to Equilibrium and Non - Equilibrium Isotope Effects 37
3.4.1 Introduction 37
3.4.2 A Kinetic Approach to Equilibrium Isotope Effects 37
3.4.3 Non - Reversible Chemical Reactions 39
3.5 Isotope Effects and the Transition State Theory 41
3.6 Summary 44

***Chapter* 4: The Effect of Temperature, Salinity and pH on the Distribution of ^{13}C and ^{12}C Within the ΣCO_2 System in the Marine Environment - A Review**
4.1 Introduction 45
4.2 A Thermodynamic Approach to the Fractionation of Isotopes Within the ΣCO_2 System 46
4.2.1 Introduction 66
4.2.2 The $CO_{2(g)}$ - $CO_{2(aq)}$ Equilibrium 48
4.2.3 The $CO_{2(aq)}$ - HCO_3^- Equilibrium 52
4.2.4 The HCO_3^- - CO_3^{2-} Equilibrium 59

4.3 A Kinetic Approach to the Fractionation of Isotopes Within the ΣCO_2 System 63
4.4 Summary 65

***Chapter* 5: The Effect of Temperature, Salinity and pH on the Distribution of ^{13}C and ^{12}C Within the ΣCO_2 System in the Marine Environment - Experimental Results**
5.1 Introduction 67
5.2 Materials and Methods 67
5.2.1 Calculations 68
5.2.2 Experimental Apparatus 69
5.2.3 Equilibrium Time 70
5.2.4 Sampling and Analysis 71
5.3 Experiments 74
5.3.1 Experimental Design 74
5.3.2 The pH Related Effect on $\alpha_{b/a}$ and $\alpha_{c/b}$ in Sea Water at Two Different Temperatures 77
5.3.3 The pH Related Effect on $\alpha_{b/a}$ and $\alpha_{c/b}$ at Two Different Salinities 86
5.4 Summary 89

***Chapter* 6: Changes in the Isotopic Composition of Particulate Organic Carbon and Dissolved Inorganic Carbon During an Algal Bloom in a Mesocosm**

6.1 Introduction 91
6.2 The Uptake of Inorganic Carbon by Marine Phytoplankton 92
6.3 Material and Method 96
6.3.1 The Mesocosm Facility 96
6.3.2 Sampling and Analysis 97
6.4 Results 99
6.4.1 The ΣCO_2 System 99
6.4.2 The Distribution of ^{12}C and ^{13}C Within the ΣCO_2 System and POC 101
6.4.3 Additional Parameters 104
6.5 Discussion 104
6.5.1 A Rayleigh Distillation Model 106
6.5.2 Empirical Models 111
6.5.3 Physiological Models 115
6.6 Summary 120

***Chapter* 7: Variations in the Isotopic Composition of the phytoplankton in the Menai Strait**
7.1 Introduction 124
7.2 The Study Area 124
7.3 Materials and Methods 125
7.3.1 Determination of POC, $\delta^{13}C_{POC}$ and Chlorophyll 126
7.3.2 Determination of the $[\Sigma CO_2]$, pH and $\delta^{13}C_{\Sigma CO2}$ 126
7.3.3 The Direct Determination of $\delta^{13}C_a$ 126

7.3.4 Additional Parameters 127
7.4 Results 128
7.4.1 POC and Chlorophyll 128
7.4.2 The ΣCO_2 System 129
7.4.3 The distribution of ^{12}C and ^{13}C within the ΣCO_2 System and POC 131
7.5 Discussion 134
7.5.1 First Bloom 139
7.5.2 Second Bloom 144
7.6 Summary 147

***Chapter* 8: Conclusions** 150

***Appendix* 1: A Description of the Methodology Used to Determine the Isotopic Composition of ΣCO_2 in Sea Water** A1
***Appendix* 2: A Description of the Methodology Used to Determine the Isotopic Composition of Particulate Organic Carbon** A9
***Appendix* 3: The Spectrophotometric Determination of pH in Sea Water** A14

References

Acknowledgements

I would like to thank my supervisors Dr Hilary Kennedy and Prof Peter Williams for their help and support throughout the course of this work and another thank you to Hilary for kindly allowing me to take time out from my current contract to finish this thesis. I am also indebted to Paul Kennedy for his help in the running of isotope samples and to Vivien Ellis and Sandy Hague for their technical support in general and more specifically for helping during the collection and analysis of samples for the Menai Strait study. I would also like to thank Dr Linda Godfrey who ran the $\delta^{13}C_{POC}$ samples from the mesocosm experiment and Dr Robert Byrne who reviewed the manuscript of the spectrophotometric pH methodology. I am also grateful to Prof David Tuner for allowing me to use his sea water model without which some of the calculations would not have been possible. I would finally like to thank my wife for putting up with the sometimes long hours of absence.

Chapter 1: Introduction

The realisation that man's activities have grown to such an extent that humans no longer only impact on their local environment, but also on the global environment, has highlighted our lack of understanding about the mechanisms that regulate our environment. Probably of greatest current concern are the possible impacts associated with the release of CO_2 in to the earth's atmosphere due to the combustion of fossil fuels (5.4 ± 0.5 Gt $C.yr^{-1}$, 1 Gt C = 10^{15} g.) and tropical deforestation (0.6 to 2.5 Gt $C.yr^{-1}$) which together emit ~7.0 ± 1.1 Gt $C.yr^{-1}$ (Siegenthaler and Sarmiento, 1993). The potential effects this may have on the global carbon cycle and climate are presently not well understood.

Together, the oceans of the world represent the largest reservoir of biologically available CO_2 and most of the carbon within this reservoir exists as dissolved inorganic carbon (ΣCO_2) (deep ocean ΣCO_2: 38100 Gt C, surface ocean ΣCO_2: 1020 Gt C, marine biota: 3 Gt C, dissolved organic carbon: 700 Gt C, Siegenthaler and Sarmiento, 1993). As a result the oceans may play an important chemical and/or biological role in the removal and regulation of atmospheric CO_2 (Tans *et al.*, 1990 and Siegenthaler and Joos, 1992). Current estimates suggest that the oceans may have already taken up about one third of the emissions from fossil fuel burning and deforestation (~2 Gt $C.yr^{-1}$). Most of this uptake has been simply due to the dissolution of atmospheric CO_2 in the surface waters and the subsequent transport of CO_2 laden water from the surface to the deep ocean, this process has been termed the solubility pump (Sarmiento and Siegenthaler, 1992).

Because it is difficult to directly quantify the uptake of atmospheric CO_2 ($CO_{2(g)}$) by the oceans directly, most estimates of the ocean's role have been derived by using models of varying complexity (*e.g.* Tans *et al.*, 1990 and Siegenthaler and Joos, 1992). However, the role of the marine biota in the uptake of CO_2 is not normally considered in models primarily because the biological productivity of the oceans is thought to be ultimately controlled by either nutrients, light, or grazing, but not the availability of CO_2. Nevertheless, consideration of oceanic profiles of the $[\Sigma CO_2]$ (where the square brackets denote concentration) show the surface waters (0 to 1000 m.) of the ocean (~2000 $\mu mol.kg^{-1}$) are depleted in ΣCO_2 by ~13%, compared with the deep ocean (>1000 m.) (2300 $\mu mol.kg^{-1}$)

(Volk and Hoffert, 1985). This concentration difference has been primarily (75%) attributed to the action of what has been termed the biological pump. The remainder is attributed to the solubility pump (Sarmiento and Siegenthaler, 1992). The biological pump simply results from the production of particulate organic carbon (POC) and dissolved organic carbon (DOC), by photosynthetic processes in the surface waters, that is transported to the deep ocean by sinking and/or downwelling where it is subsequently remineralised and retuned to the ΣCO_2 pool. Therefore the marine biota plays a major role in determining the distribution of ΣCO_2 in the ocean, and, through air / sea exchange, the $[CO_{2(g)}]$ in the atmosphere. The size of the particulate flux from the surface ocean is not well known and estimates range from 4 to 20 Gt $C.yr^{-1}$ (Berger *et al.*, 1989, Packard *et al.*, 1983). As there are few direct determinations of the export of DOC from the surface ocean, model simulations have been used to estimate the flux and suggest the export is ~10 Gt $C.yr^{-1}$ (Bacastow and Maier-Reimer, 1991, Najjar *et al.*, 1992). As the productivity of the marine system is generally not considered to be limited by carbon it has been difficult to see how biological processes may contribute to the uptake of anthropogenic CO_2 (*e.g.* Sarmiento and Siegenthaler, 1992), although possible mechanisms include CO_2 fertilisation, increased sinking of marine particles, changes in species composition and/or changes in the Redfield ratio of the phytoplankton.

At the most basic level, understanding of the role of the marine biota is hampered by our lack of knowledge about the primary acquisition of inorganic carbon by marine phytoplankton and how this process may be affected either directly, or indirectly by increased levels of CO_2 in the oceans and the atmosphere. For example, the level of photosynthesis in terrestrial plants which posses a C_3 type mechanism (see *CHAPTER* 6) can be enhanced by increasing the $[CO_{2(g)}]$ (*i.e.* CO_2 fertilisation). However, unless this is linked with a change in the Redfield ratio, *i.e.* increasing the ratio of C:N, such a change is unlikely to increase the biological uptake of anthropogenic CO_2. One possible mechanism for such a change is if variations in the climate shift the species composition of the algal population so it becomes dominated by algal forms with higher C:N ratios (*e.g.* Small *et al.*, 1977). Alternatively changes in the dynamics of the present system may result in the production of dissolved or particulate organic matter with a high C:N ratio.

To gain an insight into such problems it is ultimately necessary to understand the

process by which phytoplankton acquire their inorganic carbon. Early experiments (*e.g.* Small *et al.*, 1977) suggest that an increase in the concentration of dissolved molecular CO_2 ($[CO_{2(aq)}]$) did not affect the growth rate or C:N ratio of phytoplankton. In contrast, more recent experiments (Riebesell *et al.*, 1992), have shown that the growth rate of marine diatoms can be limited when the $[CO_{2(aq)}]$ is low. Simplistically, if marine phytoplankton rely on $CO_{2(aq)}$ as their only source of inorganic carbon their growth rate would be limited by the rate at which it can be supplied from the external medium and hence maybe partly dependant on its concentration. However, the mechanism by which phytoplankton acquire their inorganic carbon is not clear (see *CHAPTER* 6). Laboratory-based studies by algal physiologists suggest algae maybe able to actively transport $CO_{2(aq)}$ and/or HCO_3^- (bicarbonate) into the cell (*e.g.* Bowes, 1985, Beardall, 1985, Sharkey and Berry, 1985, Burns and Beardall, 1987) and as the HCO_3^- is normally more than 150 times more abundant than $CO_{2(aq)}$ (in the marine ΣCO_2 system) the growth rate of the algae, which use this pool, would not be expected to be affected by any changes in the $[CO_{2(aq)}]$. Alternatively it has been proposed that algae maybe able directly to fix HCO_3^- using a C_4 type metabolism (*CHAPTER* 6), although evidence now suggests that such a mechanism is unlikely to play an important role in the marine environment, if at all (Raven and Johnston, 1991, Goericke *et al.*, 1994). It has been suggested that an increase in the $[CO_{2(aq)}]$ may reduce the competitive advantage of phytoplankton with a carbon concentrating mechanism (CCM) (*i.e.* those that can actively transport dissolved inorganic carbon into their cells) and hence increase the importance of algae that are reliant on the passive diffusion of $CO_{2(aq)}$, although the impact of this on the productivity or C:N ratio of marine organisms is difficult to judge (Raven, 1991).

Studies on the isotopic ratio of ^{13}C to ^{12}C in terrestrial and marine plants have proved useful to help determine the mechanism of inorganic carbon acquisition (*e.g.* see Farquhar *et al.*, 1989 for a review). Laboratory measurements of phytoplankton cultures have shown a decrease in the isotopic difference between the algae and their inorganic carbon source when a CCM is employed (Sharkey and Berry, 1985). The large spatial variation in the isotopic composition of phytoplankton (*e.g.* Francois *et al.*, 1993, Goericke and Fry, 1994) in the marine environment is consistent with the trend expected if phytoplankton posses a CCM, *i.e.* a decrease in the difference between the isotopic

composition of the phytoplankton and their inorganic carbon source as the [$CO_{2(aq)}$] decreases (Raven, 1991).

However, interpretation of the oceanic isotope signal does not necessarily require the algae to posses a CCM. The observed changes may simply reflect a kinetic signal due to the differing [$CO_{2(aq)}$]. Indeed, it is the observation that the isotopic composition of phytoplankton correlates directly with the [$CO_{2(aq)}$] that has lead many researchers to survey the isotopic composition of phytoplankton in today's oceans (Fontugne and Duplessey, 1981, Rau *et al.*, 1991a, 1991b, 1992 and Francois *et al.*, 1993). The result of these studies has been to establish a simple model to relate the isotopic composition of phytoplankton (Rau, 1994), or the difference between the isotopic composition of phytoplankton and their inorganic carbon source (Jasper and Hayes, 1994), to the [$CO_{2(aq)}$]. This procedure has enabled the isotopic signal from organic matter in cores to be used as a proxy for the [$CO_{2(aq)}$] in ancient oceans (*e.g.* Degens *et al.*, 1968, Rau *et al.*, 1992, Francois *et al.*, 1993, Rau, 1994 and Jasper and Hayes, 1994). The results of several studies, summarised by Rau (1994), appear to show that a simple negative linear relationship between the [$CO_{2(aq)}$] and the isotopic composition of phytoplankton can account for 89% of the observed variation in the isotopic composition of phytoplankton in today's ocean. The physiological interpretation of this empirical relationship has relied on the assumption that phytoplankton are only able to use $CO_{2(aq)}$ as their inorganic carbon source (*e.g.* Rau *et al.*, 1992, Francois *et al.*, 1993). It is therefore possible to interpret the oceanic isotope signal either in terms of the uptake of $CO_{2(aq)}$ by passive diffusion or by use of a CCM.

To gain a better understanding about the relationship between the isotopic composition of phytoplankton and their inorganic carbon source and so the nature of inorganic carbon acquisition it is necessary to know the isotopic composition of the inorganic carbon source (*i.e.* $CO_{2(aq)}$ or HCO_3^-). Due to the dynamic nature of the marine ΣCO_2 system it is not possible to determine directly the isotopic composition of the different forms of inorganic carbon ($CO_{2(aq)}$, HCO_3^- and CO_3^{2-} (carbonate)). However, by determining the isotopic composition of the ΣCO_2 and the [$CO_{2(aq)}$], [HCO_3^-] and [CO_3^{2-}] (*CHAPTER* 2), it is possible to calculate the isotopic composition of the different forms of ΣCO_2 if the appropriate isotopic fractionation factors are known (*CHAPTERS* 3 and 4). The fractionation factors, which may, in this case, be viewed as ratios of the equilibrium

constants for ^{12}C and ^{13}C (see *CHAPTER* 3), are dependent on the temperature (*e.g.* Mook *et al.*, 1974, Zhang *et al.*, 1995) and possibly the ionic strength and ionic composition of the medium (*e.g.* Thode *et al.*, 1965). The fractionation factors that have been measured to date have been determined in distilled water and their direct application to sea water may not be correct and so lead to errors when calculating the isotopic composition of the different species of ΣCO_2 (*e.g.* Zhang *et al.*, 1995). If the calculated isotopic composition of $CO_{2(aq)}$ and HCO_3^- in sea water is incorrect, attempts to understand the uptake of inorganic carbon by marine phytoplankton maybe hampered by an ill defined relationship between the isotopic composition phytoplankton and their inorganic carbon source.

Therefore, given the possibility that the isotopic fractionation factors relating to the ΣCO_2 system in distilled water may not be applicable to the marine environment, one of the main aims of the work presented in this thesis was to determine the fractionation factors associated with the marine ΣCO_2 system. Due to the complex nature of the marine ΣCO_2 system and isotope effects in general the first two chapters will discuss the ΣCO_2 system and isotope effects with respect to the theories of thermodynamics and chemical kinetics as well as the transition state theory. *CHAPTER* 4 discuss the chemistry of isotopes within the ΣCO_2 system and reviews the existing information. *CHAPTER* 5 presents the results of experiments conducted to determine the fractionation factors between the various species of dissolved inorganic carbon in sea water in relation to temperature. The second part of the thesis presents the results obtained during a mesocosm experiment (*CHAPTER* 6) and a temporal study in the Menai Strait (*CHAPTER* 7). The aim of these experiments was to investigate how changes in the isotopic composition of phytoplankton during an algal bloom are related to changes in the isotopic composition and concentration of the two proposed sources of inorganic carbon, $CO_{2(aq)}$ and HCO_3^-. Based on the results of these studies inferences have been made about the most likely method of carbon acquisition employed by different populations of phytoplankton.

Chapter 2: The Basic Chemistry of the ΣCO_2 System in the Marine Environment From the Viewpoint of Thermodynamics, Kinetics and Transition State Theory

2.1 Introduction

One of the main aims of this thesis is to investigate the relationship between the isotopic composition of phytoplankton and that of their inorganic carbon source. In order to understand the complex factors affecting the distribution of ^{12}C and ^{13}C within the marine ΣCO_2 system it is necessary to understand the chemical factors that control the relative concentrations of the different species of ΣCO_2, *i.e.* $CO_{2(aq)}$, HCO_3^- and CO_3^{2-}, and how the concentrations of these species may be determined.

Within the pH range of sea water (7.5 to 8.5, Parsons *et al.*, 1984) less than 1% (<20 $\mu mol.kg^{-1}$) of the ΣCO_2 is in the form of $CO_{2(aq)}$. Despite the low concentration of $CO_{2(aq)}$ the majority of inorganic carbon fixed by photosynthetic processes in the marine environment is probably derived from $CO_{2(aq)}$ (Rau *et al.*, 1992, Rau, 1994), although certain species of phytoplankton appear to posses the ability to utilise HCO_3^- (Bowes, 1985, Beardall, 1985, Burns and Beardall, 1987, Sharkey and Berry, 1985, Raven and Johnston, 1991). Experimental results (Riebesell *et al.*, 1993) have shown that the growth rate of diatoms, which can only utilise $CO_{2(aq)}$, may be limited by the rate at which $CO_{2(aq)}$ can be supplied from the bulk medium. Under such conditions the concentration of $CO_{2(aq)}$ within the boundary layer around the phytoplankton cell or within the phytoplankter itself may not be in equilibrium with the surrounding bulk media (*e.g.* Goericke *et al.*, 1994). The degree of disequilibrium will be primarily controlled by the rate at which $CO_{2(aq)}$ can be resupplied by diffusion and the conversion from HCO_3^- versus the rate at which $CO_{2(aq)}$ is assimilated.

Much of the work conducted on the ΣCO_2 system in the marine environment uses thermodynamic principles and assumptions to understand the relationship between the concentrations of $CO_{2(aq)}$, HCO_3^- and CO_3^{2-} (Stumm and Morgan, 1981). Although the application of thermodynamic principles allows the relative concentrations of the different species of ΣCO_2 to be calculated using few macroscopic variables (Stumm and Morgan, 1981), which may be readily determined, it can not be correctly applied to systems which

are not at equilibrium. To investigate the chemistry of the ΣCO_2 system under such conditions requires the application of chemical kinetics (*e.g.* Gavis and Ferguson, 1975).

This chapter will therefore review the basic chemistry of the ΣCO_2 system as well as discussing aspects of its chemistry from the viewpoints of thermodynamics, kinetics and transition state theory. Due to the photosynthetic importance of $CO_{2(aq)}$ the majority of the discussions will focus on the reactions and relationships between $CO_{2(aq)}$ and HCO_3^-.

2.2 The Basic Chemistry of Dissolved Inorganic Carbon

The chemistry of the marine ΣCO_2 system is complex, both conceptually and practically, although the basic chemistry of the ΣCO_2 system may be simply viewed as the deprotonation reactions of a volatile diprotic acid; carbonic acid (H_2CO_3). The major reactions between the different species of ΣCO_2 and CO_2 in the gaseous phase ($CO_{2(g)}$) can be summarised as follows:

$$CO_{2(g)} \rightleftharpoons CO_{2(aq)} \qquad \textbf{(2.1)}$$

$$CO_{2(aq)} + H_2O \rightleftharpoons H_2CO_3 \qquad \textbf{(2.2)}$$

$$H_2CO_3 \rightleftharpoons H^+ + HCO_3^- \qquad \textbf{(2.3)}$$

$$HCO_3^- \rightleftharpoons H^+ + CO_3^{2-} \qquad \textbf{(2.4)}$$

The relative concentrations of the different species are primarily controlled by the pH of the system. For example, in a solution of high pH, the degree of deprotonation will be maximal and therefore CO_3^{2-} will be the dominant species (*FIGURE* 2.1) and when the pH is low the degree of protonation will be reduced and $CO_{2(aq)}$ will dominate. Within the pH range found in the marine environment (7.5 to 8.5), which is slightly on the alkaline side of neutral,

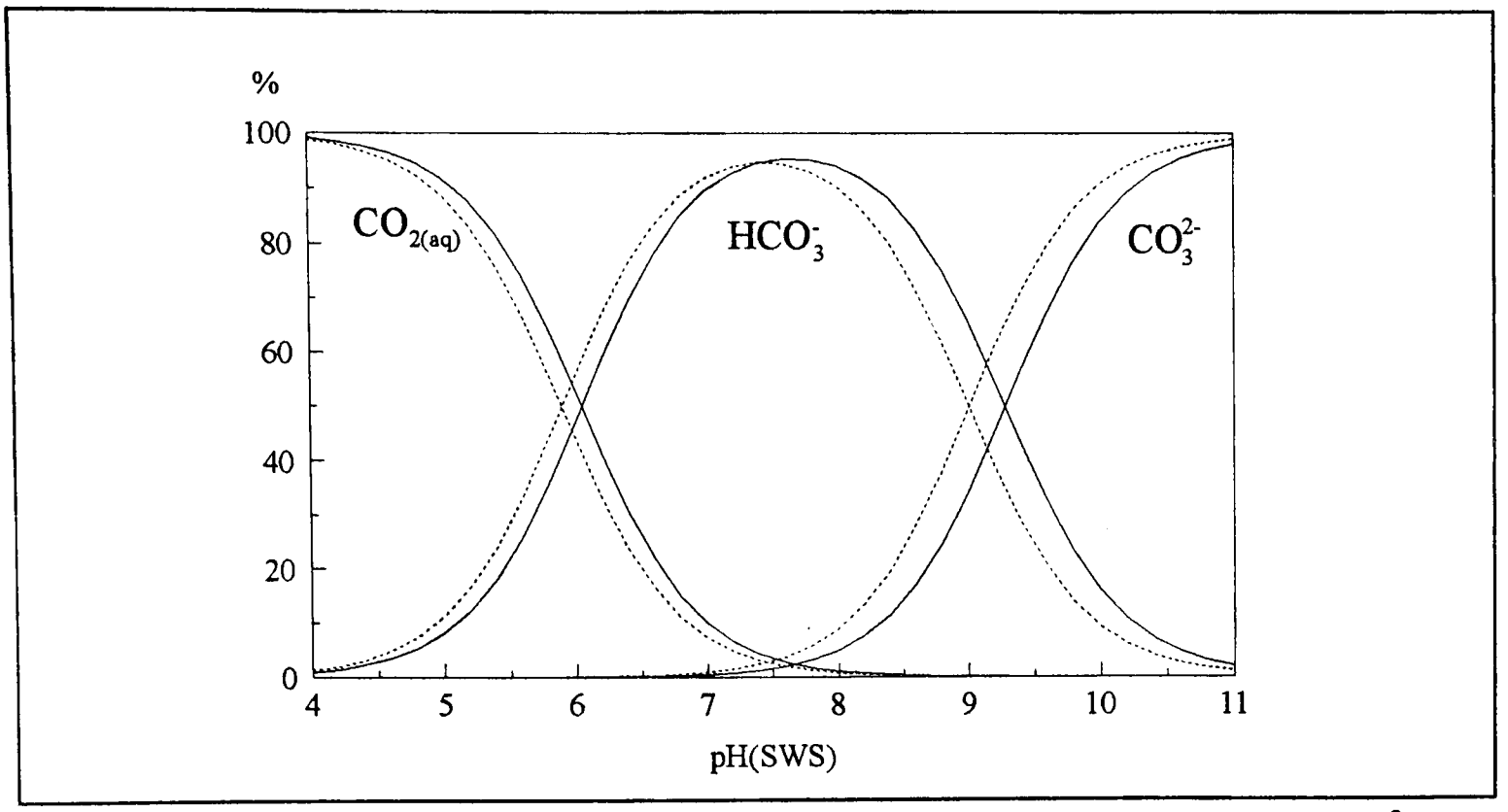

Figure 2.1 Variations in the relative concentrations (%) of $CO_{2(aq)}$, HCO_3^- and CO_3^{2-} with pH_{SWS} at 5°C (solid line) and 20°C (dashed line) in sea water (S = 35).

HCO_3^- is the dominant species (> 95 %).

As it is difficult to analytically distinguish between $CO_{2(aq)}$ and H_2CO_3 (Stumm and Morgan, 1981, DOE, 1991), mainly because of the transient nature and hence low concentration of H_2CO_3 (~0.2 to 0.3 % of the [$CO_{2(aq)}$], Skirrow, 1974, Stumm and Morgan, 1981), the reactions given in eqns. 2.2 and 2.3 are normally combined and expressed as follows:

$$CO_{2(aq)} + H_2O \rightleftharpoons H^+ + HCO_3^- \qquad \textbf{(2.5)}$$

The [ΣCO_2] is therefore given by the sum of the concentrations of the individual species of dissolved inorganic carbon, where [$CO_{2(aq)}$] also includes H_2CO_3:

$$[\Sigma CO_2] = [CO_{2(aq)}] + [HCO_3^-] + [CO_3^{2-}] \qquad \textbf{(2.6)}$$

The average oceanic [ΣCO_2] in the surface waters of the marine environment is 2000 $\mu mol.kg^{-1}$ (Volk and Hoffert, 1985) and the concentrations of $CO_{2(aq)}$, HCO_3^- and CO_3^{2-} are approximately 14, 1810 and 176 $\mu mol.kg^{-1}$ respectively.

The pH of sea water is primarily controlled by the relative concentrations of the total alkalinity (TA) and total acidity. The total alkalinity is defined as the acid neutralising capacity of a solution and the total acidity as the base neutralising capacity. As the concentration of TA is slightly greater than the total acidity concentration the pH of sea water lies on the alkaline side of neutral. The relatively high levels of alkalinity and acidity found in sea water (*e.g.* relative to freshwater) result in its high buffer capacity, *i.e.* the pH change resulting from the addition of an acid or base is small. The majority of the buffer capacity of sea water is due to the high concentration of the ΣCO_2 pool relative to other potential buffers (*e.g.* borate, the concentration of which is ~100μmol.kg^{-1}) (Skirrow, 1974). Processes which add CO_2 to the ΣCO_2 pool, such as the anthropogenic release of CO_2, will increase the acidity (due to the addition of carbonic acid), but not the total alkalinity (TA) of the system and hence decrease the pH. A decrease in the pH increases the relative concentration of $CO_{2(aq)}$ (*FIGURE* 2.1) which will "resist" the further entry of $CO_{2(g)}$ from the atmosphere (Skirrow, 1974). Similarly, the removal of $CO_{2(aq)}$ from sea water, for example by photosynthesis, decreases the acidity, but not the TA and hence raises the pH and decreases the relative concentration of $CO_{2(aq)}$ (*FIGURE* 2.1). If it is assumed that the supply of $CO_{2(aq)}$ to a cell is diffusionally controlled, a decrease in the external concentration of $CO_{2(aq)}$ will reduce the supply of $CO_{2(aq)}$ which may in turn limit the rate at which $CO_{2(aq)}$ can be fixed, *i.e.* the rate of production.

2.3 The Analytical Determination of Parameters Associated with the ΣCO_2 System

Many of the difficulties encountered when studying the marine ΣCO_2 system can be attributed to the high concentration of ΣCO_2 and hence the high levels of accuracy and precision necessary to study the relatively small effects of chemical and biological processes on the concentration of ΣCO_2. However, small changes in the $[\Sigma CO_2]$ may produce large changes in the relative concentrations of the different species, especially $[CO_{2(aq)}]$. For example, the uptake of inorganic carbon during a phytoplankton bloom in the North Atlantic only changed the $[\Sigma CO_2]$ by 2% but the $[CO_{2(aq)}]$ decreased by 25% (Rau *et al.* 1993). To investigate the potential effects of such processes on the global carbon cycle probably requires the measurements to be made with a precision of >0.1%, if accurate conclusions

are to be made (Robinson and Williams, 1991).

Due to the dynamic nature of the equilibrium between the different species of ΣCO_2 it is not possible to experimentally measure the concentrations of $CO_{2(aq)}$, HCO_3^- and CO_3^{2-} directly. However, the concentrations of the various species of ΣCO_2 may be calculated by making thermodynamic assumptions about the system under study which allow the concentrations of the individual components to be evaluated on the basis of a few analytical observations (Skirrow, 1974, Stumm and Morgan, 1981). The thermodynamic state of the ΣCO_2 system can be defined by specifying the temperature and salinity, which effectively determine the equilibrium constants (see section 2.5), and two extensive variables (*i.e.* properties which directly depend on the number of moles (Stumm and Morgan, 1981). The properties of the ΣCO_2 system which are accessible to measurement are:

i. $[\Sigma CO_2]$ - The total concentration of the ΣCO_2 pool can be determined accurately and precisely (0.025 - 0.05%) using coulometric methods (*e.g.* Robinson and Williams, 1991).

ii. fCO_2 - The fugacity of $CO_{2(aq)}$ can be determined with a precision of 0.5% (Millero *et al.* 1993) and can be related to the concentration of $CO_{2(aq)}$ by using an appropriately determined equilibrium constant (Weiss, 1974). The fugacity is normally measured by determining the CO_2 content of a small aliquot of air which has been allowed to reach equilibrium with a sample of sea water.

iii. TA - The titration, or total alkalinity, is a measure of the acid neutralising capacity of an aqueous system and is normally determined by titrating the sample with a strong acid until the required end point (equivalence point) (Stumm and Morgan, 1981) is reached, the precision has been estimated to be 2% (Millero *et al.*, 1993)

iv. pH - The pH of a sea water sample is normally determined by potentiometric methods (*e.g.* Fuhrmann and Zirino, 1988), although due to problems associated with the electrode potential chain in sea water the precision is limited (5% or 0.02 pH units, UNESCO, 1987). Recently, the precision of

oceanic pH measurements has been considerably improved (0.1% or 0.0004 pH units, Clayton and Byrne, 1993) by the use of pH indicators in conjunction with high performance spectrophotometers (See *APPENDIX* 3).

By using two of these experimentally determined parameters, in conjunction with the appropriate equilibrium constants (see section 2.5), the concentrations of $CO_{2(aq)}$, HCO_3^- and CO_3^{2-} can be calculated using the expressions given by Skirrow (1974) or DOE (1994). Examples of which are given below where pH and $[\Sigma CO_2]$ are the macroscopic observables:

$$[CO_{2(aq)}] = [\Sigma CO_2] \frac{[H^+]^2}{[H^+]^2 + K_{1\text{-}H2O} \times [H^+] + K_{1\text{-}H2O} \times K_2} \quad \textbf{(2.7)}$$

$$[HCO_3^-] = [\Sigma CO_2] \frac{K_{1\text{-}H2O} \times [H^+]}{[H^+]^2 + K_{1\text{-}H2O} \times [H^+] + K_{1\text{-}H2O} \times K_2} \quad \textbf{(2.8)}$$

$$[CO_3^{2-}] = [\Sigma CO_2] \frac{K_{1\text{-}H2O} \times K_2}{[H^+]^2 + K_{1\text{-}H2O} \times [H^+] + K_{1\text{-}H2O} \times K_2} \quad \textbf{(2.9)}$$

where $K_{1\text{-}H2O}$ and K_2 are the equilibrium constants, consistent with the adopted activity and pH scales (see below).

2.4 Activity and pH Scales

Two activity scales have been applied when studying equilibria in aqueous ionic solutions: the infinite dilution activity scale and the ionic medium activity scale (Sillén, 1966, Stumm and Morgan, 1981). The infinite dilution activity scale can be defined as follows (Sillén, 1966, Stumm and Morgan, 1981):

$$\{x\} = \gamma_x \times [x] \quad \textbf{(2.10)}$$

where {x} is the activity of species x, [x] is the concentration and γ_x is the activity coefficient. The activity coefficient is dependent on the composition and concentration of the ionic medium and hence the activity coefficient approaches one as the composition of the solution approaches pure water, *i.e.*

$$\frac{\{x\}}{[x]} \rightarrow 1 \qquad \textbf{(2.11)}$$

However, in a complex electrolyte, such as sea water, the composition of which is often constant, it has been found more convenient to define the activities using an ionic medium activity scale (Sillén, 1966). On this scale the activity coefficient approaches one as the composition of the solution approaches that of the pure *ionic* medium, as opposed to the pure medium. As the concentration of ΣCO_2 is less than 10% of the concentration of the medium ions (Stumm and Morgan, 1981) the activity coefficient remains very close to one, and hence:

$$\{x\} \approx [x] \qquad \textbf{(2.12)}$$

The ionic medium activity scale has become increasingly popular and the most recently published equilibrium constants (*e.g.* Goyet and Poison, 1989 and Roy *et al.*, 1993) have all been based on this scale.

Because of the potentiometric methods usually used to define and determine pH (Dickson, 1984), the pH of a solution is normally given the following definition:

$$pH = -\log \{H^+\} \qquad \textbf{(2.13)}$$

However, if an ionic medium activity scale is adopted, pH can be defined according to Sørenson's original definition:

$$pH = -\log [H^+] \qquad \textbf{(2.14)}$$

It is now generally accepted that a pH scale based on the hydrogen ion concentration, as opposed to activities, is probably the most meaningful for oceanic pH measurements (Dickson, 1993).

Although the pH of sea water is primarily controlled by the ΣCO_2 system other basic components, such as SO_4^{2-} and F^-, also react with H^+ and as result influence the pH of the system. It has therefore been a matter of debate whether pH definitions should account for the action of SO_4^{2-} and/or F^-. This has lead to several pH scales, in addition to the conventional NBS (National Bureau of Standards) scale, being defined for use in sea water (Dickson, 1993):

i. The "free" hydrogen ion concentration scale (pH_{free}) which does not account for the presence of either SO_4^{2-} or F^-.

ii. The "total" hydrogen ion concentration scale (pH_{total}) which only accounts for the effect of SO_4^{2-}.

iii. The "sea water" hydrogen ion concentration scale (pH_{SWS}) which includes the effect of both SO_4^{2-} and F^-.

A recent study by Dickson (1993) has indicted that sea water pH measurements should be made on the pH_{total} scale which can be defined unambiguously and is more accurate.

2.5 A Thermodynamic Approach to the Chemistry of Dissolved Inorganic Carbon

In general, when studying the relationship between the ΣCO_2 system and processes such as photosynthesis and air-sea exchange, a knowledge of the concentrations of $CO_{2(aq)}$, HCO_3^- and CO_3^{2-} is required. As the concentrations of the individual species cannot be determined directly it is necessary to calculate their concentrations from the parameters which can be measured in conjunction with the appropriate equilibrium constants (*e.g.* eqns. 2.7, 2.8 and 2.9). This is normally achieved by applying the law of mass action (equilibrium law) and hence making thermodynamic assumptions about the system under study. The primary assumptions are that the system is closed and at equilibrium (Stumm and Morgan, 1981). The validity of this assumption is dependent on the relative rates of processes which add

(*e.g.* the addition of $CO_{2(aq)}$ due to respiration) or remove (*e.g.* the removal of $CO_{2(aq)}$ by photosynthesis) different species of ΣCO_2 in relation to the rate of the reactions between the different constituents (*i.e.* $CO_{2(aq)}$, HCO_3^- and CO_3^{2-}). When studying the marine ΣCO_2 system of the bulk medium in the marine environment this assumption is probably always correct. However, the validity may not be so certain in micro-environments such as within the boundary layers surrounding individual phytoplankton cells.

By applying thermodynamic principles the following equilibrium equations for the reactions given in eqns 2.1, 2.5 and 2.4 can be written, where $K_{1\text{-}H2O}$ and K_2 are the equilibrium constants expressed on the ionic medium activity scale and K_0 is Henry's law constant:

$$K_0 = \frac{[CO_{2(aq)}]}{f_{CO_2}} \qquad \textbf{(2.15)}$$

$$K_{1\text{-}H2O} = \frac{[H^+]\,[HCO_3^-]}{[CO_{2(aq)}]} \qquad \textbf{(2.16)}$$

$$K_2 = \frac{[H^+]\,[CO_3^{2-}]}{[HCO_3^-]} \qquad \textbf{(2.17)}$$

The term f_{CO2} is the fugacity of the $CO_{2(aq)}$, this is basically a measure of the activity of CO_2 in the gaseous phase (Weiss, 1974). As the above equations are written in terms of the ionic medium activity scale the relative quantities of the different species of ΣCO_2 are expressed as concentrations. If the system was defined on the infinite dilution activity scale the concentration terms would be alternatively expressed as activities. Suitably defined equilibrium constants on the infinite dilution activity scale are independent of salinity. This constancy is due to the artificial concept of activity which is a device intended to preserve

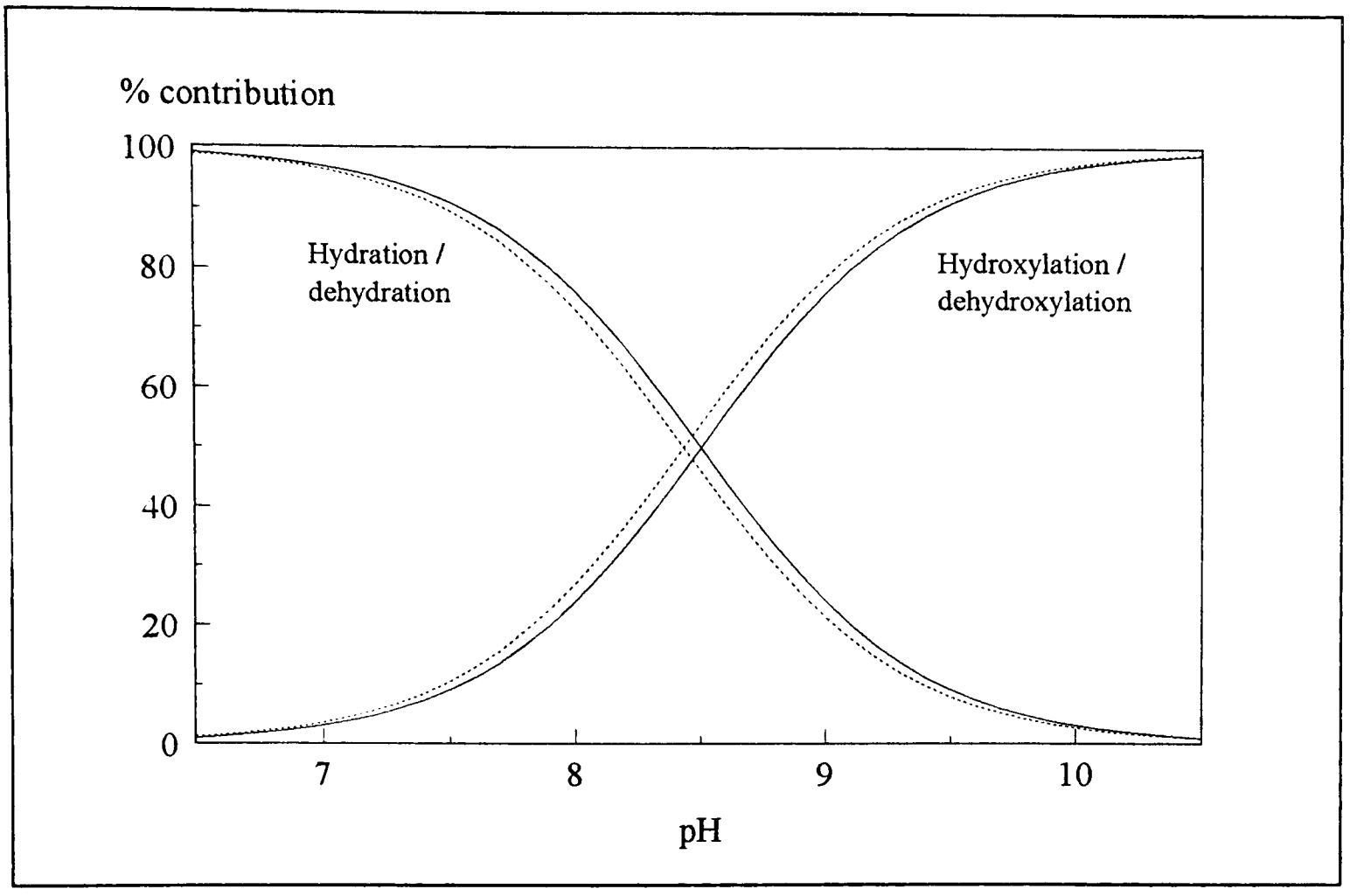

Figure 2.2 The effect of pH on the relative contribution (%) of the hydration / dehydration and hydroxylation / dehydroxylation reaction mechanisms to the overall interconversion of $CO_{2(aq)}$ and HCO_3^- at 5°C (dashed line) and 20°C (solid line) in sea water (S = 35). The contribution of each reaction mechanism was calculated using the data of Johnson (1982) in conjunction with equations 2.33 and 2.34 as described in the text.

the thermodynamic simplicity of the relationship established in ideal systems (Skirrow, 1974). It is also worth noting that due to the combination of eqns. 2.3 and 2.4 the equilibrium constant $K_{1\text{-}H2O}$ is strictly a composite acidity constant and therefore the term $[CO_{2(aq)}]$ also includes a contribution form H_2CO_3 (Stumm and Morgan, 1981). The term apparent equilibrium constant is usually used to describe the equilibrium constants which have been defined using mixed activity scales (*e.g.* Merbach *et al.*, 1973).

The equilibrium expression given in eqn. 2.16 applies to the hydration / dehydration reaction given in eqn. 2.5. However, the inter-conversion of $CO_{2(aq)}$ and HCO_3^- only proceeds dominantly (> 99 %) via the hydration / dehydration reaction pathway below a pH of ~6. At pHs greater than 11 the majority (>99 %) of the inter- conversion proceeds via the alternative hydroxylation / dehydroxylation reaction which is given below.

$$CO_{2(aq)} + OH^- \rightleftharpoons HCO_3^- \qquad \textbf{(2.18)}$$

Table 2.1 The calculated changes in the free energy (ΔG°) and equilibrium constants for the hydration / dehydration ($K_{1\text{-}H2O}$) and hydroxylation / dehydroxylation ($K_{1\text{-}OH}$) (see eqns. 2.16 and 2.19) reactions between $CO_{2(aq)}$ and HCO_3^- and the deprotonation of HCO_3^- (K_2). The K_x - thermodynamic, salinity = 0 results have been calculated using eqn. 2.20 and the salinity = 35 results have been calculated using the expressions given by Goyet and Poison (1989) (The values of $K_{1\text{-}OH}$ have been determined by dividing $K_{1\text{-}H2O}$ by K_W. K_W has been calculated at the appropriate temperature and salinity using the expression given by Dickson and Riley (1979)). The K_x - kinetic equilibrium constants have been calculated using the principle of microscopic reversibility (eqns. 2.29 and 2.30) along with the appropriate rate constants determined by Johnson (1982), the value of K_w used when salinity = 0 is given by Stumm and Morgan (1981, page 127) and when salinity = 35 the values obtained from Dickson and Riley (1979) have been used.

Reaction	**ΔG° ($kj.mol^{-1}$)**	**K_x - Thermodynamic**		**K_x -Kinetic**	
		Salinity = 0	**Salinity = 35**	**Salinity = 0**	**Salinity = 35**
$K_{1\text{-}H2O}$	36.34	4.297×10^{-7}	1.410×10^{-6}	4.908×10^{-7}	1.034×10^{-6}
$K_{1\text{-}OH}$	-43.55	4.266×10^{7}	2.368×10^{7}	3.707×10^{7}	1.611×10^{7}
K_2	58.87	4.851×10^{-11}	1.187×10^{-9}	-	-

At intermediate pHs (6 to 11) the reaction between $CO_{2(aq)}$ and HCO_3^- can proceed via both pathways simultaneously and the contribution of each reaction mechanism to the overall inter-conversion of $CO_{2(aq)}$ and HCO_3^- is dependent on pH (see *FIGURE* 2.2). It is therefore possible to write the following equilibrium relationship for the hydroxylation / dehydroxylation reaction:

$$K_{1\text{-}OH} = \frac{[HCO_3^-]}{[CO_{2(aq)}]\,[OH^-]} \qquad \textbf{(2.19)}$$

The effect of the hydroxylation / dehydroxylation reaction on the equilibrium between $CO_{2(aq)}$ and HCO_3^- is sometimes disregarded when studying the ΣCO_2 system in sea water (*e.g.* Goericke *et al.*, 1994). However, within the pH range encountered in the marine environment (7.5 to 8.5), 10 to 55 % of the $CO_{2(aq)}$ - HCO_3^- inter - conversion may proceed via the hydroxylation / dehydroxylation pathway (see *FIGURE* 2.2). It is therefore necessary

to understand the relationship between $K_{1\text{-}H2O}$ and $K_{1\text{-}OH}$ as it would appear that at intermediate pHs both equilibria may need to be taken into consideration.

From the difference in the ΔG^{e}_{f} (Gibbs free energy of formation) of the reactants and products the change in the overall Gibbs free energy associated with each reaction mechanism (ΔG^{e}), at standard temperature and pressure (298.15 K, 10^5 Pa) can be calculated. Using these calculated ΔG^{e} values the equilibrium constants may be determined using the equation given below:

$$\ln K = \frac{-\Delta G^{e}}{R \times T} \qquad \textbf{(2.20)}$$

where ln K is the natural logarithm of the equilibrium constant, T is the absolute temperature and R is the gas constant (8.314 $J.mol^{-1}.K^{-1}$). The values of $K_{1\text{-}H2O}$ and $K_{1\text{-}OH}$ calculated on a thermodynamic basis are given in *TABLE* 2.1.

From the calculated ΔG^{e} values for each reaction mechanism it is apparent that the dehydration and hydroxylation reactions decrease the energy of the system and are therefore thermodynamically favourable. It is also apparent from the results in *TABLE* 2.1 that the equilibrium constants $K_{1\text{-}H2O}$ and $K_{1\text{-}OH}$ are not equal but they are related by the disassociation constant for water, K_W:

$$\frac{K_{1\text{-}H2O}}{K_{1\text{-}OH}} = K_W \qquad \textbf{(2.21)}$$

Equilibrium constants defined on the ionic medium activity scale are normally functions of temperature, pressure and solution composition (Stumm and Morgan, 1981). The effect of the temperature on the equilibrium constant can be predicted using the Gibbs - Helmholtz equation (*e.g.* Stumm and Morgan, 1981) to calculate ΔG^{e} and therefore K using eqn 2.20, or alternatively using the van't Hoff equation. The effect of ionic strength (I) on an equilibrium constant can be predicted using empirical equations such as the Güntelberg approximation given below (Stumm and Morgan, 1981):

$$pK = p^0K + \frac{0.5 \times (z_{HB}^2 - z_B^2) \times \sqrt{I}}{1 + \sqrt{I}} \qquad \textbf{(2.22)}$$

where $pK = -\log K$, z_{HB} and z_B are the charges of the acid and base respectively and p^0K is the equilibrium constant at an ionic strength of 0 $mol.kg^{-1}$. The Güntelberg approximation may be used for ionic solutions composed of several electrolytes although it should strictly be used for solutions with ionic strengths of less than 0.5 $mol.kg^{-1}$ (sea water is ~0.7 $mol.kg^{-1}$) (see Stumm and Morgan, 1981).

However, due to the high levels of precision and accuracy required when studying the marine ΣCO_2 system it is necessary to determine directly the effect of temperature and salinity on the equilibrium constant, as general empirical relationships, based on ionic strength, may not accurately account for the combined effects of the electrolytes found in sea water. As is apparent from the equilibrium expression (eqns. 2.16 and 2.17), the equilibrium constant will be dependent on the activity and pH scales used to experimentally determine $K_{1\text{-}H2O}$ and K_2. The temperature and salinity dependence of the equilibrium constant, $K_{1\text{-}H2O}$ and K_2, has been frequently determined using different activity and pH scales (*e.g.* Buch *et al.*, 1932, Lyman, 1956, Hanson, 1973, Merbach *et al.*, 1973, Goyet and Poison, 1989, Roy *et al.*, 1993). The most recent determinations (*e.g.* Hanson, 1973, Goyet and Poison, 1989, and Roy *et al.*, 1993) have been consistently expressed on an ionic medium activity scale although Goyet and Poison (1989) used the pH_{SWS} scale and Roy *et al.* (1993) used the pH_{total} scale. The constants used during this study will be as determined by Goyet and Poison (1989). The choice of constants was primarily determined by the sea water model (Prof. David Turner) used to calculate *in situ* pH [1] (see *APPENDIX* 3) and perform some of the equilibrium calculations. However, the pH measurements during this

---

1 To calculate the pH at *in situ* temperatures requires a model capable of iteratively calculating the *in situ* pH from the TA and $[\Sigma CO_2]$ (the exact procedure is detailed in *APPENDIX 3*). The model of Prof. David Turner provided this iterative facility and therefore, to maintain consistency, this model was used to perform all calculations associated with the ΣCO_2 system.

study were made on the pH_{total} scale which is not consistent with the results of Goyet and Poison (1989). The following equation can be used convert pH measurements made on the pH_{total} to the sea water scale (Dickson, 1993):

$$pH_{SWS} = pH_{total} + \frac{\Sigma F^-}{K_{HF}} \qquad \textbf{(2.23)}$$

where ΣF^- is the total concentration of fluoride and K_{HF} is the acid dissociation constant for hydrogen fluoride (Roy *et al.*, 1993). However, as the difference between the two scales is small (~0.02 pH units) and only effects the calculated $[CO_{2(aq)}]$ by ~5% and the $[HCO_3^-]$ by ~1 % the pH results presented here have not been corrected.

The temperature (T) (-1°C to 40°C) and salinity (S) (10 to 50) dependent values of $K_{1\text{-}H2O}$ can be calculated using the following equation (Goyet and Poison, 1989):

$$pK_{1\text{-}H2O} = 812.27 / T + 3.356 - 0.00171 \times S \times \ln T + 0.000091 \times S^2 \qquad \textbf{(2.24)}$$

The reaction between HCO_3^- and CO_3^{2-} is a simple protonation / deprotonation reaction which only occurs via the one reaction mechanism (eqn 2.4) and therefore the equilibrium expression given in eqn. 2.17 completely and correctly describes the chemistry of the reaction. The changes in the Gibbs free energy and the equilibrium constant associated with the reaction have been calculated and the results are given in *TABLE* 2.1. It is apparent from the change in free energy that the reverse reaction, *i.e.* the formation of HCO_3^-, is thermodynamically favourable. The temperature (-1°C to 40°C) and salinity (10 to 50) dependence of K_2, determined by Goyet and Poison (1989), will again be used throughout this study and the values of K_2 may be calculated using the following expression:

$$pK_2 = 1450.87 / T + 4.604 - 0.00385 \times S \times \ln T + 0.000182 \times S^2 \qquad \textbf{(2.25)}$$

In summary, the interconversion of $CO_{2(aq)}$ and HCO_3^- can proceed via two alternative reaction pathways, both of which are important within the pH range found in marine and aquatic environments. Each reaction mechanism is characterised by a distinct,

but related equilibrium constant and the calculated [$CO_{2(aq)}$] and [HCO_3^-] are not dependent on the reaction mechanism. As the pH of the solution increases the hydroxylation / dehydroxylation reaction becomes increasingly more important. The importance of changes in the reaction mechanism with pH, as well as the effect of temperature and salinity in determining the distribution of isotopes between $CO_{2(aq)}$ - HCO_3^- and HCO_3^- - CO_3^{2-} will be discussed in detail in *CHAPTER* 4.

2.6 A Kinetic Approach to the Chemistry of Dissolved Inorganic Carbon

By using a thermodynamic approach to study the chemistry of the ΣCO_2 system information can be easily gained about the equilibrium composition of the ΣCO_2 pool and the direction of a spontaneous reaction (Stumm and Morgan, 1981). However, a thermodynamic approach cannot yield information about the rate at which equilibrium is achieved (Frost and Pearson, 1958, Stumm and Morgan, 1981). In order to gain information about the rates and mechanism of a chemical reaction a kinetic approach must be adopted (*e.g.* Frost and Pearson, 1958, Laidler, 1965, Denbeigh, 1981, Stumm and Morgan, 1981). The theory of chemical kinetics may be applied when studying chemical reactions under equilibrium and non - equilibrium conditions (Stumm and Morgan, 1981).

Although the theories of thermodynamics and chemical kinetics are distinct, they can both be used to study systems at equilibrium by applying the principle of microscopic reversibility (*e.g.* Frost and Pearson, 1948, Laidler, 1965, Denbeigh, 1981, Stumm and Morgan, 1981). The principle of microscopic reversibility simply states that for a dynamic reaction at equilibrium, the thermodynamic equilibrium constant is equal to the ratio of the forward (k_f) and reverse (k_r) rate constants.

Using a kinetic approach, the velocity of the forward (v_{CO2}) and reverse (v_d) reactions associated with the hydration / dehydration reaction between $CO_{2(aq)}$ and HCO_3^- may be written as follows:

$$v_{CO2} = k_{CO2}[CO_{2(aq)}] \qquad \textbf{(2.26)}$$

$$v_d = k_d [HCO_3^-] [H^+] \quad \textbf{(2.27)}$$

where k_{CO2} (s^{-1}) and k_d ($dm^3.mol^{-1}.s^{-1}$) are the respective hydration and dehydration rate constants. At equilibrium, as the concentrations of $CO_{2(aq)}$, HCO_3^- and H^+ are constant, the velocity of the forward reaction must be equal to the velocity of the reverse reaction and hence:

$$k_{CO2} [CO_{2(aq)}] - k_d [HCO_3^-] [H^+] = 0 \quad \textbf{(2.28)}$$

Rearrangement of this expression yields the following relationship which links the concepts of thermodynamics and kinetics:

$$K_{1-H2O} = \frac{k_{CO2}}{k_d} = \frac{[H^+][HCO_3^-]}{[CO_{2(aq)}]} \quad \textbf{(2.29)}$$

An expression for the hydroxylation / dehydroxylation reaction mechanism may be derived in a similar manner:

$$K_{1-OH} = \frac{k_{OH}}{k_{HCO3-}} = \frac{[HCO_3^-]}{[OH^-][CO_{2(aq)}]} \quad \textbf{(2.30)}$$

where k_{OH} ($mol.dm^{-1}.s^{-1}$) and k_{HCO3-} (s^{-1}) are the hydroxylation and dehydroxylation rate constants respectively.

The temperature (5 to 35°C) and salinity (3.40 to 37.06) dependence of the rate constants, k_{CO2}, k_{OH}, k_d and k_{HCO3-}, have been determined (Johnson, 1982) and can be

Table 2.2 Coefficients for eqn. 2.31 which can be used to calculate the temperature and salinity dependence of the rate constants k_{CO2}, k_{OH}, k_d and k_{HCO3-} (Johnson, 1982). The rate constant for the hydroxylation reaction has been expressed as $k_{OH}.K_W$.

Rate constant	A	B	D($\times 10^{-4}$)	E
k_{CO2}	1246.98	0	-6.19	-183.0
$k_{OH}.K_W$	-930.13	0.110	3.10	140.9
k_d	1346.24	-0.126	-6.44	-196.4
k_{HCO3-}	-2225.22	-0.049	8.91	336.6

calculated using the following expression in conjunction with the appropriate constants given in *TABLE* 2.2:

$$\ln k = A + B \times S^{0.5} + D/T + E \times \ln T \qquad \textbf{(2.31)}$$

The expressions given in eqns. 2.29 and 2.30 can be confirmed by calculating the appropriate rate constants and comparing the equilibrium constants predicted using the principle of microscopic reversibility with those calculated using a thermodynamic approach. The results given in *TABLE* 2.1 appear to generally confirm the applicability of both approaches when considering the ΣCO_2 system at equilibrium although the calculated equilibrium constant for the hydroxylation / dehydroxylation reaction is lower than expected particularly when S = 35. This maybe partly attributable to a difference of pH scales as the kinetic measurements made by Johnson (1982) were determined on the NBS scale and Goyet and Poison (1989) used the sea water scale.

A further comparison may also be made by comparing the effect of temperature and salinity on the equilibrium constants $K_{1\text{-}H2O}$* and $K_{1\text{-}OH}$* (the * indicates the values have been calculated from the rate constants by applying the principle of microscopic reversibility), with the experimentally determined equilibrium constants of Goyet and Poison (1989). In order to compare $K_{1\text{-}OH}$* directly with the values determined by Goyet and Poison (1989) the values must be multiplied by K_W (eqn. 2.21). *FIGURES* 2.3 and 2.4 plot the variations in $K_{1\text{-}H2O}$* and $K_{1\text{-}OH}$*.K_W with temperature and salinity alongside the values of $K_{1\text{-}H2O}$ determined by Goyet and Poison (1989). In *FIGURE* 2.3 $K_{1\text{-}H2O}$* and $K_{1\text{-}OH}$*.K_W appear to

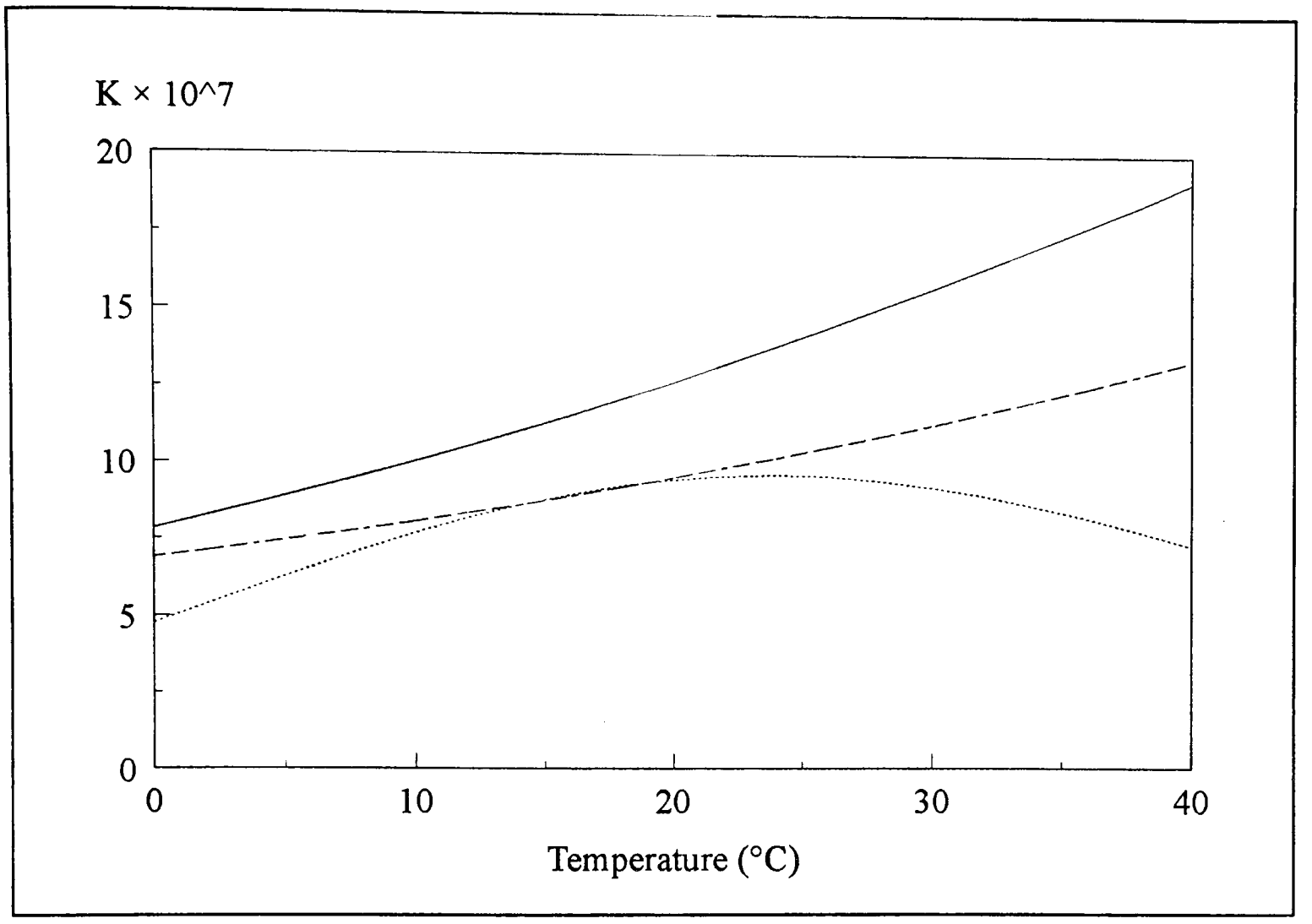

Figure 2.3 Variations in $K_{1\text{-}H2O}$* (long dash) and $K_{1\text{-}OH}.K_W$ * (short dash) with temperature in comparison with the experimentally determined results of Goyet and Poison (1989) (solid line) (S = 35). *$K_{1\text{-}OH}$ has been multiplied by K_W to aid comparison (*e.g.*, eqn. 2.21).

be subject to a temperature error although the error associated with $K_{1\text{-}OH}$*.K_W is generally larger and non-linear in comparison with $K_{1\text{-}H2O}$*. This maybe attributable to the larger errors (50 %) associated with the determination of $k_{HCO3\text{-}}$ with the equipment used by Johnson (1982). In *FIGURE* 2.4 the general agreement between the equilibrium constants is good. The offset between $K_{1\text{-}H2O}$ and $K_{1\text{-}H2O}$* is of a similar size to the offset observed in *FIGURE* 2.3. The agreement between $K_{1\text{-}OH}$*.K_W and the results of Goyet and Poison (1989) is surprisingly good considering the non - linearity of the data with respect to temperature. However, this agreement can be attributed to the temperature (25°C) chosen to plot *FIGURE* 2.4, the apparent agreement becomes increasingly worse at temperatures below 10°C and above 30°C.

As previously discussed, the interconversion between $CO_{2(aq)}$ and HCO_3^- at intermediate pHs can proceed via both reaction mechanisms simultaneously. As the rate constants for each reaction mechanism are different, the overall rate of the forward (k_h`) and

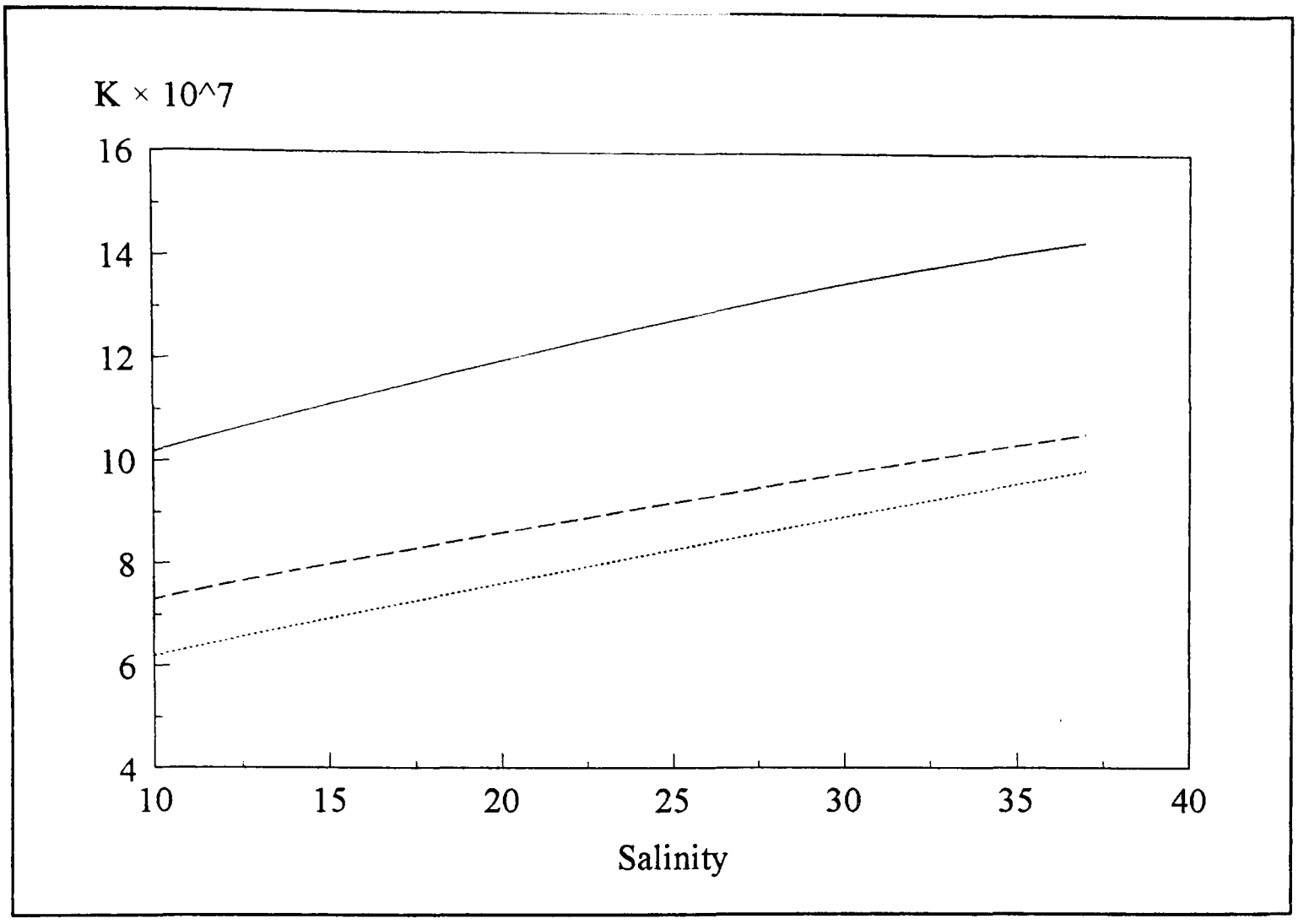

Figure 2.4 Variations in $K_{1\text{-}H2O}$* (long dash) and $K_{1\text{-}OH}$*.K_W (short dash) with salinity in comparison with empirically determined results of Goyet and Poison (1989) (solid line) (temperature = 25°C). $K_{1\text{-}OH}$* has been multiplied by K_W to aid comparison (*e.g.* eqn. 2.21).

reverse (k_d`) reactions will be dependent on the contribution of each reaction mechanism and hence pH (*FIGURE* 2.2). The following expressions can be used to calculate $k_h$` and k_d`:

$$k_h' = k_{CO2} + k_{OH}[OH^-] = k_{CO2} + k_{OH}\frac{K_W}{[H^+]} \qquad \textbf{(2.33)}$$

$$k_d' = k_d[H^+] + k_{HCO3-} \qquad \textbf{(2.32)}$$

The contribution of each reaction mechanism, k_{CO2} and k_{OH}, to the overall rate of hydration (*FIGURE* 2.2) can be calculated at different pHs by expressing k_{CO2} and $k_{OH} \times (K_W / [H^+])$, as a percentage of k_h`. A similar approach may be used to calculate the percentage contribution of $k_d$ and $k_{HCO3-}$ to $k_d$`.

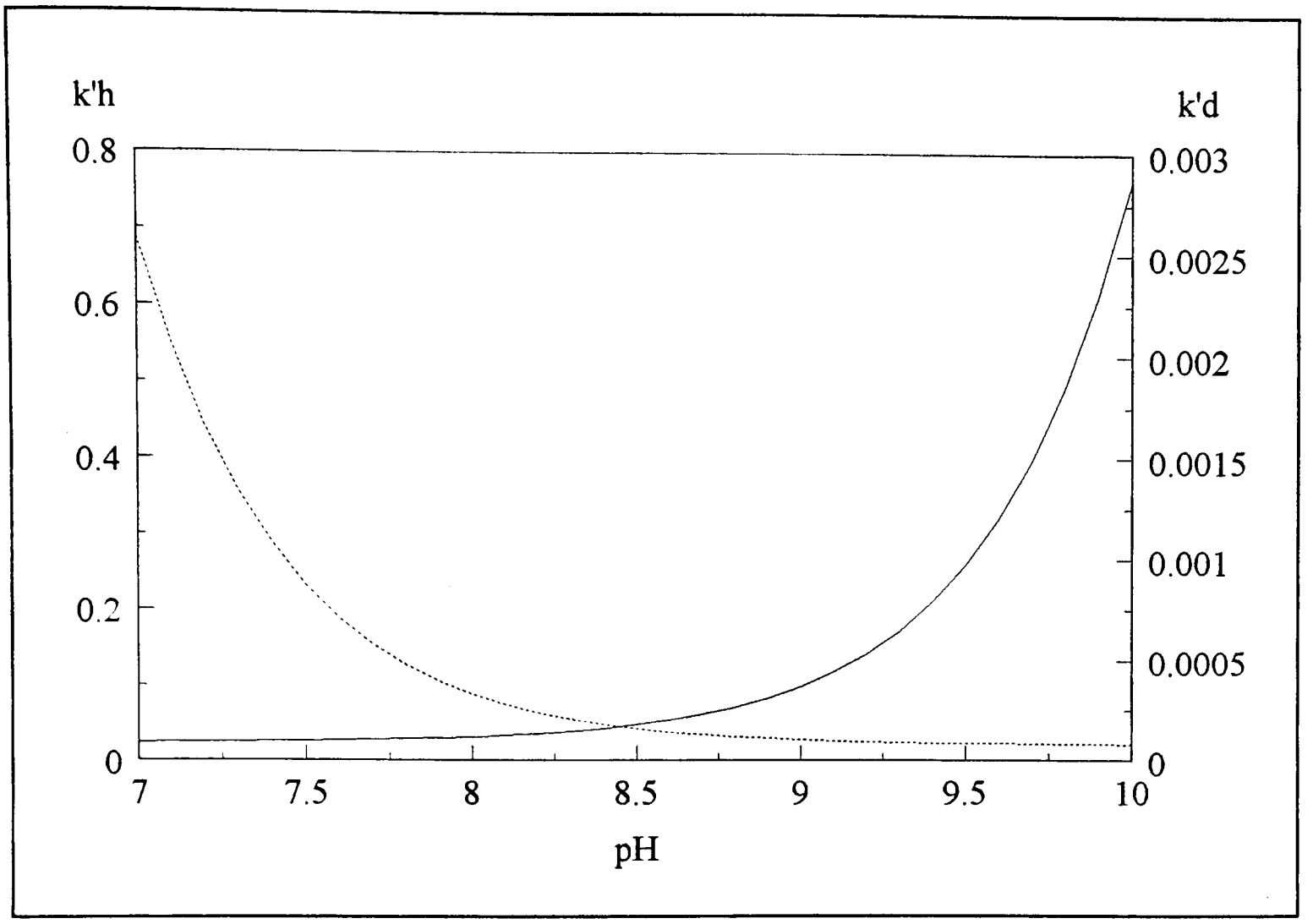

Figure 2.5 Variations in the overall rate of the forward (k_h') (solid line) and reverse (k_d') (dashed line) between $CO_{2(aq)}$ and HCO_3^- in sea water (S = 35) at 20°C using the rate constants determined by Johnson (1982) in conjunction with eqns. 2.32 and 2.33.

It is important to note that k_d` decreases as pH increases (*FIGURE* 2.5). This may have implications when considering the uptake of $CO_{2(aq)}$ by phytoplankton as the removal of $CO_{2(aq)}$ will increase the pH and hence decrease the rate at which $CO_{2(aq)}$ can be resupplied by the HCO_3^- pool. The validity of the equilibrium assumption may therefore decrease when studying processes, such as photosynthesis, if the pH of the bulk medium or within the boundary layer around the cell is high.

Little information appears to exist concerning the rate of reaction between HCO_3^- and CO_3^{2-}. The lack of data is partly due to the rapidity of the deprotonation reaction (Skirrow, 1974) which makes attempts to determine the rate constants experimentally difficult, but also reduces the need to know the rate constants as the assumption of equilibrium is probably always valid.

It is therefore important to decide whether a particular problem is concerned with equilibria or rates (Denbigh, 1981), although this decision ultimately requires a kinetic

knowledge of the system under study. It is also important to note that an equilibrium approach is not appropriate when studying a system at steady state. Therefore as processes, such as photosynthesis, remove inorganic carbon from the ΣCO_2 pool, the assumption of equilibrium, especially within the boundary layer surrounding the cell, is probably not always correct, and the degree of error introduced by such an assumption may only be assessed by studying the system using a kinetic approach.

2.7 The Dissolved Inorganic Carbon System and the Transition State Theory

The transition state theory, or activated complex theory, attempts to identify the principle features governing the rates of chemical reactions (Atkins, 1994) and it is widely used to interpret kinetic observations in solutions (Stumm and Morgan, 1981). The important features of the transition state theory for the following hypothetical reaction are summarised in *FIGURE* 2.6:

$$X + Y \rightleftharpoons Z \qquad \textbf{(2.34)}$$

The basic theory envisages the formation of a high energy, activated complex, during the course of a chemical reaction. The zero - point energy levels of the reactants and products are given by the sum of the potential energies of the individual species and the potential energy necessary to form the activated complex is given by the activation energy, E_a. The difference between the potential energy of the reactants and products is equal to the Gibbs free energy change associated with the reaction, from which the equilibrium constant can be calculated. This is important as it illustrates how the theories of kinetics and thermodynamics are conceptually related. Furthermore it demonstrates that a kinetic approach yields information about the reaction mechanism, in terms of the activation energy, as well as the equilibrium constant, whereas a thermodynamic approach only yields information about the equilibrium constant.

The activation energy of a reaction can be related to its rate constant through the expression proposed by Arrhenius:

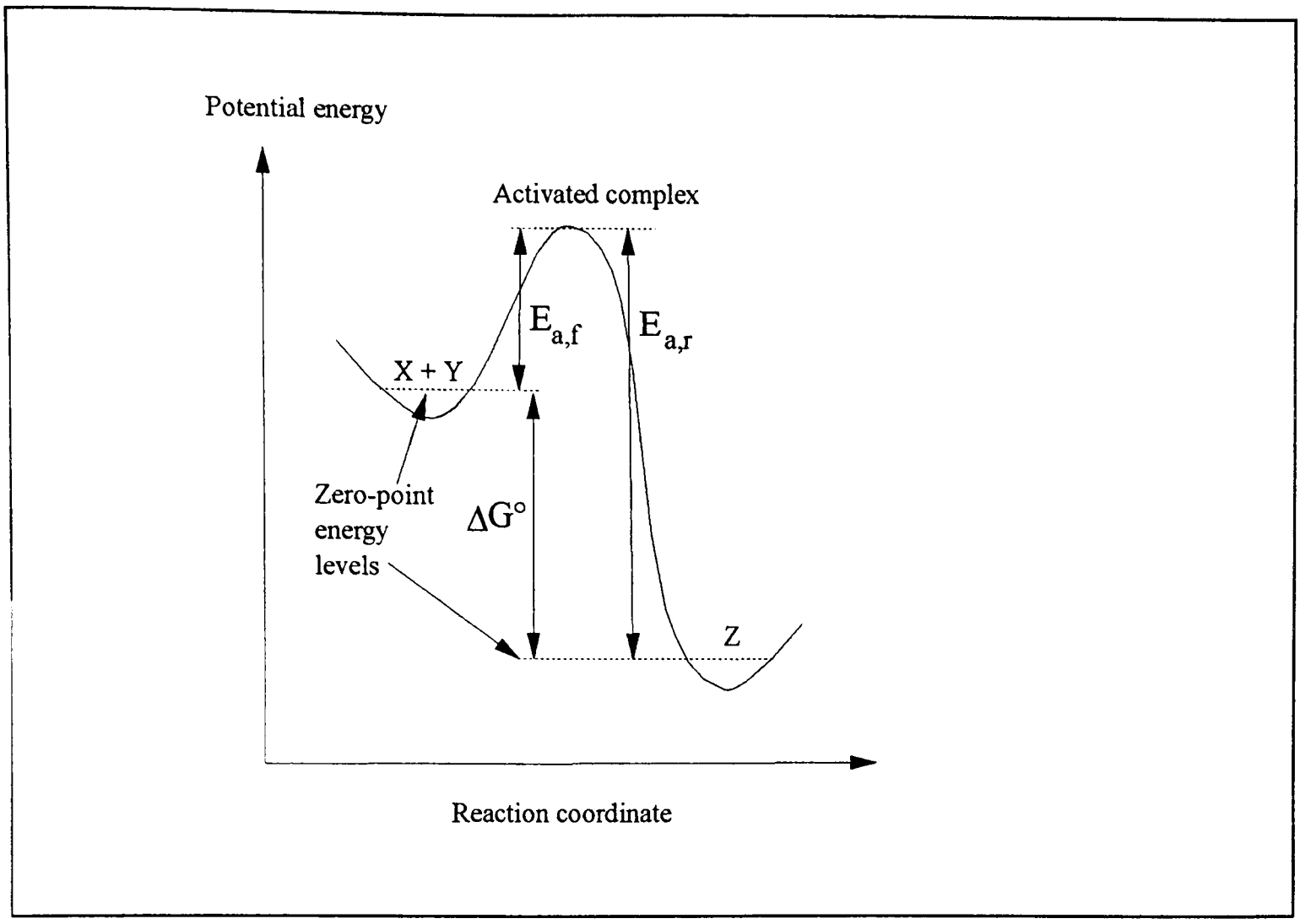

Figure 2.6 A reaction profile for the hypothetical, reversible reaction given in eqn. 2.34, where $E_{a,f}$ and $E_{a,r}$ are the activation energies associated with the forward and reverse reactions and ΔG° is the Gibbs free energy change associated with the reaction. The reaction coordinate represents the course of an individual reaction event.

$$\ln k = \ln \theta - \frac{E_a}{R T} \qquad \textbf{(2.35)}$$

where ln k is the natural logarithm of the rate constant, R is the gas constant and T is the absolute temperature. The frequency factor, θ, is basically a measure of the rate of collisions between reactant molecules (Atkins, 1994). Therefore slow reactions will be characterised by low values of θ, and / or high activation energies (Stumm and Morgan, 1981).

Using a classical Arrhenius plot the activation energy can be determined, if the temperature dependence of a rate constant is known, by plotting the natural logarithm of k against 1 / T. From the slope of the line, which is equal to E_a / R the activation energy can be calculated (Atkins, 1994). Therefore, using the rate constants determined by Johnson (1982), the activation energies relating to the hydration, dehydration, hydroxylation and

Table 2.3 Activation energies calculated using the data of Johnson (1982) and eqn. 2.35. The calculations were performed at a salinity of 0 and therefore the value of K_W given in Stumm and Morgan (1981) was used to calculate k_{OH}. Activation energies determined during previous studies are given for comparison

Reaction mechanism	Johnson, (1982)		Previous studies	
	E_a (kJ.mole^{-1})	E_a (kcal.mole^{-1})	E_a (kcal.mole^{-1})	Author
k_{CO2}	77.16	18.44	19.000	Gibbons and Edsall, 1963
k_{OH}	20.53	4.91	13.250	Pinsent *et al.*, 1956
k_d	65.91	15.75	16.900	Daziel, 1953, Sirs, 1958a, b
k_{HCO3-}	63.89	15.27	-	

dehydroxylation reactions have been calculated and are given in *TABLE* 2.3 along with the activation energies determined in previous studies. The agreement between the activation energies calculated using the data determined by Johnson (1982) and previous studies is generally adequate, although the comparison is particularly poor for the hydroxylation reaction. By comparing the plots used to calculate the activation energy of the reaction from Johnson's data with that of Pinsent *et al.* (1956) it is apparent that the difference between the calculated activation energies could be at least partly attributed to the non-linearity of Johnson's data. The non-linearity may either reflect some error in the determination of k_{OH} by Johnson (1982) or it maybe due to changes in the frequency factor (eqn. 2.35) with temperature (Laidler, 1965).

Using the calculated activation energies it is possible to represent schematically the changes in potential energy that occur during the hydration / dehydration and the hydroxylation / dehydroxylation reactions (*FIGURE* 2.7). The zero - point energy levels for HCO_3^- and $HCO_3^- + H^+$ are coincident because H^+ is not thermodynamically different from elemental hydrogen and therefore the Gibbs free energy of formation of H^+ is zero. The diagram clearly demonstrates how the energetics of each reaction mechanism differ.

The reaction between HCO_3^- and CO_3^{2-} cannot be interpreted using the transition state theory because as the appropriate rate constants have not been determined.

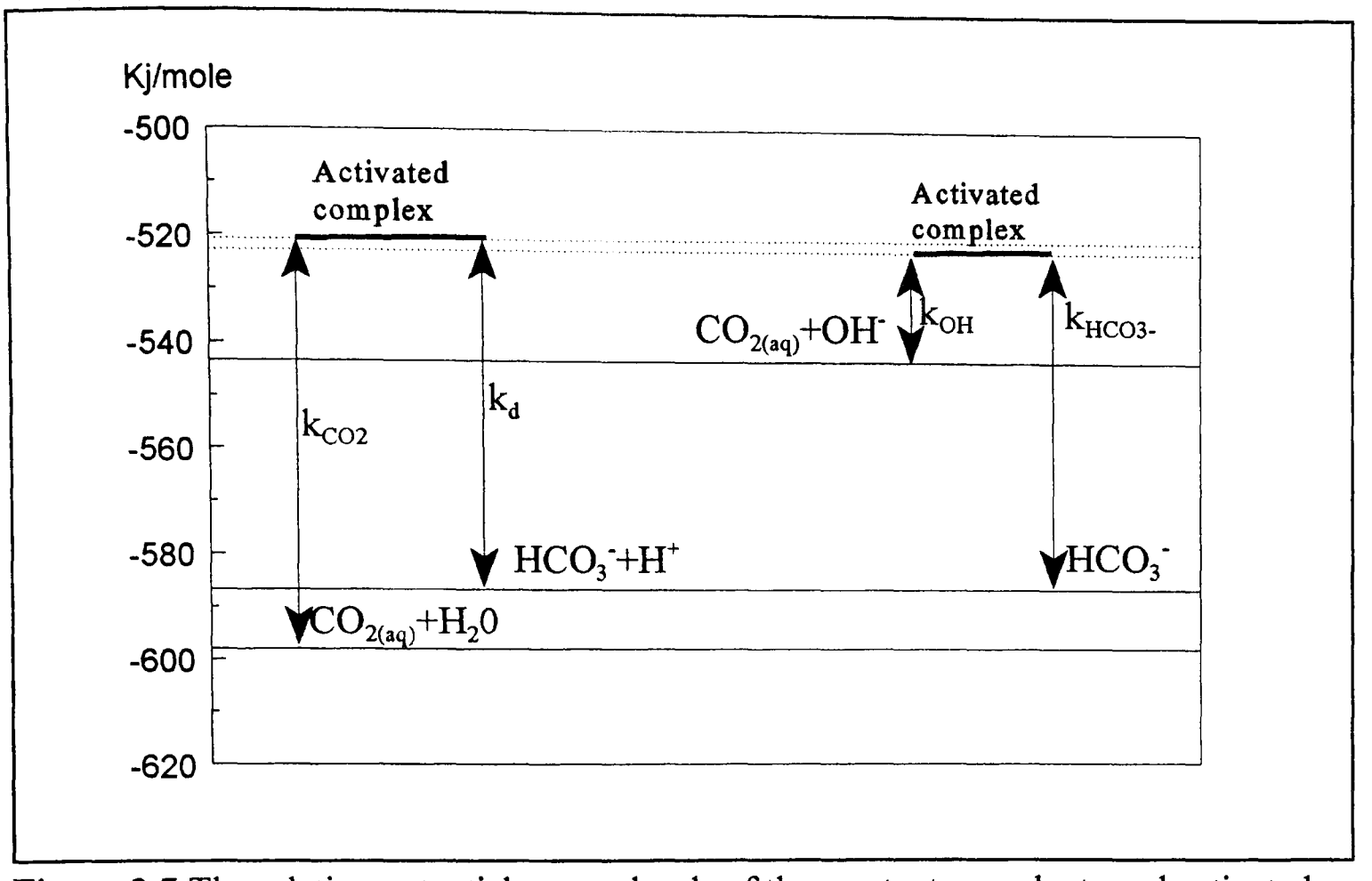

Figure 2.7 The relative potential energy levels of the reactants, products and activated complexes participating in the hydration / dehydration and hydroxylation / dehydroxylation reactions

2.6 Summary

The main aim of this chapter has been to generally describe the basic chemistry of the ΣCO_2 from the viewpoints of thermodynamic, kinetics and transition state theory. Specifically it has outlined some of the approaches and methods used to determine and calculate the concentrations of $CO_{2(aq)}$, HCO_3^- and CO_3^{2-} within the marine environment and has introduced the different activity and pH scales which can be used. It has also highlighted the controlling role pH plays in the determination of the relative concentrations of the various species within the ΣCO_2 system.

Another aim of the chapter has been to emphasise the importance of the different reaction mechanisms between $CO_{2(aq)}$ and HCO_3^- and how these distinctly different pathways of interconversion may be studied using the theories of thermodynamic, kinetics and transition state theory. The important fact that the rates of the hydration, dehydration,

hydroxylation and dehydroxylation reactions are different and that the relative contribution to the overall rate of the forward and reverse reaction varies with pH has been discussed.

This final point maybe of particular importance when studying the uptake of $CO_{2(aq)}$ by phytoplankton and ultimately, with respect to this thesis, the variation in the isotopic composition of the phytoplankton. This is because the photosynthetic removal of $CO_{2(aq)}$ will increase the pH of the bulk medium and more importantly the pH within the boundary layer around an individual cell and within it. As an increase in pH favours the slower dehydroxylation pathway and decreases the $[CO_{2(aq)}]$ the supply of $CO_{2(aq)}$ to the cell by diffusion will be reduced and hence the disequilibrium between the cell and in the bulk medium will be increased.

Chapter 3: Isotope Theory

3.1 Introduction

Isotope studies are normally concerned with the partitioning of isotopes between different pools and understanding the factors and processes (biological, chemical, or physical) controlling their distribution (Bigeleisen, 1965). Chemical isotope effects, as opposed to physical isotope effects (*e.g.* evaporation and diffusion), can be divided into two distinct groups (Owens, 1987, Broecker and Oversby, 1971):

i. Equilibrium isotope effects - The distribution of isotopes between the reactant and product pools of a chemical reaction at equilibrium.

ii. Kinetic isotope effects - Changes in the isotopic composition of the reactant and product pools during an irreversible chemical reaction.

However, from a chemical viewpoint, equilibria may be described either on a thermodynamic or a kinetic basis and the term "kinetic", as applied by physical chemists, need not necessarily apply to irreversible chemical reactions. Similarly, the above classification scheme does not account for the important group of reversible chemical reactions which are not at equilibrium. Therefore in order to avoid confusion, and to maintain consistency, the terms "kinetic" and "kinetic isotope effects" will be used when discussing isotope effects within the context of chemical kinetics and will include both reversible and irreversible chemical reactions.

The main aims of this section are to define the basic terminology associated with isotope studies and to discuss isotope theories from both a thermodynamic and kinetic viewpoint.

3.2 Definitions

Two stable isotopes of carbon exist, ^{12}C and ^{13}C, ^{12}C accounts for 98.89% of all carbon and ^{13}C for 1.11% (Fritz and Fontes, 1980, Ehleringer and Rundel, 1988). Although it is difficult to routinely determine the absolute abundance of isotopes in a sample, small differences in the isotopic ratio of two compounds can be determined with great accuracy and precision

using a dual inlet, triple collecting mass spectrometer, such as the V. G. Isogas SIRA II used during this study. Due to the technical problems associated with the determination of absolute abundances (Mariotti *et al.*, 1981), isotope ratios are normally expressed relative to a standard using the "δ" notation, where, for carbon:

$$\delta^{13}C_Y = \frac{R_Y - R_{standard}}{R_{standard}} = \frac{R_Y}{R_{std}} - 1 \qquad \textbf{(3.1)}$$

where R_Y and $R_{standard}$ are the carbon isotope ratios ($^{13}C/\ ^{12}C$) of the sample and standard respectively. The international standard for carbon is a fossilised Belemnite from the PeeDee formation in Southern Carolina (Craig, 1953) and the ratio of $^{13}C/^{12}C$ is taken as 11237.2 $\pm 9\times10^{-6}$ (Ehleringer and Rundel, 1989). As natural variations in the relative abundances of ^{13}C and ^{12}C are small, a common convention is to express the δ value in parts per thousand or per mil (‰) (Mariotti *et al.*, 1981):

$$\delta^{13}C_Y(‰) = \delta^{13}C_Y \times 1000 \qquad \textbf{(3.2)}$$

The relative partitioning of isotopes between different pools is normally quantified by expressing the distribution as an abundance ratio which is usually termed the fractionation factor, α, where:

$$\alpha_{Z/Y} = \frac{R_Z}{R_Y} \qquad \textbf{(3.3)}$$

where Y and Z are the reactant (substrate) and product pools respectively. Alternatively, the fractionation factor may also be expressed in terms of δ values:

$$\alpha_{Z/Y} = \frac{1000 + \delta^{13}C_Z}{1000 + \delta^{13}C_Y} \qquad \textbf{(3.4)}$$

However, the above definitions are not set by convention and some workers define $\alpha_{z/y}$ as R_y / R_z (*e.g.* Fritz and Fontes, 1980).

As isotope effects are often small (except for those associated with the lighter elements, *e.g.* H), the fractionation factor is normally close to unity and usually only varies in the second or third decimal place. As a result, it is often more convenient to express the difference between the isotopic composition of two pools as an enrichment factor:

$$\epsilon_{Z/Y}(‰) = (\alpha_{Z/Y} - 1) \times 1000 \qquad \textbf{(3.5)}$$

which may also be defined as follows (Mariotti *et al.*, 1981):

$$\epsilon_{Z/Y} = \frac{\delta^{13}C_Z - \delta^{13}C_Y}{1 + (\delta^{13}C_Y / 1000)} \qquad \textbf{(3.6)}$$

As the term in parenthesis is normally small (*i.e.* $\delta^{13}C_Y << 1000$), the equation can be reduced to:

$$\epsilon_{Z/Y} \approx \delta^{13}C_Z - \delta^{13}C_Y \qquad \textbf{(3.7)}$$

The enrichment factor may also be referred to as the discrimination (*e.g.* O'Leary, 1981) or isotope separation factor (Fritz and Fontes, 1980).

3.3 A Thermodynamic Approach to Equilibrium Isotope Effects

Isotope effects arise because of slight differences in the behaviour of isotopes of the same element (Bigeleisen, 1965). In the context of thermodynamics the slight variations in behaviour may be attributed to differences in the free energy and hence internal energy (heat capacity and entropy) of the different isotopic species (Broecker and Oversby, 1971). Equilibrium isotope effects have been successfully predicted using statistical mechanics (*e.g.* Bigeleisen and Mayer, 1947, Bigeleisen, 1965, Bigeleisen *et al.*, 1973) and using this

approach, isotope effects have been mainly attributed to the effect of an additional neutron on the atomic or molecular vibrations (Bigeleisen, 1965). The substitution of a heavy isotope, in place of a lighter isotope, will decrease the vibrational frequency of that molecule (see section 3.5) (Broecker and Oversby, 1971).

Equilibrium isotope effects, for single isotopes, are normally considered in terms of exchange reactions, *e.g.*:

$$Z + {}^{*}Y \leftrightharpoons {}^{*}Z + Y \qquad \textbf{(3.8)}$$

where Z and Y are compounds which include an element that exists in two isotopic forms and * indicates the presence of the heavier isotope. The equilibrium constant for the above reaction may be expressed as follows:

$$K = \frac{[{}^{*}Z][Y]}{[Z][{}^{*}Y]} \qquad \textbf{(3.9)}$$

By rearranging the above expression it becomes apparent that the equilibrium fractionation factor is the same as the equilibrium constant for an isotope exchange reaction (Fritz and Fontes, 1980):

$$K = \frac{[{}^{*}Z]/[Z]}{[{}^{*}Y]/[Y]} = \frac{R_Z}{R_Y} = \alpha_{Z/Y} \qquad \textbf{(3.10)}$$

In the same way as equilibrium constants, fractionation factors are also affected by temperature. The effect of temperature can be predicted by either using the principles of thermodynamics (Broecker and Oversby, 1971) or statistical mechanics (*e.g.* Thode *et al.*, 1965). It has been found that α is normally correlated to the absolute temperature (T) by a polynomial relationship of the form (Fritz and Fontes, 1980):

$$1000 \times \ln \alpha = A + B \times T^{-1} + C \times T^{-2} \qquad \textbf{(3.11)}$$

where A, B and C are constants. Within small ranges, at low temperatures, variations in the fractionation factor can be described by a simple linear relationship (Fritz and Fontes, 1980):

$$1000 \times \ln \alpha = A + B \times T^{-1} \quad \textbf{(3.12)}$$

When considering an isotope exchange reaction at equilibrium, it may be conceptually clearer to consider the distribution of each isotope independently. For example, the exchange reaction previously considered (eqn. 3.8) can be written as follows:

$$X + Y \leftrightharpoons Z \quad \textbf{(3.13)}$$

$$X + {}^{*}Y \leftrightharpoons {}^{*}Z \quad \textbf{(3.14)}$$

Therefore, as both isotopes behave independently, the following mass balance expressions may be written to describe the equilibrium distribution of each isotope:

$$K_i = \frac{[Z]}{[X][Y]} \quad \textbf{(3.15)}$$

$$K_i^{*} = \frac{[{}^{*}Z]}{[X][{}^{*}Y]} \quad \textbf{(3.16)}$$

where K_i and K_i^{*} are termed the isotope specific equilibrium constants. Furthermore, it can be shown that the fractionation factor is equal to the ratio of the isotope specific equilibrium constants:

$$\frac{K_i^*}{K_i} = \frac{\left(\frac{[^*Z]}{[X][^*Y]}\right)}{\left(\frac{[Z]}{[X][Y]}\right)} \tag{3.17}$$

$$= \frac{[^*Z]}{[X][^*Y]} \times \frac{[X][Y]}{[Z]} \tag{3.18}$$

$$= \frac{[^*Z]}{[Z]} \times \frac{[Y]}{[^*Y]} \tag{3.19}$$

$$= \frac{[^*Z]/[Z]}{[^*Y]/[Y]} = \alpha_{Z/Y} \tag{3.20}$$

and hence

$$\alpha_{Z/Y} = \frac{K_i^*}{K_i} \tag{3.21}$$

Therefore the equilibrium fractionation factor can be viewed as a ratio of the isotope specific equilibrium constants and variations in the fractionation factor with temperature can be attributed to small differences in the response of the isotope specific equilibrium constants to a temperature change.

The effect of ionic strength on the fractionation factor does not appear to have been investigated in detail. The only study to have been conducted (Thode *et al.*, 1965) found that the fractionation factors were dependent on the strength and composition of the ionic medium. As discussed in the preceding chapter, the equilibrium constant for a reaction, defined on the ionic medium activity scale, is partly dependent on the ionic strength of the

medium. Therefore, the isotope specific equilibrium constants may also be expected to be affected by the ionic strength of the medium. If changes in K and $^*K$ with ionic strength do occur, and if the changes are not proportional to each other, the fractionation factor will also change.

An attempt is made in the subsequent chapter to investigate theoretically the effect of ionic strength on the fractionation factors relating to the ΣCO_2.

3.4 A Kinetic Approach to Equilibrium and Non-Equilibrium Isotope Effects

3.4.1 Introduction

Unlike a thermodynamic approach, a description of isotope effects from the viewpoint of chemical kinetics can theoretically account for the distribution of isotopes under conditions of equilibrium, disequilibrium, steady state and during an irreversible chemical reaction. Therefore, although kinetic isotope data can be more difficult to obtain and more complex to apply, a kinetic approach may be used to understand a wider variety of natural situations without the need for thermodynamic assumptions which may introduce errors.

3.4.2 A Kinetic Approach to Equilibrium Isotope Effects

The hypothetical reaction previously discussed may be written as follows for each isotope, in the terms of chemical kinetics:

$$X + Y \underset{k_r}{\overset{k_f}{\rightleftharpoons}} Z \qquad \textbf{(3.22)}$$

$$X + {}^*Y \underset{k_r^*}{\overset{k_f^*}{\rightleftharpoons}} Z^* \qquad \textbf{(3.23)}$$

where k_f, k_r, k_f^* and k_r^* are the isotope specific rate constants associated with the forward (f) and reverse (r) reactions. By applying the principle of microscopic reversibility to a dynamic chemical reaction at equilibrium, it can be shown that the equilibrium constant is equal to the ratio of the forward and reverse rate constants. If this principle is extended, the equilibrium fractionation factor may be expressed as the ratio of the isotope specific rate constants:

$$\alpha_{Z/Y} = \frac{K^*}{K} = \frac{k_f^* / k_r^*}{k_f / k_r} \qquad \textbf{(3.24)}$$

Similarly, the fractionation factors associated with the forward (α_f) and reverse (α_r) reaction can be expressed in terms of isotope specific rate constants:

$$\alpha_f = \frac{k_f^*}{k_f} \qquad \textbf{(3.25)}$$

$$\alpha_r = \frac{k_r^*}{k_r} \qquad \textbf{(3.26)}$$

and related to the equilibrium fractionation factor:

$$\alpha_{Z/Y} = \frac{\alpha_f}{\alpha_r} \qquad \textbf{(3.27)}$$

Practical use can be made of the above relationship (*e.g.* O'Leary *et al.*, 1992, Marlier and O'Leary, 1984). For example, if the equilibrium fractionation factor and kinetic fractionation

factor associated with the forward reaction are known, the fractionation factor associated with the reverse reaction can be calculated. Alternatively, the above relationship can be used to check the measured fractionation factors associated with the forward and reverse reactions against a previously determined equilibrium fractionation factor (*e.g.* O'Leary *et al.*, 1992, Marlier and O'Leary, 1984).

3.4.3 Non-reversible Chemical Reactions

During an irreversible chemical reaction, the products cannot re-equilibrate with the reactant reservoir as the rate of the reverse reaction is negligible. As the reaction proceeds the isotopic composition of both the reactant and product pools will change as a function of the residual material left and the isotopic fractionation factor (Broecker and Oversby, 1971, Fritz and Fontes, 1980, Mariotti *et al.*, 1981,). Therefore, for the following irreversible reaction:

$$Y \rightarrow Z \qquad \textbf{(3.28)}$$

$$Y^{*} \rightarrow Z^{*} \qquad \textbf{(3.29)}$$

the rate at which Y and $^{*}Y$ change may be expressed as follows (Broecker and Oversby, 1971):

$$\frac{dY^{*}}{dY} = \frac{k_f^{*}}{k_f} \times \frac{[Y^{*}]}{[Y]} = \alpha_f \times \frac{[Y^{*}]}{[Y]} \qquad \textbf{(3.30)}$$

It can be shown (Broecker and Oversby, 1971) that the course of an irreversible reaction obeys a Rayleigh type equation which was derived by Lord Rayleigh to describe the fractional distillation of mixed liquids (Mariotti *et al.*, 1981):

$$R = R_0 \times f^{\alpha-1} \qquad \textbf{(3.31)}$$

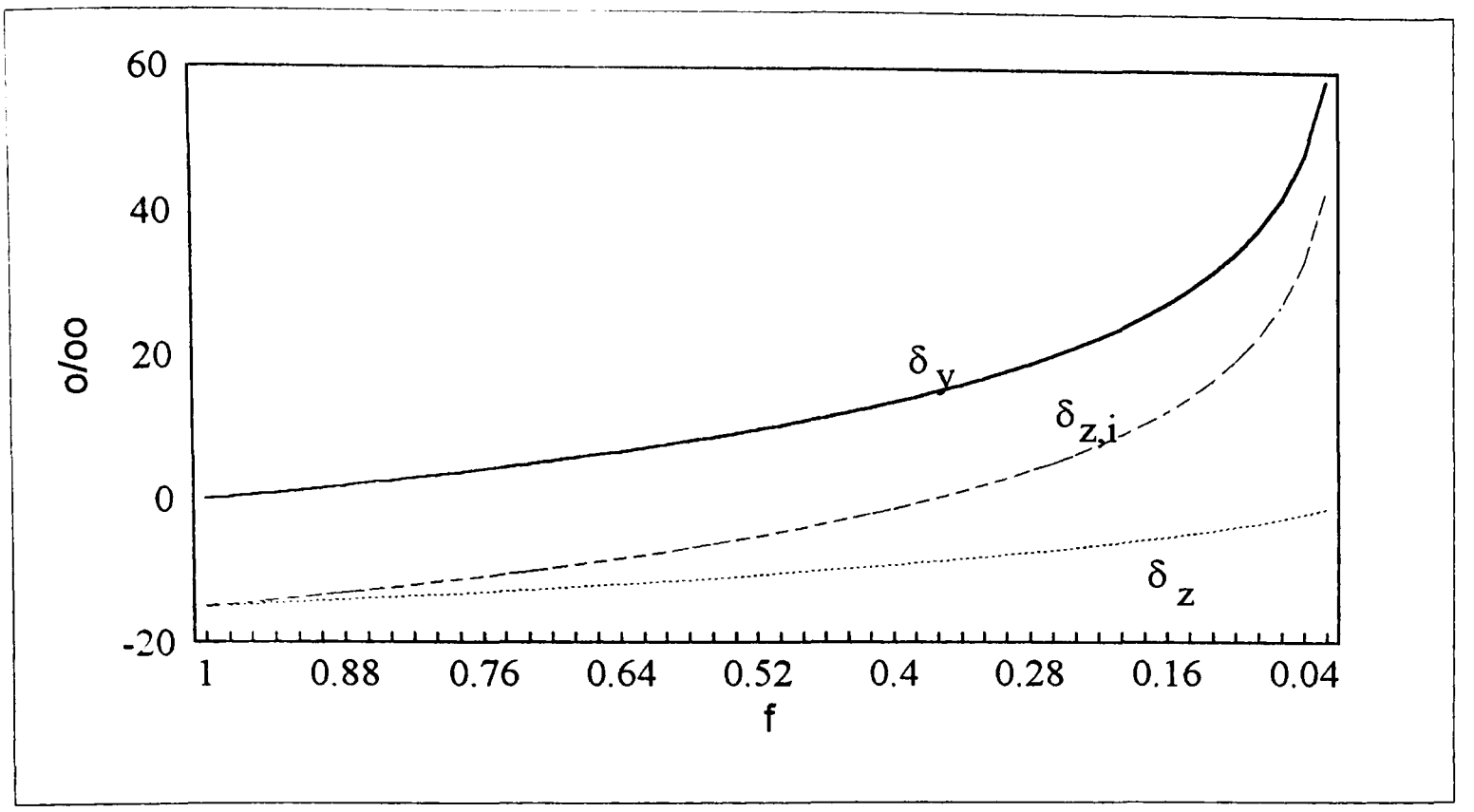

Figure 3.1 Changes in the isotopic composition of the reactant (δ_Y), instantaneous product ($\delta_{Z,i}$) and accumulated product (δ_Z) pools during an irreversible chemical reaction in a closed system, where f is the fraction of the reactant pool remaining and $\epsilon_{Z/Y}$ =-15‰.

Where R and R_0 are the isotope ratios of the reactant pool at time t and time zero respectively and f is the fraction of the reactant pool remaining at time t (Broecker and Oversby, 1971, Fritz and Fontes, 1981, Mariotti *et al.*, 1981). Changes in the isotopic composition of the reactant, accumulated product and instantaneous product pools during a reaction may be modelled using the derived equations given below (Mariotti *et al.*, 1981):

$$\delta_Y = (\epsilon_{Z/Y} \times \ln f) + \delta_{Y,0} \qquad \textbf{(3.34)}$$

$$\delta_{Z,i} \approx \delta_Y + \epsilon_{Z/Y} \qquad \textbf{(3.32)}$$

$$\delta_Z = \delta_{Y,0} - \epsilon_{Z/Y} \times \left(\frac{f \times \ln f}{1 - f} \right) \qquad \textbf{(3.33)}$$

where δ_Y, δ_Z, $\delta_{Y,0}$ and $\delta_{Z,0}$ are the isotopic composition of the reactant (Y) and accumulated product (Z) pools at time t and t_0 respectively, $\delta_{Z,i}$ is the instantaneous product and $\epsilon_{Z/Y}$ is

the enrichment factor. Equation 3.33 is a simplified relationship which holds for $\epsilon < \pm 20‰$ and $\delta_{y,0} \approx 0$, however, under more extreme conditions the following form should be applied (Mariotti *et al.*, 1981):

$$\epsilon_{Z/Y} = \frac{1000 \times \ln\left(\frac{10^{-3} \times \delta_Y + 1}{10^{-3} \times \delta_{Y,0} + 1}\right)}{\ln f} \qquad \textbf{(3.35)}$$

FIGURE 3.1 illustrates how the isotopic composition of the reactant, accumulated product and instantaneous product change during an irreversible chemical reaction as it goes to completion. It is important to note that the isotopic composition of the accumulated product pool at the end of the reaction is equal to the isotopic composition of the reactant pool at t_0.

3.5 Isotope Effects and the Transition State Theory

During an irreversible chemical reaction the isotopic composition of the product pool is normally preferentially enriched with the lighter isotope (Broecker and Oversby, 1971, O'Leary *et al.*, 1992). If a reversible reaction is considered, the isotope effect associated with the forward and reverse reactions would show a similar enrichment (*i.e.* $\alpha_f < 1$ and $\alpha_r < 1$).

The factors leading to the preferential enrichment of the lighter isotope in the product reservoir may be best illustrated by considering the effect in the terms of the transition state theory using the hypothetical reaction discussed previously. *FIGURE* 3.2 illustrates the important features of the transition state theory which control the distribution of isotopes between the reactant and product reservoirs during a reversible reaction.

Isotopic substitution changes the vibrational frequency of a molecule (Bigeleisen, 1949, Bigeleisen, 1965, Broecker and Oversby, 1971) and as the vibrational frequency depends inversely on the masses of the atoms in the molecule (Bigeleisen, 1965) the substitution of a heavy isotope in place of its lighter counterpart will reduce the vibrational frequency. As the zero-point energy of a molecule is dependent on the vibrational frequency,

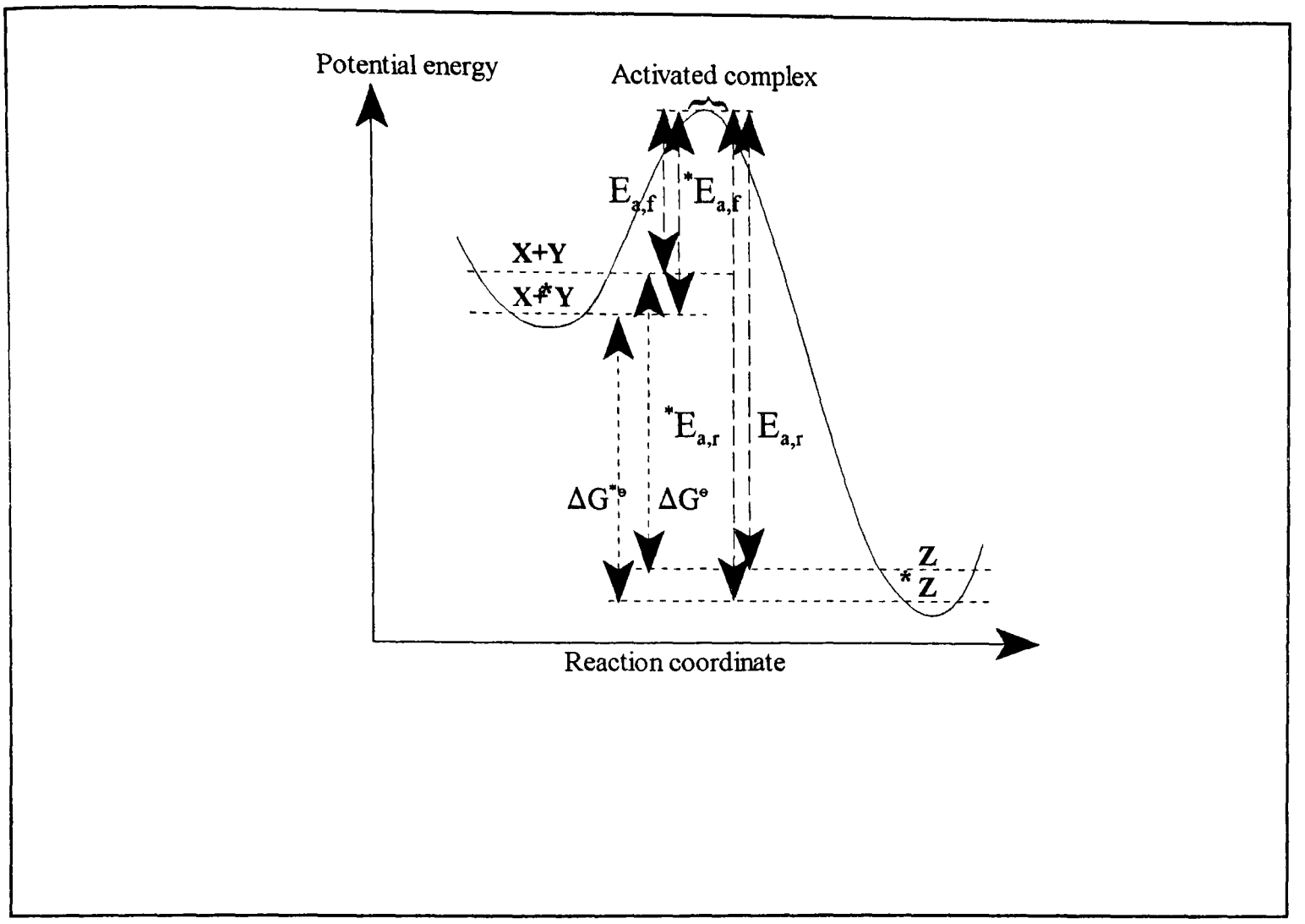

Figure 3.2 Isotope effects and the transition state theory during a reversible chemical reaction (eqns. 3.13 and 3.14). The dashed, horizontal lines represent the isotope specific zero-point energy levels. The zero-point energy levels of the heavier isotopic species (*) is lower than its lighter counterpart and therefore the activation energy associated with the heavier isotope is larger.

the lower vibrational frequency of the heavier isotope will decrease the zero-point energy. Although isotopic substitution influences the zero-point energy of a molecule (*FIGURE* 3.2), it does not normally alter the whole reaction profile (Laidler, 1965) and this has been attributed to the fact that the relevant vibration in the activated complex has a very low force constant (Atkins, 1994). Therefore, the substitution of a lighter isotope by its heavier counterpart decreases the zero-point energy and hence increases the activation energy (*FIGURE* 3.2) and according to the equation given by Arrhenius, an increase in activation energy decreases the rate constant (eqn. 2.35).

The fractionation factor associated with the forward reaction may therefore be related to the isotope specific activation energies using a classical Arrhenius approach:

$$\alpha_f = \frac{k_f^*}{k_f} = \frac{\theta \times e^{-{}^*E_{a,f}/R\times T}}{\theta \times e^{-E_{a,f}/R\times T}} \qquad \textbf{(3.36)}$$

A similar expression can be written for the reverse reaction.

It may therefore be possible to qualitatively predict relative isotope effects associated with the forward and reverse reactions during a dynamic chemical reaction. If the activation energy of a reaction is large, it may generally be expected that the isotope effect would be small because the relative differences in the isotope specific activation energies would be small in relation to the activation energy. For example, in the hypothetical example illustrated in *FIGURE* 3.2, the fractionation factor associated with the forward reaction would be expected to be larger than the fractionation associated with the reverse reaction. However, if the activation energy of the forward and reverse reactions are similar, the relative differences in energy between the isotope specific zero-point energies will be increasingly important in determining the relative isotope effects of the forward and reverse reactions making any qualitative predictions less reliable.

The relationship between the theories of thermodynamics and kinetics can be well illustrated by applying the transition state theory (*CHAPTER* 2). A similar approach may also be used when considering the distribution of isotopes in a system at equilibrium. *FIGURE* 3.2 also illustrates the relationship between the isotope specific activation energies and the isotope specific Gibbs free energy change ($\Delta G^{\ominus}$ and $\Delta G^{\ominus *}$) associated with the reaction. It is therefore possible to relate the equilibrium fractionation factors to either the isotope specific rate constants or the isotope specific Gibbs free energy change as follows:

$$\alpha_{Z/Y} = \frac{k_f^*}{k_r^*} \times \frac{k_r}{k_f} = \exp\left(\frac{-\Delta G^{\ominus *}}{R \times T}\right) \times \exp\left(\frac{-\Delta G^{\ominus}}{R \times T}\right) \qquad \textbf{(3.37)}$$

The isotope specific equilibrium constants can be calculated from $\Delta G^{\ominus}$ and $\Delta G^{\ominus *}$ using eqn.

2.20.

Therefore, the interpretation of isotope effects in terms of the transition state theory ultimately allows the principle factors governing equilibrium and non-equilibrium isotope effects (*i.e.* vibrational frequencies and isotope specific activation energies) to be understood and illustrates the relationship between the alternative approaches of thermodynamics and kinetics.

3.6 Summary

The main aims of this chapter have been to introduce and define the basic terminology associated with isotope studies in general, and more specifically, with reference to ^{12}C and ^{13}C. In addition, the factors controlling the distribution of isotopes from the viewpoints of thermodynamics, kinetics and transition state theory have been discussed.

It has been demonstrated that equilibrium fractionation factors can be directly related to the isotope specific equilibrium constants for a particular reaction, and ultimately, through the kinetic and transition state theories to the isotope specific rate constants and isotope specific activation energies. Despite the inter relationship between the different theories it is again important to stress that thermodynamics can only be used to study isotope effects under conditions of equilibrium. If steady state, non-equilibrium or irreversible isotope reaction are to be studied it is necessary to use a kinetic approach. This point is discussed latter in the thesis, in *CHAPTERS* 7 and 8, where equilibrium models have been used to try and interpret isotope effects observed during the uptake of inorganic carbon by phytoplankton.

A Rayleigh distillation model has also been discussed. The use of this model allows changes in the isotopic composition of the reactant, product and instantaneous product pools to be predicted during an irreversible chemical reaction. However, it is also important to note that the equations given are simplified derivations and therefore caution must exercised to ensure that they are not used to study situations where they are not applicable, for example, if the enrichment factor is >20‰ (*e.g.* Mariotti *et al.* 1981).

Chapter 4: The Effect of Temperature, Salinity and pH on the Distribution of ^{13}C and ^{12}C within the ΣCO_2 System in the Marine Environment - A Review

4.1 Introduction

Due to the biochemical and geochemical importance of the ΣCO_2 system it is important understand the factors and processes that control the distribution of ^{12}C and ^{13}C between the various species of inorganic carbon within the ΣCO_2 pool under equilibrium and non-equilibrium conditions.

Many studies have been conducted to determine the effect of temperature (*e.g.* Thode *et al.*, 1965, Deuser and Degens, 1967, Wendt, 1968, Vogel *et al.*, 1970, Mook *et al.*, 1974, Zhang *et al.*, 1995) on the isotopic fractionation of carbon between $CO_{2(g)}$, $CO_{2(aq)}$, HCO_3^- and CO_3^{2-}. However, the only study which has been conducted to examine the effect of ionic strength and composition on the fractionation of isotopes within the ΣCO_2 system (Thode *et al.*, 1965) suggests that the fractionation factors are affected by both the ionic strength and composition of the medium. Therefore the application of fractionation factors, derived in distilled water, to study the distribution of ^{12}C and ^{13}C in sea water maybe incorrect and lead to errors when calculating the isotopic composition of the different forms of ΣCO_2 (*e.g.* Zhang *et al.*, 1995). Furthermore, it is suggested that the equilibrium and kinetic fractionation factors associated with hydration / dehydration and hydroxylation / dehydroxylation reactions maybe different and hence dependent on the pH of the medium.

This section will review the existing kinetic and thermodynamic data relating to the fractionation of isotopes within the ΣCO_2 system and investigate the theoretical possibility of isotope effects which are dependent on the pH or ionic strength of the solution in the context of thermodynamics.

4.2 A Thermodynamic Approach to the Fractionation of Isotopes within the ΣCO_2 System

4.2.1 Introduction

The use of stable isotopes to study the distribution and flow of material between separate reservoirs normally requires information about the isotopic composition of the different pools. However, due to the dynamic chemistry of the ΣCO_2 system only the isotopic composition of the ΣCO_2 pool can be measured directly ($R_{\Sigma CO2}$). As previously discussed, a similar problem exists when information about the concentrations of $CO_{2(aq)}$, HCO_3^- and CO_3^{2-} is required. The problem can be overcome by applying thermodynamic principles thus allowing the equilibrium concentrations $CO_{2(aq)}$, HCO_3^- and CO_3^{2-} to be calculated from a few observables. Similarly, a thermodynamic approach may be adopted when calculating the isotopic composition of the different forms of dissolved inorganic carbon. However, the isotope specific equilibrium constants which are normally expressed as fractionation factors, applicable to the thermodynamic state of the system must also be known, along with the $R_{\Sigma CO2}$. The equation given below summarises the isotopic mass balance of the ΣCO_2 system:

$$R_{\Sigma CO2} \times [\Sigma CO_2] = R_a \times [a] + R_b \times [b] + R_c \times [c] \qquad \textbf{(4.1)}$$

To aid clarity the terms: $CO_{2(aq)}$, HCO_3^- and CO_3^{2-} have been replaced by a, b and c respectively. The fractionation factors between $CO_{2(aq)}$ - HCO_3^- and HCO_3^- - CO_3^{2-} can be defined as follows:

$$\alpha_{b/a} = \frac{R_b}{R_a} \qquad \textbf{(4.2)}$$

By using equation 4.1 in conjunction with eqns. 4.2 and 4.3, a mass balance expression may

$$\alpha_{c/b} = \frac{R_c}{R_b} \tag{4.3}$$

be derived, written in terms of R_b:

$$R_{\Sigma CO2} \times [\Sigma CO_2] = \left(\frac{R_b \times [a]}{\alpha_{b/a}} \right) + (R_b \times [b]) + (R_b \times \alpha_{c/b} \times [c]) \tag{4.4}$$

By rearrangement an expression can be obtained to calculate R_b if $R_{\Sigma CO2}$, $[CO_{2(aq)}]$, $[HCO_3^-]$ and $[CO_3^{2-}]$ are known:

$$R_b = \frac{R_{\Sigma CO2} \times [\Sigma CO_2]}{\frac{[a]}{\alpha_{b/a}} + [b] + (\alpha_{c/b} \times [c])} \tag{4.5}$$

Similar expressions may also be obtained for R_a and R_c:

$$R_a = \frac{R_{\Sigma CO2} \times [\Sigma CO_2]}{[a] + (\alpha_{b/a} \times [b]) + (\alpha_{c/b} \times \alpha_{b/a} \times [c])} \tag{4.6}$$

$$R_c = \frac{R_{\Sigma CO2} \times [\Sigma CO_2]}{\frac{[a]}{\alpha_{c/b} \times \alpha_{b/a}} + \frac{[b]}{\alpha_{c/b}} + [c]} \tag{4.7}$$

In order to make use of the above expressions it is necessary to know the fractionation factors, $\alpha_{b/a}$ and $\alpha_{c/b}$, and how they vary in relation to the thermodynamic state of the system. However, as it is not possible to measure the isotopic composition of the

different forms of ΣCO_2 directly the fractionation factors are usually determined with respect to the isotopic composition of CO_2 in gaseous phase.

The subsequent sections review the existing thermodynamic data and discuss and calculate the possible effect of ionic strength on the fractionation factors and how $\alpha_{b/a}$ and $\alpha_{c/b}$ maybe affected by the pH of the medium.

4.2.2 The $CO_{2(g)}$ - $CO_{2(aq)}$ Equilibrium

The isotopic fractionation between $CO_{2(g)}$ and $CO_{2(aq)}$ is normally determined in an acidified solution in which the ΣCO_2 is solely comprised of $CO_{2(aq)}$. The two phases are allowed to reach isotopic equilibrium after which the isotopic composition of the phases, R_a and R_g (where g represents $CO_{2(g)}$), are measured thus allowing the fractionation factor, $\alpha_{a/g}$, to be directly calculated:

$$\alpha_{a/g} = \frac{R_a}{R_g} \qquad \textbf{(4.8)}$$

The isotopic fractionation associated with the equilibrium between $CO_{2(g)}$ - $CO_{2(aq)}$ is small (Vogel, 1960, Thode *et al.*, 1964, Wendt, 1968, Vogel *et al.*, 1970, Zhang *et al.*, 1995) in comparison with the fractionation factor associated with the equilibrium between $CO_{2(aq)}$ and HCO_3^-(see section 4.2.3). Early measurements indicated the preferential enrichment of ^{12}C in the aqueous phase (*e.g.* Vogel, 1960, $\alpha_{a/g}$=0.9995 ± 0.0002, $\epsilon_{a/g}$=-0.5‰ (reported in Wendt, 1968, temperature not given), Wendt, 1968, $\alpha_{a./g}$=0.9994 ± 0.0009, $\epsilon_{a/g}$=-0.6‰ (7°C)) and this "unusual" isotope effect (O`Leary *et al.*, 1992) was subsequently confirmed by the high precision measurements of Vogel *et al.* (1970). This reversal of the "normal" isotope effect has been attributed to the binding energy term of the molecule containing the lighter isotope outweighing the extra vibrational degree of freedom, associated with dissolution, which normally favours the heavier isotope (Vogel *et al.*, 1970).

Thode *et al.* (1964) have attempted to predict $\alpha_{a/g}$ in relation to temperature using statistical mechanics to calculate the partition coefficients from experimentally determined vibrational frequencies. However, the published results, given as K_0 by Thode *et al.* (1964), appear to predict the preferential enrichment of ^{13}C in the aqueous phase (*i.e.* K_0=1.0008).

Table 4.1 Linear and second order polynomial expressions of the form given in eqns. 3.11 and 3.12 have been fitted to the results of previous studies by minimising the residual sum of squares (RSS). The calculated constants are given below along with the calculated standard errors. Linear regressions were only employed where there was insufficient data to perform a polynomial regression (Wendt, $\alpha_{b/g}$, Zhang *et al.* , $\alpha_{a/g}$ and $\alpha_{b/g}$) or where the data was too scattered to justify a polynomial regression (Zhang *et al.*, $\alpha_{c/g}$).

Author	Fractionation factors	Constants:			Temperature range (°C)	No. of data points	RSS
		A	B	C			
Vogel *et al.* (1970)	$1000.\ln\alpha_{a/g}$	1.93±0.32	-1423±196	1.58×10^{5} $\pm2.9\times10^{4}$	0 - 60	7	4.2×10^{-5}
Zhang *et al.* (1995)	$1000.\ln\alpha_{a/g}$	0.200 $\pm4.6\times10^{-3}$	-414±26	-	5 - 25	4	4.6×10^{-5}
Deuser and Degens (1967)	$1000.\ln\alpha_{b/g}$	95.86±0.84	-5.7×10^{4} $\pm4.8\times10^{4}$	9.1×10^{6} $\pm6.9\times10^{6}$	0 - 30	10	0.645
Wendt (1968)	$1000.\ln\alpha_{b/g}$	-8.26±0.12	5049±674	-	7 - 28	3	1.5×10^{-2}
Mook *et al.* (1974)	$1000.\ln\alpha_{b/g}$	-23.7±1.9	9258 $\pm1.2\times10^{3}$	5.3×10^{4} $\pm2.0\times10^{4}$	5 - 126	36	0.258
Zhang *et al.* (1995)	$1000.\ln\alpha_{b/g}$	-23.496 $\pm2.3\times10^{-2}$	9.37×10^{3} $\pm1.3\times10^{2}$	-	5 - 25	4	1.1×10^{-3}
Thode *et al.* (1965)	$1000.\ln\alpha_{c/g}$	-28.5±2.2	1.25×10^{4} $\pm1.3\times10^{3}$	-5.3×10^{5} $\pm1.9\times10^{5}$	0 - 50	19	7.8×10^{-3}
Zhang *et al.* (1995)	$1000.\ln\alpha_{c/g}$	-7.33±0.45	$4\times10^{3}\pm2\times10^{3}$	-	5 - 25	6	0.8

Furthermore, division of the associated partition coefficients ($Q^{13}_{CO2(g)}/Q^{12}_{CO2(g)}$ by $Q^{13}_{CO2(aq)}/Q^{12}_{CO2(aq)}$) to calculate K_0 gives results which are different from the values of K_0 given alongside in the same table (Table 3, Thode *et al.*, 1964). Therefore as it is not clear how Thode *et al.* (1964) arrived at the results given for the temperature dependence of $\alpha_{a/g}$ their results will not be used.

Vogel *et al.* (1970) appear to have conducted the first experiment to determine how $\alpha_{a/g}$ is affected by temperature (0 to 60°C) (*FIGURE* 4.1). A polynomial expression, of the form given in eqn. 3.11, has been fitted to their results and the calculated constants (A, B and C) are given in *TABLE* 4.1. It is apparent that the degree of fractionation decreases as the temperature increases (*FIGURE* 4.1). The fractionation factor determined

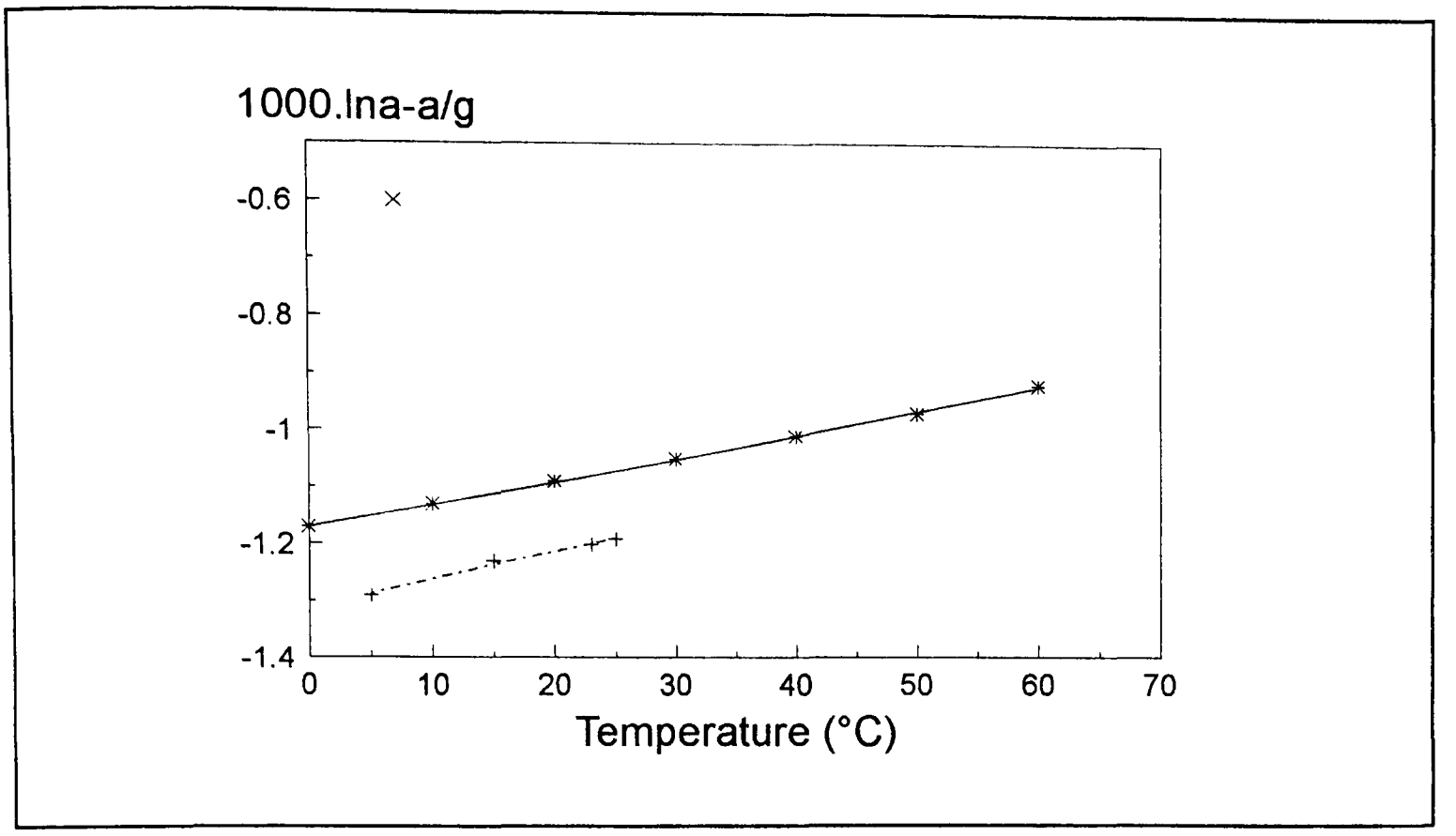

Figure 4.1 The effect of temperature on the fractionation factor $\alpha_{a/g}$ as determined by Wendt (1968) (×), Vogel *et al.* (1970) (*) and Zhang *et al.* (1995) (+). The lines have been fitted to the data by minimising the RSS and the appropriate constants are given in *TABLE* 4.1.

by Vogel *et al.*(1970) is approximately twice as large as the value reported by Wendt (1968).

The recently published results of Zhang *et al.* (1995), who have comprehensively redetermined the fractionation factors associated with the ΣCO_2 system, are given alongside the results of Wendt (1968) and Vogel *et al.* (1970) in *FIGURE* 4.1. A linear expression of the form given in eqn. 3.12 was fitted to their results (*FIGURE* 4.1) and the calculated constants (A and B) are given in *TABLE* 4.1. A comparison of the results of Zhang *et al.* (1995) with those of Vogel *et al.* (1970) indicate that although the slopes are similar to the results of Zhang *et al.* (1995) are ~0.1‰ more negative. Neither the results of Vogel *et al.* (1970) nor Zhang *et al.* (1995) agree with the earlier determination of Wendt (1968). As pointed out by Zhang *et al.* (1995), the difference between the various studies is unlikely to be inter-laboratory offset as $\alpha_{a/g}$ depends on relative measurements, and is more likely to be caused by a difference between the experimental methods.

Due to the dynamic nature of the ΣCO_2 system the isotopic effects associated with the different species are normally determined relative to the isotopic composition of $CO_{2(g)}$. In order to separately measure the equilibrium isotopic composition of the gaseous and

aqueous phases the two phases must be separately sampled without disturbing the equilibrium. Two main methods have been employed to separately sample the two phases:

i. Quickly freezing the aqueous phase to allow the gaseous phase to be removed (*e.g.* Vogel *et al.*, 1970).

ii. Removing the gas phase sufficiently quickly to ensure the equilibrium distribution of isotopes between the two phases is not significantly altered (Zhang *et al.*, 1995).

Both these techniques assume that the disturbance to the equilibrium distribution of isotopes is minimal. Errors in this assumption maybe at least partly responsible for the small variations between the different data sets. An additional source of error maybe related to the extraction and purification of the CO_2 from the different phases. If the extraction is incomplete, the isotopic composition of the CO_2 which is collected may not reflect the isotopic composition of the sample and as a result the calculated fractionation factor will be incorrect.

The fractionation factor can also be related to the isotope specific equilibrium constants, $^{12}K_0$ and $^{13}K_0$:

$$\alpha_{a/g} = \frac{K_0^{13}}{K_0^{12}} \qquad (4.9)$$

and therefore a decrease in the fractionation factor, as temperature increases, can be interpreted as a decrease in the difference between the isotope specific equilibrium constants.

The chemical equilibrium between $CO_{2(g)}$ and $CO_{2(aq)}$ is dependent on salinity, although only slightly (Weiss, 1974). No investigation appears to have been undertaken to determine if the equilibrium fractionation factor, $\alpha_{a/g}$, is affected by ionic strength, or more specifically the salinity of sea water.

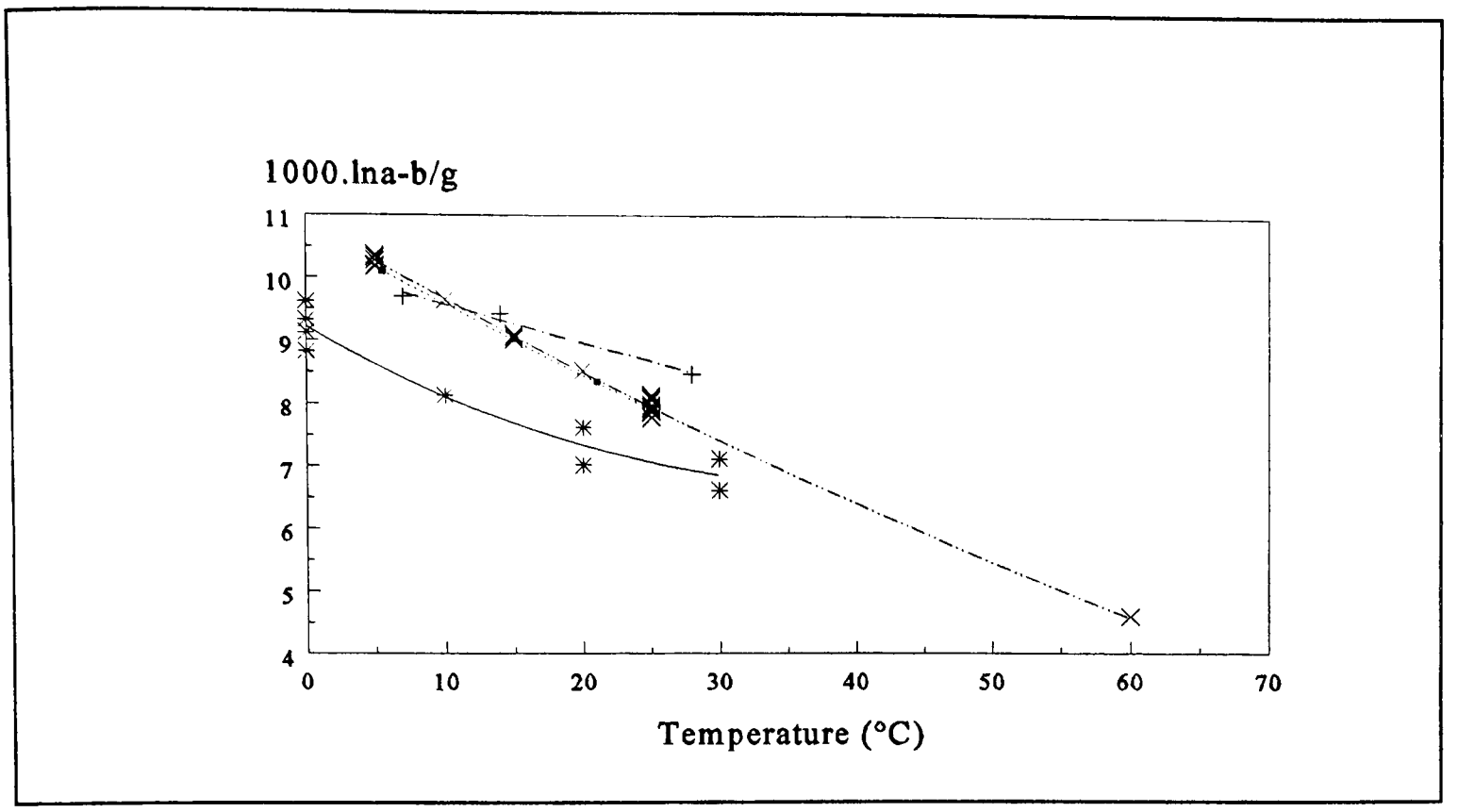

Figure 4.2 The effect of temperature on the fractionation factor $\alpha_{b/g}$ as determined by; Deuser and Degens (1967) (*), Wendt (1968) (+), Mook *et al.* (1974) (×) and Zhang *et al.* (1995) (■). Lines of the form given in eqns. 3.11 and 3.12 have been fitted to the data and the calculated constants are given in *TABLE* 4.1.

The temperature related experimental results of Vogel *et al.* (1970) and Zhang *et al.* (1995) represent the most comprehensive data sets although it not obvious which results are more accurate. The results of Vogel *et al.* (1970) were determined over a greater temperature range (0 to 60°C), contain more data points (7) and are slightly more precise (*i.e.* a lower residual sum of squares) (*TABLE* 4.1). It is for these reasons that the results of Vogel *et al.* (1970) will be used during this study.

4.2.3 The $CO_{2(aq)}$ - HCO_3^- Equilibria

It has long been recognised that the oceanic ΣCO_2 system is enriched in ^{13}C relative to the isotopic composition of atmospheric CO_2 (Reid and Urey, 1943, Craig, 1953, Abelson and Hoering, 1961) and this has been attributed to the relatively large isotope effect (7 to 8‰) associated with the $CO_{2(aq)}$ - HCO_3^- equilibria. Latter studies (Deuser and Degens, 1967, Wendt, 1968, Mook *et al.*, 1974, Lesniak and Sakai, 1989, Zhang *et al.*, 1995) have focussed on improving the accuracy and precision with which this fractionation factor is known as well as determining the effect of temperature over environmental (0 to 40°C) (Deuser and Degens, 1967, Wendt, 1968, Lesniak and Sakai, 1989, Zhang *et al.*, 1995) and geological (5 to 125°C) (Mook *et al.*, 1974) temperature ranges.

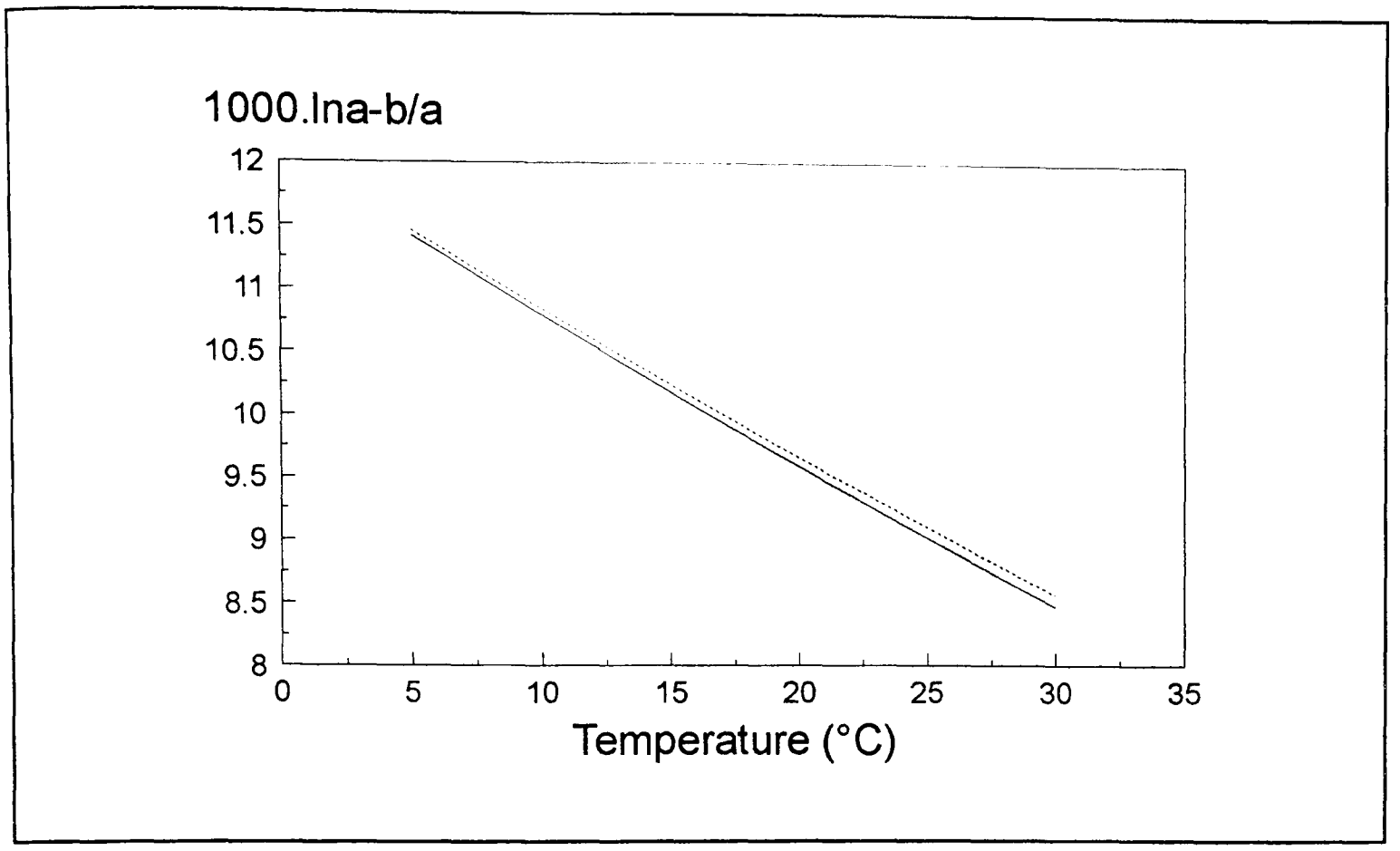

Figure 4.3 The effect of temperature on the fractionation factor $\alpha_{b/a}$ as determined from the studies of Vogel *et al.* (1970) and Mook *et al.* (1974) (solid line) and Zhang *et al.* (1995) (dashed line) using eqn. 4.11. See text for further explanation.

The fractionation factor between $CO_{2(g)}$ and HCO_3^-, from which $\alpha_{b/a}$ can be calculated (see below), is normally determined in solutions of approximately neutral pH to maximise the concentration of HCO_3^-. However, the fractionation factor between $CO_{2(g)}$ and CO_3^{2-} is not well known and to avoid the introduction of errors by using this term, the pH of the solution can be slightly decreased to eliminate CO_3^{2-} and increase the concentration of $CO_{2(aq)}$ which can be accurately corrected for.

The effect of temperature on fractionation factors can normally be described by a second order polynomial expression (eqn. 3.11) (Fritz and Fontes, 1981). However, different studies have used a variety of different expressions to describe their results and, as a consequence, it is often difficult to compare the results of different studies. In order to overcome this problem a polynomial expression has been fitted to the temperature related results (*FIGURE* 4.2) determined by Deuser and Degens (1967) and Mook *et al.* (1974) and the calculated constants are given in *TABLE* 4.1. Attempts were also made to describe the results of Wendt (1968) and Zhang *et al.* (1995) using the same polynomial expression. However, it became apparent that the calculated value of the constant C was less than the calculated standard error. This was interpreted as indicating that the data could be

adequately described by a linear expression. The data of Wendt (1968) and Zhang *et al.* (1995) were therefore fitted to a linear expression of the form given in eqn. 3.12 (*FIGURE* 4.2) and the constants (A and B) are given in *TABLE* 4.1. It is apparent from *FIGURE* 4.2 that an increase in temperature again decreases the degree of fractionation. It can also be seen that the experimentally determined values of $\alpha_{b/g}$ vary by as much as 2‰ and there is also a considerable variation between the form and the slope of the fitted lines. It is again probable that the differences between the isotope effects determined by the different groups can be attributed to problems associated with the separation of the gaseous and aqueous phases and the incomplete removal of CO_2 from the sample.

Despite the differences between the various data sets the agreement between the results of Mook *et al.* (1974) and Zhang *et al.* (1995) is good with a difference of ~0.1‰ at 5°C and decreasing to ~0.04‰ at 25°C. Therefore, as the data set determined by Mook *et al.* (1974) is more comprehensive (27 data points as opposed to four) the polynomial expression fitted to their data will be used to describe the effect of temperature on $\alpha_{b/g}$ during this study.

As it is not possible to directly determine the fractionation factor associated with the equilibrium between $CO_{2(aq)}$ and HCO_3^- ($\alpha_{b/a}$) by experiment, it must be calculated using the fractionation factors that can be determined, *i.e.* $\alpha_{b/g}$ and $\alpha_{a/g}$, and the following expression:

$$\alpha_{b/a} = \frac{\alpha_{b/g}}{\alpha_{a/g}} \qquad \textbf{(4.10)}$$

The effect of temperature on $\alpha_{b/a}$ may therefore be calculated by combining the polynomial relationships derived from the results of Vogel *et al.*(1970) and Mook *et al.* (1974) with eqn. 4.10. The results obtained in this manner were then fitted to a polynomial relationship (eqn. 3.11) to describe the effect of temperature on $\alpha_{b/a}$ (*FIGURE* 4.3), the calculated constants are given in *TABLE* 4.2. *FIGURE* 4.3 graphically compares the relationship between $\alpha_{b/a}$ and temperature as determined from the results of Vogel *et al.* (1970) and Mook *et al.* (1974) and the results of Zhang *et al.* (1995). The agreement between the two data sets is good, <0.1‰.

Table 4.2 Linear and second order polynomial regressions have been fitted to the calculated values of $1000.\ln\alpha_{b/a}$ and $1000.\ln\alpha_{c/b}$ (see eqns. 3.11 and 3.12) At different temperatures. The appropriate constants along with the standard errors and RSS are given below.

Author	**Fraction ation Factors**	**Contants**			**RSS**
		A	**B**	**C**	
Vogel *et al.* (1970)/Mook *et al.* (1974)	$1000.\ln\alpha_{b/a}$	$-25.629 \pm 5\times10^{-3}$	10683 ± 3	$-10.5\times10^{4} \pm 5\times10^{2}$	2.7×10^{-5}
Zhang *et al.* (1995)	$1000.\ln\alpha_{b/a}$	-23.69 ± 0.01	9776 ± 6	$5\times10^{2}\pm9$	3.2×10^{-5}
Mook *et al.* (1974)/Thode *et al.* (1965)	$1000.\ln\alpha_{c/b}$	-4.79 ± 0.02	$3.26\times10^{3} \pm13$	$-5.80\times10^{5} \pm1.9\times10^{3}$	2.6×10^{-5}
Zhang *et al.* (1995)	$1000.\ln\alpha_{c/b}$	16.17 ± 0.02	5401 ± 1		9.7×10^{-4}

If it is assumed the isotope specific equilibrium constant for ^{12}C ($^{12}K_{1\text{-}H2O}$) is equal to the published values of $K_{1\text{-}H2O}$ (Goyet and Poison, 1989), the isotope specific equilibrium constant for ^{13}C can be calculated by rearranging the following expression:

$$\alpha_{b/a} = \frac{^{13}K_{1\text{-}H2O}}{^{12}K_{1\text{-}H2O}} \qquad \textbf{(4.11)}$$

Although the fractionation factors determined in dilute ionic media have been applied to study the distribution of ^{12}C and ^{13}C within the marine ΣCO_2 system experimental (*e.g.* Thode *et al.*, 1965) and basic thermodynamic principles suggest this may not be correct. If the isotope specific equilibrium constants ($^{12}K_{1\text{-}H2O}$ and $^{13}K_{1\text{-}H2O}$) are altered by changes in the ionic composition and strength of the medium and these relative changes are not proportional, $\alpha_{b/a}$ will change. The possible effect of increased ionic strength on the fractionation factor between $CO_{2(aq)}$ and HCO_3^- is demonstrated below. The theoretical value of the equilibrium constant, $K_{1\text{-}H2O}$, was previously calculated (*TABLE* 2.1). Therefore using the above relationship (eqn. 4.11), and taking $\alpha_{b/a}$ as 1.0091 at 298.15 K, $^{13}K_{1\text{-}H2O}$ can be

estimated:

$$^{13}K_{1\text{-}H2O} = 1.0091 \times 4.297\times10^{-7} = 4.336\times10^{-7} \quad \textbf{(4.12)}$$

By applying the Güntelberg approximation (see eqn. 2.23) the effect of increasing the ionic strength of the medium to 0.72 moles.dm^{-3} on $^{12}K_{1\text{-}H2O}$ can be estimated:

$$p\,^{12}K_{1\text{-}H2O} = -6.3668 + \left(\frac{0.5 \times 1 \times \sqrt{0.72}}{1 + \sqrt{0.72}} \right) \quad \textbf{(4.13)}$$

$$= -6.3668 + 0.2295 = -6.1373 \quad \textbf{(4.14)}$$

$$^{12}K = 7.289\times10^{-7} \quad \textbf{(4.15)}$$

and similarly for $^{13}K_{1\text{-}H2O}$:

$$p\,^{13}K_{1\text{-}H2O} = -6.3629 + 0.2295 = -6.1334 \quad \textbf{(4.16)}$$

$$^{13}K_{1\text{-}H2O} = 7.355\times10^{-7} \quad \textbf{(4.17)}$$

and hence when the ionic strength is equal to 0.72 moles/dm^{-3}:

$$\frac{^{13}K_{1\text{-}H2O}}{^{12}K_{1\text{-}H2O}} = \alpha_{b/a} = 1.0091 \quad \textbf{(4.18)}$$

Therefore, as maybe expected, due to the form of the Güntelberg approximation (*i.e* no mass dependent terms), the ionic strength does not have any effect on the distribution of

isotopes. However, this is only a basic and general empirical relationship and does not take into account the specific effects which may arise due to the ionic composition and concentration of sea water, such as the interaction between HCO_3^- and CO_3^{2-} and ions within the medium (*i.e.* the formation of complexes). The potential of such ionic effects is of particular concern when studying the distribution of ^{12}C and ^{13}C within the marine ΣCO_2 system. However, studies by Thode *et al.* (1965) and Zhang *et al.* (1995) have suggested that these effects maybe largely confined to the equilibrium between HCO_3^- and CO_3^{2-} due to the complexation of CO_3^{2-} with Mg^{2+} ions.

The fractionation factor, $\alpha_{b/a}$, as determined by previous studies strictly corresponds to hydration / dehydration reaction between $CO_{2(aq)}$ and HCO_3^- and therefore may be more completely written as $\alpha_{b/a\text{-}H2O}$. However, the inter-conversion between $CO_{2(aq)}$ and HCO_3^- can also proceed by the alternative hydroxylation / dehydroxylation pathway. It maybe possible, by applying simple thermodynamic principles, to theoretically calculate if the fractionation factors associated with the hydration / dehydration and hydroxylation / dehydroxylation ($\alpha_{b/a\text{-}OH}$) reactions are different.

In the terms of thermodynamics, the equilibrium constant is ultimately a function of the relative energies of the reactants and products. The Gibbs free energy of the reactants and products are calculated from the Gibbs free energy of formation of the individual species involved in the reaction (*e.g.* $CO_{2(aq)}$, H^+ and HCO_3^-) which are not dependent on the reaction mechanism. As the fractionation factor can be viewed as the ratio of isotope specific equilibrium constants it is theoretically possible to calculate the change in Gibbs free energy associated with ^{12}C and ^{13}C for the hydration / dehydration reaction (*i.e.* the isotope specific Gibbs free energy change) from the isotope specific equilibrium constants using eqn. 2.20 (page 17):

$$\Delta^{12}G^{\ominus}_{1\text{-}H2O} = \ln(4.297\times10^{-7}) \times -8.314 \times 298.15 = 36.340 \text{ KJ.mol}^{-1} \qquad \textbf{(4.19)}$$

$$\Delta^{13}G^{e}_{1\text{-}H2O} = \ln(4.336 \times 10^{-7}) \times -8.314 \times 298.15 = 36.318 \text{ KJ.mol}^{-1} \quad \textbf{(4.20)}$$

Isotopic substitution will only alter the ΔG^e of the isotope bearing molecules and therefore the free energy of other ionic or molecular species involved in the reaction, such as H_2O and H^+, will not be affected. It is therefore possible, as the ΔG_f^e are additive, to calculate the Gibbs free energy change associated with just $CO_{2(aq)}$ and HCO_3^- by removing the contribution of H_2O (-237.13 KJ.mol^{-1}) and H^+ (0 KJ.mol^{-1}) to the overall Gibbs free energy change associated with the hydration / dehydration reactions for ^{12}C and ^{13}C respectively:

$$36.340 + (-237.13) - 0 = -200.79 \text{ KJ.mol}^{-1} \quad \textbf{(4.21)}$$

$$36.318 + (-237.13) - 0 = -200.81 \text{ KJ.mol}^{-1} \quad \textbf{(4.22)}$$

As $CO_{2(aq)}$ and HCO_3^- both partake in the hydroxylation / dehydroxylation reaction the above numbers can be used, in conjunction with the free energy of OH^- (-157.24 KJ.mol^{-1}) to calculate the overall energy change associated with the hydroxylation / dehydroxylation reaction for each isotope:

$$\Delta^{12}G^{e}_{1\text{-}OH} = -200.79 - (-157.24) = -43.55 \text{ KJ.mol}^{-1} \quad \textbf{(4.23)}$$

$$\Delta^{13}G^{e}_{1\text{-}OH} = -200.81 - (-157.24) = -43.57 \text{ KJ.mol}^{-1} \quad \textbf{(4.24)}$$

And therefore the isotope specific equilibrium constants for the hydroxylation / dehydroxylation reactions can be calculated as follows:

$$\ln {}^{12}K_{1\text{-}OH} = \frac{-43.55}{-8.314 \times 298.15} = 17.56885 \quad \textbf{(4.25)}$$

$$\ln {}^{13}K_{1\text{-}OH} = \frac{-43.57}{-8.314 \times 298.15} = 17.5769 \quad \textbf{(4.26)}$$

and hence:

$${}^{12}K_{1\text{-}OH} = 4.2663 \times 10^{7} \quad \textbf{(4.27)}$$

$${}^{13}K_{1\text{-}OH} = 4.3009 \times 10^{7} \quad \textbf{(4.28)}$$

The fractionation factor associated with the hydroxylation / dehydroxylation reaction, $\alpha_{b/a\text{-}OH}$ can be calculated:

$$\alpha_{1\text{-}OH} = \frac{{}^{13}K_{1\text{-}OH}}{{}^{12}K_{1\text{-}OH}} = \frac{4.3009 \times 10^{7}}{4.2663 \times 10^{7}} = 1.0081 \quad \textbf{(4.29)}$$

Therefore it can be demonstrated that the fractionation factor is not affected by the reaction mechanism as the calculated value of $\alpha_{b/a\text{-}OH}$ is 1.0081 at 25°C ($\epsilon_{b/a\text{-}OH}$= -8.1‰) is approximately equal to the fractionation factor associated with the hydration / dehydration pathway.

4.2.4 The HCO_3^- - CO_3^{2-} Equilibria

It should be possible to determine the fractionation factor between $CO_{2(g)}$ and CO_3^{2-} by increasing the pH of the medium so CO_3^{2-} becomes an increasingly important species.

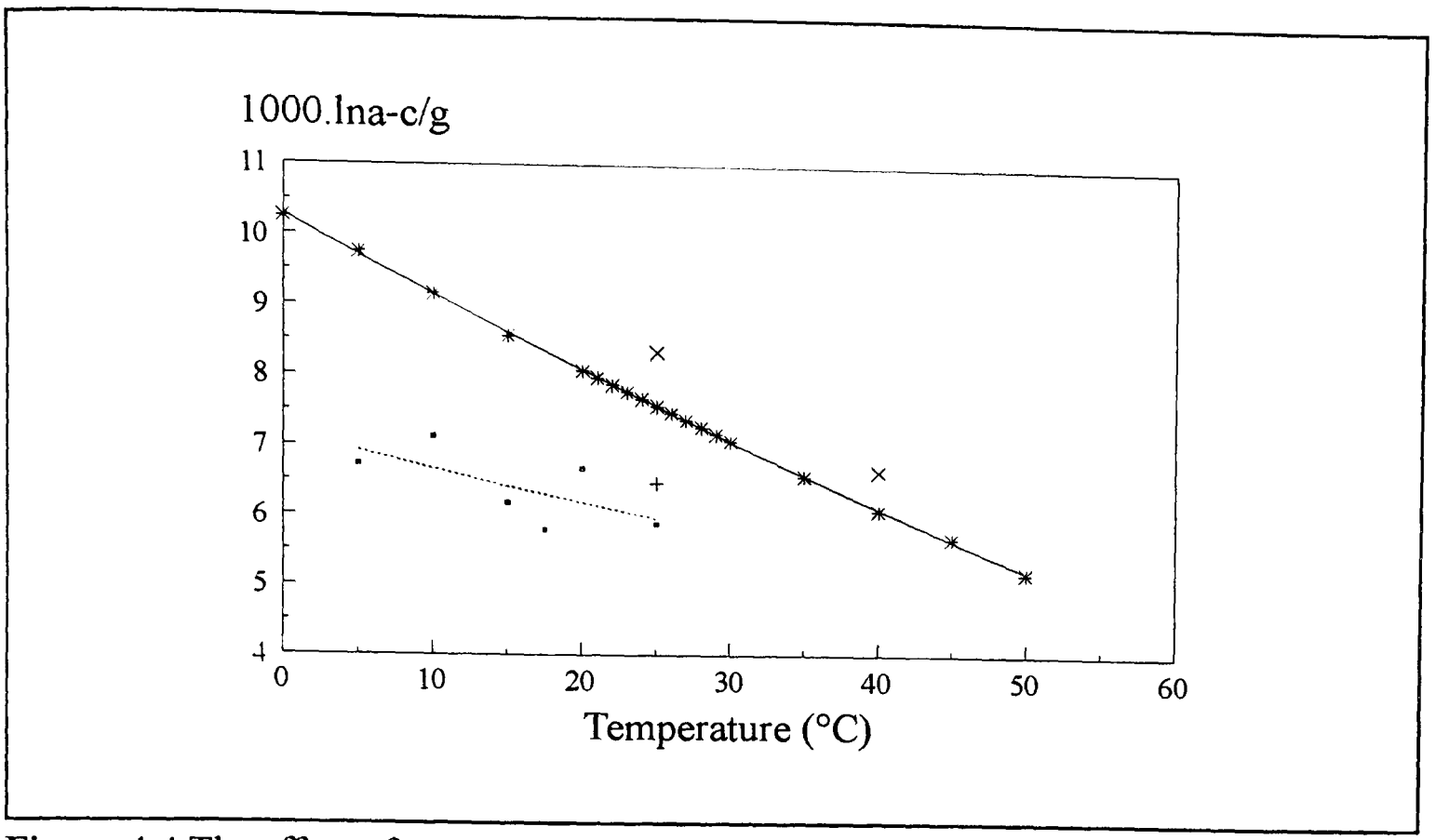

Figure 4.4 The effect of temperature on $\alpha_{c/g}$ as determined by Thode *et al.* (1965) (*), Turner (1982) (+), Lesniak and Sakai (1989) (×) and Zhang *et al.* (1995) (■). The lines represent the best fit (minimal RSS) linear (eqn. 3.12) or non-linear regressions (eqn. 3.11), the associated constants are given in *TABLE* 4.1

Nevertheless it has proved difficult to satisfactorily measure $\alpha_{c/g}$ (Mook *et al.*, 1974, Deines *et al.*, 1974, Zhang *et al.*, 1995) by using this experimental approach. This maybe at least partly attributable to the low concentration of $CO_{2(aq)}$ when CO_3^{2-} forms a sufficient proportion of the ΣCO_2 pool as well as the problems associated with the separation of the gaseous and aqueous phases and complete extraction of CO_2 from the separated pools.

Theoretical calculations by Thode *et al.* (1965), based on measured vibrational frequencies, indicate that the fractionation factor between $CO_{2(g)}$ and CO_3^{2-} is ~1.007, although the exact value is dependent on temperature. A polynomial expression has been fitted to the calculated results of Thode *et al.* (1965) (*FIGURE* 4.4) and the calculated constants are given in *TABLE* 4.1. Thode *et al.* (1965) also conducted a series of experiments to confirm the theoretical calculations, although the results show a considerable lack of reproducibility and an equal lack of agreement with the results of the theoretical calculations, ranging from 1.0066 (6.6‰) to 1.0166 (16.6‰) at 27°C.

Lesniak and Sakai (1989) experimentally determined $\alpha_{c/g}$ at two temperatures, 25°C ($\alpha_{c/g}$=1.00838, $\epsilon_{c/g}$=8.38‰) and 40°C ($\alpha_{c/g}$=1.00667, $\epsilon_{c/g}$=6.67‰) using an open system approach to avoid problems associated with the low concentration of $CO_{2(g)}$. The results of

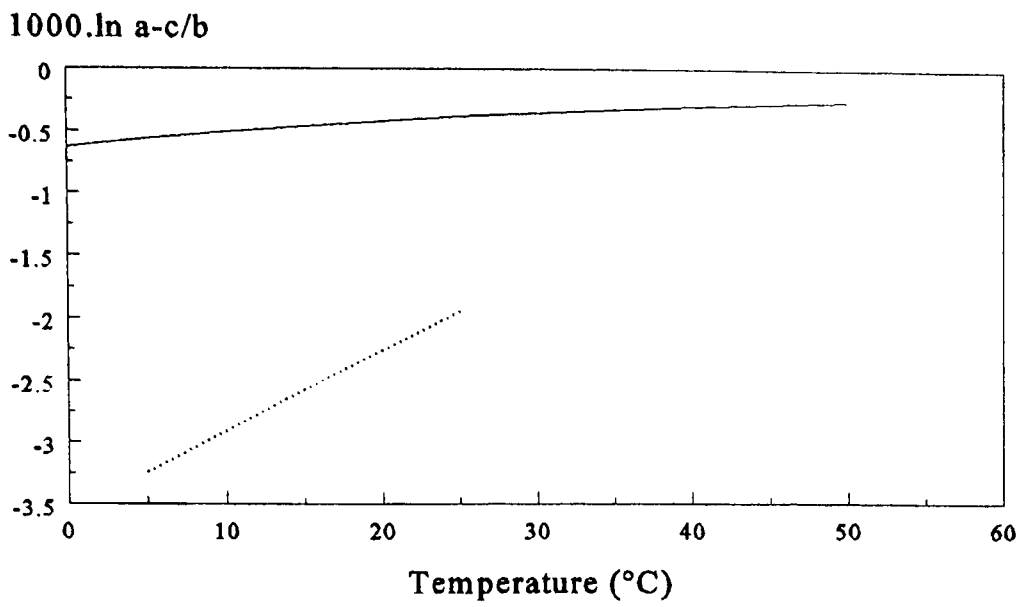

Figure 4.5 The effect of temperature on $\alpha_{c/b}$ as determined from the studies of Mook *et al.* (1974) and Thode *et al.* (1965) (solid line) and Zhang *et al.* (1995) (dashed line). See text for explanation.

Lesniak and Sakai (1989) (*FIGURE* 4.4) are ~1‰ greater than the calculated results of Thode *et al.* (1965) although the slope of the temperature change appear to be similar (*FIGURE* 4.4). A subsequent study conducted by Turner (1982) at a single temperature (25°C) determined $\epsilon_{c/g}$ to be -6.45‰, over 1‰ less than the theoretical results of Thode *et al.*(1965). Most recently Zhang *et al.* (1995) have attempted to clear up some of the confusion by conducting a series of experiments over a range of temperatures (5 to 25°C). Unfortunately their results are ~2 to 3‰ lower than the results of Thode *et al.* (1965) and the slope of the temperature effect is less.

The studies conducted by Mook *et al.* (1974) used the results of Thode *et al.* (1965) when calculating $\alpha_{b/g}$ using a mass balance approach. It is difficult to choose which set of results, those of Thode *et al.* (1965) or Zhang *et al.* (1995), are more accurate. In order to maintain consistency with previous studies the results of Thode *et al.* (1965) will be used during this study.

The temperature dependence of the fractionation factor between HCO_3^- and CO_3^{2-} pools in dilute ionic medium may therefore be calculated using the equation given below in conjunction with the fitted temperature dependent relationships obtained to describe $\alpha_{b/g}$ and

$\alpha_{c/g}$ (see *TABLE* 4.1). A polynomial expression (eqn. 3.11) was again fitted to the results (*FIGURE* 4.5) and the appropriate constants are given in *TABLE* 4.2.

$$\alpha_{c/b} = \frac{\alpha_{c/g}}{\alpha_{b/g}} \qquad \textbf{(4.30)}$$

The results of Zhang *et al.* (1995) were similarly treated although linear expressions were used to describe the data. As is apparent from *FIGURE* 4.5 there is poor agreement between the data of Thode *et al.* (1965) and Zhang *et al.* (1995). Despite choosing to use the results of Thode *et al.* (1965) during this study it is important to note that these results have been estimated using vibrational frequency data and not directly determined. The similarity of the experimentally derived data of Lesniak and Sakai (1989) to the results of Thode *et al.* (1965) lends greater credence to both studies. However, the results of Zhang *et al.* (1995) represent the largest experimentally derived data set and therefore must be rejected with caution.

Recent experiments by Zhang *et al.* (1995) have indicated that the measured isotopic enrichment between $CO_{2(g)}$ and the ΣCO_2 pool in sea water was larger than the expected enrichment predicted using the fractionation factors determined by themselves in dilute ionic media. It was suggested, on the basis of the results of Thode *et al.* (1965), that the value of $\alpha_{c/b}$ in sea water maybe decreased by the formation of the neutral complex $MgCO_3$ which has been calculated to be the dominant form (60-70%) of CO_3^{2-} (Stumm and Morgan, 1981). This decrease in $\alpha_{c/b}$ has been attributed to changes in the vibrational frequencies associated with the formation of the complex (Thode *et al.*, 1965) which favours $^{13}CO_3^{2-}$ complexation. However, it must also be pointed out that the enrichment factor determined by Zhang *et al.* (1995) using sea water is consistent with the enrichment factor expected if the fractionation factors derived by Vogel *et al.* (1970), Mook *et al.* (1774) and Thode *et al.* (1965) were used to calculate the $\delta^{13}C_{\Sigma CO2}$. This may suggest that either; 1. The values of $\epsilon_{c/b}$ determined by Zhang *et al.* (1995) are incorrect or not applicable, or; 2. That the results of Thode *et al.* (1965) should be used when studying the distribution of isotopes within the marine ΣCO_2 pool. Therefore, the values of $\epsilon_{c/b}$ determined by Thode *et al.* (1965) appear to be the most applicable to sea water, and as this study is mainly concerned with the sea water the use of the values determined by Thode *et al.* (1965) would seem

preferable.

4.3 A Kinetic Approach to the Fractionation of Isotopes within the ΣCO_2 System

The kinetic fractionation factors associated with the forward and reverse reactions of a dynamic reaction can be theoretically and practically (Marlier and O'Leary, 1984) related to the corresponding equilibrium fractionation factor (eqn. 3.27). Therefore, for the hydration / dehydration reaction between $CO_{2(aq)}$ and HCO_3^- the following reaction schemes may be written for both isotopes with the corresponding isotope specific rate constants:

$$^{12}CO_{2(aq)} + H_2O \underset{^{12}k_d}{\overset{^{12}k_{CO2}}{\rightleftharpoons}} H^+ + H\,^{12}CO_3^- \qquad \textbf{(4.31)}$$

$$^{13}CO_{2(aq)} + H_2O \underset{^{13}k_d}{\overset{^{13}k_{CO2}}{\rightleftharpoons}} H^+ + H\,^{13}CO_3^- \qquad \textbf{(4.32)}$$

Therefore at equilibrium:

$$\alpha_{b/a\text{-}H2O} = \frac{^{13}K_{1\text{-}H2O}}{^{12}K_{1\text{-}H2O}} = \frac{^{13}k_{CO2}/^{13}k_d}{^{12}k_{CO2}/^{12}k_d} = \frac{\alpha_{CO2}}{\alpha_d} \qquad \textbf{(4.33)}$$

The kinetic fractionation factors, α_{CO2} and α_d, have both been determined and are given in *TABLE* 4.3. The isotope effects for both the forward and reverse reactions are less than unity. This can be attributed to the greater activation energy normally required by the heavier isotope (O'Leary *et al.*, 1992) (*e.g. FIGURE* 3.2). The validity of the measured values of α_{CO2} and α_d may be assessed by substituting them into the eqn. 4.33 and comparing

Table 4.3 Kinetic fractionation factors associated with the hydration (α_{CO2}), dehydration (α_d), hydroxylation (α_{OH}) and dehydroxylation (α_{HCO3-}) reactions between $CO_{2(aq)}$ and HCO_3^-. Data is also given for the fractionation associated with the forward ($\alpha_{CO2\text{-}CAT}$) and reverse ($\alpha_{d\text{-}CAT}$) reactions when catalysed by carbonic anhydrase. Figures in parenthesis indicate the data has been calculated from existing data (see text for details) and * indicates that the data has been estimated.

Reaction	**$\alpha = {}^{13}k / {}^{12}k$**	**Temperature (°C)**	**Author(s)**
α_{CO2}	0.9931±0.0003	24	Marlier and O'Leary, 1984
α_d	0.9855±0.0007	24	Marlier and O'Leary, 1984
$\alpha_{CO2\text{-}CAT}$	(0.9989)	25	This study
$\alpha_{d\text{-}CAT}$	0.9900±0.0004	25	Paneth and O'Leary, 1985
α_{HCO3-}	0.9900*	25?	O'Leary *et al.*, 1992
α_{OH}	(0.9812)*	25?	This study

the answer (1.007 ± 0.0008) to the experimental value of $\alpha_{b/a\text{-}H2O}$ (1.0090) determined by Mook *et al.* (1974).

The effect of the enzyme Carbonic Anhydrase, which catalyses the interconversion between $CO_{2(aq)}$ and HCO_3^-, on the kinetic fractionation factor associated with the dehydration reaction has also been determined (Paneth and O'Leary, 1985) and is given in *TABLE* 4.3. The fractionation factor for the catalysed hydration reaction has not been determined experimentally. However, as the equilibrium constant and hence the isotope specific equilibrium constants are not affected by catalysis the fractionation factor for the hydration reaction can be calculated from the equilibrium fractionation factor as follows:

$$\alpha_{CO2\text{-}CAT} = \alpha_{b/a} \times \alpha_{d\text{-}CAT} = 1.0090 \times 0.9900 = 0.9989 \qquad \textbf{(4.34)}$$

The kinetic fractionation factor associated with the hydroxylation / dehydroxylation reaction may again be related to $\alpha_{b/a}$ as follows:

$$\alpha_{b/a} = \frac{^{13}K_{1\text{-}OH}}{^{12}K_{1\text{-}OH}} = \frac{^{13}k_{OH}/^{13}k_{HCO3\text{-}}}{^{12}k_{OH}/^{12}k_{HCO3\text{-}}} = \frac{\alpha_{OH}}{\alpha_{HCO3\text{-}}} \qquad \textbf{(4.35)}$$

The fractionation factor associated with the dehydroxylation reaction is reported to be (O'Leary *et al.*, 1992) slightly less than the fractionation factor associated with the catalysed dehydration reaction (*TABLE* 3.4) and so $\alpha_{HCO3\text{-}}$ may be estimated using eqn. 4.35.

4.4 Summary

The main aim of this chapter has been to review the numerous studies which have been conducted to determine the isotope fractionation factors associated with the ΣCO_2 system in an attempt to highlight the best data sets in terms of precision and consistency. As a result it has been decided that the results of Vogel *et al.* (1970), Mook *et al.* (1974) and Thode *et al.* (1965) are probably the best measurements of $\alpha_{a/g}$, $\alpha_{b/a}$ and $\alpha_{c/b}$ respectively. Most of the studies which have attempted to determine $\alpha_{a/g}$ and $\alpha_{b/a}$ are in close agreement, however, there does appear to be considerable disagreement between the values of $\alpha_{c/b}$ determined by various researchers and their is an obvious requirement for the equilibrium isotope effect associated with this reaction to be studied further by experimentation.

An additional aim of this chapter was to investigate the applicability of the various fractionation factors, which have been determined in dilute ionic media, to isotopic studies in the marine environment. By applying a simple empirical formula it was found that the ionic strength of the medium does not theoretically effect the distribution of isotopes within the ΣCO_2 pool. However, this is contrary to the experimental results of Thode *et al.* (1965) which suggested that both the ionic strength and the composition of the medium may be important, and in particular, that $MgCO_3$ complexes may have an important influence of the distribution of isotopes between HCO_3^- and CO_3^{2-} in sea water. The simple method used here to theoretically investigate the potential of such ionic isotope effects is basic and although empirical it does not specifically account for the effect of complexation and any differential effect complexation may hav on the compounds containing either ^{12}C or ^{13}C.

Therefore, there is an obvious need for direct experimental measurements to be

made to determine the values of $\alpha_{b/a}$ and $\alpha_{c/b}$ in sea water and the attempts to do this are discussed in the following chapter.

Although the equilibrium fractionation of isotopes between the $CO_{2(aq)}$ and HCO_3^- pools is not effected by the pH of the medium, the kinetic fractionation factors associated with the different reaction mechanisms are distinct. This may be of particular importance when studying systems which are not at equilibrium. An obvious example of this, in the context of this thesis, is the distribution of isotopes within the ΣCO_2 pool around an actively photosynthesising phytoplankton cell. The distribution of isotopes between the various species of ΣCO_2 within these micro environments will be effected not only by the degree of disequilibrium, which is ultimately a function of rates, but also the pH which will determine the importance of the various reaction mechanisms and hence, because of the differing isotopic signal, the distribution of isotopes.

Chapter 5: The Effect of Temperature, Salinity and pH on the Distribution of ^{13}C and ^{12}C Within the ΣCO_2 System in the Marine Environment - Experimental Results.

5.1 Introduction

Simple thermodynamic considerations of the ΣCO_2 system do not predict any salinity or pH effect on the fractionation factors; $\alpha_{a/g}$, $\alpha_{b/a}$ or $\alpha_{c/b}$ (see *CHAPTER* 4) . However, recent measurements made in sea water by Zhang *et al.* (1995) appear to show a pH related isotope effect, possibly associated with $\alpha_{c/b}$, which has been attributed to the formation of $MgCO_3$ complexes (Thode *et al.*, 1965, Zhang *et al.*, 1995). Based on their findings, Zhang *et al.* (1995) proposed a carbonate dependent correction factor to account for the observed discrepancy between the measured and calculated values of $\delta^{13}C_{\Sigma CO2}$ of sea water when in equilibrium with $CO_{2(g)}$ of a known isotopic composition. However, as pointed out by Zhang *et al.* (1995), HCO_3^- also forms complexes in sea water (Stumm and Morgan, 1981) and therefore a general correction factor, based on the proportion of carbonate, does not explicitly deal with the possible effect of HCO_3^- complexes and how they may affect the isotopic composition of $CO_{2(aq)}$, HCO_3^- and CO_3^{2-} ($\delta^{13}C_a$, $\delta^{13}C_b$, $\delta^{13}C_c$).

The main aim of the experiments reported in this section were to look for the existence of pH related isotope effects in sea water, at two temperatures, and to compare the results with a similar experiment conducted in distilled water to ascertain the magnitude of any salinity effect.

5.2 Materials and Methods

It was suggested in the previous chapter that some of the observed discrepancies between the fractionation factors, especially $\alpha_{c/b}$, determined by different workers, maybe at least partly attributable to problems associated with the separation of the aqueous and gaseous phases. An additional source of error could be associated with the extraction efficiency of the procedures used to strip and collect CO_2 from the gaseous and aqueous samples. The design of the experimental apparatus used during this experiment was specifically developed to reduce the potential errors introduced by these problems when sampling the $\delta^{13}C_g$ and

$\delta^{13}C_{\Sigma CO2}$. This was achieved by conducting the experiments using equipment which allowed the gaseous and aqueous phases to be rapidly brought in to chemical and isotopic equilibrium and subsequently isolated. The experiments were also conducted at atmospheric pressure which allowed the aqueous phase to be easily sampled without disturbing the equilibrium. The $\delta^{13}C_g$ and $\delta^{13}C_{\Sigma CO2}$ could then be determined using extraction procedures which had been previously determined to be 99.5% efficient.

The following sections detail the apparatus, methods and calculations used during this study.

5.2.1 Calculations

Using the equations given below, the isotopic composition of the HCO_3^- and CO_3^{2-} pools can be calculated, if the $[CO_{2(aq)}]$, $[HCO_3^-]$, $[CO_3^{2-}]$, R_a and $R_{\Sigma CO2}$ are known:

$$R_b = \frac{R_{\Sigma CO2} \times [\Sigma CO_2] - R_a \times [a]}{[b] + \alpha_{c/b} \times [c]} \qquad \textbf{(5.1)}$$

$$R_c = \frac{R_{\Sigma CO2} \times \Sigma CO_2 - R_a \times ([a] + \alpha_{b/a} \times [b])}{[c]} \qquad \textbf{(5.2)}$$

The isotopic composition of $CO_{2(aq)}$ can be calculated from R_g using the following equation:

$$R_a = \alpha_{a/g} \times R_g \qquad \textbf{(5.3)}$$

The appropriate fractionation factors for substituting into the above equations may be calculated at different temperatures using the polynomial and linear relationships given in *TABLES* 4.1 and 4.2. The values of $\alpha_{b/a}$ and $\alpha_{c/b}$ may then be calculated by substituting the values of R_b and R_c into eqns. 4.2 and 4.3.

One of the main aims of this study was to investigate the potential effect of salinity and pH on the previously determined fractionation factors. However, it is important to note

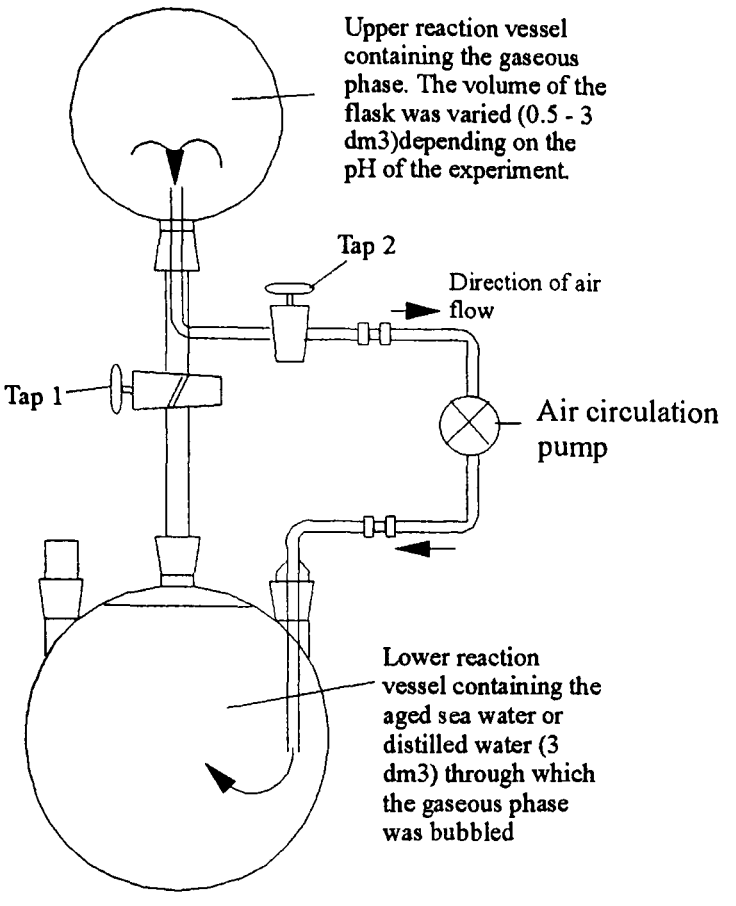

Figure 5.1 The experimental apparatus used during this study.

from eqns 5.1 and 5.2 that in order to calculate R_b or R_c one of the predetermined fractionation factors must be substituted into the equation. If the previously determined fractionation factors are incorrect the calculated values of R_b or R_c maybe in error. This problem is normally circumvented by first determining $\alpha_{b/a}$ at a pH which is sufficiently low to eliminate CO_3^{2-}, therefore eliminating the need to know $\alpha_{c/b}$, and then determining R_c and hence $\alpha_{c/b}$ (*e.g.* Zhang *et al.*, 1995). As it was decided to conduct the experiments within the pH range found in the marine environment the pH was not sufficiently low to assume the $[CO_3^{2-}]$ to be negligible and therefore this potential source of error must be taken into account when analysing the data.

The $[CO_{2(aq)}]$, $[HCO_3^-]$ and $[CO_3^{2-}]$ were calculated using the sea water model developed by Prof. D. Turner to maintain consistency (see page 18).

5.2.2 Experimental Apparatus

All of the experiments were conducted using the experimental apparatus shown in *FIGURE* 5.1. The apparatus was designed to facilitate the rapid equilibrium between the gaseous and

PAGE

NUMBERING

AS ORIGINAL

Sample was then allowed to fill the bottle slowly, being careful to avoid air bubbles and excessive turbulence. The sample was allowed to overflow by two full volumes before the sample transfer tube was withdrawn. The volume of the sample was then adjusted so that an air space would occupy ~1% of the volume of the bottle after the glass stopper had been replaced. The sample was not spiked with saturated $HgCl_2$ solution because the appropriate quantity of $HgCl_2$ was added at the beginning of the experiment. This sampling protocol is based on the standard operating procedure described in DOE (1991).

Samples for the determination of $\delta^{13}C_{\Sigma CO2}$ were taken in separate borosilicate bottles. The samples were only stored in these bottles temporarily before being transferred to 10 cm^3 borosilicate ampoules for permanent storage (see *APPENDIX* 1). The $\delta^{13}C_{\Sigma CO2}$ was determined using a modified technique which was based on the methodology employed by McCorkle (1987). This method allowed both the $\delta^{13}C_{\Sigma CO2}$ and $[\Sigma CO_2]$ to be determined simultaneously from the same sample with a precision, determined from replicate standards, of ± 0.05 ‰ and ± 10 $\mu moles.kg^{-1}$ respectively. Replicate internal standards were run during the preparation of $\delta^{13}C_{\Sigma CO2}$ samples for mass spectrometric determination. A detailed description of the method is given in *APPENDIX* 1.

The $[\Sigma CO_2]$ was determined using an automated coulometric titration system. The exact apparatus has been described by Robinson and Williams (1991) and the precision of the method has been determined to be σ_{n-1} = 0.5 to 1 $\mu mol.kg^{-1}$ (0.025 to 0.05 %). Samples were stored under water prior to analysis to reduce evaporation.

Samples to determine $[\Sigma CO_2]$ by the manometric procedure were taken at the end of every experiment, whilst samples to measure $[\Sigma CO_2]$ coulometrically were only taken during experiment one (see section 5.3.1). *FIGURE* 5.3 plots the $[\Sigma CO_2]$ results obtained using the coulometric system against the manometrically determined results. The $[\Sigma CO_2]$ determined using the manometer are offset from the results obtained with the coulometer by -62 ± 16 $\mu mol.kg^{-1}$. Therefore, although the manometric method is not as accurate, the precision is good. The offset maybe due to poor or incorrect calibration of the manometer, or, incomplete stripping and collection of $CO_{2(g)}$ after acidification of the sample. The impact of this offset on the calculated values of $\epsilon_{b/a}$ was determined by calculating the values of $\epsilon_{b/a}$ determined using the manometric and coulometric results. It was found that the results were

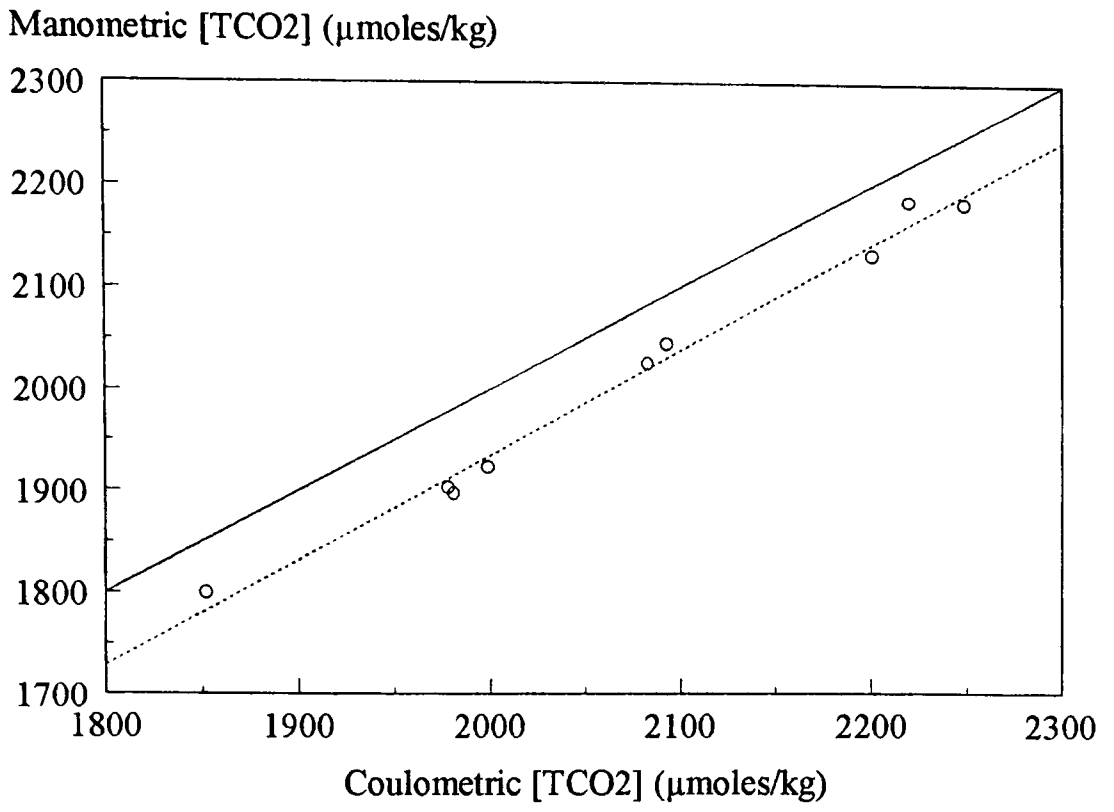

Figure 5.3 Variations in the [ΣCO_2] as determined from replicate samples measured using a coulometric and manometric procedure. The best fit line (dashed line) and 1:1 line (solid line) are also shown.

not significantly different and therefore any errors introduced by using the manometric results are small.

Two methods were employed to measure pH. For the experiments conducted in sea water a spectrophotometric technique was employed (see *APPENDIX* 3) and for the experiments conducted in distilled water the conventional potentiometric technique was used. Samples for the spectrophotometric determination of pH were directly transferred from the experimental apparatus to a 10 cm spectrophotometer cell via the sample transfer tube. The cell was filled slowly and allowed to overflow by at least two volumes before the stoppers were inserted, ensuring no air bubbles were present. The pH was then determined (± 0.002 pH units) immediately using a diode array spectrophotometer (Hewlett-Packard, 8452 A) and the indicator *m*-cresol purple. The methodology and calculations were based on the protocol described by Clayton and Byrne (1993) and is detailed in *APPENDIX* 3.

Samples for the potentiometric determination of pH were taken by filling a beaker (~100 cm^3) from the sample transfer tube at the end of the experiment. The mV reading of

the sample was then immediately determined using an Orion combination electrode and Orion expandable ion analyser. The sample was continuously stirred using a magnetic stirrer and placed in a water bath at the experimental temperature to reduce temperature changes. The electrode was then calibrated using three IUPAC primary pH standards (Vogel, 1989) and the pH calculated.

The samples for the determination of $\delta^{13}C_g$ were obtained by cryogenic extraction. The upper reaction vessel was attached to the vacuum line and then the sample was slowly pumped through a series of traps; the first trap was a water trap cooled to ~ -95°C with a $N_{2(l)}$ / ethanol slush, and the second two traps were cooled with $N_{2(l)}$ to trap $CO_{2(g)}$. The quantity of $CO_{2(g)}$ collected was measured manometrically and then transferred to the mass spectrometer. The precision of the technique, which was determined on replicate samples, was ± 0.05 ‰ with a yield of 99.5 % ± 0.3 %.

Salinity samples from the sea water experiments were transferred to standard salinity bottles for storage prior to determination using a standardised Autosal (Model 8400A) type salinometer (σ_{n-1} = 0.002 salinity units). Temperature measurements were made using a Comark 9001 thermometer in conjunction with a Comark type K (± 0.2°C) Thermocouple.

Carbon isotope ratios were determined on a V.G. Isogas, SIRA II mass spectrometer and are reported relative to the PDB standard.

5.3 Experiments

5.3.1 Experimental Design

In order to assess the effect of temperature, salinity and pH on $\alpha_{b/a}$ and $\alpha_{c/b}$ a series of three experiments were conducted:

i. *Experiment 1*: To assess the pH related effect on the fractionation factors $\alpha_{b/a}$ and $\alpha_{c/b}$ in sea water at 20°C.

ii. *Experiment 2*: To assess the pH related effect on the fractionation factors $\alpha_{b/a}$ and $\alpha_{c/b}$ in sea water at 5°C.

iii. *Experiment 3*: To assess the pH related effect on the fractionation factors $\alpha_{b/a}$ and $\alpha_{c/b}$ in distilled water at 20°C.

Each experiment consisted of ~9 different runs which were conducted at different pHs. *TABLE* 5.1 gives the temperature, salinity and pH of each run for experiments 1 to 3.

Experiments 1 and 2 used different batches of aged sea water which had been collected offshore in the Irish sea and aged for several months after which time the sea water was filtered through a 0.4 μm membrane filter under positive pressure. The pH was adjusted by either bubbling with $N_{2(g)}$ (CO_2-free), to increase the pH, or with compressed air to decrease the pH. Once the correct pH had been achieved 3 dm^3 of the water was taken and gently poured (to reduce pH changes due to the exchange of $CO_{2(g)}$ with the atmosphere) into the lower flask and 3 cm^3 of saturated $HgCl_2$ solution added. The upper reaction vessel, which had been previously evacuated, was then allowed to fill with air after which the apparatus was assembled (*FIGURE* 5.1), placed in the water bath and the pump connected. The size of the upper flask varied depending on the pH of the experiment (0.5 to 3 dm^3 for experiments one and two). When the pH is high the $[CO_{2(g)}]$, relative to the $[\Sigma CO_2]$, is very low and hence the volume of the upper flask must be large enough to ensure sufficient amounts of $CO_{2(g)}$ are available for mass spectrometric analysis. Similarly samples taken to determine $\delta^{13}C_{\Sigma CO2}$ at the end of high pH runs had an increased risk of contamination from atmospheric $CO_{2(g)}$ during sample transfer due to the low $[CO_{2(aq)}]$. The experiment commenced when the pump was started. From the results of the experiment conducted to assess how quickly isotopic equilibrium was achieved between the two phases it was found that equilibrium appeared to be reached within half an hour at a pH of 8.1. It was therefore decided that the duration of each run should be 2 hours to ensure isotopic equilibrium. At the end of each run the pump was stopped and taps one and two were closed. Sampling then proceeded as described earlier.

Part of the aim of experiment 3 was to look for any pH related effect on the fractionation factors $\alpha_{b/a}$ and $\alpha_{c/b}$ in distilled water and to examine any such effect over a large pH range (~6 to 10). It was not possible to extend the pH range of the

Table 5.1 Summary of results for experiments 1, 2 and 3. The pH results have been temperature corrected using the method described in *APPENDIX* 3, section A3.4.3.

Expt no.	Run no.	Temperature (°C)	Salinity	$[\Sigma CO_2]$, $\mu mol.kg^{-1}$	pH_{SWS}	$\delta^{13}C_g$(‰)	$\delta^{13}C_{\Sigma CO2}$(‰)
1	A	20.1	34.552	1593	8.494	-12.31	-3.21
1	B	20.1	34.567	1897	8.277	-14.18	-6.09
1	C	20.1	34.587	2045	8.111	-15.05	-7.53
1	D	20.1	34.59	2185	7.815	-17.59	-9.65
1	E	19.9	34.632	1800	8.45	-14.46	-7.98
1	F	20.1	34.624	1903	8.303	-16.15	-9.29
1	G	20.0	34.632	2026	8.129	-17.80	-10.54
1	H	20.0	34.637	2132	7.926	-20.06	-12.70
1	I	20.0	34.633	2078	7.946	-20.44	-12.86
1	J	20.1	34.662	2183	7.817	-21.25	-13.68
1	K	20.1	34.7	1923	8.272	-18.72	-12.18
2	A	4.9	34.081	2219	7.849	-14.60	-4.87
2	B	4.3	34.084	2163	8.029	-14.19	-4.63
2	C	4.9	34.081	2129	8.076	-13.91	-4.42
2	D	4.8	34.089	2078	8.218	-13.29	-4.09
2	E	4.9	34.107	1942	8.388	-12.54	-3.64
2	F	5.2	34.121	1866	8.498	-11.17	-3.39
2	G	4.8	34.131	1869	8.524	-11.21	-3.30
2	H	4.9	34.142	1816	8.589	-10.79	-2.81
2	I	5.0	34.168	1775	8.654	-10.60	-2.64
3	A	20.0	0	993	5.382	-37.99	-38.11
3	B(2)	20.0	0	1048	6.632 .	-30.13	-25.81
3	C	20.0	0	1686	7.278	-20.70	-13.52
3	E	19.8	0	2057	7.945	-15.87	-7.76
3	J(1)	20.4	0	4773	8.883	-27.12	-21.36
3	J(2)	20.0	0	4450	9.392	-21.67	-20.07
3	J(3)	20.0	0	3886	9.804	-14.91	-16.97
3	K	20.2	0	4500	9.939	-12.81	-16.67

experiment any higher because the difference between the relative concentrations of $CO_{2(g)}$ and ΣCO_2 would be too great. The volume of the upper flask was 0.5 dm^3 for the runs conducted at the lowest pHs and up to 5 dm^3 for the high pHs.

To achieve the required pH for the individual runs in experiment 3 differing quantities of either Na_2CO_3 and $NaHCO_3$ were added to the distilled water so the resultant pH was slightly higher than required. The pH was then adjusted by blowing $CO_{2(g)}$ into the solution until the correct pH was reached. Once the correct pH was achieved the solution

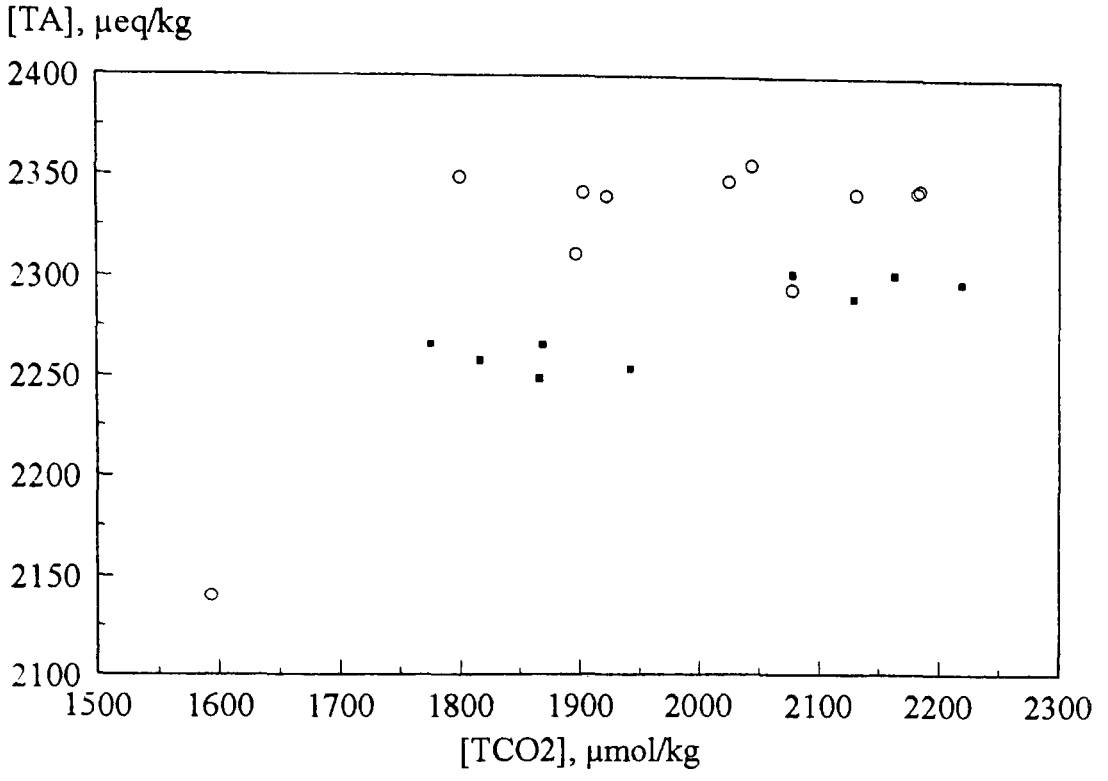

Figure 5.4 Total Alkalinity values for each of the individual experimental runs conducted during experiments one (o) and two (■).

($3\ dm^3$) was carefully transferred to the lower flask and the apparatus was assembled as described for experiments 1 and 2.

5.3.2 The pH Related Effect on $\alpha_{b/a}$ and $\alpha_{c/b}$ in Sea Water at Two Different Temperatures

The results of experiments one and two are given in *TABLE* 5.1. Using the pH, [ΣCO_2], temperature and salinity results the concentrations of CO2(aq), HCO_3^- and CO_3^{2-} were calculated using the sea water model written by Prof. David Turner, the results are given in *TABLE* 5.2 along with the calculated total alkalinity (TA). As the TA of sea water does not change when CO_2 is added or removed the TA should be constant for each experiment. The calculated TAs have been plotted in *FIGURE* 5.4 in relation to the [ΣCO_2]. It is apparent that the TA's for experiment 1 are generally in agreement with each other (2319 ± 62

Table 5.2 Chemical and isotopic parameters calculated from the experimental results. The isotopic composition of the different ΣCO_2 pools have been calculated using eqns 5.1 and 5.2, assuming either the values of $\alpha_{c/b}$ or $\alpha_{b/a}$ determined during previous studies are correct.

Expt no.	Run no.	TA, μeq. kg^{-1}	$[CO_{2(aq)}]$ μmole $s.kg^{-1}$	$[HCO_3^-]$ μmoles. kg^{-1}	$[CO_3^{2-}]$ μmole $s.kg^{-1}$	Calculated assuming $\alpha_{c/b}$ is correct					Calculated assuming $\alpha_{b/a}$ is correct				
						$\delta^{13}C_a$ (‰)	$\delta^{13}C_b$ (‰)	$\delta^{13}C_c$ (‰)	$\alpha_{b/a}$	$\epsilon_{b/a}$ (‰)	$\delta^{13}C_a$ (‰)	$\delta^{13}C_c$ (‰)	$\delta^{13}C_b$ (‰)	$\alpha_{c/b}$	$\epsilon_{c/b}$ (‰)
1	A	2140	3.1	1221	369	-13.38	-3.22	-3.63	1.0103	10.30	-13.38	-1.43	-3.88	1.0025	2.46
1	B	2311	6.7	1599	291	-15.25	-6.05	-6.47	1.0093	9.34	-15.25	-8.01	-5.77	0.9978	-2.25
1	C	2358	11.1	1807	227	-16.12	-7.24	-7.66	1.0090	9.02	-16.12	-12.44	-6.65	0.9942	-5.83
1	D	2344	24.6	2032	129	-18.66	-9.75	-10.16	1.0091	9.08	-18.66	-18.67	-9.21	0.9905	-9.55
1	E	2349	4.0	1412	384	-15.53	-7.71	-8.12	1.0080	7.95	-15.53	-14.28	-6.03	0.9917	-8.29
1	F	2342	6.3	1587	310	-17.21	-9.14	-9.56	1.0082	8.21	-17.21	-16.68	-7.75	0.9910	-8.99
1	G	2348	10.5	1783	232	-18.87	-10.25	-10.67	1.0088	8.78	-18.87	-17.11	-9.41	0.9922	-7.77
1	H	2342	18.4	1954	160	-21.12	-12.64	-13.05	1.0087	8.67	-21.12	-24.69	-11.69	0.9869	-13.15
1	I	2294	17.1	1899	162	-21.51	-12.95	-13.36	1.0087	8.75	-21.51	-23.56	-12.08	0.9884	-11.62
1	J	2343	24.5	2029	129	-22.31	-13.51	-13.92	1.0090	9.00	-22.31	-23.50	-12.90	0.9893	-10.74
1	K	2340	6.9	1621	295	-19.78	-12.09	-12.50	1.0078	7.85	-19.78	-22.08	-10.35	0.9881	-11.86
2	A	2298	34.0	2110	75	-15.73	-4.66	-5.23	1.0112	11.24	-15.73	-12.52	-4.40	0.9918	-8.15
2	B	2302	21.9	2034	107	-15.32	-4.46	-5.03	1.0110	11.03	-15.32	-15.23	-3.92	0.9886	-11.36
2	C	2290	19.0	1990	120	-15.04	-4.28	-4.84	1.0109	10.93	-15.04	-14.20	-3.71	0.9895	-10.53
2	D	2302	13.1	1906	159	-14.42	-4.05	-4.62	1.0105	10.52	-14.42	-16.43	-3.06	0.9866	-13.41
2	E	2254	8.0	1721	213	-13.67	-3.53	-4.10	1.0103	10.28	-13.67	-13.85	-2.33	0.9885	-11.55
2	F	2249	5.7	1601	259	-12.30	-3.14	-3.70	1.0093	9.28	-12.30	-17.03	-0.98	0.9839	-16.06
2	G	2266	5.4	1595	269	-12.34	-3.42	-3.99	1.0090	9.03	-12.34	-18.54	-0.96	0.9824	-17.59
2	H	2258	4.4	1513	298	-11.92	-2.38	-2.94	1.0097	9.65	-11.92	-12.20	-0.56	0.9884	-11.65
2	I	2266	3.6	1440	331	-11.74	-2.29	-2.86	1.0096	9.55	-11.74	-11.17	-0.38	0.9892	-10.79
3	A	-	902.5	90	0	-39.03	-28.98	-29.39	1.0105	10.46	-39.03	-	-	-	-
3	B(2)	-	376.7	671	0	-31.18	-22.80	-23.21	1.0086	8.65	-31.18	-	-	-	-
3	C	-	189.5	1495	1	-21.76	-12.48	-12.89	1.0095	9.49	-21.76	-	-	-	-
3	E	-	54.6	1995	7	-16.93	-7.51	-7.93	1.0096	9.59	-16.93	-27.39	-7.44	0.9799	-20.10
3	J(1)	-	14.4	4609	150	-28.17	-21.33	-21.73	1.0070	7.04	-28.17	-97.87	-18.85	0.9195	-80.53
3	J(2)	-	3.9	4027	419	-22.74	-20.03	-20.44	1.0028	2.77	-22.74	-84.91	-13.32	0.9274	-72.56
3	J(3)	-	1.2	3062	823	-15.98	-16.89	-17.30	0.9991	-0.92	-15.98	-55.96	-6.50	0.9502	-49.79
3	K	-	0.9	3288	1211	-13.88	-16.56	-16.97	0.9973	-2.71	-13.88	-49.98	-4.40	0.9542	-45.78

μeq.kg^{-1}), although the TA for runs A, B and I appear to be too low. These results have been rejected which improved the precision of the estimated TA (2346 ± 6 μeq.kg^{-1}). A plot of $[\Sigma CO_2]$ against TA for experiment 2 suggests the data maybe divided in two groups on the basis of their calculated TA (2276 ± 22 μeq.kg^{-1}). There is no evidence to suggest one set of results is preferable to the other and the difference may reflect a small change in one

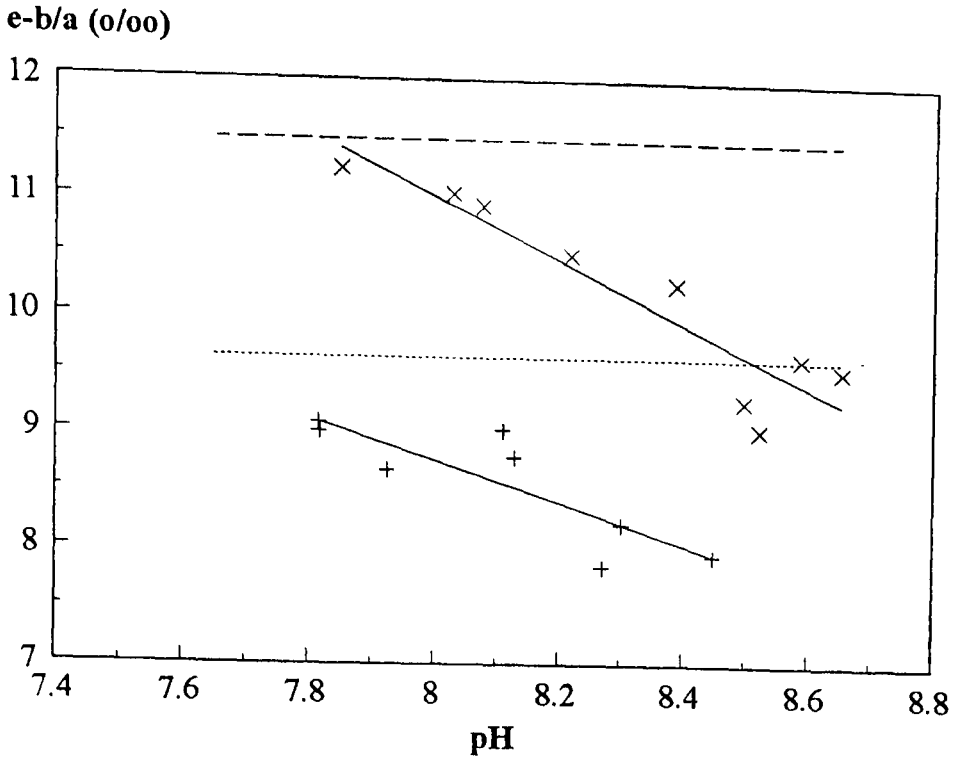

Figure 5.5 The effect of pH on $\epsilon_{b/a}$ at two temperature in sea water; 20°C (+) and 5°C (×). The solid lines represent the linear regressions given by the following equations: $\epsilon_{b/a}$= 22.97 (±0.29) - 1.78 (±0.47) × pH (r^2 =0.70) and $\epsilon_{b/a}$ = 32.38 (±0.33) - 2.67 (±0.42) × pH (r^2 =0.85) at 20°C and 5°C respectively. The dashed lines are the results obtained by Vogel *et al.* (1970) / Mook *et al.* (1974) at 20°C (short dash) and 5°C (long dash).

of the methods that was not noted. Therefore no data from experiment two will be rejected.

Using the data given in *TABLES* 5.1 and 5.2 in conjunction with eqns. 4.2, 4.3 and 5.1 to 5.3 the fractionation and enrichment factors associated with the $CO_{2(aq)}$ -HCO_3^- equilibria can be calculated. The results are given in *TABLE* 5.2 and *FIGURE* 5.5. From *FIGURE* 5.5 it is apparent that $\epsilon_{b/a}$, at both temperatures varies in relation to pH, the value of $\epsilon_{b/a}$ decreasing as the pH increases. It was suggested in *CHAPTER* 4 that the equilibrium fractionation factors associated with the hydration / dehydration and hydroxylation / dehydroxylation reactions between $CO_{2(aq)}$ and HCO_3^- may be different. If such a difference was present the overall fractionation factor would be expected to vary in a sigmoid fashion with pH, constant below a pH of 6, (where the hydration / dehydration reaction is dominant) and above a pH of 11 (where the hydroxylation / dehydroxylation predominates) and variable at intermediate pHs. The value of $\alpha_{b/a}$ at the intermediate pHs would reflect the contribution of each reaction mechanism to the overall interconversion of $CO_{2(aq)}$ and HCO_3^-.

The results obtained during experiments one and two all fall within the intermediate pH range and therefore according to this hypothesis $\epsilon_{b/a}$ would be expected to be dependent on pH.

However, according to the thermodynamic arguments and calculations given in *CHAPTER* 4, a suitably defined fractionation factor should be independent of pH. As the results of experiments one and two are unlikely to violate the laws of thermodynamics, an alternative explanation must be sought to account for the experimental observations. The subsequent discussions in this section will therefore focus on the following possible factors which may have given rise to the apparent relationship between $\epsilon_{b/a}$ and pH:

1. Isotopic equilibrium within the system was not achieved within the experimental period of two hours.

2. The value of the fractionation factor $\alpha_{c/b}$ used to calculate $\alpha_{b/a}$ was incorrect.

3. The values of $\alpha_{b/a}$ and $\alpha_{c/b}$ derived by previous studies are not applicable to the sea water system.

1. When calculating $\epsilon_{b/a}$ it was assumed that the experimental system had achieved isotopic equilibrium by the end of each two hour run. Preliminary experiments suggested that isotopic equilibrium was reached within half an hour of the experiment starting, even if the degree of isotopic disequilibrium was large. Chemical equilibrium within the ΣCO_2 pool is normally achieved within 20 - 200 seconds (Johnson, 1982). Therefore the slowest processes effecting the rate at which chemical and isotopic equilibrium is achieved within the experimental system is probably the diffusion of CO_2 across the gas / liquid interface (*e.g.* Zhang *et al.*, 1995). The rate at which CO_2 exchange occurs between the gaseous and aqueous phases is not dependent on pH and therefore the rate at which isotopic equilibrium is achieved would be expected to be independent of pH. The apparently rapid rate at which isotopic equilibrium was achieved within this experimental system can be attributed to the circulation of the gaseous phase through the aqueous phase.

The volume of the upper reaction vessel was increased from 0.5 dm^3 to ~3 dm^3 as the experimental pH was increased. This increase in the volume of the upper reaction vessel would be expected to increase the time taken to achieve isotopic equilibrium, although it

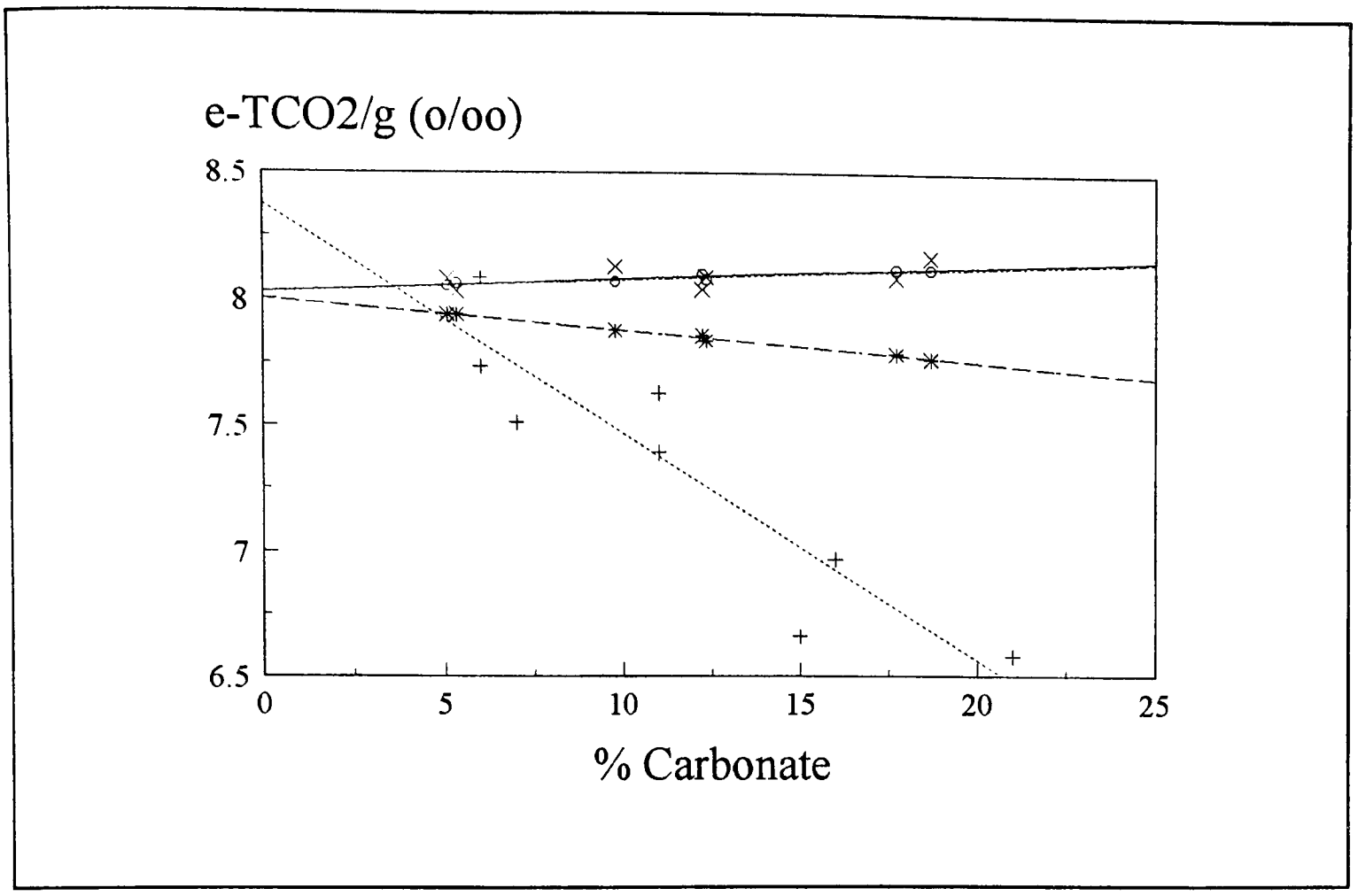

Figure 5.6 The isotopic fractionation between sea water and air when in isotopic equilibrium at different pHs (% CO_3^{2-}). The × are values measured by Zhang *et al.* (1995), o and * are the predicted values calculated using the enrichment factors derived by Thode *et al.* (1965) / Vogel *et al.* (1970) / Mook *et al.* (1974) and Zhang *et al.* (1995) respectively and + are the results determined during this study at 20°C, the other values were determined at 23°C. The lines represent the best linear fit to the respective data sets.

seems unlikely to increase the time required to reach equilibrium by four times, especially given the high flow rate of the pump.

If there is a problem with isotopic equilibrium not being achieved by the end of the experiment, it is more likely to be associated with the experimental runs conducted at high pHs. This is because isotopic equilibrium was confirmed experimentally to be achieved with 0.5 hours at a pH of 8.1 and the larger size of the upper reaction vessel used in the high pH experiments may increase the time taken to reach equilibrium. Therefore if the results of the experiments conducted above this pH are temporally rejected the mean enrichment factors for the two experiments can be calculated; $\epsilon_{b/a} = 8.91 \pm 0.18$ ‰ (20°C) and $\epsilon_{b/a} = 11.07 \pm 0.16$ ‰ (5°C). If these values are compared with those calculated using the combined results of Vogel *et al.* (1970) / Mook *et al.* (1974) , 9.64‰ and 11.49‰ respectively, it can be seen that the enrichment factors calculated during this study are significantly less, 0.73‰ at 20°C

and 0.42‰ at 5°C, than those previously determined. The agreement is poorer still when compared with the data obtained by Zhang *et al.* (1995). Therefore, even if the data from the runs conducted at higher pHs are rejected there is still an offset between the results of this study and previous studies.

2. It has been suggested that the enrichment factor, $\epsilon_{c/b}$, maybe particularly susceptible to the effects of complexation in an ionic medium and therefore the application of data derived in distilled water to the marine environment may lead to errors when calculating the distribution of isotopes within the marine ΣCO_2 system (Zhang *et al.*, 1995). Zhang *et al.* (1995) came to this conclusion after using their experimentally derived results and the data of Thode *et al.* (1965), Vogel *et al.* (1970) and Mook *et al.* (1974) to try and predict the isotopic composition of sea water ($\delta^{13}C_{\Sigma CO2}$) in equilibrium with air of a known isotopic composition at 23°C. The results of their study are plotted along side the results obtained during this study in *FIGURE* 5.6. The values measured by Zhang *et al.* (1995) of $\epsilon_{\Sigma CO2/g}$ agree well with the value predicted by using the data of Thode *et al.* (1965), Vogel *et al.* (1970) and Mook *et al.* (1974). The difference between the measured values of $\epsilon_{\Sigma CO2/g}$ and those predicted using the enrichment factors determined by Zhang *et al.* (1995) can be attributed to the larger, more negative value of $\epsilon_{c/b}$ determined by Zhang *et al.* (1995) (*FIGURE* 4.5). This has the effect of decreasing $\epsilon_{\Sigma CO2/g}$ as the $\%CO_3^{2-}$ increases. The variation in $\epsilon_{\Sigma CO2/g}$ in relation to the $[CO_3^{2-}]$ measured during experiment 1 would suggest that $\epsilon_{c/b}$ in sea water maybe larger and more negative than the value obtained by Zhang *et al.* (1995) and other studies conducted in distilled water. This is contrary to the results of sea water experiments of Zhang *et al.* (1995) which suggest that the effect of an ionic medium decreases the degree of fractionation between HCO_3^- and CO_3^{2-} and as a result leads to an increase in the value of $\epsilon_{\Sigma CO2/g}$ as the pH increases. It was on the basis of these results Zhang *et al.* (1995) suggested a correction factor for $\epsilon_{\Sigma CO2/g}$ which was dependent on the $[CO_3^{2-}]$ in sea water.

Given the good agreement between the values of $\epsilon_{b/a}$ determined by Vogel *et al.* (1970) / Mook *et al.* (1974) and Zhang *et al.* (1995) it will be assumed the values of $\epsilon_{b/a}$ determined by Mook *et al.* (1974) are correct and that any apparent pH isotope effect can be attributed to $\epsilon_{c/b}$ which is not well known. The values of $\epsilon_{c/b}$ at different pHs and temperatures have been calculated for experiments 1 and 2 using eqns. 4.3 and 5.2. The

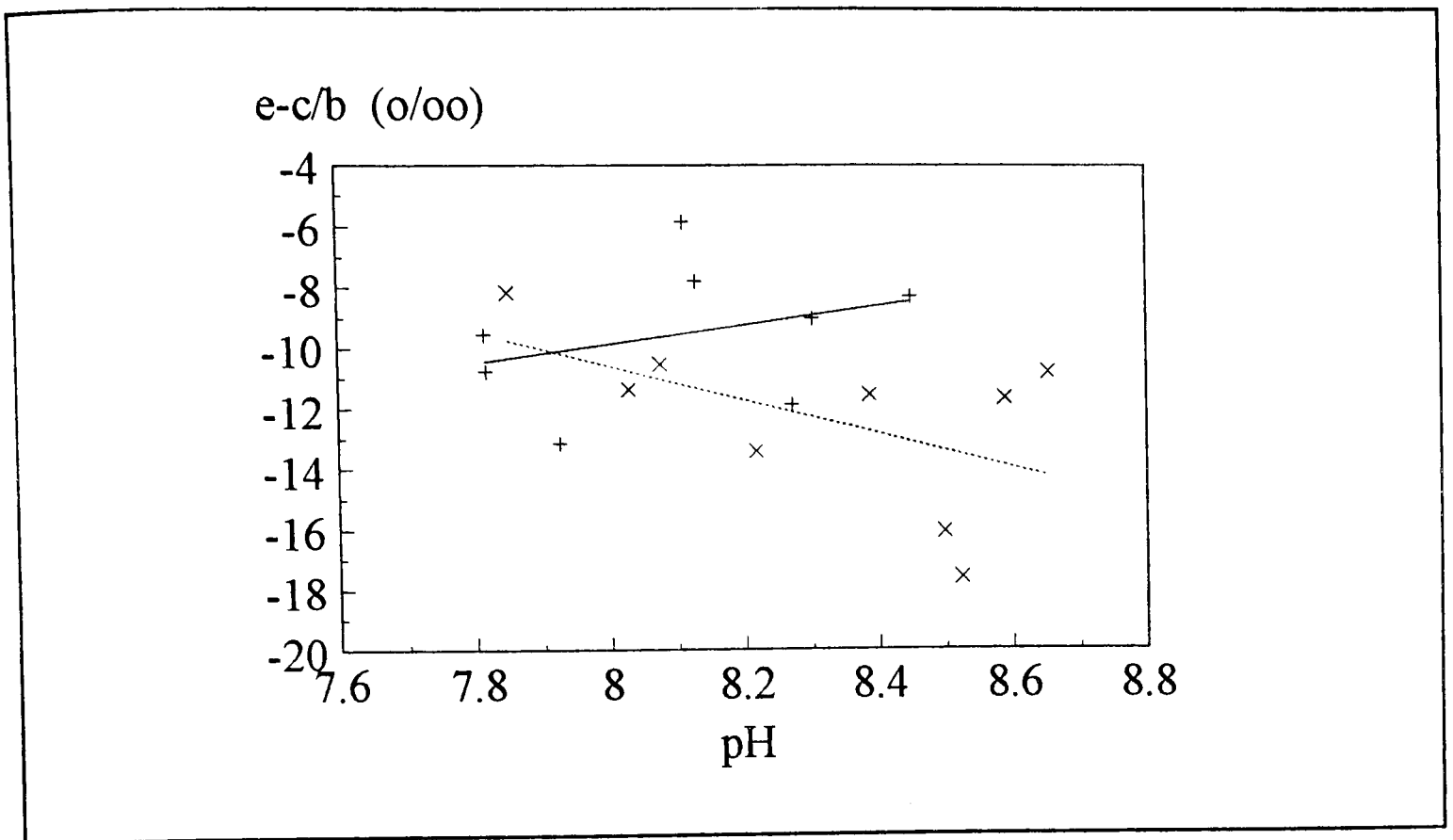

Figure 5.7 The effect of pH on $\epsilon_{c/b}$ at two temperatures, 20°C (+) and 5°C (×), if it is assumed the values of $\epsilon_{b/a}$ determined by Vogel *et al.*(1970) / Mook *et al.*(1974) are correct. The lines represent the best linear fit and can be described by the following equations: $\epsilon_{c/b}$ (20°C) = -35.0 (±2.4) + 3.1 (±3.9) × pH ($r^2 = 0.1$) (solid line) and $\epsilon_{c/b}$ (5°C) = 34.2 (±2.6) - 5.6 (±3.3) × pH ($r^2 = 0.3$) (dashed line).

results obtained in this manner are given in *TABLE* 5.2 and are plotted in *FIGURE* 5.7. Linear regressions of the data are also plotted and the relevant equations are given in the legend. From the low r^2 values it is apparent that there is no correlation between $\epsilon_{c/b}$ and pH. The value of $\epsilon_{c/b}$ can therefore be estimated by calculating the mean value of $\epsilon_{c/b}$ for each temperature; $\epsilon_{c/b} = -9.5 \pm 2.3$ ‰ at 20°C, and $\epsilon_{c/b} = -12.3 \pm 2.9$ ‰ at 5°C. The values of $\epsilon_{c/b}$ calculated from experiments 1 and 2 are somewhat larger than the values determined by previous studies (see *FIGURE* 4.5).

3. Finally, if it is assumed that neither $\epsilon_{b/a}$ or $\epsilon_{c/b}$ should show any pH dependence and that previously derived estimates are not applicable to sea water, it is possible to iteratively fit the experimental results to fractionation factors which are independent of pH. This can be achieved by substituting different values of $\epsilon_{c/b}$ into eqn. 5.1 until the gradient of $\epsilon_{b/a}$ versus pH approaches zero. *TABLE* 5.3 gives the calculated values of $\alpha_{b/a}$ and $\epsilon_{b/a}$

Table 5.3 The values of $\epsilon_{b/a}$ and $\epsilon_{c/b}$ that have been iteratively fitted to the experimental results so neither enrichment factor show any pH dependence. The values of $\epsilon_{c/b}$ - estimated are the values calculated by substituting the fitted value of $\epsilon_{b/a}$ into eqn. 5.2 to estimate the errors associated with the fitted value of $\epsilon_{c/b}$. The results of previous studies are given for comparison.

Expt	Temp. (°C)	S	$\alpha_{b/a}$ - fitted	$\epsilon_{b/a}$ - fitted	$\epsilon_{b/a}$, Vogel *et al.* (1970) / Mook *et al.*(1974)	$\epsilon_{b/a}$, Zhang *et al.* (1995)		
1	20	35	1.00948 $\pm 2.6\times10^{-4}$	9.48 ± 0.26	9.64	9.71	-	-
2	5	34	1.001167 $\pm 3.4\times10^{-4}$	11.67 ± 0.34	11.49	11.53	-	-
3	20	0	1.0095 $\pm 1.1\times10^{-3}$	9.5 ± 1.2	9.64	9.71	-	-
Expt	**Temp. (°C)**	**S**	**$\alpha_{c/b}$ - fitted**	**$\epsilon_{c/b}$ - fitted**	**$\alpha_{c/b}$ - estimated**	**$\epsilon_{c/b}$ - estimated**	**$\epsilon_{c/b}$, Thode *et al.* (1965) / Mook *et al.*(1974)**	**$\epsilon_{c/b}$, Zhang *et al.* (1995)**
1	20	35	0.99196	-8.037	0.9919 $\pm 2.2\times10^{-3}$	-8.1 ± 2.2	-0.42	-2.25
2	5	34	0.98561	-14.3	0.9858 $\pm 2.4\times10^{-3}$	-14.2 ± 2.4	-0.57	-3.24
3	20	0	0.9480	-52.0	0.939 $\pm 1.6\times10^{-2}$	-61 ± 16	-0.42	-2.25

along with the fitted values of $\alpha_{c/b}$ and $\epsilon_{c/b}$ and the values of $\epsilon_{b/a}$ calculated for the individual runs are also plotted in *FIGURE* 5.8. The mean value of $\epsilon_{b/a}$ was then substituted into eqn. 5.2 for each run at the different temperatures to determine the errors associated with the fitted values of $\epsilon_{c/b}$, the values of $\epsilon_{c/b}$ determined in this way and the errors are also given in *TABLE* 5.3. The mean values of $\epsilon_{b/a}$ calculated using this approach are not significantly different from the values determined by Mook *et al.* (1974) or Zhang *et al.* (1995). However, the fitted values of $\epsilon_{c/b}$ are considerably more negative than the results of previous studies. The difference between the values of $\epsilon_{c/b}$ obtained by this approach and the values determined by Thode *et al.* (1965) and Zhang *et al.* (1995) at the two temperatures are significantly different. The relationship between $\alpha_{c/b}$ and temperature can be described by the following linear expression:

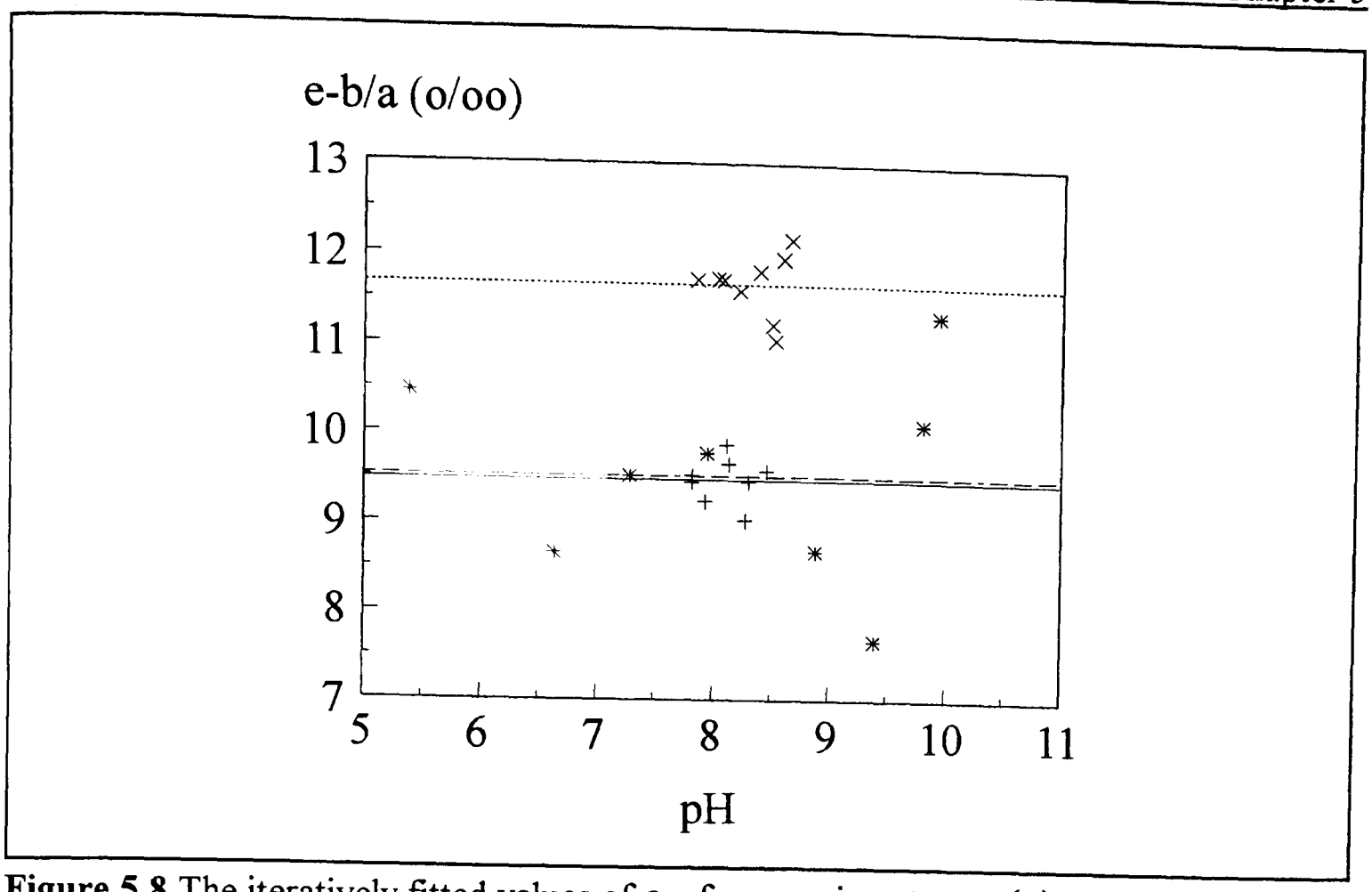

Figure 5.8 The iteratively fitted values of $\epsilon_{b/a}$ for experiments one (+), two (×) and three (*). The best fit lines for each experiment have also been given (solid, short dash, long dash respectively).

$$1000 \ln \alpha_{c/b} = -134 + 0.43 \times T \qquad \textbf{(5.4)}$$

Therefore by using this iterative approach any apparent dependency of $\epsilon_{b/a}$ and $\epsilon_{c/b}$ on pH can be eliminated. The calculated values of $\epsilon_{b/a}$ at the two temperatures also agree closely with the values determined by previous studies. However the estimated values of $\epsilon_{c/b}$ are considerably more negative than the values found by other studies (*e.g.* Thode *et al.*, 1965, Turner, 1982, Lesniak and Sakai, 1989, Zhang *et al.*, 1995) although the results do lie closer to the results of Zhang *et al.* (1995) which represent the most comprehensive set of experimentally derived data.

It has been suggested (Thode *et al.*, 1965, Zhang *et al.*, 1995) that the size of $\alpha_{c/b}$ maybe decreased in sea water due to the formation of $MgCO_3$ complexes which favour $^{13}CO_3^{2-}$. The experimental results presented here suggest that the opposite is true, *i.e.* the CO_3^{2-} is preferentially enriched in $^{12}CO_3^{2-}$. These measurements therefore represent the first attempt to directly determine $\alpha_{c/b}$ in sea water and although they maybe unexpected there seems to be no obvious reason to reject them.

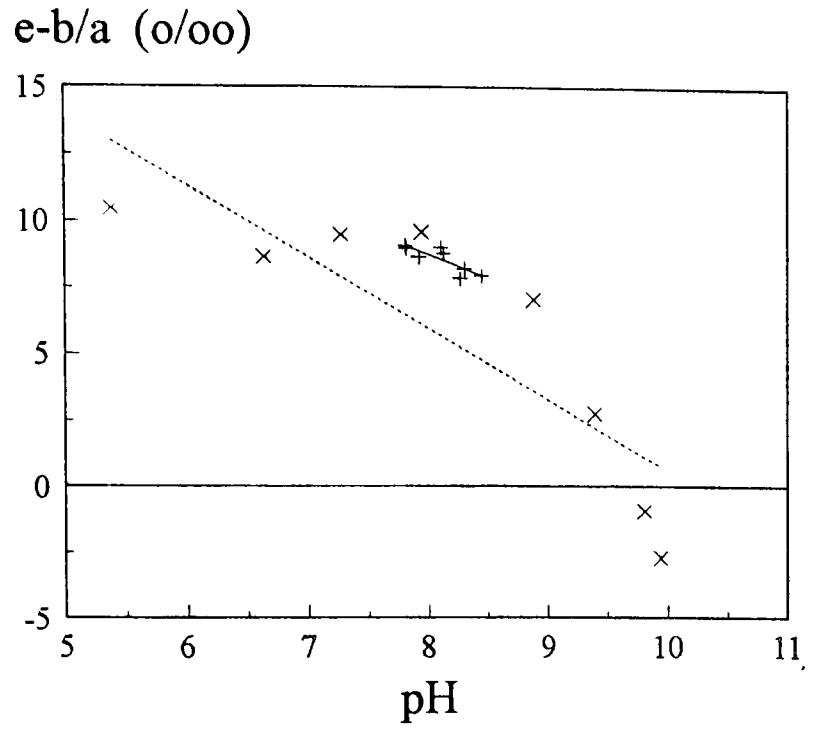

Figure 5.9 The pH related effect on the value of $\epsilon_{b/a}$ calculated using eqns. 5.1 and 4.2 and previously determined values of $\epsilon_{c/b}$. The results are from experiments one and three, conducted at two different salinities, 35 (+) and ~0 (×). The fitted lines can be described by the following linear expressions: $\epsilon_{b/a}$ = 22.97 (± 0.29) - 1.78 (± 0.47) × pH, (r^2 = 0.71) and $\epsilon_{b/a}$ = 27.4 (± 2.9) - 2.68 (± 0.67) × pH, (r^2 = 0.73) for experiments one and three respectively.

5.3.3 The pH Related Effect on $\alpha_{b/a}$ and $\alpha_{c/b}$ at Two Different Salinities

To investigate the possible effect of pH on the fractionation and enrichment factors at two different salinities the results of experiments one and three will be used (*TABLE* 5.1). Experiment one was conducted using aged sea water and experiment three used distilled water. *FIGURE* 5.9 plots the effect of pH on $\epsilon_{b/a}$ calculated using eqn. 5.1 and the calculated values are also given in *TABLE* 5.2. Despite the similar r^2 values obtained for the linear regressions performed on both data sets (see legend, *FIGURE* 5.9) the calculated standard errors associated with both the constant and the slope for experiment three are larger than experiment one. Inspection of *FIGURE* 5.9 indicates that the data from experiment 3 is probably best described by a non-linear fit. In fact the form of the line resembles a portion of the hypothesised sigmoidal fit which may be expected if the fractionation factors associated with the hydration / dehydration and hydroxylation / dehydroxyaltion reaction are different. The line would be expected to show another plateau as the pH increased above 11. However, such a hypothesis is not thermodynamically consistent and therefore the results will be discussed in the context of the three possible

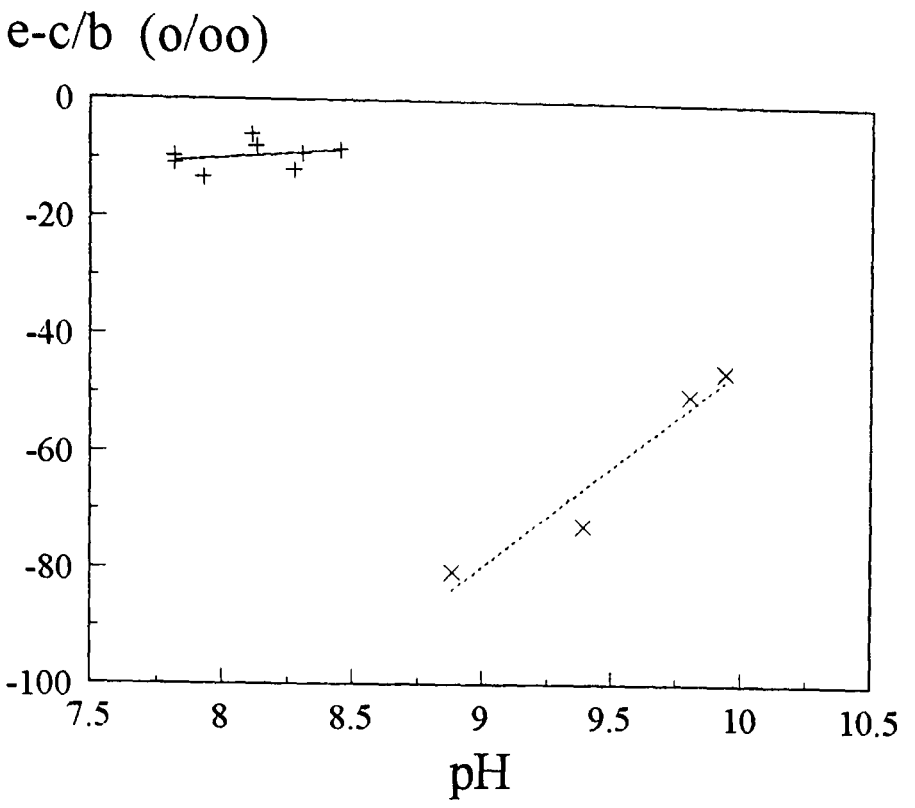

Figure 5.10 Variations in $\epsilon_{c/b}$ with pH at two different salinities, 35 (+) and ~0 (×). The best fit lines can be described by the following equations for each salinity respectively: $\epsilon_{c/b}$ = -35.0 (±2.4) + 3.1 (±3.9) × pH (r^2 = 0.1) and $\epsilon_{c/b}$ = -390.7 (±5.4) + 34.6 (±6.5) × pH (r^2 = 0.9).

factors (see page 80) that may give rise to such a pH effect.

1. It was previously suggested that the data obtained from experiments conducted at pHs greater than ~8.1 maybe erroneous because isotopic equilibrium may not have been achieved within the closed system by the end of the experiment. Due to the higher pHs in experiment 3 the volume of the upper reaction vessel was increased to 5 dm^3 and as a result the likelihood of a more persistent disequilibrium was increased. Therefore if the values of $\epsilon_{b/a}$ obtained by runs conducted at pHs of <~8.1 are averaged it is found that $\epsilon_{b/a}$ = 8.90 ‰ ± 0.18 (S = 35) and $\epsilon_{b/a}$ = 9.54 ‰ ± 0.74 (S=0). The value of $\epsilon_{b/a}$ calculated for experiment three agrees well and is not significantly different from the values obtained by Mook *et al.* (1974) and Zhang *et al.* (1995) (*TABLE* 5.3). However, the calculated value of $\epsilon_{b/a}$ for experiment one is significantly lower than the value determined by the previous studies, although it is not significantly different from the value obtained from experiment three due to the large standard error associated with this result. As the pH range of experiment one was limited the [CO_3^{2-}] contributed between 5 and 10% to the [ΣCO_2] during the runs conducted at low pHs. If the previously estimated value of $\epsilon_{c/b}$ is incorrect this proportion

of CO_3^{2-} is sufficient to decrease the calculated value of $\epsilon_{b/a}$. This was demonstrated at the end of the previous section.

2. If it is assumed that the value of $\epsilon_{b/a}$ determined by previous studies is correct the value of $\epsilon_{c/b}$ can be calculated using eqn. 5.2. The results are given in *TABLE* 5.2 and *FIGURE* 5.10. The values of $\epsilon_{c/b}$ have not been calculated for the first few runs of experiment three. This is because the $[CO_3^{2-}]$ contributed <0.3% to the $[\Sigma CO_2]$ which is less than the standard error associated with the manometric determination of $[\Sigma CO_2]$ (σ_{n-1} = 0.5%). The statistical information relating to the linear regressions performed on the calculated values of $\epsilon_{c/b}$ (see legend, *FIGURE* 5.10) for experiment three indicate the data is well described by a linear relationship. The values of $\epsilon_{c/b}$ for experiment three are somewhat larger than the values calculated for experiment one and those determined during previous studies and show a high degree of pH dependence, changing from ~ -80‰ to ~-50‰ over a range of one pH unit. However the values of $\epsilon_{c/b}$ calculated from experiment 1 are not dependent on pH as shown by the low value of r^2 (0.1).

3. Thermodynamic theory suggests that the fractionation factors should not be dependent on pH. It is therefore possible to iteratively fit a value of $\epsilon_{c/b}$ to the results of experiment three using eqn. 5.1 so that neither $\epsilon_{b/a}$ or $\epsilon_{c/b}$ are pH dependent. The fitted value of $\epsilon_{c/b}$ along with the mean value of $\epsilon_{b/a}$ is given in *TABLE* 5.3 and plotted in *FIGURE* 5.8. Despite the large error associated with the estimate of $\epsilon_{b/a}$ the average value agrees very well with the results of Mook *et al.* (1974) and Zhang *et al.* (1995) and the value of $\epsilon_{b/a}$ estimated from experiment one using the same fitting procedure (*TABLE* 5.3).

The fitted value of $\epsilon_{c/b}$ (-52‰) is very large in comparison with the values determined in previous theoretical and experimental studies ($\epsilon_{c/b}$ ≈-3.5 to -0.5 ‰). The errors associated with this value were estimated by substituting the fitted value of $\epsilon_{b/a}$ into eqn. 5.2 for each run. It was found that the values of $\epsilon_{c/b}$ calculated in this manner were highly scattered, particularly when the pH was low. This was attributed to the low $[CO_3^{2-}]$ and as a result these values were omitted when estimating the errors associated with $\epsilon_{c/b}$. The value of $\epsilon_{c/b}$ and its errors calculated in this manner are given in *TABLE* 5.3. The errors associated with this value are large and therefore it is probably not wise to draw any conclusions from this estimate.

5.4 Summary

The aim of this section of the thesis was to directly determine the fractionation factors associated with the ΣCO_2 system in sea water.

The results obtained by applying a predetermined fractionation factor to calculate an unknown fractionation factor appeared to suggest $\epsilon_{b/a}$ and/or $\epsilon_{c/b}$ maybe pH dependent. However, using an iterative approach, to fit both $\epsilon_{b/a}$ and $\epsilon_{c/b}$ simultaneously to a set of results, any apparent pH dependence was eliminated and the values of $\epsilon_{b/a}$ obtained in this manner, at different temperatures agree closely with the results of previous studies (*TABLE* 5.3). The values of $\epsilon_{b/a}$ determined at the same temperature in distilled water and sea water do not differ significantly and therefore indicate there is no ionic dependent isotope effect associated with $\epsilon_{b/a}$.

The values of $\epsilon_{c/b}$ for the sea water experiments, which were again calculated using the iterative procedure, were somewhat larger than both the theoretical predictions of Thode *et al.* (1965) and the experimental results of Zhang *et al.* (1995). Although these experimental results represent the first attempt to directly determine $\epsilon_{c/b}$ in sea water earlier studies have suggested that the isotope effects associated with the HCO_3^-/CO_3^{2-} reaction in sea water maybe diminished (relative to the values obtained for measurements made in media with a low ionic strength) due to the formation of $MgCO_3$ complexes which appear to be preferentially enriched in $^{13}CO_3^{2-}$ (Thode *et al.*, 1965). Therefore these results suggest that there is an ionic isotope effect associated with $\epsilon_{b/c}$ although the magnitude and direction of this effect is not as predicted by previous studies.

The results of experiment three, which was conducted in distilled water, again appear to generally confirm the previously determined values of $\epsilon_{b/a}$ but also suggest the $\epsilon_{c/b}$ is very large and negative. As the discrepancy between the results of this experiment and the previous studies is very large, it would seem prudent to reject the value of $\epsilon_{c/b}$ determined by this experiment.

Given the large discrepancy between the values of $\epsilon_{c/b}$ determined during this study and previous studies, it would seem likely that there maybe an inherent deficiency associated with the experimental apparatus and/or experimental methodology used during this study.

However, there does not appear to be any obvious reason to suspect the experimental apparatus or experimental design. The most likely source of variability and as a result, the largest source of error is the relative lack of precision associated with the determination of $\delta^{13}C_{\Sigma CO2}$. Therefore, if this work were to be repeated a necessary modification would be to run replicate $\delta^{13}C_{\Sigma CO2}$ samples to reduce variation associated with this result. It is recommended that at least three replicates should be run to maximise the accuracy of the determination. Similarly, given the potential of a persistent disequilibrium between the gaseous and aqueous phases, particularly at the higher pHs, it would seem sensible to confirm the rate at which isotopic equilibrium is achieved over a range of pHs.

Chapter 6: Changes in the Isotopic Composition of Particulate Organic Carbon and Dissolved Inorganic Carbon During an Algal Bloom in a Mesocosm.

6.1 Introduction

The isotopic composition of phytoplankton in the marine environment varies widely (-35 to -18 ‰, Goericke and Fry, 1994), both temporally (Rau *et al.*, 1992) and spatially (Fontugne and Duplessey, 1981, Rau *et al.*, 1991a, 1991b, Francois *et al.*, 1993). As a result of experiments conducted both in the laboratory and in the field, numerous factors have been suggested to account for the observed variations: species composition of the phytoplankton (Falkowski, 1991), temperature (Degens *et al.*, 1968, Fontugne and Duplessey, 1981, Goericke and Fry, 1994), the metabolic pathway used during the fixation of inorganic carbon (Descolas-Gross and Fontugne, 1985, Beardall *et al.*, 1976), the $[CO_{2(aq)}]$ (Rau *et al.*, 1992), growth rate (Goericke *et al.*, 1994, Laws *et al.*, 1995), cell size (Goericke *et al.*, 1994), the active uptake of inorganic carbon (Raven and Johnston, 1991, Sharkey and Berry, 1985) and the permeability of the cell wall (Rau *et al.*, 1992, Francois *et al.*, 1993).

However, despite the apparent complexity it has been shown that a simple negative linear relationship between $[CO_{2(aq)}]$ and the isotopic composition of suspended particulate organic matter ($\delta^{13}C_{POC}$) can account for 89% of the variation in the $\delta^{13}C_{POC}$ seen in today's oceans (Rau *et al.*, 1992). Similar non - linear (Jasper and Hayes, 1994) and logarithmic (Popp *et al.*, 1989) models relating $[CO_{2(aq)}]$ to the isotopic enrichment between $CO_{2(aq)}$ and POC, $\epsilon_{POC/a}$ (see eqns. 3.4 and 3.5 for definition), have been developed which appear equally effective (Rau, 1994) at describing present day observations.

Research into the existence of a simple relationship between $[CO_{2(aq)}]$ and $\delta^{13}C_{POC}$ or $\epsilon_{POC/a}$ has been primarily stimulated by the possibility that the $[CO_{2(aq)}]$ in ancient oceans may be reconstructed from changes in the $\delta^{13}C_{POC}$ and/or algal specific biomarkers preserved in the sedimentary records, and ultimately, assuming air/sea equilibrium, atmospheric levels of $CO_{2(g)}$ (Rau, 1994, Jasper and Hayes, 1994). However, accurate reconstruction of ancient $[CO_{2(aq)}]$ ultimately requires an understanding of the physiological processes involved during the acquisition of inorganic carbon in case environmental perturbations have altered any apparent relationship derived from modern oceans (Rau *et al.*, 1992, Francois

et al., 1993). Despite the success of these simple models, attempts have been made to introduce a greater degree of physiological correctness into the models by accounting for changes in the demand of $CO_{2(aq)}$ relative to its supply (Rau *et al.*, 1992, Francois *et al.*, 1993). Other basic physiological models have tried to account for the existence of active uptake systems (Sharkey and Berry, 1985, Hayes, 1993) and different metabolic pathways (Goericke *et al.*, 1994).

Within the oceanic environment the $\delta^{13}C_{POC}$ probably closely represents the isotopic composition of the phytoplankton ($\delta^{13}C_P$). However, in certain regions, such as coastal areas, the relative contribution of detritus to the overall POC pool may be greater and hence, if the isotopic composition of the detritus is not similar to the $\delta^{13}C_P$, alter any apparent relationship between the bulk $\delta^{13}C_{POC}$ and $[CO_{2(aq)}]$. Similarly, when the phytoplankton growth is rapid the $\delta^{13}C_{POC}$ and $\delta^{13}C_P$ will not reflect the isotopic composition of freshly formed organic matter (*e.g.* Raven and Johnston, 1991). Under such circumstances it maybe necessary to study the isotopic composition of algal specific compounds such as alkenones (*e.g.* Jasper and Hayes, 1994) or porphyrins (*e.g.* Hayes *et al.*, 1989). During this study it will be generally assumed that the $\delta^{13}C_{POC}$ is equivalent to $\delta^{13}C_P$.

This section will firstly review the possible mechanisms by which inorganic carbon may be acquired by marine microalgae and then discuss the results obtained during a mesocosm study in the context of some of the models and mechanisms which have been suggested.

6.2 The Uptake of Inorganic Carbon by Marine Phytoplankton

Terrestrial plants can be divided into two distinct metabolic groups on the basis of their isotopic composition; C_3 plants, which use Rubisco (ribulose 1,5 - bisphosphate carboxylase - oxygenase) as the primary carboxylation enzyme during the fixation of inorganic carbon ($\delta^{13}C$ = -28.1 ± 2.5 ‰, O'Leary, 1981) and C_4 plants which utilise PEPC (phosphoenolpyruvate carboxylase) (-13.5 ± 1.5 ‰, O'Leary, 1981). The isotopic distinction between the two groups has been primarily attributed to the different enrichment factors associated with Rubisco (-29 ‰, Roeske and O'Leary, 1984) and PEPC (-2 ‰, O'Leary *et al.*, 1981) and the isotopic composition of the inorganic substrate, CO_2 for

Rubisco and HCO_3^- for PEPC. An additional β-carboxylation enzyme (*i.e.* C_4 type metabolism) is also found in algae, PEPCK (PEP-carboxykinase) which appears to have a variable enrichment factor (-24 to -40 ‰, Arnelle and O'Leary, 1992) and uses CO_2 as its substrate.

The wide variation in the isotopic composition of marine phytoplankton has lead to the suggestion that different species of algae may employ either C_3 or C_4 metabolisms (Descolas-Gross and Fontugne, 1990). Direct measurements of the activities of PEPC and PEPCK in natural phytoplankton communities have indicated the presence of both enzymes, although the activity of PEPCK was normally greater than PEPC (Descolas-Gross and Fontugne, 1988, 1990). Culture experiments using *Skeletonema costatum* have indicated the activity of PEPCK relative to Rubisco is low (PEPCK : Rubisco < 0.01) (Descolas-Gross and Fontugne, 1985). Similarly, short term incubation experiments ($H^{14}CO_3^-$) using a variety of species have indicated that primary carboxylation was mediated by Rubisco (*e.g.* Kerby and Raven, 1985) and if β-carboxylation did occur it could not account for more than 25% of the net carbon fixation in phytoplankton (Beardall, 1989). At present it seems to be generally agreed that all marine phytoplankton posses typical C_3 metabolisms (Raven and Johnston, 1991, Goericke *et al.*, 1994) and even those species with C_4 characteristics, such as the high activity of β-carboxylation enzymes, are in fact C_3 with "C_4-like" gas exchange characteristics (Kerby and Raven, 1985). Therefore it seems unlikely that the diverse isotopic composition of oceanic phytoplankton can be simply attributed to different metabolic pathways.

As all marine phytoplankton appear to be characterised by C_3 metabolic pathways, CO_2 must ultimately be the inorganic substrate fixed during carboxylation. If it is assumed that all of the CO_2 fixed enters the cell by passive diffusion it is possible to represent the uptake of inorganic carbon by a simple two step process as follows (O'Leary, 1981, Francois *et al.*, 1993):

$$C_e \underset{k_{-1}}{\overset{k_1}{\rightleftharpoons}} C_i \xrightarrow{k_2} C_{org} \qquad \textbf{(6.1)}$$

where C_e is the $[CO_{2(aq)}]$ in the bulk medium, C_i is the $[CO_{2(aq)}]$ within the cell, C_{org} is the photosynthate, k_1 and k_{-1} are the diffusional rates of CO_2 into and out of the cell and k_2 is the rate of the irreversible carboxylation reaction. Each step in the above reaction will also fractionate the isotopes to a different extent. The isotopic fractionation associated with the diffusion of $CO_{2(aq)}$ is small, -0.7 ‰ (O'Leary, 1984) and as the fractionation associated with diffusion into the cell is the same as the reverse process, at equilibrium there will be no net fractionation associated with this step. The isotopic enrichment associated with the fixation of CO_2 by Rubisco present in phytoplankton has not been directly determined although evidence indicates (Raven and Johnston, 1991) that it is similar to the value found in higher plants, -29 ± 1 ‰ (Roeske and O'Leary, 1984).

If a slowly growing phytoplankton cell is considered, the internal carbon pool will be in chemical and isotopic equilibrium with the external medium and the isotopic fractionation associated with Rubisco will be fully expressed and hence $\epsilon_{POC/a}$ = -29 ‰. As the $\delta^{13}C_a$ within the oceans varies from ~-7.5 ‰ to ~-10.0 ‰ (Francois *et al.*, 1993), depending on the temperature, the expected minimum $\delta^{13}C_{POC}$ would be expected to be -36.5 ‰ to -39.0 ‰, which is close to the minimum values observed in the southern ocean, -35 ‰ (Goericke and Fry, 1994). Alternatively for a phytoplankton cell whose growth rate is high and all the available $CO_{2(aq)}$ that diffuses into the cell is fixed, $\epsilon_{POC/a}$ would be expected to approach or equal the isotopic fractionation associated with the diffusion of $CO_{2(aq)}$. Therefore the maximum expected $\delta^{13}C_{POC}$ value would be expected to approach or be equal to -8 ‰ to -11‰. The maximum value observed in the present day ocean is ~-16 ‰ (Rau, 1994), somewhat lower than the predicted maximum. However, algae would only be expected to approach the maximum isotopic composition under conditions of high growth and low $[CO_{2(aq)}]$, which is probably not common within the marine environment.

Experimental evidence suggests (*e.g.* Bowes, 1985, Beardall, 1985, Burns and Beardall, 1987, Sharkey and Berry, 1985, Raven and Johnston, 1991) that some marine phytoplankton posses the ability to take up inorganic carbon ($CO_{2(aq)}$ and/or HCO_3^-) actively (Badger, 1987), but do not seem to actively concentrate inorganic carbon intracellularly relative to the concentration in sea water (see Raven and Johnston, 1991, Goericke *et al.*, 1994). The active uptake of inorganic carbon when the $[CO_{2(aq)}]$ is low will enhance the productivity and alter the isotopic composition of the algae (Beardall *et al.*, 1982, Sharkey

and Berry, 1985). The change in the isotopic composition associated with the active uptake of inorganic carbon will depend on the isotopic composition of species actively transported (*i.e.* $CO_{2(aq)}$ or HCO_3^-) and the degree of 'leakiness' of the cell (*e.g.* Sharkey and Berry, 1985, Hayes, 1993). The degree of leakiness of the cell is a complex parameter which mainly depends on the permeability of the cell wall, the rate of active transport and the rate of carboxylation. Direct measurements of the enrichment factor associated with a culture of *Chlamydomonas reinhardtii* grown at low [$CO_{2(aq)}$] which was actively transporting inorganic carbon (Sharkey and Berry, 1985) found $\epsilon_{POC/a}$ =-4 ‰, although it was not known which species was transported, it was assumed to be HCO_3^-. The enrichment factor determined on the same culture, under high [$CO_{2(aq)}$], found $\epsilon_{POC/a}$ = -28‰, and when the culture was grown at low [$CO_{2(aq)}$] with the addition of a carbonic anhydrase (CA) inhibitor the enrichment factor increased from -4 ‰ and approached the levels measured in the high [$CO_{2(aq)}$] culture. The termination of active transport by the addition of a CA inhibitor and the subsequent change in $\epsilon_{POC/a}$ also indicates that the isotopic fractionation associated with Rubisco maybe fully expressed, even if [$CO_{2(aq)}$] is low. These experiments therefore provide a direct measure of $\epsilon_{POC/a}$ associated with a cell which is actively transporting inorganic carbon and indicate the apparent importance of CA to the carbon concentrating mechanism (CCM). Cultures of *Chlorella emersonii*, grown under conditions of low [$CO_{2(aq)}$], were found to have an $\epsilon_{POC/a}$ of -6.8 ‰ to -8.2 ‰, this was attributed to the operation of a CCM (Beardall *et al.*, 1982).

If it is assumed that the values of $\epsilon_{POC/a}$ determined in the above experiments (-4 to -8 ‰) are representative of a cell totally reliant on actively transported inorganic carbon the maximum value of $\delta^{13}C_{POC}$ observed in the oceans would be expected to be ~ -11.5 ‰ to ~-14 ‰, in fairly good agreement with the observed maximum (~-16 ‰). However, the isotopic composition of phytoplankton naturally varies between -37 ‰ to -16 ‰ and does not appear to consist of two distinct isotopic groups representing algae with and without the ability to actively take up inorganic carbon. This graded variability may therefore indicate that the contribution made by actively transported carbon to the overall carbon requirement of the cell may vary in a controlled fashion, for example, in response to [$CO_{2(aq)}$] and the photosynthetic demand for CO_2.

Therefore, in summary, three broad theories, concerning the acquisition and

fixation of inorganic carbon have been suggested to account for the variation in the $\delta^{13}C_{POC}$ observed in the ocean:

i. The passive diffusion of $CO_{2(aq)}$ into the cell folowed by fixation by Rubisco. The observed changes in the $\delta^{13}C_{POC}$ would therefore be attributed to the increasing isotopic disequilibrium between the ΣCO_2 within the cell and in the bulk medium as the $[CO_{2(aq)}]$ decreases and maybe a measure of the degree of carbon limitation.

ii. The use of different metabolic pathways, *i.e.* C_3 or C_4 types, during the fixation of inorganic carbon. The observed variation of $\delta^{13}C_{POC}$ with $CO_{2(aq)}$ could therefore be explained by changes in the relative proportion of phytoplankton with the differenr metabolic pathways.

iii. The active uptake of HCO_3^- by phytoplankton cells followed by carboxylation by Rubisco. The shift in the $\delta^{13}C_{POC}$ in relation to the $[CO_{2(aq)}]$ therefore represents a graded change in the relative proportions of $CO_{2(aq)}$ and HCO_3^- entering the cell, the amount of actively transported HCO_3^- increasing as the $[CO_{2(aq)}]$ decreases.

Various empirical models, *i.e.* derived from direct measurements made in the field (*e.g.* Popp *et al.*, 1989, Rau *et al.*, 1992, Rau, 1994, Jasper and Hayes, 1994), and physiological models, *i.e.* based on the different mechanisms of inorganic carbon uptake and fixation (*e.g.* Francois *et al.*, 1993, Hayes, 1993), have been developed in an attempt to account for the observed variations in the oceanic $\delta^{13}C_{POC}$ signal. These various model will be applied to the data presented in an attempt to determine the mechanisms and pathways which maybe used by the phytoplankton during the study periods.

6.3 Material and Methods

6.3.1 The Mesocosm Facility

The mesocosm facility was situated in a small, sheltered bay (Knebel vig) in the north of Jutland, Denmark. Each mesocosm was 1 m in diameter and ~4 m deep and was made from translucent polyethylene. The mesocosm was open to the atmosphere but closed to the

sediment. The water enclosed within the mesocosm was mixed by a wind driven paddle so the rate of mixing was dependent on the wind speed. The experiment was initiated by the addition of nutrients (12 July 1992, day 0), nitrate and phosphate, so the initial concentrations in the bag were 21 $\mu mol.dm^{-3}$ and 2 $\mu mol.dm^{-3}$ respectively. An additional, unscheduled nitrate addition of unknown concentration was also made on the 25 July (day 13).

6.3.2 Sampling and Analysis

A depth integrated water sample was obtained every day from the mesocosm by combining equal volumes of pre-screened (200 μm mesh) water taken from the surface, mid-depth, and bottom of the mesocosm using a hand held water sampler (2 dm^3). The water sample was returned to the field laboratory for processing where aliquots were removed for the determination of POC, PON, $\delta^{13}C_{POC}$, chlorophyll, nitrate, phosphate and silicate.

POC and PON samples were obtained by filtering an appropriate volume of the depth integrated sample through a 25 mm, precombusted (500°C), Whatman GF/F filter. The filters were then stored frozen (-20°C) until required for analysis. Just prior to analysis the samples were removed from the freezer and acid fumed overnight (concentrated HCl) to remove any inorganic carbonate which maybe present. The POC and PON content of the sample was then determined using a Europa Roboprep PCN analyser.

Samples for the determination of $\delta^{13}C_{POC}$ were similarly treated, although 47 mm, precombusted (500°C), Whatman GF/F filters were used instead. The $\delta^{13}C_{POC}$ (± 0.1 ‰) was determined from acid fumed samples using conventional off-line Dumas combustion methods in sealed quartz tubes, followed by cryogenic distillation under vacuum to clean the liberated $CO_{2(g)}$. The isotope ratio was determined using a V.G. Isogas Sira II mass spectrometer. A detailed account of the exact methodology is given in *APPENDIX* 2.

The concentration of chlorophyll within the mesocosm was determined using a technique described by Jespersen and Christifferson (1987) (±0.5 $\mu gChl.dm^{-3}$) which uses ethanol as the extraction solvent. Nutrient determinations were carried out every three days using the methods described by Parsons *et al.* (1984b). The samples taken on days when nutrient determinations were not carried out were frozen until required.

Table 6.1 Data from samples collected during the mesocosm experiment. * indicates the data has been interpolated.

Date	Day	Salinity	Temp. (°C)	Silicate (µM)	Phosphate (µM)	Nitrate (µM)	$[\Sigma CO_2]$ (µmol/kg)	$\delta^{13}C$ ΣCO_2 (‰)	POC (µM)	$\delta^{13}C$ POC (‰)	Chl. (µg/l)
12-Jul-92	0	16.65	19.6*	2.2	1.97	21.2	1675	-0.11	87.5	-17.99	-
13-Jul-92	1	16.64	19.6	2.4	1.9	17.8	1674	0.201	80	-18.45	1.46
14-Jul-92	2	-	18.95	2.1	1.56	7.5	1627*	0.544*	93	-14.41	-
15-Jul-92	3	16.63	17.8	-	0.68	3	1579	0.886	127	-11.68	16.6
16-Jul-92	4	-	17.3	1.9	0.8	0.3	1494	0.782	224	-9.76	-
17-Jul-92	5	-	17.7	1.4	0.7	-	1427	1.153	308	-8.29	15.3
18-Jul-92	6	-	18.1	-	0.29	0.17	1366*	1.456*	307	-8.06	14.7
19-Jul-92	7	-	17.7	2.1	-	0.02	1305	1.758	425	-7.36	12
20-Jul-92	8	16.88	18.4	1.8	1.38	0.48	1319	1.35	343	-7	9.6
21-Jul-92	9	-	19.35	1.6	0.17	1.46	1300	1.108	423	-7.59	7.8
22-Jul-92	10	-	18.85	1.5	0.1	0.24	1368	1.229	460	-7.04	8
23-Jul-92	11	-	18.6	1.1	0.2	0.38	1327	1.443	416	-7.25	5.9
24-Jul-92	12	-	19.3	1.2	0.3	0.09	1356	1.400*	417	-6.4	7.5
25-Jul-92	13	-	19.5	1.2	-	0.13	1392	1.357	265	-8.3	3.7
26-Jul-92	14	-	19.7	0.74	0.2	-	1422	1.081	300	-7.25	4.2
27-Jul-92	15	-	19.15	1.1	0.1	1.25	1444	0.732	363	-7.43	4.8
28-Jul-92	16	-	19.15*	0.92	-	0.72	1499	0.635	214	-8.66	9.7
29-Jul-92	17	-	19.15*	0.76	0.15	0.13	1496	0.606	226	-8.45	14.3

Samples for the determination of $\delta^{13}C_{\Sigma CO2}$ (± 0.05 ‰) and $[\Sigma CO_2]$ (± 10 µmol.kg^{-1}) were also taken everyday. However, due to the sensitive nature of the ΣCO_2 system caution was exercised to avoid the loss, or gain of $CO_{2(g)}$ from, or to, the sample. Samples were therefore directly obtained from the hand held sampler by transferring the water sample to a 250 cm^3 borosilicate glass bottle, via a sample tube in the field. The sample was then immediately poisoned with saturated mercuric chloride solution (250 µdm^3 per 250 cm^3) before it was returned to the laboratory, in a cool box, and filtered under a nitrogen ($CO_{2(g)}$ free) atmosphere in to a pre - weighed 10 cm^3 borosilicate ampoule which was flame sealed for permanent storage. The ΣCO_2 was liberated from the sample by acidification (H_3PO_4) under vacuum followed by cryogenic distillation to purify the $CO_{2(g)}$ (McCorkle *et al.*, 1985). The $[\Sigma CO_2]$ was obtained manometrically prior to mass spectrometric determination. A detailed account of the methodology is given in *APPENDIX* 1.

The temperature of the mesocosm was monitored daily. Salinity samples were taken infrequently during the experiment and stored in dedicated salinity bottles prior to determination using a standardised Autosal (Model 8400 A) salinometer (σ_{n-1}=0.02).

Table 6.2 Calculated parameters of the ΣCO_2 system. The values have been calculated by assuming the [TA] remained constant (1803 $\mu eq.kg^{-1}$) throughout the experiment. * indicates data has been interpolated.

Day	Temp. (°C)	Salinity (average)	$[\Sigma CO_2]$ (µmol/kg)	$[CO_{2(aq)}]$ (µmol/kg)	$[HCO_3^-]$ (µmol/kg)	$[CO_3^{2-}]$ (µmol/kg)	pH_{sws}	pCO2 µatm/kg
0	19.6*	16.7	1675	12.85	1557	106	8.077	355
1	19.6	16.7	1674	12.71	1555	106	8.081	351
2	18.95	16.7	1627*	8.73	1480	139	8.229	237
3	17.8	16.7	1579	6.15	1400	173	8.368	161
4	17.3	16.7	1494	3.61	1255	235	8.558	93.2
5	17.7	16.7	1427	2.47	1140	285	8.676	64.6
6	18.1	16.7	1366*	1.77	1034	330	8.776	46.7
7	17.7	16.7	1305	1.24	928	375	8.885	32.5
8	18.4	16.7	1319	1.36	953	365	8.85	36.4
9	19.35	16.7	1300	1.25	920	379	8.864	34.2
10	18.85	16.7	1368	1.81	1038	329	8.759	49
11	18.6	16.7	1327	1.43	967	359	8.833	38.5
12	19.3	16.7	1356	1.71	1017	338	8.772	46.8
13	19.5	16.7	1392	2.09	1079	311	8.707	57.7
14	19.7	16.7	1422	2.48	1131	289	8.651	68.9
15	19.15	16.7	1444	2.79	1169	272	8.621	76
16	19.15*	16.7	1499	3.83	1263	232	8.517	104
17	19.15*	16.7	1496	3.76	1258	234	8.523	103

6.4 Results

6.4.1 The ΣCO_2 System

At least two macroscopic variables are required to define the ΣCO_2 system sufficiently to calculate the $[CO_{2(aq)}]$, $[HCO_3^-]$ and $[CO_3^{2-}]$. However, the only parameter of the ΣCO_2 system that was directly determined was the $[\Sigma CO_2]$, measured manometrically during the preparation of the $\delta^{13}C_{\Sigma CO2}$ samples.

Therefore, in order to obtain the necessary data it was assumed the pCO_2 of the water in the mesocosm was in equilibrium with the atmosphere (355 µatm, Keeling and Whorf, 1991) on day 0. By making this assumption it was possible to calculate the [TA] of

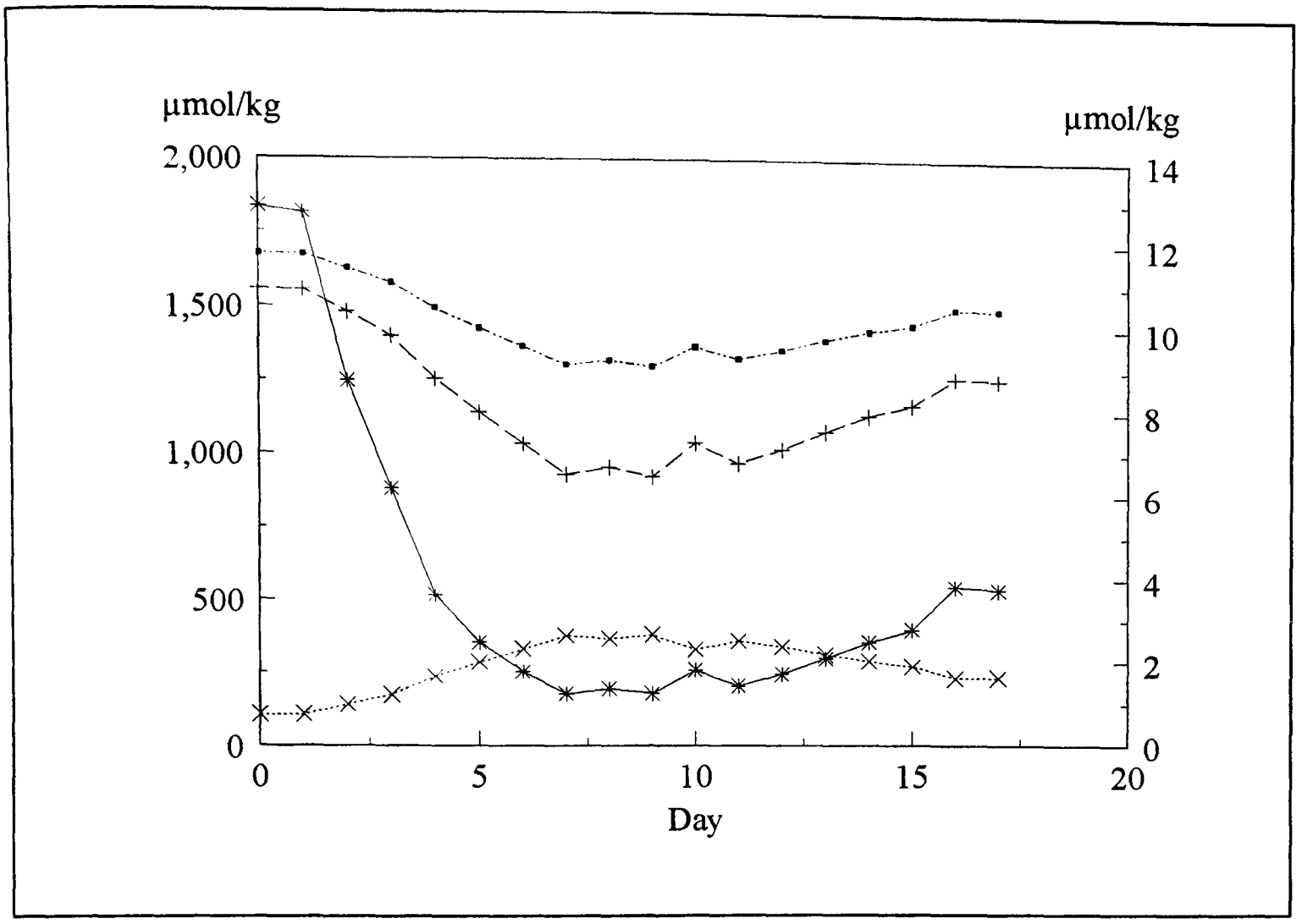

Figure 6.1 Variations the [ΣCO_2] (■), [HCO_3^-] (+), [CO_3^{2-}] (×) and [$CO_{2(aq)}$] (*). The [$CO_{2(aq)}$] has been plotted on the secondary y axis to aid clarity.

the mesocosm water using the sea water model. As TA is a conservative property (*i.e.* a temperature independent property if expressed using $\mu eq.kg^{-1}$) (Stumm and Morgan, 1981) which remains constant during the removal of CO_2 , the [TA] of the mesocosm should remain constant throughout the experimental period assuming no calcifying organisms were present and the effect of changes in the concentration of nitrate was negligible. Therefore, using the estimated [TA] (1803 $\mu eq.kg^{-1}$) in conjunction with the directly determined values of [ΣCO_2], temperature and salinity (*TABLE* 6.1), the values of other parameters associated with the ΣCO_2 system were calculated (*TABLE* 6.2, *FIGURE* 6.1). As salinity samples were only taken intermittently the average salinity was taken ($S = 16.7 \pm 0.1$) and assumed to remain constant.

Due to the loss of some samples the [ΣCO_2] data set was not complete. To aid subsequent modelling the [ΣCO_2], for the days where there was no information, was inferred by assuming it was equal to the mean of the [ΣCO_2] measured on the day prior and the day after the absent sample.

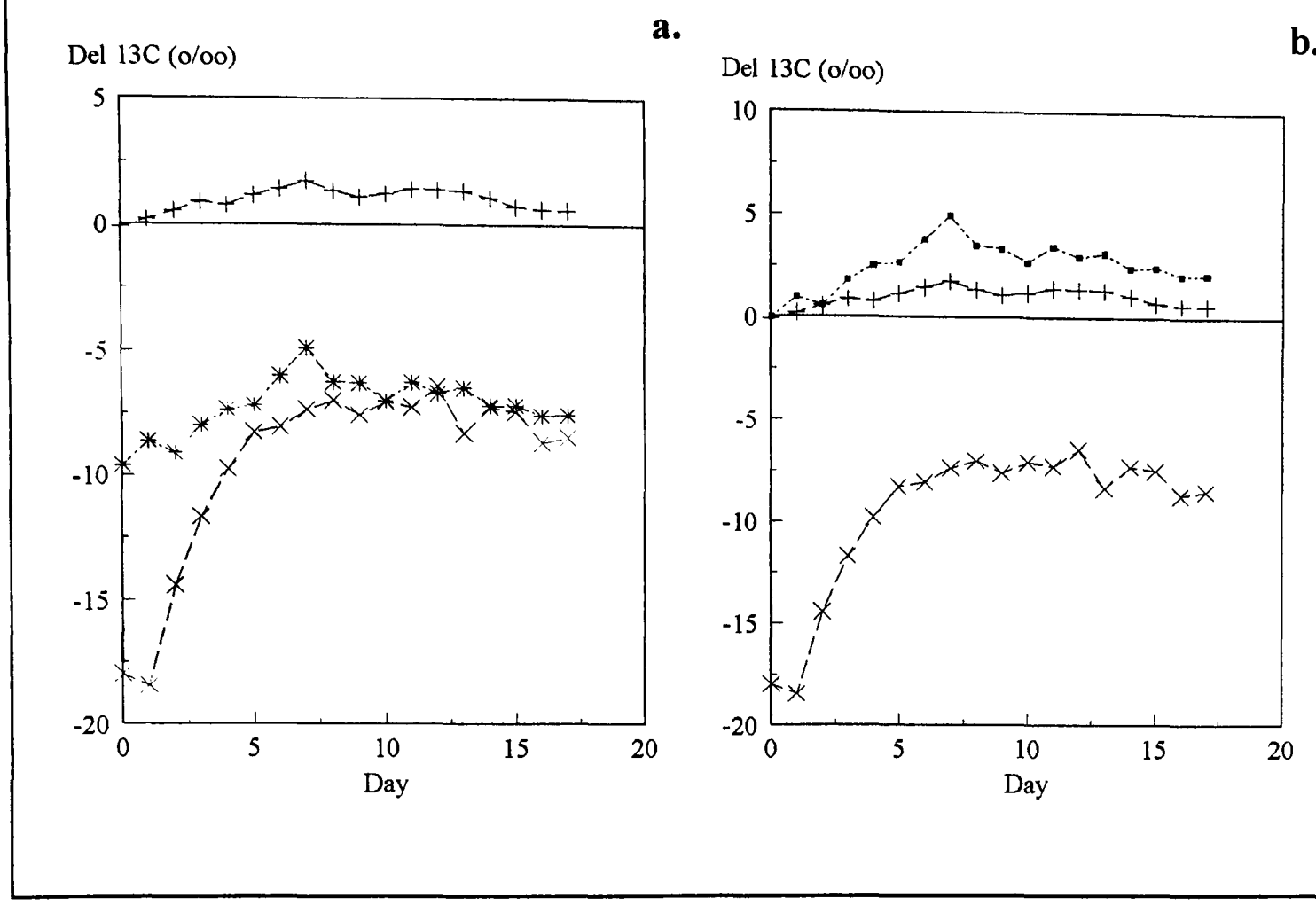

Figure 6.2 Variations in the isotopic composition of (a) $CO_{2(aq)}$ (*) and (b) HCO_3^- (■). The isotopic composition of the POC (×) and ΣCO_2 (+) pools have also been plotted to aid comparison.

During the experiment the [ΣCO_2] reduced from 1675 μmol.kg^{-1} on day 0 to 1300 μmol.kg^{-1} on day 9, a decrease of 22%, after which the concentration rose until it reached ~90% of it's original concentration (*FIGURE* 6.1). The [$CO_{2(aq)}$] is calculated to decrease from ~12 μmol.kg^{-1} to ~1 μmol.kg^{-1}, a drop of 92% (*FIGURE* 6.1).

6.4.2 The Distribution of ^{12}C and ^{13}C Within the ΣCO_2 System and POC

When trying to study the relationship between the isotopic composition of phytoplankton and their source of inorganic carbon it is important to know how ^{12}C and ^{13}C are distributed between the various species within the ΣCO_2 system. In order to calculate the values of $\delta^{13}C_a$, $\delta^{13}C_b$ and $\delta^{13}C_c$ (see eqn. 4.5 - 4.7, section 4.2.1) it is necessary to use the correct fractionation factors which relate to the thermodynamic state of the system under study. The experimental evidence presented in *CHAPTER* 5 suggests that the application of the values of $\alpha_{c/b}$, obtained from the theoretical and experimental studies conducted in media of low

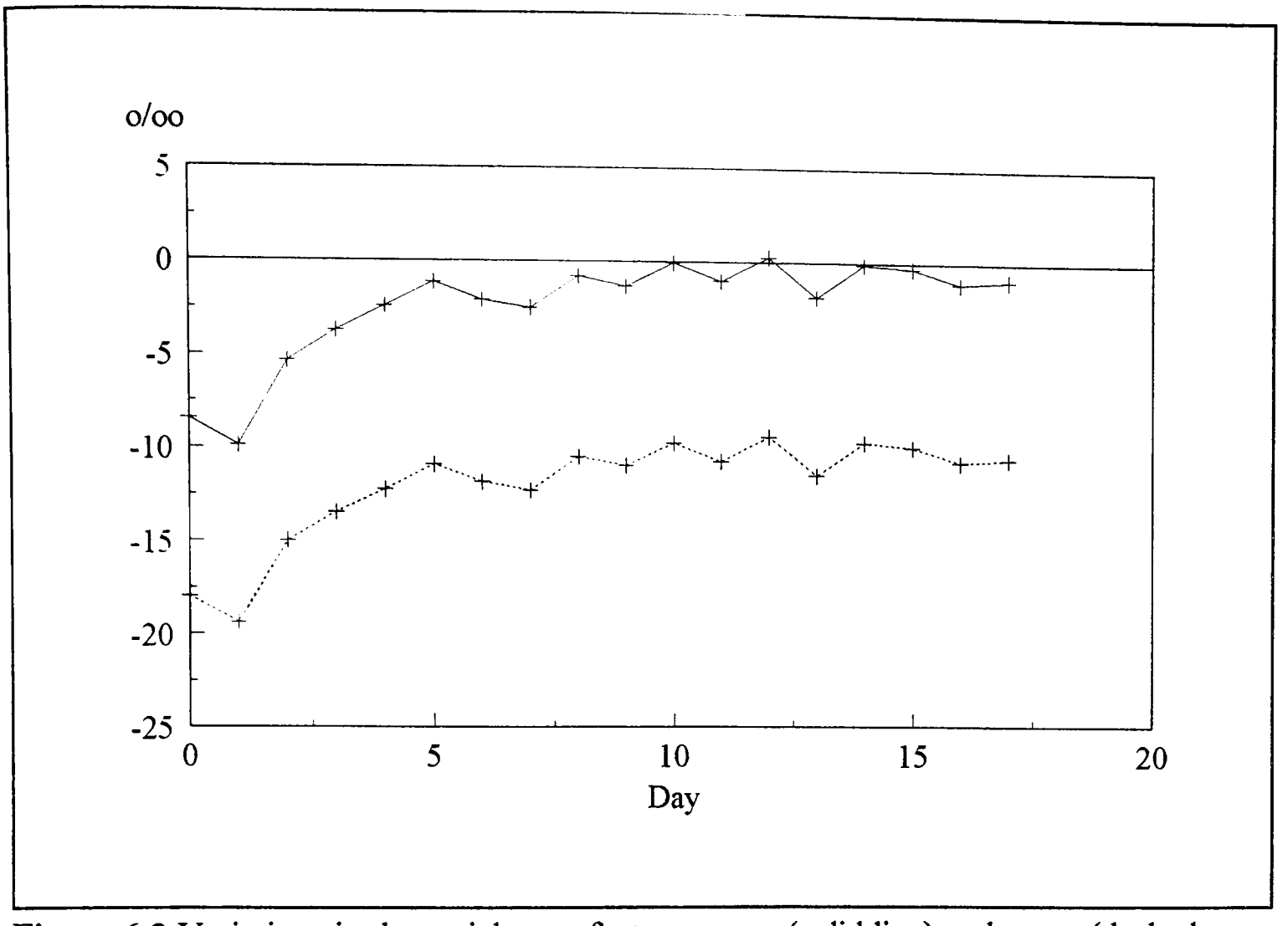

Figure 6.3 Variations in the enrichment factors; $\epsilon_{POC/a}$ (solid line) and $\epsilon_{POC/b}$ (dashed line).

ionic strength, to the marine environment maybe incorrect. However, given the large difference between the values of $\alpha_{c/b}$ determined during this study in comparison with the previous studies, which have indirectly explored the effect of a sea water medium on $\alpha_{c/b}$, the values determined here will be applied with caution. Similarly, the evidence presented in *CHAPTER* 5 suggests $\alpha_{b/a}$ is not significantly altered by the ionic composition of sea water. For the sake of brevity and simplicity the effect of applying the previously determined values and $\alpha_{c/b}$ on the calculated values of $\delta^{13}C_a$, $\delta^{13}C_b$ and $\delta^{13}C_c$ will only be discussed where their application may alter the conclusions which have been drawn. Changes in $\delta^{13}C_a$ and $\delta^{13}C_b$ during the experiment are plotted in *FIGURE* 6.2 along with the $\delta^{13}C_{POC}$ to aid comparison between the results.

The changes in the $\delta^{13}C_{POC}$ were large, increasing from ~-18 ‰ to ~-7‰ in 9 days and thereafter remaining relatively constant (*TABLE* 6.1 and *FIGURE* 6.2). The results obtained during a similar mesocosm study (Nakatsuka *et al.*, 1992) found that the $\delta^{13}C_{POC}$ decreased after the bloom maximum and then returned to the original pre-bloom level.

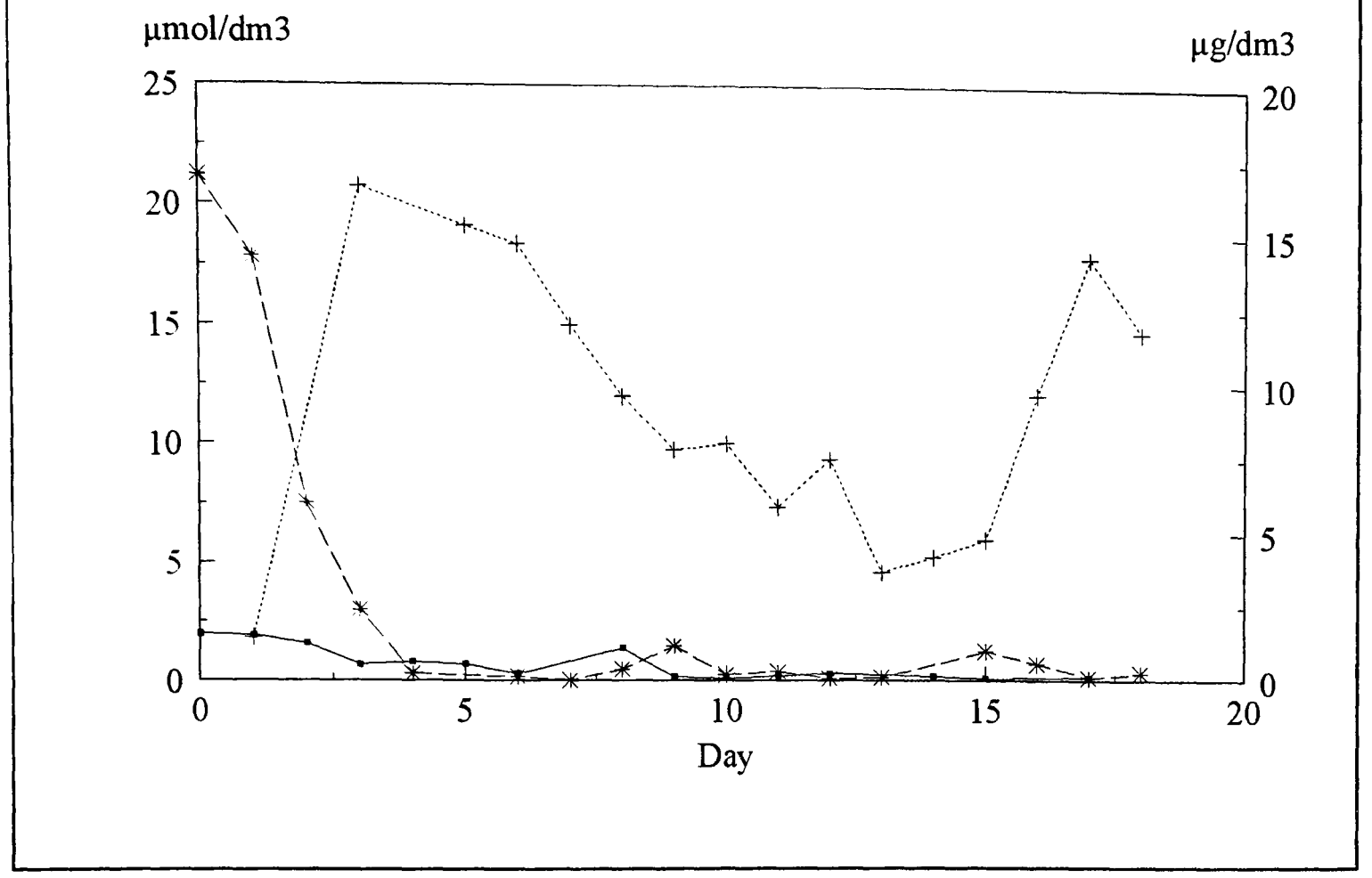

Figure 6.4 Nitrate (*), phosphate (■) and chlorophyll (+, secondary y axis) changes during the course of the mesocosm experiment.

However, their experiment lasted 24 days, 7 days longer than the experiment conducted during this study and the period when the $\delta^{13}C_{POC}$ most rapidly decreased was during the last week of the experiment. The apparent constancy observed in this experiment maybe also attributable to the additional, unscheduled, addition of nitrate made on day 13. If this had not occurred, and the duration of the experiment was longer, the $\delta^{13}C_{POC}$ during this study may have also decreased.

From *FIGURE* 6.2 it is readily apparent that the changes in the isotopic composition of $\delta^{13}C_{POC}$ are much larger than the observed changes in either $\delta^{13}C_a$ or $\delta^{13}C_b$. In fact the $\delta^{13}C_{POC}$ values are approximately equal to the values of $\delta^{13}C_a$, for the majority of the experiment.

The estimated enrichment factors between $CO_{2(aq)}$ and POC, $\epsilon_{POC/a}$, and HCO_3^- and POC, $\epsilon_{POC/b}$, have also been calculated using eqns. 3.4 and 3.5 and are plotted in *FIGURE* 6.3. The values of $\epsilon_{POC/a}$ are predicted to rapidly decrease as the bloom develops and by day 5, $\epsilon_{POC/a} \approx 0‰$, after which it remains relatively constant and close to zero.

6.4.3 Additional Parameters

The concentration of nitrate within the enclosure decreased from ~21 $\mu mol.dm^{-3}$ on day 0 to ~0 $\mu mol.dm^{-3}$ by the fourth day (*TABLE* 6.1, *FIGURE* 6.4). For the rest of the experiment the nitrate concentration remained low although it appeared to increase on day 9 and day 15. The latter increase is due to the second addition of nitrate on day 13 and as no nitrate results were obtained for day 14 the additional nitrate was first detected on day 15. The concentration of chlorophyll increased rapidly and appeared to peak on day 3. Samples were not taken every day during the early stage of the experiment and as a result the peak may not have coincided with our sampling. The chlorophyll concentration shows a large response to the second nitrate addition reaching a peak on day 17.

6.5 Discussion

Much of the data concerning the acquisition of inorganic carbon by marine phytoplankton has either been derived from laboratory based culture experiments or inferred from the isotopic composition of oceanic phytoplankton populations. Mesocosm experiments represent an opportunity to acquire a well constrained data set obtained in a semi-natural environment using natural populations of phytoplankton. The extreme nature of the algal bloom and the depletion of the $CO_{2(aq)}$ pool also provides the opportunity to test many of the empirical and physiological models under extreme conditions. The discussions will therefore mainly focus on the applicability of existing empirical and physiological models to the data presented here and any inferences that may be made about the nature of inorganic carbon acquisition by phytoplankton within the mesocosm.

To start with some basic deductions can be made, based on the three basic theories, which have been previously suggested (see page 96), about the uptake of inorganic carbon during the bloom without the use of modelling. Firstly, if the inorganic carbon assimilated by phytoplankton was purely via the passive diffusion of $CO_{2(aq)}$ the isotopic composition of the phytoplankton would be expected to approach, but not exceed, the isotopic composition of their inorganic carbon source, $\delta^{13}C_a$ (Hayes, 1993) (see section 6.2, page 97), *i.e.* $\epsilon_{POC/a} \leq 0$. This is because the isotopic fractionation associated with a reaction in a single direction (in this case the fixation of $CO_{2(aq)}$) is normally less than one. From

FIGURE 6.4 it is apparent that $\epsilon_{POC/a}$ generally remains less than zero, accept for one occasion, indicating the $CO_{2(aq)}$ could be the exclusive source of inorganic carbon. However, if the values of $\delta^{13}C_a$ had been calculated using the values of $\alpha_{c/b}$ derived by previous studies (*i.e.* Thode *et al.*, 1965) the $\delta^{13}C_{POC}$ would have exceeded the values of $\delta^{13}C_a$ by day 5 (*i.e.* $\epsilon_{POC/a} > 0$) and remain larger, by up to 2‰, for the duration of the experiment. This, according to Hayes (1993), would lead to the conclusion that $CO_{2(aq)}$ entering the cell by passive diffusion could not be the sole source of inorganic carbon.

These contrary conclusions highlight the importance of ensuring the fractionation factors applied to the marine ΣCO_2 system are correct, although based on the findings of the previous chapter the results presented here are not inconsistent with the assimilation of $CO_{2(aq)}$ by passive diffusion.

However, because of the extreme nature of the bloom, which rapidly diminished the $[CO_{2(aq)}]$ in the bulk medium, it is probable that the ΣCO_2 pool within the cell was not in equilibrium with the external medium. As the fixation of CO_2 by Rubisco shows a large discrimination against $^{13}CO_2$ the internal ΣCO_2 pool may become enriched in $^{13}CO_{2(aq)}$. As estimates of $\epsilon_{POC/a}$ are in relation to the isotopic composition of $CO_{2(aq)}$ in the bulk medium, no account is taken of this possible isotopic disequilibrium. Therefore, although the values of $\epsilon_{POC/a}$ either approach, or exceed zero (depending on the value of $\alpha_{c/b}$), this does not necessarily exclude $CO_{2(aq)}$ as the ultimate source of inorganic carbon as the enrichment factor, in relation to the isotopic composition of $CO_{2(aq)}$ within the cell may still be less than zero. In addition, due to the decrease in the rate at which $CO_{2(aq)}$ is replenished by the HCO_3^- pool as the pH increases (*e.g.* see *FIGURE* 2.5), the potential of a chemical and isotopic disequilibrium between the ΣCO_2 pool in the bulk medium and within the cell is increased as the bloom develops.

The calculated values of $\delta^{13}C_a$ rely on the assumption that the ΣCO_2 system within the enclosure was in chemical equilibrium with the atmosphere on day 0. In order to asses the effect of this assumption the values of $\delta^{13}C_a$ have been recalculated, assuming the $[CO_{2(aq)}]$ was 6 $\mu mol.kg^{-1}$ on day 0, for days 0, 4 and 9 respectively; $\delta^{13}C_a$ = -8.6, -7.0, -6.0 ‰. By comparison with the $\delta^{13}C_{POC}$ results in *TABLE* 6.1 it is apparent even if the initial $[CO_{2(aq)}]$ was 50 % lower, the value of $\delta^{13}C_a$ at bloom maximum is still less negative than

the $\delta^{13}C_{POC}$. Therefore the assumption of atmospheric equilibrium does not greatly effect relationship between the $\delta^{13}C_a$ and $\delta^{13}C_{POC}$.

According to the second theory, if the phytoplankton present within the enclosure were able to fix inorganic carbon via a C_4 type metabolism, using PEPC, the maximum value obtained by the phytoplankton maybe expected to be ~-2 ‰ less than the isotopic composition of the HCO_3^- pool. However, from the calculated values of $\epsilon_{POC/b}$ (*FIGURE* 6.3) the minimum enrichment factor, relative to HCO_3^- is ~-10 ‰. This does not necessarily indicate that PEPC was not important but merely indicates that the fixation of inorganic carbon was not solely via a C_4 type mechanism. Although, given the conclusions that no marine phytoplankton appear to posses a C_4 type mechanism (Raven and Johnston, 1991, Goericke *et al.*, 1994), this would seem an unlikely explanation.

The third possible mechanism of inorganic carbon acquisition is that the algae present within the enclosure may have employed some form of carbon concentrating mechanism (CCM) to enhance the supply of $CO_{2(aq)}$ to Rubisco. According to the experiments conducted by Beardall *et al.* (1982) and Sharkey and Berry (1985) the isotopic enrichment associated with the concentrating mechanism is -4 to -8 ‰, relative to $CO_{2(aq)}$. As $\epsilon_{POC/a} \rightarrow 0$ ‰, this would suggest that the use of a concentrating mechanism could not easily explain the observed values of $\delta^{13}C_{POC}$.

Therefore, by simple consideration of the results it would suggest that the phytoplankton, present within the enclosure are exclusive users of $CO_{2(aq)}$ and as the [$CO_{2(aq)}$] decreases, C_i also decreases (eqn. 6.1) and the enrichment factor associated with Rubisco cannot be fully expressed, *i.e.* $\epsilon_{POC/a} \rightarrow 0$ ‰ .

The subsequent sections will examine the applicability of several published empirical and physiological models to the results obtained during the mesocosm study in an attempt to ascertain the mechanism of inorganic carbon acquisition. In addition an attempt will also be made to use a Rayliegh type distillation model (see section 3.4.3)

6.5.1 A Rayleigh Distillation Model

Rayleigh distillation models have been successfully applied to predict the changes in the isotopic composition of the reactant and product pools during an irreversible chemical

reaction in a closed system (*e.g.* Mariotti *et al.*, 1981). Assuming the absence of air/sea exchange the mesocosm is effectively a closed system and as a result it maybe possible to use a Rayleigh type model (see section 3.4.3) to predict changes in the isotopic composition of the phytoplankton as a function of the proportion of the reactant pool remaining (f). An important assumption concerning the Rayleigh model is that the enrichment factor remains constant throughout the course of the experiment. From *FIGURE* 6.3 which plots the calculated enrichment factors assuming either $CO_{2(aq)}$ or HCO_3^- are inorganic carbon sources, it is apparent that this assumption maybe in error as $\epsilon_{POC/a}$ and $\epsilon_{POC/b}$ both decrease by ~10‰. However, the values calculated maybe termed the "apparent" enrichment factor as they do not reflect true difference between the isotopic composition of the inorganic carbon pool and the instantaneous product because of the diluting effect of the existing POC pool (see *FIGURE* 3.1). As a result the apparent enrichment factor would be expected to decrease as the substrate pool was diminished and when f→0 the values of the apparent enrichment factor would be expected approach zero.

An additional problem is encountered when trying to define the substrate pool, which in this case, is the ΣCO_2 pool. The ΣCO_2 pool cannot be described as a single pool from the isotopic viewpoint due to the differing isotopic compositions of $CO_{2(aq)}$, HCO_3^- and CO_3^{2-}. For example, if it is initially assumed that the phytoplankton growth is sustained by the passive diffusion of $CO_{2(aq)}$, using a C_3 type mechanism, the enrichment factor would be expected to be equal to the enrichment factor determined for Rubisco, -29 ‰. In fact, this enrichment factor will not be directly applicable if ΣCO_2 is defined as the substrate pool and must be corrected to obtain $\epsilon_{POC/\Sigma CO2}$, the enrichment factor between ΣCO_2 and POC. Due to variations in the concentrations $CO_{2(aq)}$, HCO_3^- and CO_3^{2-} $\epsilon_{POC/\Sigma CO2}$ will not be constant throughout the whole experiment. However, given the dominance of the HCO_3^- pool within the ΣCO_2 system the correction can be simplified to represent the isotopic enrichment between the $CO_{2(aq)}$ and HCO_3^- pools, ~-10 ‰ and the effective enrichment factor that will apply will be taken as -39 ‰.

Due to the presence of POC within the mesocosm at the start of the experiment the $\delta^{13}C_{POC}$ predicted by the model will not be fully expressed. The $\delta^{13}C_{POC}$ predicted by the model has to be modified to account for this dilution. This correction was achieved using the following equation which is based on a mass balance relationship:

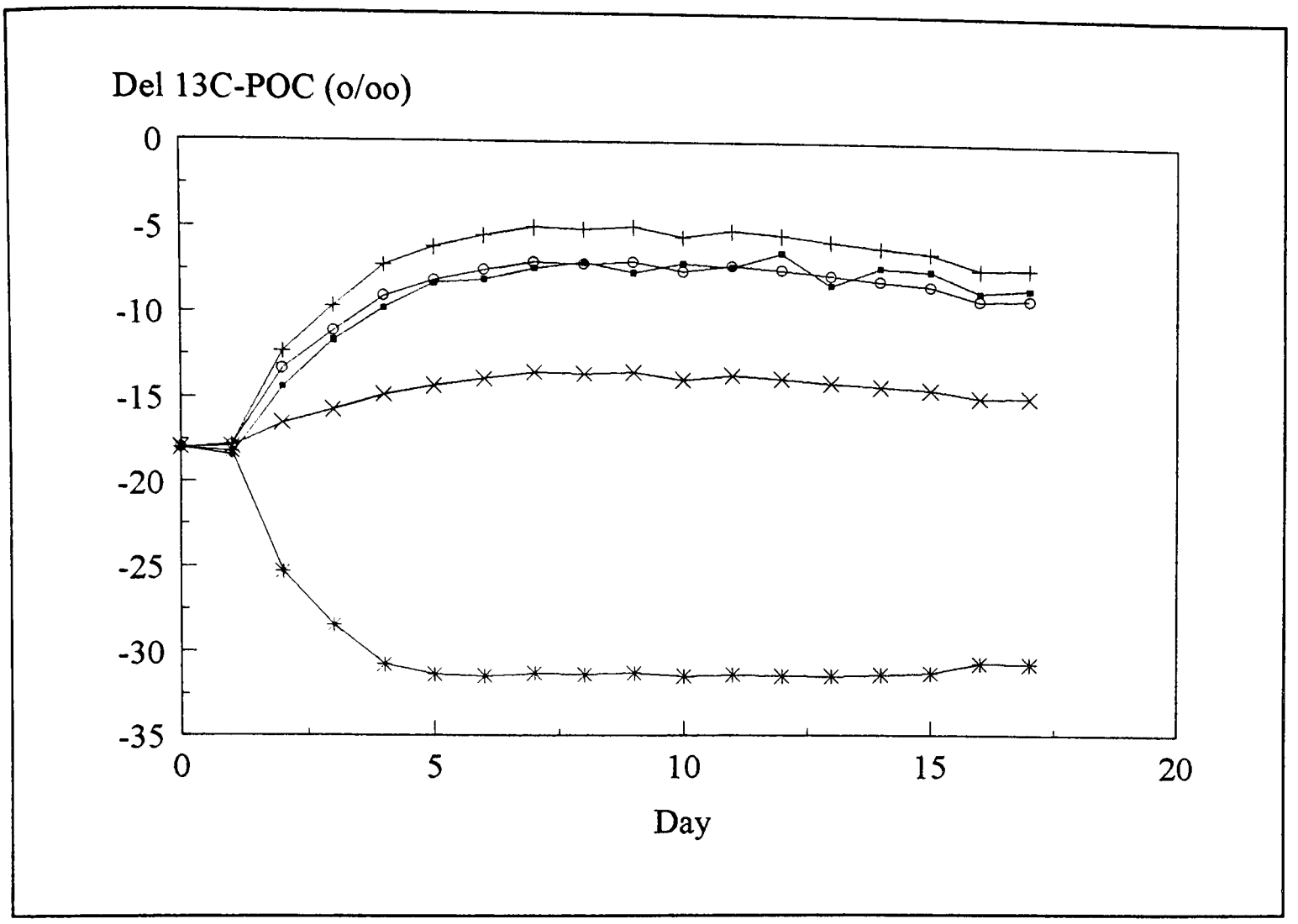

Figure 6.5 Predicted variations in the isotopic composition of POC using a Rayleigh distillation model assuming the enrichment factor, $\epsilon_{POC/\Sigma CO2}$ is equal to; -39 ‰ (*), -2 ‰ (+), -14 ‰ (×) and -4.9 ‰ (o). The measured $\delta^{13}C_{POC}$ has also been plotted to aid comparison (■).

$$\delta^{13}C_{POC-t+} = \frac{\delta^{13}C_{POC-t0} \times [POC]_{t0} + \delta^{13}C_{POC-t} \times ([\Sigma CO_2]_{t0} - [\Sigma CO_2]_t)}{[POC]_{t0} + [\Sigma CO_2]_{t0} - [\Sigma CO_2]_t} \qquad \textbf{(6.2)}$$

where $\delta^{13}C_{POC-t0}$, $[\Sigma CO_2]_{t0}$ and $[POC]_{t0}$ are the observed isotopic composition and concentration of the ΣCO_2 and POC pools on day 0, and $\delta^{13}C_{POC-t}$ and $[\Sigma CO_2]_t$ are the calculated isotopic compositions of the accumulated POC and the $[\Sigma CO_2]$ at time t, predicted by the Rayleigh fractionation model, and $\delta^{13}C_{POC-t+}$ is the predicted isotopic composition of the combined POC pool at time t.

FIGURE 6.5 plots the values of $\delta^{13}C_{POC-t+}$ predicted using eqns. 3.34 and 6.2, assuming $\epsilon_{POC/\Sigma CO2}$ = -39 ‰. It is apparent that there is no agreement between the predicted values of $\delta^{13}C_{POC-t+}$ and those directly determined during the experiment. Not only are the values far too negative but they show that the $\delta^{13}C_{POC}$ decreases rather than increases over the course of the experiment. In conclusion, the chosen enrichment factor, which represented

the passive diffusion of $CO_{2(aq)}$ and subsequent carboxylation via Rubisco, is far too negative and this may indicate:

i. That the majority of the carboxylation occurring in the enclosure is not mediated by Rubisco.

ii. The existence of a CCM which will alter the apparent enrichment factor (Beardall *et al.*, 1982, Sharkey and Berry, 1985).

iii. The enrichment factor is not constant and varies in response to another parameter such as [$CO_{2(aq)}$] or the enrichment factor chosen for Rubisco (which has been derived from higher, terrestrial plants) may not be applicable to marine phytoplankton, or the phytoplankton present during this experiment (Goericke *et al.*, 1994).

Firstly, if Rubisco was not the primary carboxylation enzyme, fixation maybe occurring via a β-carboxylation pathway, mediated either by PEPC or PEPCK. The enrichment factor associated with PEPCK appears to be variable (Arnelle and O'Leary, 1992), but it is generally thought to be similar to Rubisco, and as the substrate utilised by PEPCK is $CO_{2(aq)}$, the overall enrichment associated with fixation via PEPCK would be similar to Rubisco. On the other hand, the enrichment factor associated with PEPC is small, -2 ‰, relative to HCO_3^- which is the substrate. The model has been re-run assuming PEPC is the primary carboxylation enzyme where the effective enrichment factor, $\epsilon_{POC/\Sigma CO2}$, will be taken as -2 ‰ given the dominance of HCO_3^- within the ΣCO_2 pool. The agreement between the predicted and measured values of $\delta^{13}C_{POC}$ is good (*FIGURE* 6.5), although the model generally predicts the $\delta^{13}C_{POC}$ to be too high by 2 to 3 ‰.

The isotopic enrichment that occurs whilst a CCM is in operation has been determined to be -4 to -8‰, relative to $CO_{2(aq)}$ (Beardall *et al.*, 1982, Sharkey and Berry, 1985). If the ΣCO_2 is the defined substrate pool this value must be corrected by -10 ‰ (see above) to give the effective enrichment factor (-14 ‰) which describes the active uptake of inorganic carbon. The predicted and determined values of $\delta^{13}C_{POC}$ are not in good agreement (*FIGURE* 6.5), the predicted values are ~6 ‰ too low. This would indicate that the simple model of a CCM does not easily account for the observed changes in $\delta^{13}C_{POC}$. However,

several different mechanisms by which carbon may be actively transported have been suggested (*e.g.* Badger, 1987) and it is probable that each type of mechanism maybe associated with a different enrichment factor and different substrate. There is also the possibility that different mechanisms may operate at different times, depending on the pH of the enclosure (Thielmann *et al.*, 1990), or their operation maybe intermittent.

Finally the predicted values of $\delta^{13}C_{POC}$ were fitted to the observed data by adjusting the value of $\epsilon_{POC/\Sigma CO2}$ until a best fit was obtained (minimising the residual sum of squares) (*FIGURE* 6.5). The value obtained in this manner was -4.9 ‰, which can be taken to be equivalent to $\epsilon_{POC/b}$ ~ -4.9 ‰, due to the dominance of HCO_3^- and $\epsilon_{POC/a}$ of ~5.1 ‰. This result would suggest that HCO_3^- is likely to be the inorganic carbon source as most isotope fractionations associated with a reaction in a single direction are negative, *i.e.* the lighter isotope reacts faster. A positive enrichment factor, which would result if $CO_{2(aq)}$ was assumed to be the inorganic carbon source, would be unlikely (O'Leary *et al.*, 1992). The good agreement between the fitted values of $\delta^{13}C_{POC}$ and the directly determined $\delta^{13}C_{POC}$ suggest that the enrichment factor between the phytoplankton and their inorganic carbon source is not variable.

It is important to note that the predicted values of $\delta^{13}C_{POC}$ in *FIGURE* 6.5 have been corrected for POC which was present at the beginning of the experiment and it was assumed this correction applied throughout the experiment. This is unlikely to be the case as much of the organic POC was probably gradually removed from the suspended POC pool by sinking and re mineralisation. In the absence of this residual pool the predicted $\delta^{13}C_{POC}$ would be less negative (~-4.5 ‰) and the agreement with the measured values would be diminished.

In conclusion, according to the Rayleigh distillation model, the uptake of inorganic carbon by phytoplankton within the enclosure can be described by a constant enrichment factor of ~-4.9 ‰, and the likely substrate is HCO_3^-. This is close to the value expected if the phytoplankton were operating a β-carboxylation pathway with PEPC as its primary enzyme. The slight difference maybe attributable to either the fractionation that may occur during the active transport of HCO_3^- across the cell wall, which although small, is likely to be negative or the presence of other, isotopically light, phytoplankton with different uptake mechanisms.

Although this conclusion is theoretically consistent with the use of a C_4 type metabolism, with PEPC as the primary carboxylation enzyme, it is not supported by experimental evidence. Experimental evidence suggests that fixation by PEPC accounts for less than 25% of net carbon fixation (Beardall, 1989) and that all phytoplankton possess a C_3 type metabolism (Raven and Johnston, 1991), making this conclusion difficult to accept.

A major potential problem resulting from the application of a Rayleigh distillation model is associated with treating the entire ΣCO_2 pool as the substrate pool. It is arguable that the $CO_{2(aq)}$ pool should be defined as the substrate pool when it is assumed $CO_{2(aq)}$ is the form of inorganic carbon entering the cell. This maybe particularly important for the results presented here as the $[CO_{2(aq)}]$ decreased by 90% during the course of the experiment which would have direct implications on the diffusional flux of $CO_{2(aq)}$ into the cell. However, as the Rayleigh distillation model is ultimately a mathematical simplification, used to describe kinetic changes during the distillation of two liquids, is probably not wise to manipulate or force the simplified model by defining $CO_{2(aq)}$ as the substrate because of its dynamic relationship with HCO_3^-. Therefore, any conclusions reached by applying this model must be treated with caution.

6.5.2 Empirical Models

Simple empirical models have been developed by fitting data obtained in the field (Popp *et al.*, 1989, Rau *et al.*, 1992, Rau, 1994) or from geological cores (Jasper and Hayes, 1994), which relate changes in $\delta^{13}C_{POC}$, or $\epsilon_{POC/a}$, to $[CO_{2(aq)}]$, to simple linear, non-linear and logarithmic models. Such a relationship was originally proposed by Degens *et al.* (1968) on the basis of laboratory based culture experiments although the existence of such a relationship has been subsequently demonstrated both in lake based (McCabe, 1985) and marine studies (Rau *et al.*, 1989, Rau *et al.*, 1991a, Rau *et al.*, 1991b, Rau *et al.*, 1992, Rau, 1994). However, the principle limitation of these simple models has been their limited physiological basis and therefore, although they may well describe the relationship in today's oceans, it does not advance our understanding about the physiological origins of such a relationship and how it maybe altered by environmental changes.

The simple inverse linear model relating $\delta^{13}C_{POC}$ to $[CO_{2(aq)}]$ has been mainly advanced by Rau and his coworkers (Rau *et al.*, 1989, Rau *et al.*, 1991a, Rau *et al.*, 1991b,

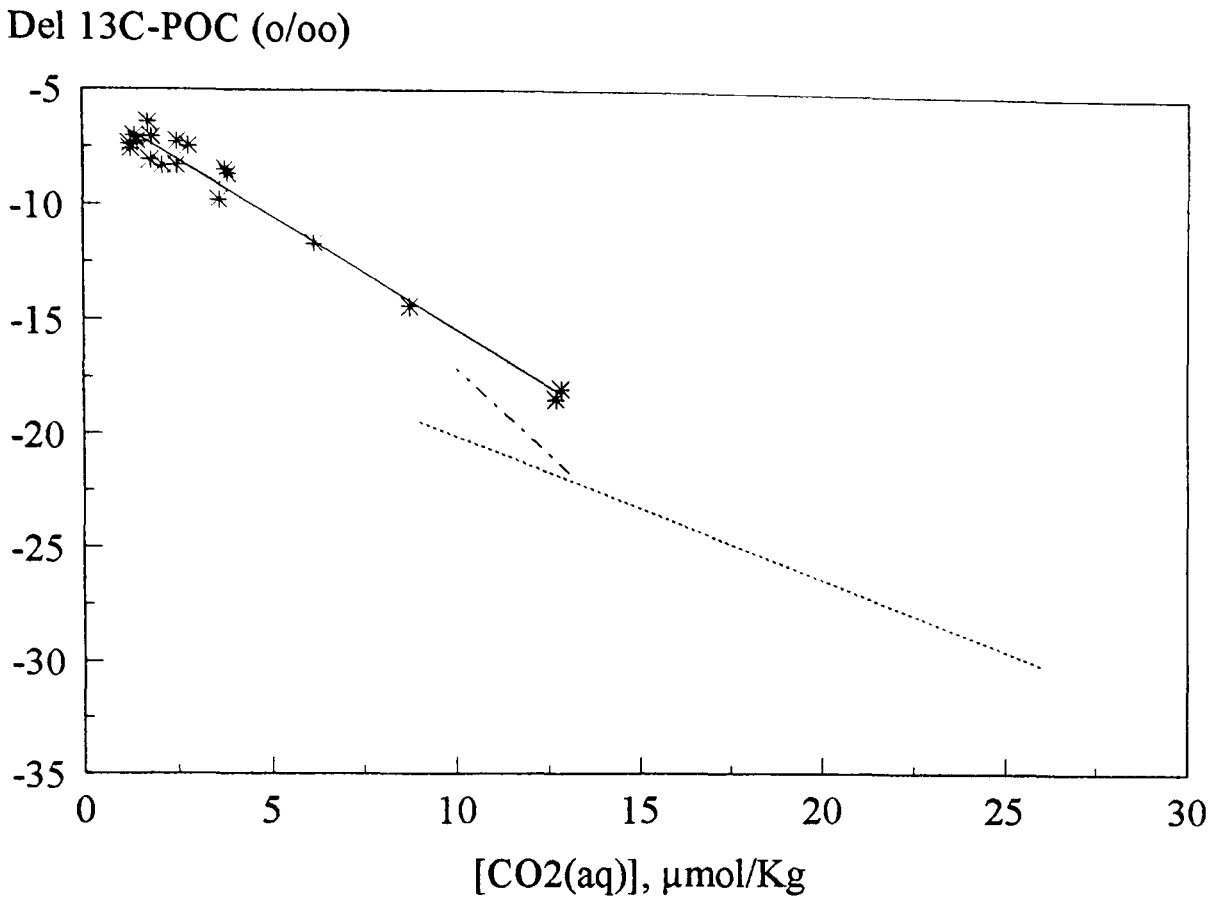

Figure 6.6 The $\delta^{13}C_{POC}$ in relation to $[CO_{2(aq)}]$ during the mesocosm experiment. A linear regression has been fitted to the data ($\delta^{13}C_{POC}$=-0.98 (±0.04) × $[CO_{2(aq)}]$ - 5.6 (±0.6)) (solid line) to aid comparison with previous models; Rau *et al.* (1992)($\delta^{13}C_{POC}$=1.5 × $[CO_{2(aq)}]$ - 2.1) (long dash) and Rau (1994) ($\delta^{13}C_{POC}$=-0.628 × $[CO_{2(aq)}]$ - 13.8) (short dash).

Rau *et al.*, 1992, Rau, 1994). In order to compare the relationship between $\delta^{13}C_{POC}$ and $[CO_{2(aq)}]$ derived during this study, with those of previous studies, a linear relationship has been fitted to the data and the results are plotted in *FIGURE* 6.6. It is difficult to tell if the relationship derived during this study is significantly different from the previous studies because the errors associated with the slopes and constants have not been given. However, given the spread of results in the data set published by Rau (1994) and the errors introduced by assuming the ΣCO_2 system within the mesocosm was in chemical equilibrium with the atmosphere on day 0 it is likely that it is not significantly different. The data derived in previous studies related to water masses where the $[CO_{2(aq)}]$ ranged from 9 to 26 $\mu mol.kg^{-1}$, whereas the data presented here is estimated to range from 12 to 1 $\mu mol.kg^{-1}$. Therefore the results presented here represent an extension of the existing data set.

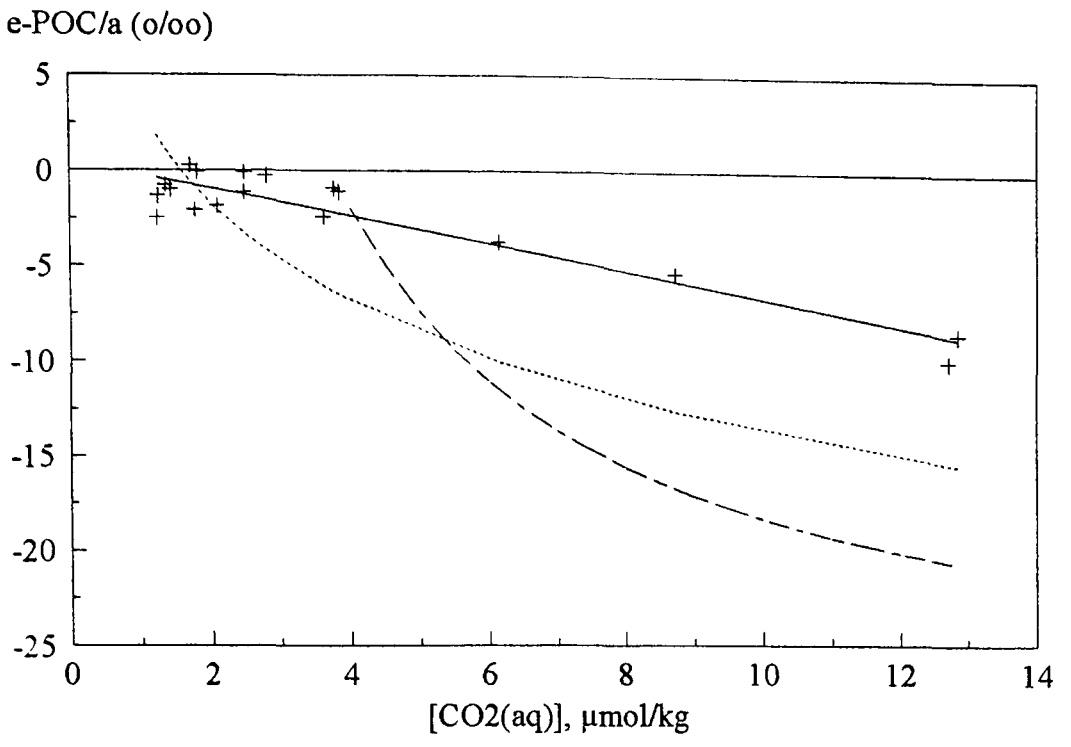

Figure 6.7 Variations in $\epsilon_{POC/a}$ (+) and $[CO_{2(aq)}]$ determined during this study. A linear regression has been fitted to the data and may be described by the following expression; $\epsilon_{POC/a} = -0.72\ (\pm 0.06) \times [CO_{2(aq)}] + 0.5\ (\pm\ 1.0)$, solid line. The relationship between $\epsilon_{POC/a}$ and $[CO_{2(aq)}]$ given by Popp *et al.* (1989) (short dash) and Jasper and Hayes (1994) (long dash) have also been plotted.

If the relationship given by Rau (1994) is extrapolated so $[CO_{2(aq)}] = 0$, the maximum predicted value of $\delta^{13}C_{POC} = -13.8$ ‰. But the mesocosm results show the $\delta^{13}C_{POC}$ can become less negative, -5.6 ‰. Thus the empirical model of Rau (1994) may not be applicable to situations where $[CO_{2(aq)}]$ is low.

The isotopic composition of the phytoplankton will also be influenced by the isotopic composition of their inorganic carbon source, which is assumed to be $CO_{2(aq)}$ (Rau *et al.*, 1992, Rau, 1994, Jasper and Hayes, 1994). The model proposed by Rau (1994) does not account for variations in the isotopic composition of $CO_{2(aq)}$, either within today's ocean, or in the past. Therefore an implicit assumption in its application is that the isotopic composition of $CO_{2(aq)}$ and atmospheric $CO_{2(g)}$ are in equilibrium and has not changed over geological time.

In order to overcome this problem similar non - linear and logarithmic models have been developed based on the relationship between $\epsilon_{POC/a}$ and $[CO_{2(aq)}]$ to account for variations in $\delta^{13}C_a$ (Jasper and Hayes, 1994, Popp *et al.*, 1989 respectively). A linear regression has been fitted to the calculated values of $\epsilon_{POC/a}$ and the results are plotted in *FIGURE* 6.7. The values of $\epsilon_{POC/a}$ predicted using the models of Popp *et al.* (1989) and Jasper and Hayes (1994) have also been plotted in *FIGURE* 6.7. A comparison of the predicted values of $\epsilon_{POC/a}$ from other studies with those directly calculated from the experimental results indicate the agreement is poor, the predicted values are generally too negative when the $[CO_{2(aq)}]$ is high and become positive when the concentration is low. The model of Popp *et al.* (1989) was calibrated using the results of lake based studies (McCabe, 1985) and the Jasper and Hayes (1994) model used the $\delta^{13}C$ values from alkenones and foraminiferal carbonates from geological cores. Therefore any differences between these models and the relationship derived in the mesocosm may be at least partly attributable to the different methods calibration. Another more probable cause of error is the value of $[CO_{2(aq)}]$ estimated during this study. If the $[CO_{2(aq)}]$ were lower than the assumed values the agreement between $\epsilon_{POC/a}$ estimated during this study and previous studies would be improved. It is assumed, for the purpose of these models, that phytoplankton are exclusive users of $CO_{2(aq)}$. When the $[CO_{2(aq)}]$ is high the isotopic enrichment associated with Rubisco will be fully expressed and when the $[CO_{2(aq)}]$ is low the $\delta^{13}C_{POC}$ will approach the isotopic composition $CO_{2(aq)}$ pool. However, simple linear models such as Rau's assume that the $\delta^{13}C_a$ is constant, *i.e.* in equilibrium with the atmosphere and the value of $\delta^{13}C_{POC}$ will continue to increase as the $[CO_{2(aq)}]$ increases. The advantage of the non-linear models based on $\epsilon_{POC/a}$ is that they take account of variations of $\delta^{13}C_a$ and assume the value of $\epsilon_{POC/a}$ will approach the isotopic enrichment expressed by Rubisco as the $[CO_{2(aq)}]$ increases. However, as revealed by the data set presented here none of the proposed models appear applicable to situations where the $[CO_{2(aq)}]$ is low. The results presented here suggest that the relationship between $[CO_{2(aq)}]$ and $\epsilon_{POC/a}$ at low $[CO_{2(aq)}]$ is linear and as the $[CO_{2(aq)}]$ approaches zero $\epsilon_{POC/a}$ approaches zero. Conversely it may not be applicable to use the regression equations obtained from this study when the $[CO_{2(aq)}]$ is high.

6.5.3 Physiological Models

Using the simple two step scheme given in eqn. 6.1, Farquhar *et al.* (1982) proposed a model to describe the isotopic composition of C_3 terrestrial plants which accounted for the relative effects of changes in the external concentration of $[CO_{2(g)}]$ and the rate of carboxylation. This model, given below, has been rewritten to describe the isotopic composition of a phytoplankton cell, using the terminology used during this study:

$$\delta^{13}C_{POC} = \delta^{13}C_a + \epsilon_{i/e} + f(\epsilon_R - \epsilon_{e/i}) \qquad \textbf{(6.3)}$$

where f is the proportion of intracellular inorganic carbon which leaks back into the environment, $\epsilon_{i/e}$ and $\epsilon_{e/i}$ are the isotopic enrichments associated with the diffusion of $CO_{2(aq)}$ into and out of the cell and ϵ_R is the net isotopic enrichment associated with fixation of inorganic carbon. The leakiness of a cell, reliant on the passive diffusion of $CO_{2(aq)}$, is basically a measure of the degree of isotopic disequilibrium between $[C_e]$ and $[C_i]$ and may be expressed more explicitly as (Francois *et al.*, 1993) :

$$f = \frac{k_{-1}[C_i]}{k_1[C_e]} \qquad \textbf{(6.4)}$$

Therefore, if a C_3 phytoplankton cell is considered, which is solely reliant on the passive diffusion of $CO_{2(aq)}$, ϵ_R will be -27 ‰, the net enrichment associated with the fixation of CO_2 by Rubisco. The isotopic enrichment associated with the diffusion of $CO_{2(aq)}$ is small, and will be assumed to be -1 ‰. As the uptake of inorganic carbon is by passive diffusion it will be assumed $\epsilon_{i/e}$ is equal to $\epsilon_{e/i}$. When the cell is growing slowly the internal carbon pool will be in chemical and isotopic equilibrium with the $CO_{2(aq)}$ in the bulk medium and as $f \rightarrow 1$, eqn. 6.3 can be simplified to:

$$\delta^{13}C_{POC} = \delta^{13}C_a + \epsilon_R \qquad \textbf{(6.5)}$$

Under conditions of high growth the internal carbon pool will become depleted and $f \rightarrow 0$ and:

$$\delta^{13}C_{POC} = \delta^{13}C_a + \epsilon_{i/e} \qquad \textbf{(6.6)}$$

A modified form of this model has been applied by Rau *et al.* (1992) to interpret the observed changes in the $\delta^{13}C_{POC}$ during a phytoplankton bloom in the north Atlantic. The model used by Rau *et al.* (1992) did not take into account variations in the $\delta^{13}C_a$ and therefore its applicability to situations where $\delta^{13}C_a$ cannot be assumed to remain constant is limited. The modified version of the model used by Francois *et al.* (1993) takes account of possible variations in $\delta^{13}C_a$ by expressing the output of the model as $\epsilon_{POC/a}$:

$$\epsilon_{POC/a} = \epsilon_{i/e} + \left(1 - \frac{[C_e] - [C_i]}{[C_e]} \times (\epsilon_R - \epsilon_{e/i})\right) \qquad \textbf{(6.7)}$$

and using the above enrichment factors the model simplifies to:

$$\epsilon_{POC/a} = -27 + \frac{26\,([C_e] - [C_i])}{C_e} \qquad \textbf{(6.8)}$$

Using this relationship it is possible to plot the isopleths of $\epsilon_{POC/a}$ for a constant $[C_e]$ - $[C_i]$ and given $[CO_{2(aq)}]$ (*FIGURE* 6.8). The values of $\epsilon_{POC/a}$ have also been plotted. However according to the model the minimum value of $\epsilon_{POC/a}$ that may be obtained is -1 ‰, the isotopic enrichment due to the passive diffusion of $CO_{2(aq)}$ and the estimates of $\epsilon_{POC/a}$ data are observed to increase beyond this. One possible cause of this apparent inconsistency maybe related to the term associated with the isotopic enrichment due to the diffusion of $CO_{2(aq)}$ in and out of the cell. If these terms were removed from the model the minimum value of $\epsilon_{POC/a}$ predicted by the model would be zero. *FIGURE* 6.8 replots the predicted isopleths for constant $[C_e]$ - $[C_i]$ along with the calculated values of $\epsilon_{POC/a}$. The values of $\epsilon_{POC/a}$ remain negative and within the range of the model. The validity of removing the terms associated with the diffusion of $CO_{2(aq)}$ is difficult to justify except on the grounds that the values of $\epsilon_{POC/a}$ predicted by this study are now within the range of the model. However, as the model does not appear to have been explicitly tested at low $[CO_{2(aq)}]$ their inclusion has not been experimental verified. If the omission of these terms cannot be justified, the effect of their inclusion on the predicted values of $\epsilon_{POC/a}$ (1‰), relative to the overall changes in $\epsilon_{POC/a}$

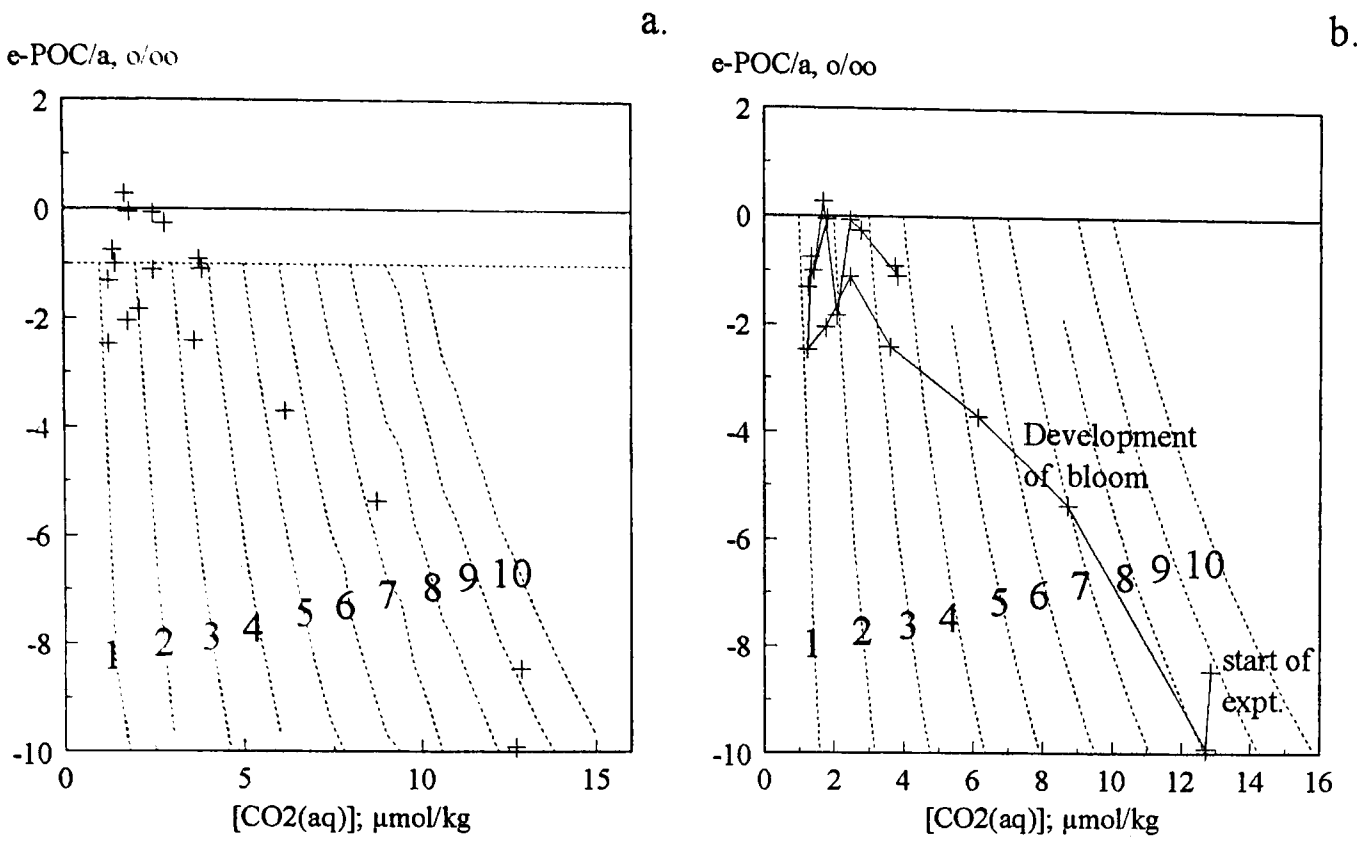

Figure 6.8 The calculated values of $\epsilon_{POC/a}$ have been plotted in relation to the $[CO_{2(aq)}]$. The dashed lines represent the expected isopleths of $\epsilon_{POC/a}$ at a specified $[CO_{2(aq)}]$ and constant $[C_e]$ - $[C_i]$ (1 - 10 µmol.kg^{-1}). Graph **a** uses the model given by Francois *et al.* (1993) which takes account of the fractionation associated with the diffusion of $[CO_{2(aq)}]$. This determines the minimum isotopic enrichment (-1 ‰) which is represented by the horizontal dashed line. Graph **b** uses the modified version of the model which does not take account of the isotopic enrichment associated with the diffusion of $CO_{2(aq)}$ and therefore the minimum enrichment factor associated with this model is 0 ‰. The course of the bloom has been represented by joining the data points sequentially (solid line).

observed during this study (10‰), is minor. It is worth noting at this stage that if the values of $\delta^{13}C_a$ had been calculated using previously estimated and determined values of $\alpha_{c/b}$ the values of $\epsilon_{POC/a}$ would have been ~2‰ more positive, increasing the discrepancy with the model.

At the start of the experiment the values of $\epsilon_{POC/a}$ rapidly increase from ~-9 ‰ to ~-1 ‰ and $[C_e]$ - $[C_i]$ rapidly decreases 8 µmol.kg^{-1} to 2 µmol.kg^{-1}, which according to the model (Francois *et al.*, 1993) indicates the growth rate rapidly declined during the growth phase of the bloom (*i.e.* the difference between $[C_e]$ and $[C_i]$ indicates the degree of disequilibrium between the internal and external pools, this has been suggested to be related to the rate of carboxylation and hence growth rate, Rau *et al.*, 1992). This would seem

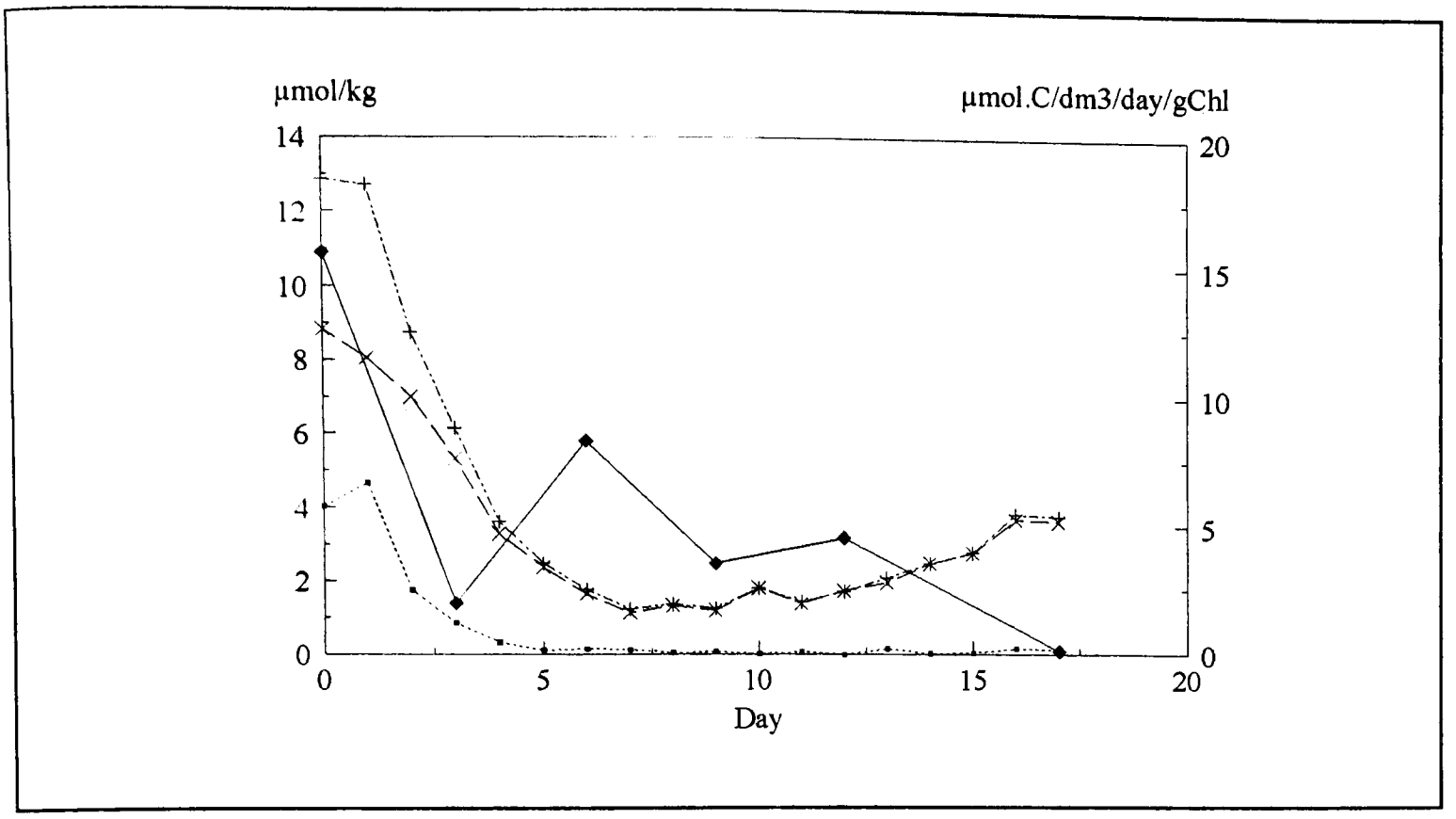

Figure 6.9 Variations in the chlorophyll specific productivity (◆) (secondary y axis), $[CO_{2(aq)}](\mu mol.kg^{-1})$ (+), $[C_i](\mu mol.kg^{-1})$ (×) and $[C_e] - [C_i](\mu mol.kg^{-1})$ (■) during the mesocosm bloom. The $[C_i]$ and $[C_e] - [C_i]$ have been calculated using the model given in eqn. 6.7 although the terms associated with the isotopic enrichment of $CO_{2(aq)}$ during diffusion have been removed as discussed in the text.

contrary to expectations as the development of a bloom maybe expected to be associated with a rise in the specific growth rate. $H^{14}CO_3^-$ productivity measurements, conducted by other participants of the experiment (Dr. B. Rieman, *pers. comm.*), indicate (*FIGURE* 6.9) a decrease in the rate of chlorophyll specific productivity during the growth phase of the bloom, corroborating the predictions of the model. These results suggest that the following scenario could explanation of the isotope data:

i. Phytoplankton present in the enclosure at the beginning of the experiment were nutrient deficient but carbon sufficient and hence $\epsilon_{POC/a}$ would be expected to be large.

ii. The addition of nutrients stimulated the growth and division of cells. However, the $[CO_{2(aq)}]$ was already low enough to limit the growth rate, indicated by a decrease in $[C_e] - [C_i]$. The high carbon demand by Rubisco in relation to the rate at which $CO_{2(aq)}$ could be supplied by diffusion resulted in a decrease in $\epsilon_{POC/a}$.

iii. As the phytoplankton continued to grow the [$CO_{2(aq)}$] was further depleted, increasing the degree of carbon limitation still further and hence decreasing [C_e] - [C_i] and decreasing $\epsilon_{POC/a}$.

iv. As the [$CO_{2(aq)}$] approached zero the isotopic composition of the phytoplankton approached the $\delta^{13}C_a$. As the demand remained high relative to the [$CO_{2(aq)}$], $\epsilon_{POC/a}$ remained low for the rest of the experiment.

It is also possible that changes in the membrane permeability or cell size may have accounted for some of the observed changes but as no measurements were taken to define these parameters it is difficult to comment on their potential impact (Francois *et al.*, 1993).

An additional line of evidence may be obtained by considering the relationship between [C_e] and [C_i] more closely. At the start of the experiment [C_e] - [C_i] = 8 to 9 $\mu mol.kg^{-1}$. As the bloom starts to develop the [C_e] decreases and by day 4 was less than 8 $\mu mol.kg^{-1}$ and as a result a gradient of 8 $\mu mol.kg^{-1}$ between [C_e] and [C_i] could not be maintained. If [C_i] decreased alongside [C_e], but at a lower rate, the gradient between [C_e] -[C_i] would decrease and limit the diffusional supply of $CO_{2(aq)}$ to Rubisco. As the bloom develops the [C_i] continues to decrease rapidly as the [C_e] decreases (*FIGURE* 6.9) until [C_i] $\approx$ 0 $\mu mol.kg^{-1}$. Such a low value of [C_i] would have to indicate that the growth rate was limited by the rate at which $CO_{2(aq)}$ could be resupplied from the external medium.

The results presented here are not easily interpreted, but the above explanation is consistent with the productivity measurements. If the [$CO_{2(aq)}$] was higher, and the growth rate was not limited by the supply of inorganic carbon the values of $\epsilon_{POC/a}$ would be expected to plot along or close to one of the isopleths, indicating a constant growth rate or even cut across the isopleths so [C_e] - [C_i] increased due to the increased rate of carboxylation and hence decreased [C_i]. By interpreting the model in this manner it may be possible to discover if the growth rate of a phytoplankton community is limited by the supply of $CO_{2(aq)}$.

The above discussion relies on the acceptance of the values of $\alpha_{c/b}$ derived in *CHAPTER* 5. If $\epsilon_{POC/a}$ was recalculated using the values of $\alpha_{c/b}$ determined by Thode *et al.* (1965), $\epsilon_{POC/a}$ would be remain positive throughput the majority of the study period. According to Hayes (1993) positive values of $\epsilon_{POC/a}$ would indicate that $CO_{2(aq)}$ may not be

the exclusive source of inorganic carbon. Hayes suggested the following model to describe the relationship between $\epsilon_{POC/a}$ and the cell leakiness during the active transport of inorganic carbon, which is of similar form to the passive diffusion model (see eqn. 6.3):

$$\epsilon_{POC/a} = \epsilon_{b/a} + \epsilon_{i/e} + f \times (\epsilon_R - \epsilon_{e/i}) \qquad \textbf{(6.9)}$$

where $\epsilon_{i/e}$ represents the isotopic enrichment associated with the active transport of HCO_3^-, $\epsilon_{e/i}$ is the enrichment factor associated with the diffusion of $CO_{2(aq)}$ out of the cell and $\epsilon_{b/a}$ is the isotopic enrichment factor between $CO_{2(aq)}$ and HCO_3^-, ~ 10 ‰ . The value of $\epsilon_{i/e}$ is not known (Sharkey and Berry, 1985) but is estimated to be small and negative (Hayes, 1993) and will be assumed to be -1 ‰. The small values of the enrichment factor associated with the bloom maximum and post bloom periods ($\epsilon_{POC/a} \rightarrow 0$) are not inconsistent with the active transport model. However, experimental evidence, obtained from culture experiments, suggests the value of $\epsilon_{POC/a}$ associated with a phytoplankton which possess a CCM is -4 to -8‰, somewhat larger than the values observed here. Similarly, as the bloom progresses and the $[CO_{2(aq)}]$ in the bulk medium diminishes the disequilibrium between $[C_i]$ and $[C_e]$ would be expected to increase the leakiness of the cell. The observed decrease in the leakiness of the cell from ~0.67 to 0.39 maybe explained by simultaneous decrease in the permeability of the cell wall and hence increased efficiency of the CCM.

The growth rate or uptake rate of phytoplankton with the ability to operate a CCM would be expected to be independent of the $[CO_{2(aq)}]$. However, the productivity measurements appear to indicate a large decrease in the chlorophyll specific uptake rates by day 3 which is in advance of the nutrient pools becoming depleted. This apparent decrease in uptake rates, prior to the depletion of the nutrients indicate that $[CO_{2(aq)}]$ maybe limiting the specific uptake rate of inorganic carbon by phytoplankton within the mesocosm and therefore it would seem unlikely that the phytoplankton were able to use the HCO_3^- pool.

6.6 Summary

This mesocosm experiment provided the opportunity to obtain a well constrained isotopic data set. Due to the intense nature of the phytoplankton bloom which occurred in the

mesocosm, $\delta^{13}C_{POC}$ samples were obtained over a wide range of $[CO_{2(aq)}]$. Therefore the results presented here represent an extension to the range of the existing oceanic data set. It has been possible to apply a Rayleigh model as well as a variety of different empirical and physiological models to the data in order to investigate the possible mechanisms(s) of carbon acquisition used by the phytoplankton within the enclosure.

However, the application of the different models has not led to a clear signal indicating which mechanism of inorganic carbon acquisition is employed by the phytoplankton. Nevertheless, the data presented here agreed well with the empirical models of Rau (*i.e.* Rau *et al.*, 1992, Rau, 1994) despite the implicit assumption made about the isotopic composition of $CO_{2(aq)}$. In addition, the application of the physiological model, modified by Francois *et al.* (1993), indicated that the specific growth rate of the phytoplankton within the enclosure was probably limited by the $[CO_{2(aq)}]$ in the bulk medium as the bloom developed. This prediction was corroborated by the productivity data.

However, this interpretation of the data largely relies on the acceptance of this values of $\alpha_{c/b}$ determined during this study. If the results were re analysed using the previously determined values of $\alpha_{c/b}$, the values of $\epsilon_{POC/a}$, over a large period of the experiment, would be positive and hence the conclusion drawn would be more difficult to accept.

A more important criticism concerns the attempts made by the physiological models to describe the internal inorganic carbon pool within the cell. The Francois *et al.* (1993) model assumes this pool is solely composed of $CO_{2(aq)}$. Other studies (*e.g.* Beardall and Raven, 1981, Raven and Johnston, 1991) indicate that this is not the case as HCO_3^- and CO_3^{2-} are also present and that the $[\Sigma CO_2]$, within the cell, is similar to the external medium (Raven and Johnston, 1991). In addition, the models probably do not fully account for the dynamic, kinetic complexities of the ΣCO_2 pools within the cell and boundary layer surrounding an actively photosynthesising cell and the resultant kinetic isotope effects.

On balance, given the models which are currently available, it is therefore concluded that the phytoplankton within the enclosure were most likely to acquire their inorganic carbon exclusively by the passive diffusion of $CO_{2(aq)}$ into the cell.

PAGE

NUMBERING

AS ORIGINAL

Chapter 7: Variations in the Isotopic Composition of the Phytoplankton in the Menai Strait

7.1 Introduction

Although a large amount of data has now been acquired concerning the spatial variations of the isotopic composition of phytoplankton within the oceanic environment, information concerning the temporal variability is limited (*e.g.* Rau *et al.*, 1992). Furthermore, there appears to be very little information concerning the spatial (Kopczyńska *et al.*, 1995) and temporal (Wainwright and Fry, 1994) variability of the $\delta^{13}C_{POC}$ in coastal marine environments and any information which does exist has been largely collected during estuarine studies as the marine end member (*e.g.* Tan and Strain, 1983, Fogel *et al.*, 1992).

In this section of the thesis isotopic data obtained during a temporal study on the Menai Strait in North Wales in the spring and early summer of 1994 will be presented. The main aim of this study was to investigate the temporal variations of $\delta^{13}C_{POC}$ and interpret the observations in terms of the possible mechanisms of inorganic carbon acquisition (see section 6.2) used by marine phytoplankton within the marine environment by applying the existing empirical models and physiological models introduced in the previous chapter.

The interpretation of the $\delta^{13}C_{POC}$ signal measured in coastal waters is potentially complex due to the input of allochthonous organic material from terrestrial and aquatic ecosystems via rivers and/or the resuspension of mainly refractory sedimentary organic matter from the within the marine environment due to mixing events (*e.g.* storms or spring tides). The potential effects of allochthonous and resuspended organic matter on the $\delta^{13}C_{POC}$ will also be investigated.

7.2 The Study Area

All samples during this study were obtained at high water from St. George's Pier, Menai Bridge, which is situated towards the north east end of the Menai Strait. The Menai Strait is a narrow body of water which is some 20 km long and separates the island of Anglesey from the mainland of North Wales. Hydrological studies have indicated that the residual flow through the Strait is in a south westerly direction, from Liverpool Bay at the north eastern end of the strait to Caernarfon, in the south west (Harvey, 1968) and that the

residence time of a parcel of water entering the Strait from the north east is approximately two days. The residual flow has been attributed to a discrepancy between the tidal ranges at either end of the strait, the range at the north east end exceeding that of the south western end (Harvey, 1968). Therefore samples taken at high water should be representative of water from Liverpool Bay (Dr. C. P. Spencer, *pers. comm.*).

Liverpool Bay represents a large, shallow (< 50 m) portion of the Irish sea, stretching from the Isle of Man in the north west to the North Wales coast in the south. Major fluvial inputs are derived from the Mersey, Dee and Ribble estuaries and Morecambe Bay (Miller, 1985) and other inputs include sewage sludge (~ 40,000 to 80,000 tonnes per year), industrial waste and dredging spoils (Norton *et al.*, 1984 in Miller, 1985). Therefore POC associated with these inputs may contribute to the $\delta^{13}C_{POC}$ signal measured in the Menai Strait although evidence suggests that the impact of the sewage sludge is not far reaching (Norton *et al.*, 1984 in Miller, 1985). An additional source of organic matter within the Strait is the discharge of partially treated sewage via sea outfalls within the Menai Strait.

7.3 Material and Methods

All samples were obtained from St. George's pier at high water by pumping water from ~1 m depth using a hand operated bilge pump. The inflow to the bilge pump was fitted with a 200 μm nylon mesh to prescreen samples and the outflow was placed at the bottom of a 10 dm^3 aspirator. As portions of this sample were to be used to determine parameters associated with the ΣCO_2 system the aspirator was allowed to overflow by at least two volumes before the effluent pipe was withdrawn. The aspirator was then covered with black plastic and returned to the laboratory where sample processing commenced immediately.

7.3.1 Determination of POC, $\delta^{13}C_{POC}$ and Chlorophyll

Samples for the determination of POC and $\delta^{13}C_{POC}$ were obtained by filtering samples through precombusted Whatman GF/F filters (25 mm and 47 mm respectively) using the sampling protocol already detailed in *CHAPTER* 6. The analytical methodologies have also been discussed in *CHAPTER* 6 and a thorough description of the $\delta^{13}C_{POC}$ analysis is given in *APPENDIX* 2.

Samples for the determination of chlorophyll concentrations were obtained by filtering ~1 dm^3 of sea water through a 47 mm Whatman GF/F filter which was frozen prior to analysis. The concentration of chlorophyll was determined by extracting the chlorophyll in 90 % acetone (10 cm^3) overnight in a fridge and measuring the fluorescence using a calibrated fluorometer (Parsons *et al.*, 1984 b).

7.3.2 Determination of the [ΣCO_2], pH and $\delta^{13}C_{\Sigma CO2}$

As the ΣCO_2 system can become modified by air/sea exchange, samples for the determination of [ΣCO_2], pH and $\delta^{13}C_{\Sigma CO2}$ were removed first from the aspirator on return to the laboratory. Samples for the determination of the [ΣCO_2] were obtained from the aspirator using protocol outlined in section 6.3.2 for $\delta^{13}C_{\Sigma CO2}$ and [ΣCO_2]. Samples were stored underwater prior to analysis. The [ΣCO_2] was determined using the automated coulometric system described by Robinson and Williams (1991).

Samples for the determination of $\delta^{13}C_{\Sigma CO2}$ were taken in a similar manner although the samples were quickly transferred from the storage bottles to ampoules and flame sealed for permanent storage using the protocol described in *APPENDIX* 1.

The samples for spectrophotometric pH determination were directly transferred to a 10 cm spectrophotometer cell from the aspirator via a length of Nalgene tubing. The pH was determined immediately using *m*-cresol purple, a detailed description of the methodology is given in *APPENDIX* 3.

7.3.3 The Direct Determination of $\delta^{13}C_a$

The $\delta^{13}C_a$ was determined using the apparatus described in *CHAPTER* 5 (see *FIGURE* 5.1). A water sample was obtained by directly filling the lower reaction vessel with water pumped directly from the Menai Strait using the bilge pump. The water pumped into the lower reaction vessel was allowed to overflow by at least two volumes before the effluent pipe was withdrawn. Saturated mercuric chloride was added immediately (1 μdm^3 per 1 cm^3) and the reaction vessel was isolated from the atmosphere by replacing all of the stoppers before the sample was returned to the laboratory. On return

Table 7.1 Summary of the state variables measured in the Menai Strait. * indicates the pH sample was stored before analysis.

Sample Date	Day of year	Temp. (°C)	Salinity	$[\Sigma CO_2]$ (µmol. kg^{-1})	$pH_{(SWS)}$	$\delta^{13}C_{\Sigma CO2}$ (‰)	$\delta^{13}C_a$ (‰)	POC (µmol $C.dm^{-3}$)	$\delta^{13}C_{POC}$ (‰)	Chl (µg.dm^{-3})
25 Feb 1994	55	3.0	33.183	2090	8.109*	0.38	-	43	-	0.8
4 Mar 1994	62	5.8	33.021	2093	8.065*	0.28	-	39	-	0.7
11 Mar 1994	69	6.8	33.473	2105	8.058	-0.23	-11.07	29	-	0.6
18 Mar 1994	76	4.7	33.601	2107	8.099*	0.12	-10.89	37	-	0.5
25 Mar 1994	83	7.6	33.461	2090	8.04	0.26	-10.75	71	-	0.8
29 Mar 1994	87	7.5	34.154	2117	8.056	0.33	-11.20	58	-22.64	1.0
7 Apr 1994	96	6.9	33.173	2084	8.075	0.12	-10.85	52	-23.36	0.8
11 Apr 1994	100	7.0	32.397	2041	8.075	0.38	-10.65	54	-22.67	1.4
18 Apr 1994	107	8.0	33.193	2042	8.145	0.76	-10.43	64	-20.49	4.2
22 Apr 1994	111	8.4	-	2013	8.135	0.64	-10.24	48	-21.97	5.0
25 Apr 1994	114	8.7	-	2031	8.141	0.50	-9.88	51	-	3.5
29 Apr 1994	118	10.0	-	2054	8.118	0.66	-9.90	46	-20.64	4.2
3 May 1994	122	10.8	-	2040	8.115	0.74	-9.75	35	-21.72	2.4
6 May 1994	125	9.8	-	2051	8.122	0.67	-10.33	32	-23.46	0.7
9 May 1994	128	10.2	-	2004	8.245	0.93	-9.28	42	-22.52	8.3
13 May 1994	132	10.9	-	1958	8.321	2.08	-8.46	78	-22.56	11.5
16 May 1994	135	11.3	-	1926	8.344	2.48	-8.74	73	-22.41	11.8

to the laboratory the lower reaction vessel was placed in to a water bath which had been previously adjusted to the temperature of the Menai Strait. The apparatus was fully assembled as shown in *FIGURE* 5.1 and described in section 5.2. The upper reaction vessel was filled with air at the beginning of the experiment . The aqueous and gaseous phases were allowed to equilibrate by circulating the gaseous phase through the aqueous phase for two hours.

After two hours the pump was stopped, taps 1 and 2 closed and samples taken for the determination of pH and $\delta^{13}C_{\Sigma CO2}$ as described in section 5.2.4. The $\delta^{13}C_g$ was also determined from the air sample in the upper reaction vessel by extracting the $CO_{2(g)}$ cryogenically as previously described (section 5.2.4). The $\delta^{13}C_a$ was then calculated using eqn. 5.3.

7.3.4 Additional Parameters

The temperature of the Menai Strait and the temperature of the water bath used during the experiment to determine $\delta^{13}C_a$ were measured using a Comark 9001 thermometer fitted with

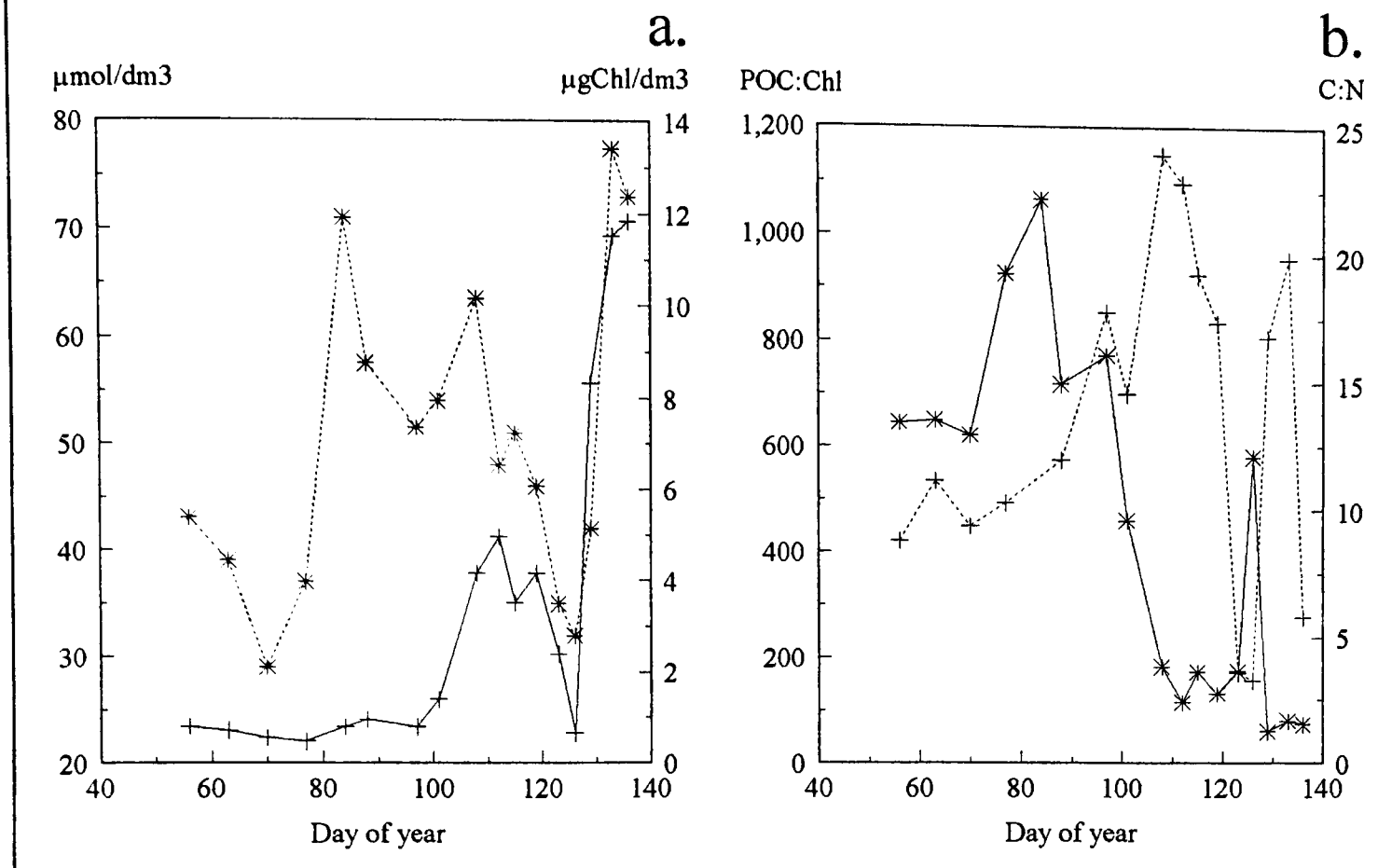

Figure 7.1 Variations in: a; the concentration of chlorophyll (+) and POC (*) and b; POC:Chl (*) and C:N (+) ratios during the temporal study in the Menai Strait

a Comark type K thermocouple (± 0.2°C). The salinity was determined from water samples which had been stored in dedicated salinity bottles using an Autosal (Model 8400A) type salinometer ($\sigma_{n-1} = 0.002$).

7.4 Results

7.4.1 POC and Chlorophyll

The period of study was characterised by initially low chlorophyll concentrations (<1 µgChl.dm^{-3}) followed by two distinct chlorophyll peaks (4.96 and 11.84 µgChl.dm^{-3} respectively), which lasted from day 97 to 123 and from 126 until the end of the study (see *TABLE* 7.1 and *FIGURE* 7.1a). The first bloom was characterised by a mixed assemblage of diatoms although *Asterionella glacialis* and *Ditylum brightwelli* were numerically dominant, the second bloom was initially dominated by the diatom *Rhizosolenia delicatula* although *Phaeocystis* bladders, which were first observed on day 129, quickly became numerically dominant (Blight *et al.*, 1996).

The levels of POC did not always reflect the changes in the concentration of chlorophyll as maybe expected. Initially POC (30 to 40 $\mu mol.dm^{-3}$, *TABLE* 7.1 and *FIGURE* 7.1a) and chlorophyll were at a minimum although the POC concentration quickly increased to ~70 $\mu mol.dm^{-3}$ (day 84) with no commensurate change in the level of chlorophyll, this change is clearly illustrated by rapid increase in the POC:Chl ratio (*FIGURE* 7.1b). It is probable, given the timing of this POC peak, that this can be attributed to the release of planktonic larvae, possibly barnacle nauplii larvae, which after release remain in the water column for about a month. The second POC peak (day 108) is coincident with the rise in chlorophyll concentration during the first bloom and is characterised by a lower POC:Chl ratio which is indicative of a phytoplankton dominated POC pool (Ducklow *et al.*, 1993). As the bloom progresses the levels of POC generally fall and by day 126 the POC, chlorophyll and POC:Chl levels have returned to their prebloom levels. The decline of the bloom can be probably attributed to the rapid sedimentation of diatoms (Kiørbe, 1993).

The second bloom develops very rapidly, with large increases in the concentration of chlorophyll, up to 8 $\mu gChl.dm^3$ in three days (days 126 to 129), and POC. The POC:Chl values during this period are consistent with organic matter which is enriched in phytoplankton.

The C:N ratios vary widely (*FIGURE* 7.1b) from values greater than 20 to values less than 5 and the highest values are generally associated with the phytoplankton blooms which would tend to indicate nitrogen deficiency. The C:N was changed little by the release of the planktonic larvae which was suggested to account for the large POC values observed from days 84 to 97.

7.4.2 The ΣCO_2 System

During the study period the $[\Sigma CO_2]$ decreased by ~250 $\mu mol.kg^{-1}$ from around 2100 $\mu mol.kg^{-1}$ to 1850 $\mu mol.kg^{-1}$ (*TABLE* 7.1, *FIGURE* 7.2a). The $[\Sigma CO_2]$ remained fairly constant during the spring until day 97 when the $[\Sigma CO_2]$ decreased by ~60 $\mu mol.kg^{-1}$ over a period of eleven days, after which the concentration remained fairly constant until day 126 when the $[\Sigma CO_2]$ again began to rapidly decrease and continued to fall until the end of the study (*FIGURE* 7.2a). The pH generally remained low, ~8.05, during the early part of the study (*TABLE* 7.1, *FIGURE* 7.2b). The high pH values recorded on day 56 and day 77 are

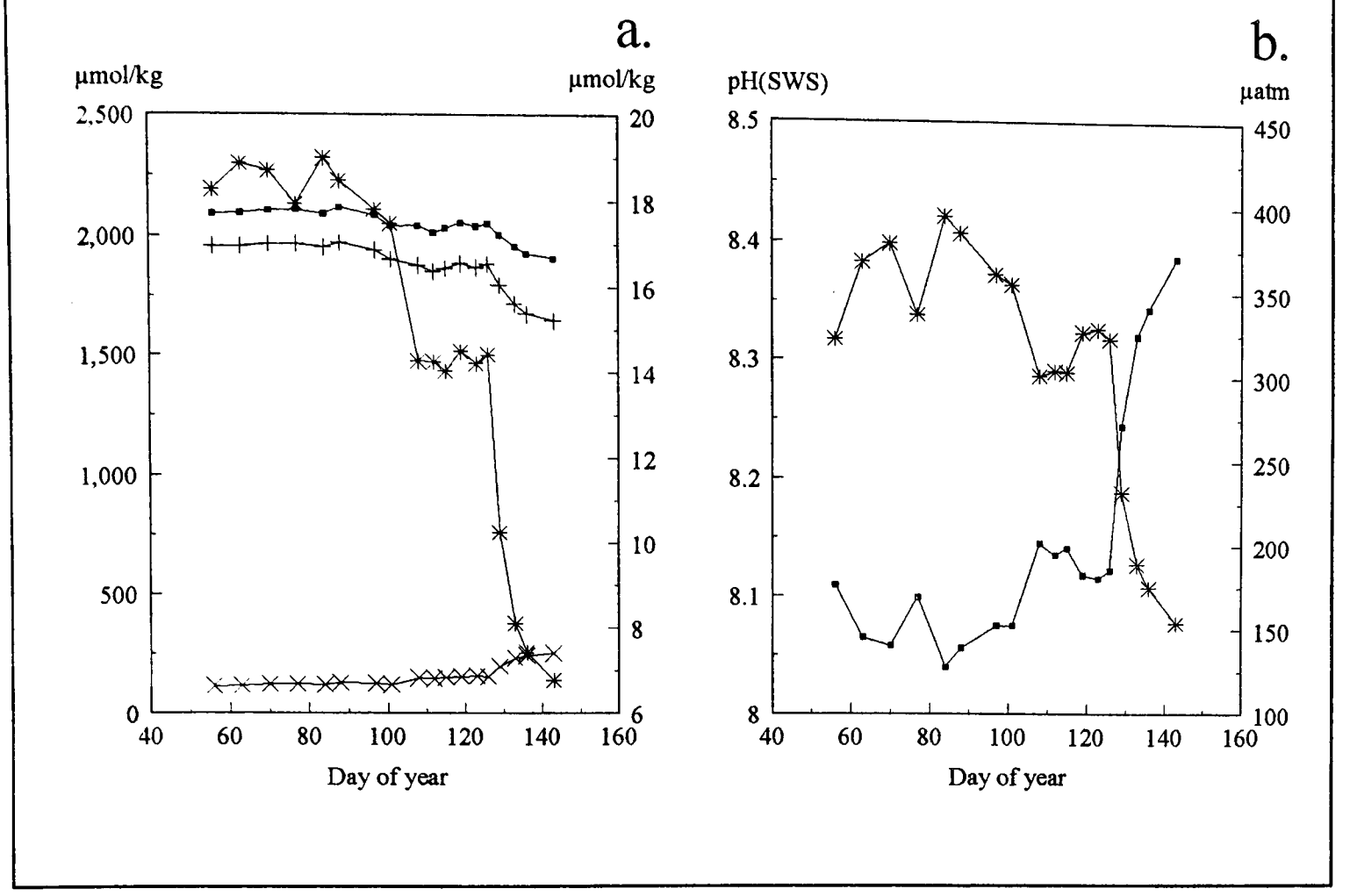

Figure 7.2 Changes in the concentrations of: a; ΣCO_2 (■), $CO_{2(aq)}$ (*), HCO_3^- (+) and CO_3^{2-} (×), b; pH_{sws} (■) and pCO_2 (*) in the Menai Strait

probably erroneous as the pH samples on these days were stored prior to determination. After day 101 the pH rose sharply to ~8.14 and remained at this level until day 126 when the pH again increased and continued to rise until the end of the study period.

The observed decreases in the [ΣCO_2] are coincident with the increases in pH. This is consistent with the removal of $CO_{2(aq)}$ from the system. The periods of rapid change are associated with periods of increasing chlorophyll concentration and therefore the changes in the ΣCO_2 system can probably be attributed to the photosynthetic uptake of $CO_{2(aq)}$ from the system.

Using the sea water model the measured pH was corrected to *in situ* temperature (see *APPENDIX* 3) and the concentration of $CO_{2(aq)}$, HCO_3^- and CO_3^{2-} have been calculated and the results are given in *TABLE* 7.2 and *FIGURE* 7.2a. As salinity measurements were not available for the whole study period the average value was used when performing these calculations for days with no salinity data.

Table 7.2 Changes in the ΣCO_2 system calculated using the sea water model (Prof. D. Turner) from pH and $[\Sigma CO_2]$ measurements. The pH measurements have been corrected to *in situ* values using the method described in *APPENDIX* 3.* indicates these are average values as no salinity data was obtained for this period.

Sample Date	Day of year	Temp. (°C)	Salinity	$[\Sigma CO_2]$ (µmol/kg)	pH_{SWS}	$[CO_{2(aq)}]$ (µmol. kg^{-1})	$[HCO_3^-]$ (µmol. kg^{-1})	$[CO_3^{2-}]$ (µmol. kg^{-1})	pCO2 µatm
25-Feb-94	56	2.98	33.183	2090	8.109	18.26	1957	115	322
04-Mar-94	63	5.8	33.021	2093	8.065	18.86	1957	117	368
11-Mar-94	70	6.82	33.473	2105	8.058	18.7	1964	122	379
18-Mar-94	77	4.68	33.601	2107	8.099	17.93	1966	123	337
25-Mar-94	84	7.57	33.461	2090	8.04	19	1951	120	395
29-Mar-94	88	7.5	34.154	2117	8.056	18.47	1971	128	385
07-Apr-94	97	6.87	33.173	2084	8.075	17.81	1941	125	361
11-Apr-94	101	7.01	32.397	2041	8.075	17.48	1902	121	355
18-Apr-94	108	8.01	33.193	2042	8.145	14.26	1878	149	301
22-Apr-94	112	8.35	33.3*	2013	8.135	14.24	1852	147	304
25-Apr-94	115	8.7	33.3*	2031	8.141	14.03	1865	152	303
29-Apr-94	119	10	33.3*	2054	8.118	14.49	1885	154	327
03-May-94	123	10.8	33.3*	2040	8.115	14.21	1869	157	329
06-May-94	126	9.8	33.3*	2051	8.122	14.41	1883	154	323
09-May-94	129	10.2	33.3*	2004	8.245	10.25	1796	198	232
13-May-94	133	10.9	33.3*	1958	8.321	8.11	1718	232	189
16-May-94	136	11.3	33.3*	1926	8.344	7.43	1675	243	175

From *FIGURE* 7.2a it can be clearly seen that there are two periods during which the $[CO_{2(aq)}]$ rapidly decreases, both of which are coincident with increases in the concentration of chlorophyll. The first decrease in the $[CO_{2(aq)}]$ appears to indicate that the primary production during the first bloom was mainly limited to the period between days 101 and 108 (*i.e.* the start of the bloom) even though the chlorophyll concentration remained high after this period, and the second increase also indicates that the highest levels of productivity were confined to the initial stages of the bloom.

7.4.3 The distribution of ^{12}C and ^{13}C within the ΣCO_2 system and POC

The isotopic composition of the ΣCO_2 pool increased during the period of study (*TABLE* 7.1, *FIGURE* 7.3). The increase was not constant and changes in the $\delta^{13}C_{\Sigma CO2}$ are confined to the periods between days 101 and 108 and from day 126 until the end of the study, although the largest and most rapid change was associated with latter period. These periods of change are again associated with periods of chlorophyll increase and as a result can be attributed to the photosynthetic removal of carbon from the ΣCO_2 system.

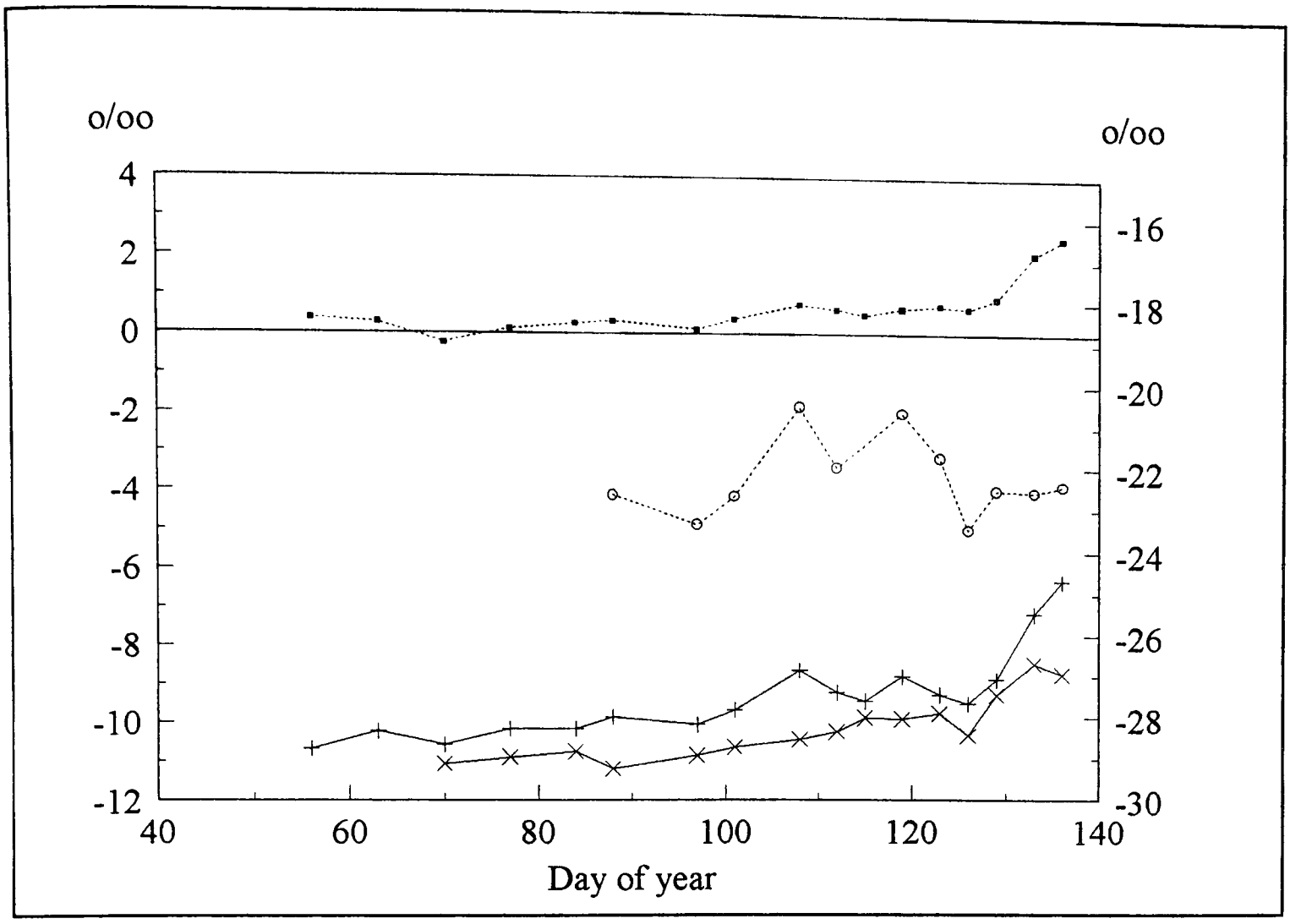

Figure 7.3 Variations in the isotopic composition of ΣCO_2 (■), $CO_{2(aq)}$ and POC (○). The isotopic composition of $CO_{2(aq)}$ has been estimated using the two different methods discussed in the text: calculated from $\delta^{13}C_{\Sigma CO2}$ (+) and directly determined (×). The $\delta^{13}C_{POC}$ results have been plotted on the secondary Y axis to aid clarity.

The isotopic compositions of $CO_{2(aq)}$, HCO_3^- and CO_3^{2-} have been calculated using the values of $\alpha_{c/b}$ determined during this study and $\alpha_{b/a}$ determined by Mook *et al.* (1974) in conjunction with eqns. 4.5 to 4.7. The calculated values of $\delta^{13}C_a$, $\delta^{13}C_b$ and $\delta^{13}C_c$ are given in *TABLE* 7.3 along with the directly determined values of $\delta^{13}C_a$.

The directly determined values of $\delta^{13}C_a$ appear to be slightly offset from the calculated values of $\delta^{13}C_a$. When $\delta^{13}C_a$ was directly determined the atmospheric flask was initially filled with air ($\delta^{13}C_g \approx -7$ ‰) which maybe expected to slightly alter the isotopic composition of $\delta^{13}C_{\Sigma CO2}$ as the sea water in the Menai Strait is not in isotopic equilibrium with the atmosphere. However, comparison of the $\delta^{13}C_{\Sigma CO2}$ values taken directly from the Menai Strait and those taken from the aqueous phase at the end of the experiment indicate that the average difference is 0.01 ‰, less than the precision of the $\delta^{13}C_{\Sigma CO2}$ technique. Therefore the air in the atmospheric vessel did not significantly alter the isotopic composition of the $\delta^{13}C_{\Sigma CO2}$ and the values of $\delta^{13}C_a$ determined in this manner probably

Table 7.3 The calculated isotopic composition of $CO_{2(aq)}$, HCO_3^- and CO_3^{2-} (see text for explanation). The directly determined values of the ΣCO_2 and $CO_{2(aq)}$ pools have also been given for comparison.

Date	Day of year	$\delta^{13}C_{\Sigma CO2}$ (‰)	Calculated $\delta^{13}C_a$ ‰	Calculated $\delta^{13}C_b$ ‰	Calculated $\delta^{13}C_c$ ‰	Directly determined $\delta^{13}C_a$ ‰
25 Feb 1994	56	0.38	-10.67	0.95	-14.31	-
4 Mar 1994	63	0.28	-10.22	1.04	-13.02	-
11 Mar 1994	70	-0.23	-10.57	0.56	-13.07	-11.07
18 Mar 1994	77	0.12	-10.17	1.24	-13.30	-10.89
25 Mar 1994	84	0.26	-10.16	0.89	-12.43	-10.75
29 Mar 1994	88	0.33	-9.86	1.20	-12.16	-11.20
7 Apr 1994	97	0.12	-10.06	1.08	-12.54	-10.85
11 Apr 1994	101	0.38	-9.68	1.44	-12.13	-10.65
18 Apr 1994	108	0.76	-8.65	2.35	-10.80	-10.43
22 Apr 1994	112	0.64	-9.21	1.74	-11.26	-10.24
25 Apr 1994	115	0.50	-9.43	1.47	-11.37	-9.88
29 Apr 1994	119	0.66	-8.80	1.96	-10.34	-9.90
3 May 1994	123	0.74	-9.27	1.38	-10.57	-9.75
6 May 1994	126	0.67	-9.49	1.28	-11.10	-10.33
9 May 1994	129	0.93	-8.87	1.86	-10.35	-9.28
13 May 1994	133	2.08	-7.18	3.48	-8.45	-8.46
16 May 1994	136	2.48	-6.32	4.30	-7.48	-8.74

closely represent the values of the *in situ* $\delta^{13}C_a$. It is worth noting that the values of $\delta^{13}C_a$ calculated using the fractionation factors determined by Thode *et al.* (1965) and Mook *et al.* (1974) (see *TABLES* 5.1 and 5.2) agree more closely with the directly determined values of $\delta^{13}C_a$.

Nevertheless, the different values of $\delta^{13}C_a$ (*FIGURE* 7.3) show the same trend of generally increasing throughout the study, although the periods of most rapid change were again associated with the second bloom. As the general trend of $\delta^{13}C_a$, estimated using the different methods are the same, the values calculated using $\alpha_{c/b}$ determined during this study will be used to maintain consistency.

The $\delta^{13}C_{POC}$ increased during the first bloom from ~ -23 ‰ to ~ -21 ‰ and returned to pre bloom levels at the end of the bloom (*FIGURE* 7.3). The $\delta^{13}C_{POC}$ values do not change during the second, larger, bloom as would have been predicted. The values of $\epsilon_{POC/a}$ and $\epsilon_{POC/b}$ (*i.e.* assuming either $CO_{2(aq)}$ or HCO_3^- are exclusive sources of inorganic carbon) have also been calculated using the expressions given in eqns. 3.4 and 3.5 and the results are plotted in *FIGURE* 7.4. Both sets appear to indicate a slight decrease in the enrichment

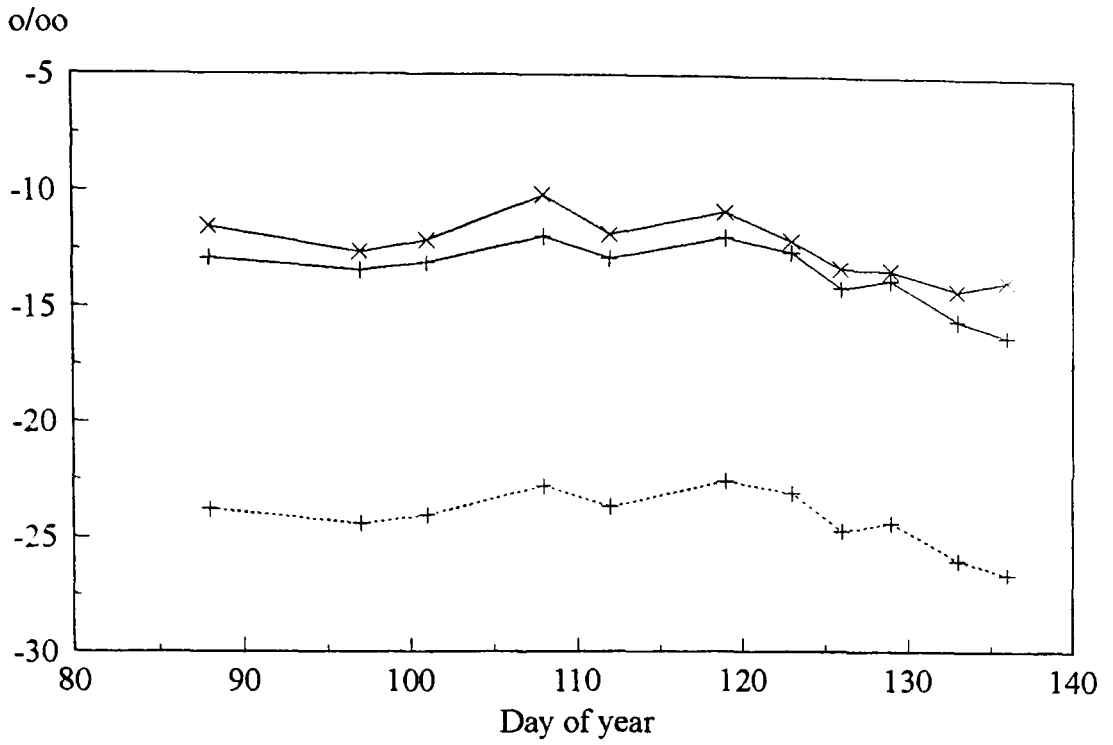

Figure 7.4 Variations in the $\epsilon_{POC/a}$ (solid lines) and $\epsilon_{POC/b}$ (dashed line). The values of $\epsilon_{POC\ a}$ have been estimated using the calculated (+) and directly determined (×) values of $\delta^{13}C_a$.

factor associated with the first bloom and an increase associated with the second bloom. The $\delta^{13}C_{POC}$ data set does not extend to the beginning of the study and only starts during the period when the POC pool was dominated by what is assumed to be planktonic larvae. The presence of these larvae may alter the isotopic composition of the POC pool and therefore the $\delta^{13}C_{POC}$ signal will no longer be representative of the phytoplankton. The $\delta^{13}C_{POC}$ value measured during the period between the two blooms, which is characterised by a sharp decline in the concentrations of POC and chlorophyll, to the levels observed before levels of larvae and phytoplankton increased, may be taken to represent the isotopic composition of the POC pool when concentration of biologically active POC is at a minimum. This value (-23.5) is close to the average value measured (-22.9 ± 0.4 ‰) during the period of larval release before the first phytoplankton bloom. This would indicate that the isotopic composition of the larvae is not significantly different the existing POC.

7.5 Discussion

Temporal and spatial variations between the oceanic $\delta^{13}C_{POC}$ signal and $[CO_{2(aq)}]$ can be well described by a simple negative linear relationship (Rau *et al.*, 1992, Rau, 1994).

Physiological explanations of this relationship have generally assumed that oceanic phytoplankton obtain their inorganic carbon by the passive diffusion of $CO_{2(aq)}$. The results presented in the previous chapter appear to generally confirm this relationship.

Comparison of the overall relationship between $\delta^{13}C_{POC}$ and $[CO_{2(aq)}]$, determined during this study, with previously derived linear, empirical relationships (*FIGURE* 7.5a) indicate that the agreement is poor. The results of this study show little overall variation (the calculated slope of the linear regression was zero) despite the large (11 $\mu mol.kg^{-1}$) change in the $[CO_{2(aq)}]$, which suggests that the isotopic composition of phytoplankton within the Menai Strait is independent of the $[CO_{2(aq)}]$. On the basis of the empirical relationships derived by previous studies and the relationship derived during the mesocosm experiment (*FIGURE* 6.6) the $\delta^{13}C_{POC}$ in the Menai Strait would have been expected to increase by either 16.5 ‰ (Rau *et al.*, 1992), 7 ‰ (Rau, 1994), or 11 ‰ (this study) for the 11 $\mu mol.kg^{-1}$ change in $[CO_{2(aq)}]$. However, despite the apparently independent nature of $\delta^{13}C_{POC}$ with respect to $[CO_{2(aq)}]$ the $\delta^{13}C_{POC}$ are numerically similar to the values predicted by the empirical linear models, although the agreement is closest when the $[CO_{2(aq)}]$ was high.

A plot of the values of $\epsilon_{POC/a}$ in relation to the $[CO_{2(aq)}]$ indicate a small overall increase in the $\epsilon_{POC/a}$ as the $[CO_{2(aq)}]$ decreases (*FIGURE* 7.5b). This trend is contrary to the that predicted by the non - linear models of Jasper and Hayes (1994) and Popp *et al.* (1989). The values of $\epsilon_{POC/a}$ determined during this study agree more closely with the predicted values of $\epsilon_{POC/a}$ when the $[CO_{2(aq)}]$ is low.

It would therefore appear that any temporal changes in the $\delta^{13}C_{POC}$ signal that may be expected as a result of deceases in the $[CO_{2(aq)}]$ are not observed in the Menai Strait. This maybe because the phytoplankton present during the study acquired their inorganic carbon via a mechanism independent of the $[CO_{2(aq)}]$ or, any changes in the isotopic composition of the phytoplankton may have been obscured by a large residual pool of biologically inactive POC. Given the coastal nature of the study site and the various potential sources of POC it seems likely that allochthonous sources of POC may have made a significant contribution to the total POC pool and $\delta^{13}C_{POC}$ signal at certain times of the year. As a result, if changes in the isotopic composition of the phytoplankton are to be interpreted in relation to the mechanism of inorganic carbon acquisition the effects of these sources must be corrected for.

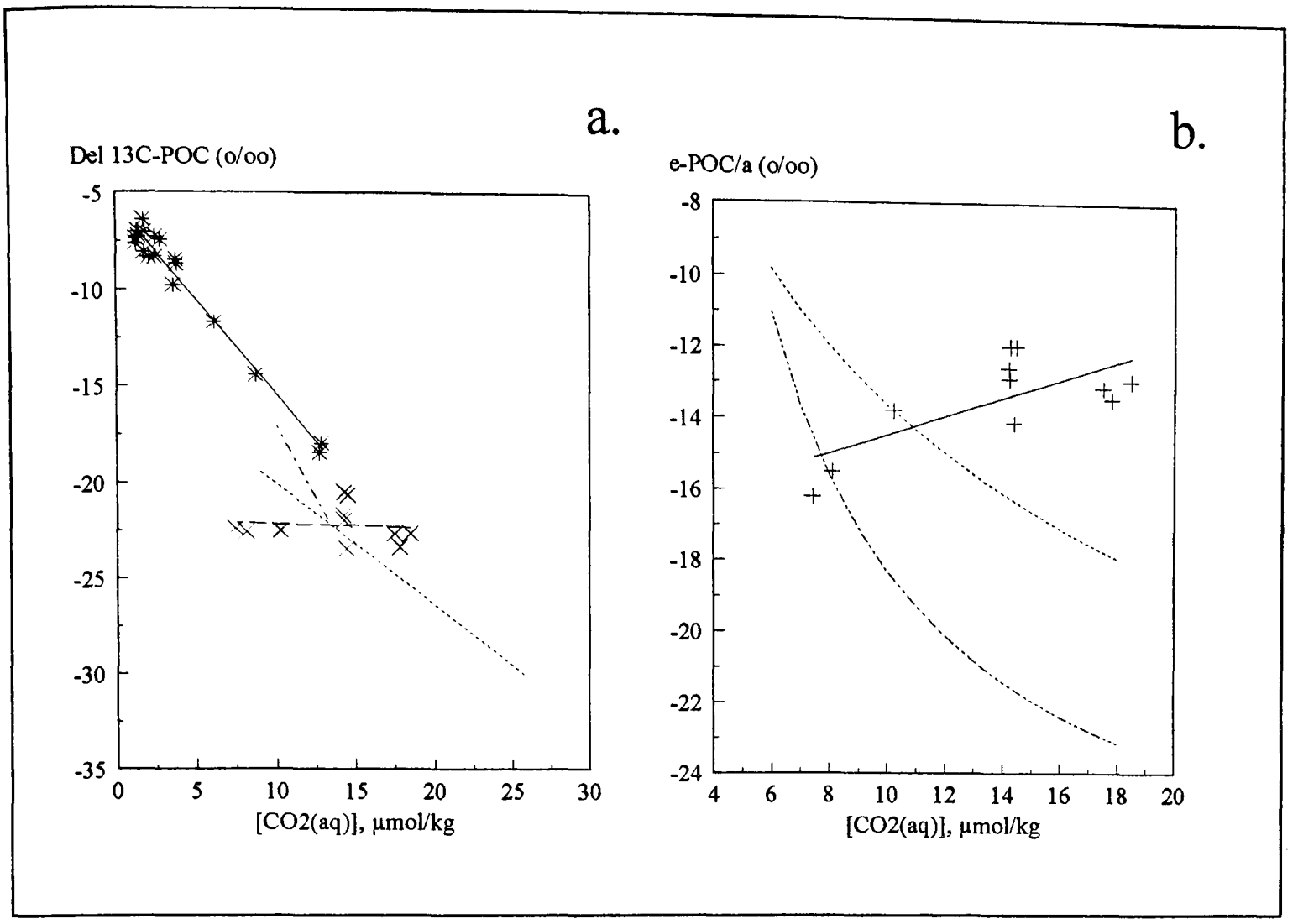

Figure 7.5 Variations in $\delta^{13}C_{POC}$ and $\epsilon_{POC/a}$ in relation to the $[CO_{2(aq)}]$.a) A linear regression ($\delta^{13}C_{POC}$ = -22 (±1) - 0.02 (±0.1) × $[CO_{2(aq)}]$) (long dash) has been fitted to the values of $\delta^{13}C_{POC}$(×) determined during this study and the empirical relationships derived by Rau *et al* (1992) (long - short dash), Rau (1994) (short dash) and the mesocosm study (*CHAPTER* 6) (solid line) are given for comparison. b) A linear regression (solid line) has been fitted to the calculated values of $\epsilon_{POC/a}$ (+) ($\epsilon_{POC/a}$ = -17 (±1) + 0.3 (±0.1) × $[CO_{2(aq)}]$). The relationships derived by Popp *et al.* (1989) (short dash) and Jasper and Hayes (1994) (long short short dash) are given for comparison.

This correction may be achieved by rearranging the following mass balance relationship:

$$\delta^{13}C_{POC} \times POC = \delta^{13}C_R \times POC_R + \delta^{13}C_P \times POC_P \qquad \textbf{(7.1)}$$

where POC_P and $\delta^{13}C_P$ are the concentration and isotopic composition of the phytoplankton pool and POC_R and $\delta^{13}C_R$ are the concentrations and isotopic composition of the residual organic material. In order to calculate $\delta^{13}C_P$ from the above relationship it is necessary to estimate POC_R and $\delta^{13}C_R$.

During the periods of low biological activity the concentration and isotopic composition of the POC pool would be expected to closely reflect POC_R and $\delta^{13}C_R$. The

periods of low biological activity (*i.e.* days 56 - 70 and day 126) during this study appear to be characterised by a relatively high level of POC (~ 30 $\mu mol.dm^{-3}$). The POC:Chl ratios associated with these periods are not characteristic of a phytoplankton POC (*e.g.* Raymont, 1980, Ducklow *et al.*, 1993) which indicates that a large amount of this organic matter is not associated with phytoplankton. By using POC:Chl ratios (80 µg:µg, Ducklow *et al.*, 1993) the amount of phytoplankton POC during the period of low biological activity is estimated to be ~ 5 $\mu mol.dm^{-3}$ and, by difference, the residual pool of organic carbon is ~25 $\mu mol.dm^{-3}$.

The $\delta^{13}C_{POC}$ during the periods of low biological activity will be dependent on the concentration and isotopic composition of the phytoplankton (POC_P and $\delta^{13}C_P$) and the residual organic material (POC_R and $\delta^{13}C_R$). If the isotopic signal from the two sources are similar the $\delta^{13}C_{POC}$ measured during these periods will closely represent the isotopic composition of the POC_R pool. Unfortunately the $\delta^{13}C_{POC}$ data does not extend to the period of low biological activity at the start of the study (days 56 - 70). However, by applying the empirical relationship of Rau (1994) it maybe possible to predict the $\delta^{13}C_P$ from $[CO_{2(aq)}]$: -25‰. This agrees closely with $\delta^{13}C_{POC}$ values recorded in the Gulf of St. Lawrence (Tan and Strain, 1983); -24‰, and Woods Hole (Wainwright and Fry, 1994); -25‰ (during the periods of low biological activity). Therefore as the predicted and measured isotopic composition of phytoplankton at similar latitudes are similar to the $\delta^{13}C_{POC}$ measured during the periods of low biological activity (day 126); -23.5‰, this value will be taken to represent POC_R.

Using the isotopic signal associated with POC_R pool in association with additional lines of evidence, it maybe possible to infer the most likely source of this pool from the three main sources:

i. The input of screened sewage directly into the Menai Strait.

ii. The input of organic matter of terrestrial and/or riverine origin via rivers discharging into Liverpool bay.

iii. The presence of a large amount of predominately refractory organic matter due to the resuspension of organic rich sediments and/or sewage sludge in Liverpool Bay.

Firstly, the input of fresh sewage via marine outfalls within the Menai Strait maybe expected to contribute significantly to the POC_R pool. The isotopic composition of sewage is -24 to -26 ‰ (Coffin *et al.*, 1994, Burnett and Schaffer, 1980, respectively) which is close to the estimated isotopic composition of the POC_R indicating that sewage may potentially be the source of the POC_R pool. However, areas of high organic input are normally characterised by a high level microbial chemoautotrophic primary production, which can replace photosynthesis as the dominant source of ecosystem energy production (Conway *et al.*, 1994). A concurrent study in the Menai Strait (Blight *et al.*, 1996) has indicated that the temporal variations of microbial numbers and activity was not characteristic of a system with high organic input, indicating that the large residual POC pool was largely refractory and therefore not derived from fresh sewage.

With respect to the second point, the impact of terrestrial and aquatic POC, entering Liverpool Bay via rivers, on the $\delta^{13}C_{POC}$ measured at Menai Bridge is probably very low. Evidence for this can be obtained from the salinity levels within the Menai Strait which remain close to the salinity of the Irish Sea. Estuarine isotope studies have indicted that when the salinity of estuary water approaches the salinity of the sea the $\delta^{13}C_{POC}$ signal is dominated by the marine system (*e.g.*, Tan and Strain, 1983).

Thirdly, the isotopic composition of sedimentary organic carbon generally reflects the isotopic composition of the phytoplankton growing in the water column (Tan and Strain, 1979). The $\delta^{13}C_P$ during this study remains constant at ~-23 ‰ which is similar to the isotopic composition of coastal marine sedimentary POC (-22 ‰) measured at similar latitudes (Tan and Strain, 1979). The C:N ratios of the POC determined during the periods of low biological activity are similar to the ratio expected in marine coastal sediments (Tan and Strain, 1979).

Therefore it will be assumed that the residual POC pool has been derived from the resuspension of sedimentary organic matter and is largely composed of refractory organic matter, the concentration and isotopic composition will be assumed to be a constant 25 $\mu mol.dm^{-3}$ and ~ -23.5 ‰ respectively throughout the study period. By rearranging the mass balance relationship (eqn. 7.1) the isotopic composition of the organic matter associated with phytoplankton during the study can be determined from the $\delta^{13}C_{POC}$. The calculated values

of $\delta^{13}C_P$ have been plotted on *FIGURE* 7.6a along with the values of $\delta^{13}C_{POC}$ for comparison.

The validity of assuming the concentration of POC_R remains constant throughout the study period is questionable. As the most likely source of the POC_R is the resuspension of sedimentary organic material the amount of resuspended material would be expected to vary in relation to the frequency and magnitude of mixing events such as storms and spring tides. As both the frequency and magnitude of these events decrease during the summer months the concentration of POC_R can also be expected to decline. If the values of $\delta^{13}C_P$ are recalculated, this time assuming the concentration of POC_R is equal to 10 $\mu mol.dm^{-3}$ the values of $\delta^{13}C_P$ decrease from -17.2 to -19.9‰ and from -21.8 to -22.2‰ on days 119 and 136 respectively. Therefore the estimates of $\delta^{13}C_P$ during the first bloom are much more susceptible to variations in the concentration of POC_R and can probably be viewed as maximum values (*i.e.* the least negative), whereas the values of $\delta^{13}C_P$ during the second bloom are not greatly affected by the assumptions made.

The isotopic composition of the POC_R is also taken to be constant throughout the study period. The validity of this assumption is not as tenuous because even if the concentration of POC_R varies in relation to mixing events the isotopic composition of the resuspended sediments will probably remain constant.

The following sections examine the applicability of existing empirical models (*e.g.* negative linear, non-linear and logarithmic models) and physiological models which have been used to describe and account for the observed variations in the $\delta^{13}C_{POC}$ of the phytoplankton. From *FIGURE* 7.6 b it is apparent that the $\delta^{13}C_P$ values during the first bloom generally increase as the $[CO_{2(aq)}]$ decreases, where as the values remain more or less constant during the second bloom. As the response of the $\delta^{13}C_P$ values appears to differ for each bloom the two events will be discussed separately in relation to the different models.

7.5.1 First Bloom

The isotopic composition of the phytoplankton, estimated using the mass balance equation, is calculated to rise by ~ 6 ‰ during this first bloom. This is larger than the change predicted by the empirical model of Rau (1994), 2.5 ‰, and the model derived from the mesocosm

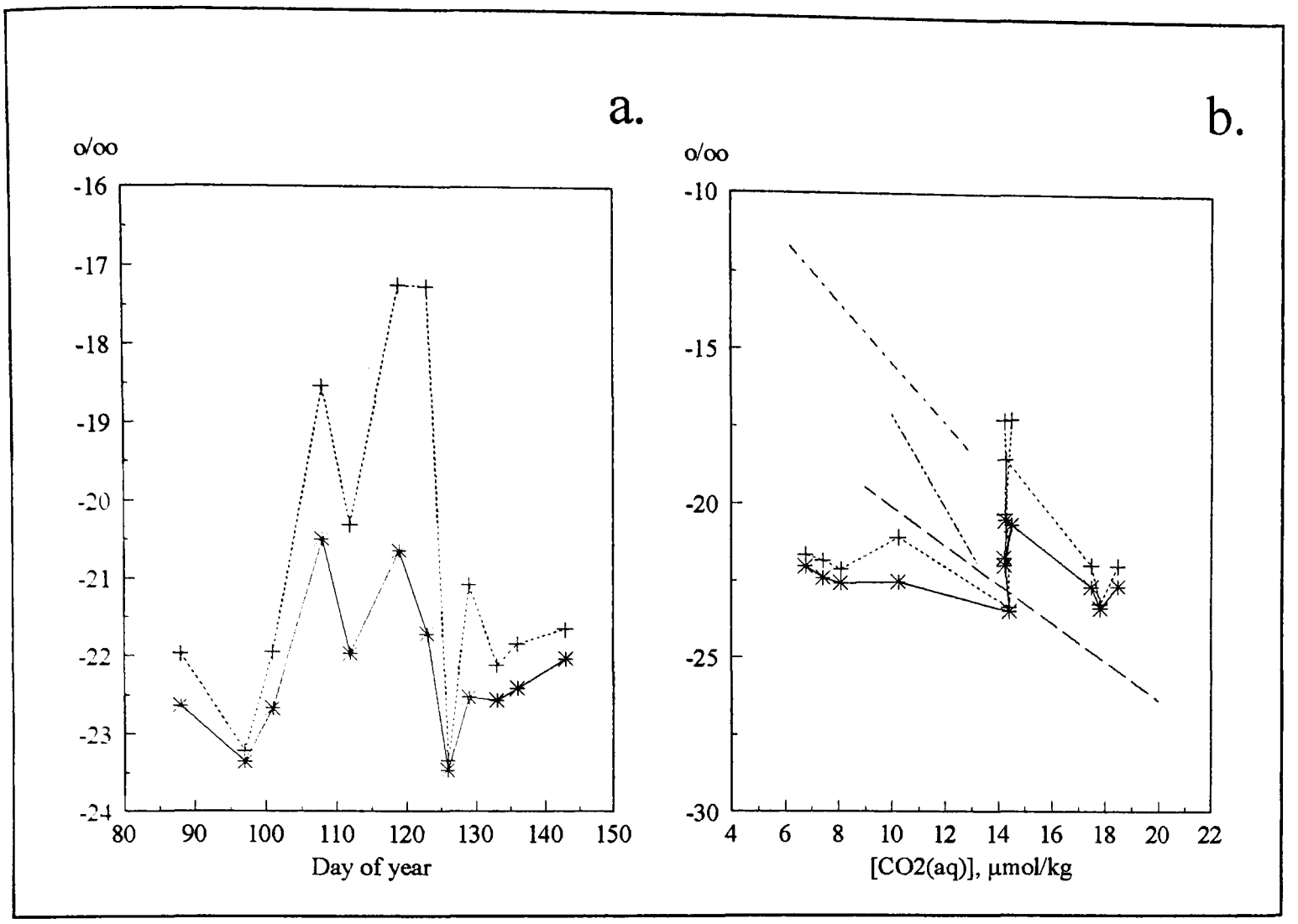

Figure 7.6 Changes in $\delta^{13}C_{POC}$ (*, solid line) and $\delta^{13}C_P$ (+, short dash) have been plotted in as a time sequence (a) and in relation to the $[CO_{2(aq)}]$ (b). The relationships between $CO_{2(aq)}$ and $\delta^{13}C_P$ determined by previous studies have been plotted for comparison; Rau *et al* (1992) (long short short dash), Rau (1994) (long dash) and mesocosm study, *CHAPTER* 6 (long short dash).

experiment, 3.9 ‰, for the 4 $\mu mol.kg^{-1}$ change in the $[CO_{2(aq)}]$ observed over the same period, although it generally agrees with the change predicted by the model derived by Rau *et al.* (1992). However, due to the assumptions made during the estimation of $\delta^{13}C_P$ the calculated rise probably represents the maximum change of $\delta^{13}C_P$. Therefore, changes in $\delta^{13}C_P$ during the first bloom seem to be generally consistent with the predictions of empirically derived models relating the $\delta^{13}C_P$ to the $[CO_{2(aq)}]$ (*FIGURE* 7.6b), which, as a result implies that $CO_{2(aq)}$, supplied by passive diffusion, is the most likely source of inorganic carbon.

The values of $\epsilon_{P/a}$ (*i.e.* the enrichment factor between $CO_{2(aq)}$ and phytoplankton POC) have also been calculated and are given in *FIGURE* 7.7 along with the non - linear models of Popp *et al.* (1989) and Jasper and Hayes (1994). The values of $\epsilon_{P/a}$ during the first bloom do not agree with the values predicted using the models, although the general trend

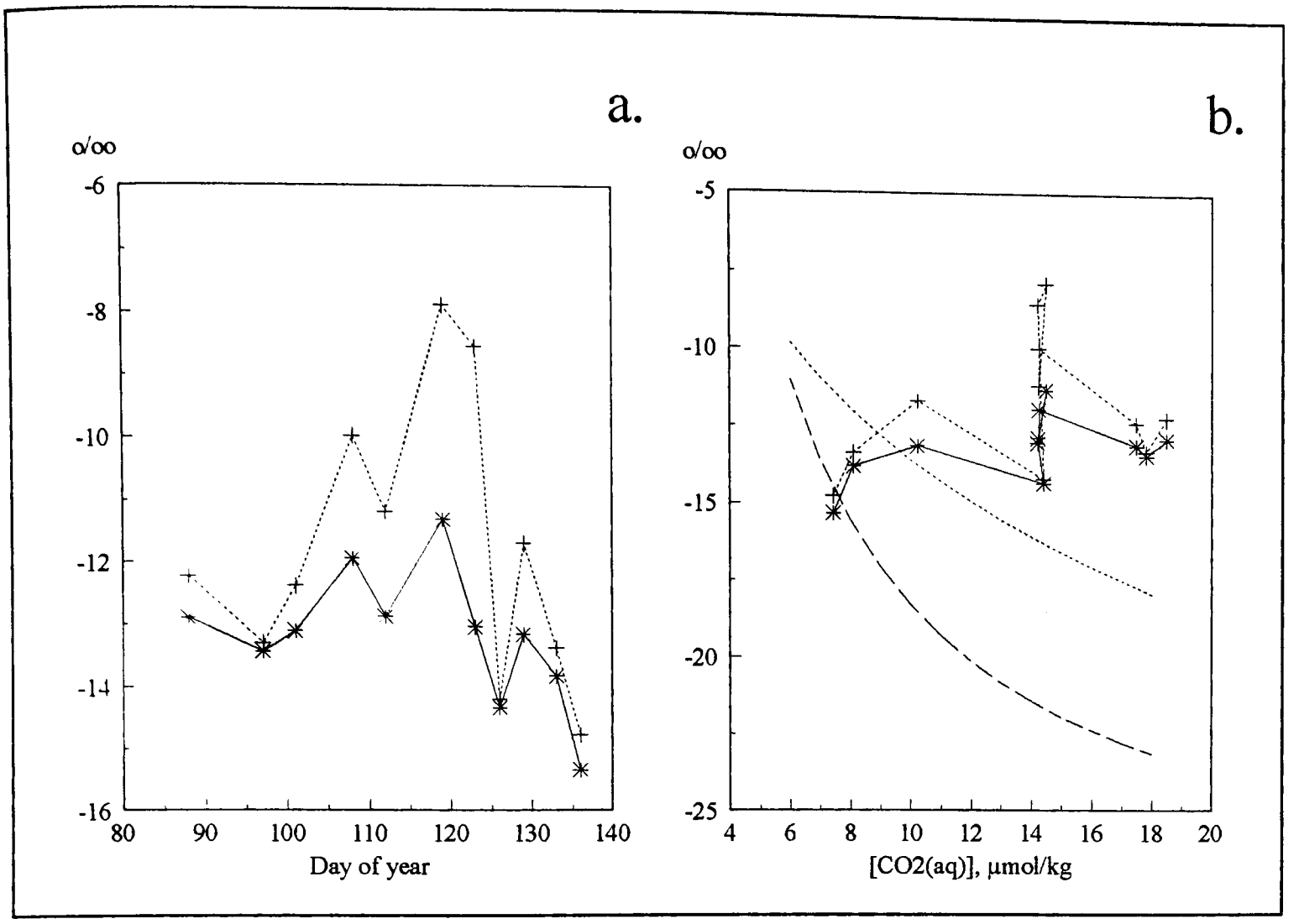

Figure 7.7 Variations in the values of $\epsilon_{POC/a}$ (*) and $\epsilon_{P/a}$ (+) in relation to: a) time (days) and b) $[CO_{2(aq)}]$. The relationships determined by Popp *et al.* (1989) (short dash) and Jasper and Hayes (1994) (long dash) have also been plotted.

of $\epsilon_{P\,a}$ decreasing as the $[CO_{2(aq)}]$ decreases is observed. A similarly large disagreement between the values of $\epsilon_{P/a}$ predicted using the Popp *et al.* (1989) and Jasper and Hayes (1994) models and the values of $\epsilon_{P/a}$ determined during the mesocosm study was also observed. The model of Popp *et al.* (1989) was calibrated using the results of lake based studies (McCabe, 1985) and the Jasper and Hayes (1994) model used the $\delta^{13}C$ values of alkenones and foraminiferal carbonates from geological cores whereas the models of Rau *et al.* (1992) and Rau (1994) have been derived from present day oceanic measurements. The methods used to calibrate the Popp *et al.* (1992) and Jasper and Hayes (1994) models may account for the observed discrepancy between these models and the models derived by Rau and by this study.

Nevertheless, despite the quantitative disagreement between the empirical models and observations made during the first bloom, there is qualitative agreement, *i.e.* decreasing values of $\epsilon_{POC/a}$ as $[CO_{2(aq)}]$ decreases, which would again suggest that $[CO_{2(aq)}]$ is the most probable photosynthetic substrate.

Although the general agreement between the various models and the results presented here for the first bloom is satisfactory, there appears to be large fluctuations in $\delta^{13}C_P$ and $\epsilon_{P/a}$ (~3‰) at the end of the bloom, which are not associated with changes in $[CO_{2(aq)}]$ (*FIGURE* 7.6 and 7.7). A similar observation was made during the study by Francois *et al.* (1993) and this was interpreted by applying the more physiologically rigorous model given in the previous chapter (see section 6.5.3, eqns. 6.7 and 6.8, page 116) which predicts $\epsilon_{P/a}$ will change in relation to $[CO_{2(aq)}]$ and/or growth rate. According to this model lower values of $\epsilon_{P/a}$ would be expected to be associated with higher growth rates.

The values of $\epsilon_{P/a}$ have been plotted in *FIGURE* 7.8 along with the changes in $\epsilon_{P/a}$ for constant levels of $[C_e] - [C_i]$ predicted by the model used by Francois *et al.* (1993) (see section 6.5.3). The model predicts that the decrease in $\epsilon_{P/a}$ towards the end of the first bloom is associated with an increase in $[C_e] - [C_i]$, which maybe interpreted as an increase in growth rate. However, the $[CO_{2(aq)}]$ and $[\Sigma CO_2]$ remained fairly constant during this period indicating a very low level of primary production which is not consistent with the higher growth rates predicted by the model.

As previously demonstrated, the predicted values of $\delta^{13}C_P$ during this period are particularly sensitive to the assumption of a constant concentration of POC_R. Therefore changes in the concentration of POC_R could easily account for the variation in the values of $\delta^{13}C_P$ predicted using the mass balance approach.

An implicit assumption made in the application of the above empirical and physiological models is that the species of phytoplankton from which the community is comprised can only derive their inorganic carbon by the passive diffusion of $CO_{2(aq)}$. It has been demonstrated (Beardall *et al.*, 1976, Burns and Beardall, 1987) that certain species of marine phytoplankton maybe able to increase the supply of inorganic carbon by the induction of a CCM (Sharkey and Berry, 1985). Culture experiments indicate that $\epsilon_{POC/a}$ (or $\epsilon_{P/a}$) associated with phytoplankton using a CCM is ~ -4 to -7 ‰ and therefore if the phytoplankton during the first bloom were able induce a CCM their isotopic composition would have been expected to be -14 to -17 ‰. The $\delta^{13}C_P$ during the first bloom approached, but did not reach, this isotopic composition. It may be suggested that the observed changes in the $\delta^{13}C_P$ represent the mixing of POC_P, with a low isotopic composition, with an

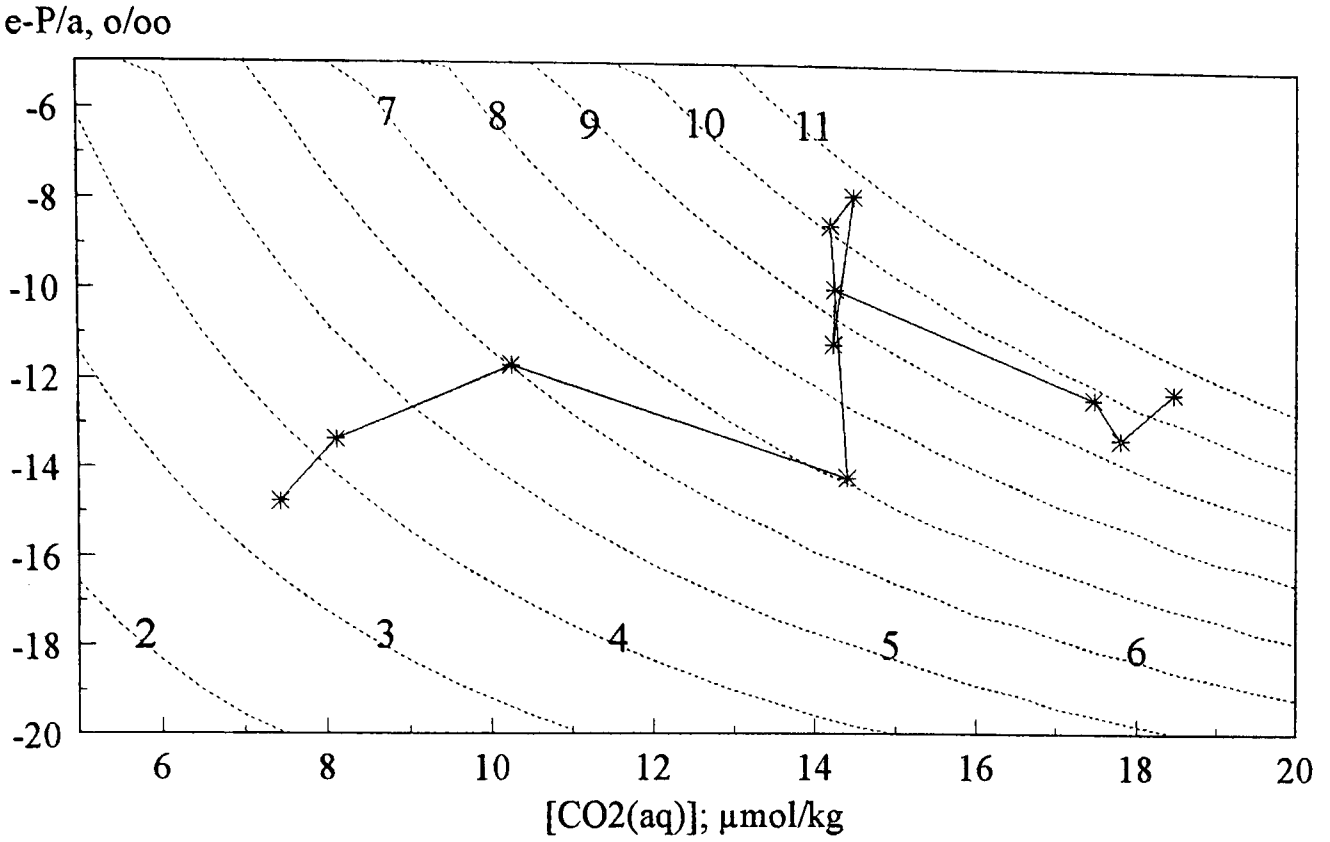

Figure 7.8 The calculated values of $\epsilon_{P/a}$ (*) are plotted along with the values of $\epsilon_{P/a}$ predicted for constant levels of $[C_e]$ - $[C_i]$ (dashed line) using the model given by Francois *et al.* (1993) (eqn. 6.8). The data points have been joined sequentially to indicate the time course.

increasing amount of new POC_P with an isotopic composition of -14 to -17 ‰ due to the presence of phytoplankton operating a CCM.

The first bloom was diatomaceous in character and was dominated by *Asterionella glacialis* and *Ditylum brightwelli*. The presence of a CCM has only been experimentally demonstrated in one diatom species; *Phaeodactylum* (Beardall *et al.*, 1976, Burns and Beardall, 1987). Other experiments (Riebesell *et al.*, 1993) using the diatoms *Ditylum brightwelli*, *Thalassiosira punctigera* and *Rhizosolenia* cf. *alata* have demonstrated that the growth rate of these diatoms is reduced when the $[CO_{2(aq)}]$ is low, which probably indicates that these species of diatoms do not possess the ability to actively transport inorganic carbon. Therefore as *Ditylum brightwelli*, which does not appear to posses a CCM, is present during the bloom and the general relationship between $\delta^{13}C_P$ and $[CO_{2(aq)}]$ is consistent with algae reliant on $CO_{2(aq)}$ it will be concluded that the algae during this initial bloom only acquire their inorganic carbon by the passive diffusion of $CO_{2(aq)}$.

The calculated increase in $\delta^{13}C_P$ during the latter part of this bloom, when the $[CO_{2(aq)}]$ remains constant is probably attributable to assumptions made during the mass balance correction rather than increases in growth rate as predicted by the physiological model of Francois *et al.* (1993).

7.5.2 Second Bloom

Despite correcting the observed $\delta^{13}C_{POC}$ values to obtain $\delta^{13}C_P$ the isotopic composition of the phytoplankton during the second bloom appear to increase only slightly (*FIGURE* 7.6). Application of the empirical models suggest the isotopic composition should have increased by either 10 ‰ (Rau *et al.*, 1992), 4 ‰ (Rau, 1994) or 7 ‰ (this study, *CHAPTER* 6) for the 8 $\mu mol.kg^{-1}$ decrease in the $[CO_{2(aq)}]$ during the second bloom. Calculated values of $\epsilon_{P/a}$ indicate that this bloom is characterised by an initial decrease followed by a more general decrease as the bloom develops (*FIGURE* 7.7). The values of $\epsilon_{P/a}$ are numerically similar to the non - linear models of Popp *et al.* (1989) and Jasper and Hayes (1994) although the general trend of $\epsilon_{P/a}$ increasing as $[CO_{2(aq)}]$ decreases is not as would be predicted by these models. Therefore the values of $\delta^{13}C_P$ and $\epsilon_{P/a}$ during the second bloom cannot be simply explained by changes in the $[CO_{2(aq)}]$.

According to the physiological model (Francois *et al.*, 1993, *CHAPTER* 6) the growth rate may be an important factor determining the isotopic composition of phytoplankton. From *FIGURE* 7.8, the growth rate is predicted to decrease during the latter stage of the bloom , *i.e.* $[C_e]$-$[C_i]$ decreases. Changes in $[\Sigma CO_2]$ (*TABLE* 7.1) indicate that the rate of net productivity, during the latter stage of the bloom, relative to the start of the bloom, decreases therefore supporting the predictions of the model. The model also indicates that the growth rate is lower during the second bloom in comparison with the first. This is inconsistent with the changes in the concentrations of chlorophyll, POC and ΣCO_2 during the second bloom which are all larger than the first bloom indicating a higher growth rate.

The second bloom was dominated by *Phaeocystis* although the diatom *Rhizosolenia delicatula* was present throughout and numerically dominant at the very start of the bloom (Blight *et al.*, 1996). Riebesell *et al.* (1992) have demonstrated that the growth of a member of the *Rhizosolenia* sp. is limited at low $[CO_{2(aq)}]$ and therefore probably does not poses a

CCM. The initial dominance of *Rhizosolenia delicatula* may account for the slight decrease in $\epsilon_{P/a}$ observed at the start of the bloom. The observed increase in $\epsilon_{P/a}$ during the rest of the bloom may be attributed to the *Phaeocystis* becoming increasingly numerous and hence dominating the isotopic signal, which would imply that the isotopic composition of *Phaeocystis* is ~ -22 ‰ and $\epsilon_{P/a} \geq$ -14 ‰. As the isotopic composition and the trend of the $\epsilon_{P/a}$ values, in relation to $[CO_{2(aq)}]$, are not as would be expected if the phytoplankton were solely reliant on the passive diffusion of $CO_{2(aq)}$, it maybe possible to infer that *Phaeocystis* possess a different mechanism of inorganic carbon acquisition. As the observed values of both $\delta^{13}C_P$ and $\epsilon_{P/a}$ appear independent of $[CO_{2(aq)}]$ it would suggest HCO_3^- maybe the form of inorganic carbon utilised via a CCM with an associated enrichment factor ($\epsilon_{P/a}$) of ≥-14‰. However, the value of $\epsilon_{P/a}$ is somewhat larger than the values previously measured during culture experiments of algae utilising a CCM (Sharkey and Berry, 1985, Burns and Beardall, 1981).

Hayes (1993) suggested the model given in eqn. 6.9 (page 120) to describe the relationship between $\epsilon_{P/a}$ and cell leakiness during the active transport of inorganic carbon, which is of similar from to the passive diffusion model introduced in *CHAPTER* 6:

By rearranging the equation the leakiness of the cells during the second bloom is estimated to be ~ 0.9, *i.e.* 90 % of the carbon pumped into the cell leaves by diffusion before it can be fixed. As the active transport of carbon has an energetic cost (*e.g.* Lucas and Berry, 1985, Raven and Johnston, 1991) it seems unlikely that the phytoplankton would employ this mechanism for so little gain (*e.g.* Fogel *et al.*, 1992).

It is therefore difficult to account for the large value of $\epsilon_{P/a}$ during the second bloom which seems to be associated with the presence of *Phaeocystis*. As the values of $\epsilon_{P/a}$ are largely independent of the $[CO_{2(aq)}]$ it seems likely that some form of CCM is operational which is possibly exclusive to *Phaeocystis*. On the basis of the large $\epsilon_{P/a}$ values (≥ -14 ‰) the following model which is represented schematically in *FIGURE* 7.9 is suggested. The basic model involves the following steps:

i. HCO_3^- is actively transported into the cell

ii. The pH within the cell (7 to 8, Burns and Beardall, 1987, Dixon *et al.*, 1989)

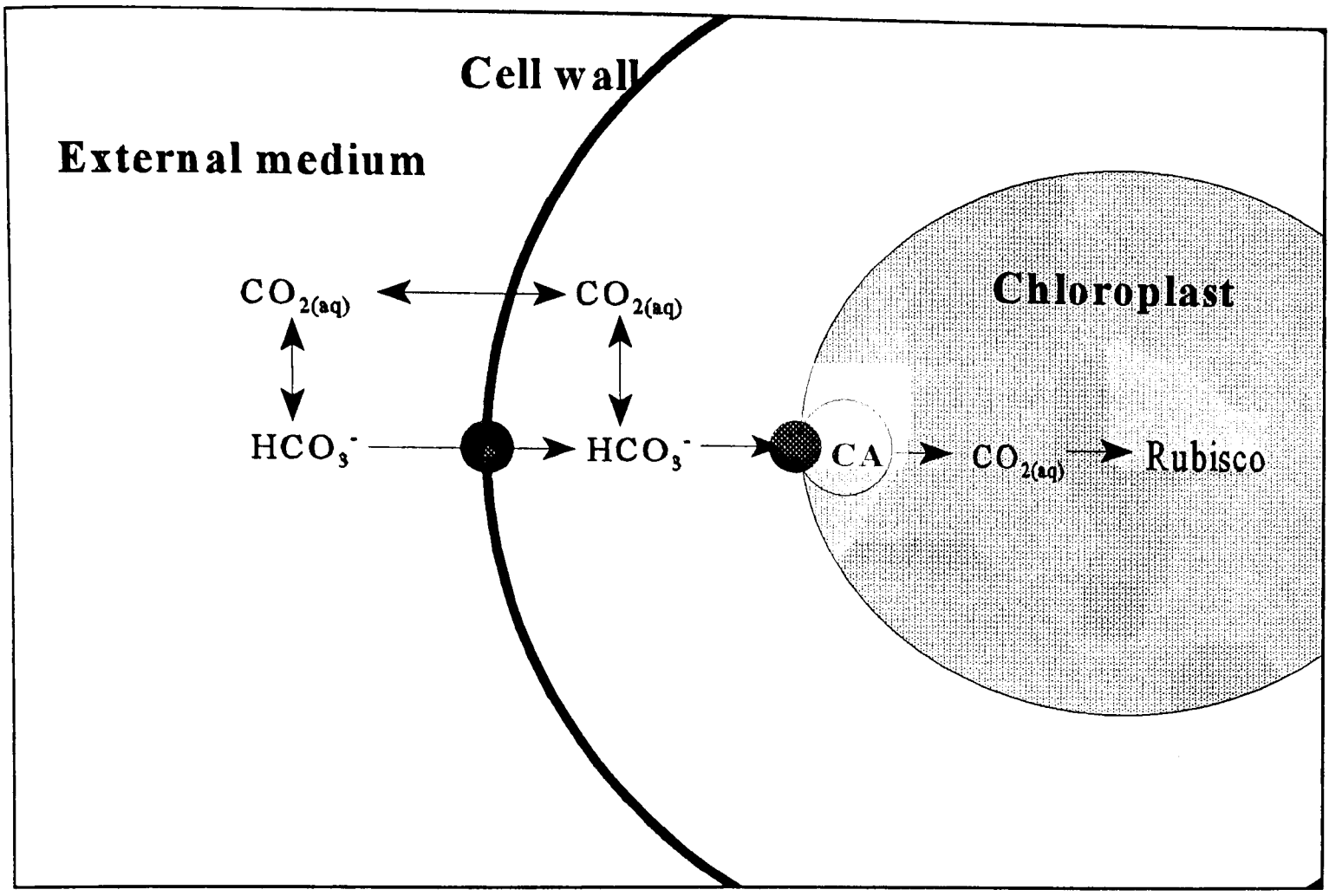

Figure 7.9 The suggested pathway carbon fixation employed by *Phaeocystis*. Double ended arrows represent reversible pathways, single ended arrows illustrate unidirectional pathways, ● indicates a HCO_3^- pump and CA is carbonic anhydrase. The dashed line between $CO_{2(aq)}$ in the cytoplasm and $CO_{2(aq)}$ within the chloroplast indicates that $CO_{2(aq)}$ maybe able to diffuse through the chloroplast membrane although this is unlikely to be a major pathway due to the low membrane permeability of the chloroplast wall. A full explanation of the model is given in the text.

is close to that of the external medium and as a result HCO_3^- is the dominant form of inorganic carbon within the cell (*e.g.* see *FIGURE* 2.1).

iii. HCO_3^- from within the cell is transported across the membrane of the chloroplast which has a relatively low permeability to $CO_{2(aq)}$. The HCO_3^- pump is closely associated with CA so all of the HCO_3^- transported into the cell is converted to $CO_{2(aq)}$. As a result of this close association there is no isotopic fractionation associated with this step and therefore the isotopic composition of $CO_{2(aq)}$ within the chloroplast is similar to the isotopic composition of HCO_3^- in the cytoplasm and the external medium.

iv. The $[CO_{2(aq)}]$ around Rubisco within the chloroplast is high due to the active transport and therefore the enrichment factor associated with the Rubisco mediated carboxylation reaction (-27 ‰) is fully expressed.

The maximum value of $\epsilon_{P/a}$ associated with this mechanism, -17 ‰ (*i.e.* $-\epsilon_{b/a} + \epsilon_R = 10 + -27$) , can only be achieved if the isotopic composition of $CO_{2(aq)}$ within the chloroplast is equal to the isotopic composition of HCO_3^- transported into the chloroplast. The dissolved inorganic carbon within the cytoplasm is predominantly composed of HCO_3^-, although there will also be a limited quantity of $CO_{2(aq)}$ either due to the diffusion of $CO_{2(aq)}$ across the membrane or due to the dehydration of HCO_3^- (possibly mediated by cytoplasmic CA). The values of ϵ_{P_a} determined during the second bloom are slightly less than the predicted enrichment associated with this mechanism and this could either be attributed to:

i. The diffusion of isotopically light $CO_{2(aq)}$ out of the cell.

ii. The low permeability of the chloroplast membrane causing the inorganic pool within the chloroplast to become enriched in $^{13}CO_{2(aq)}$ due to the preferential uptake of $^{12}CO_{2(aq)}$ by Rubisco and hence decreasing the apparent isotopic enrichment relative to the external $\delta^{13}C_a$ in the bulk medium.

iii. The presence of phytoplankton reliant on the passive diffusion of $CO_{2(aq)}$ (*i.e.* *Rhizosolenia delicatula*) with a less negative isotopic composition.

It is difficult to comment on the most likely cause of the slightly lower values of $\epsilon_{P/a}$ than would be expected from the suggested mechanism. Despite this, the general evidence indicates that *Phaeocystis* possess a HCO_3^- based CCM which is associated with a large enrichment factor ($\epsilon_{P/a} \geq$-14‰). Furthermore, as this enrichment factor is considerably larger than the values determined in other phytoplankton species operating a CCM the CCM mechanism employed by *Phaeocystis* maybe fundamentally different.

7.6 Summary

Changes in the $\delta^{13}C_{POC}$ within the oceanic environment probably closely reflect changes in $\delta^{13}C_P$. However, within coastal environments this assumption cannot be applied with the same degree of certainty because of the presence of allochthonous organic matter. Due to the apparently high concentration of refractory organic matter found within the Menai Strait an attempt has been made to correct the $\delta^{13}C_{POC}$ signal measured during this study to obtain $\delta^{13}C_P$. It has been clearly demonstrated that the difference between the $\delta^{13}C_{POC}$ and $\delta^{13}C_P$

largely depend on the isotopic composition and relative concentrations of the of the refractory organic matter and the phytoplankton pools. It was found during the first bloom that the calculated values of $\delta^{13}C_P$ were considerably different from the $\delta^{13}C_{POC}$, whereas the $\delta^{13}C_{POC}$, during the second bloom, closely reflected the calculated value of $\delta^{13}C_P$.

By removing the effect of the refractory organic matter pool it has been shown that the isotopic response of the two blooms, in relation to the $[CO_{2(aq)}]$, is distinctly different. The isotopic composition of the phytoplankton during the first bloom, which was dominated by diatoms, varied in relation to the $[CO_{2(aq)}]$. The observed variation was consistent with changes in the $\delta^{13}C_{POC}$ measured in the oceans during both spatial and temporal studies. The observed changes in the $\delta^{13}C_P$ during the first bloom have been taken as an indication that the diatoms probably acquired their inorganic carbon via the $CO_{2(aq)}$ pool, probably by passive diffusion of $CO_{2(aq)}$ into the cell.

However, the isotopic composition of the *Phaeocystis* dominated bloom showed no apparent variation in relation to the $[CO_{2(aq)}]$. It has therefore been concluded that this distinctly different isotopic signal is because *Phaeocystis* possess a fundamentally different type of inorganic carbon acquisition mechanism. As the isotopic composition is independent of the $[CO_{2(aq)}]$ this mechanism probably utilises the HCO_3^- pool, possibly via a CCM. However, as the enrichment factor asociated with this CCM is different from previously determined values a new model has been speculatively suggested to try and account for the measured value of $\epsilon_{P/a}$. The main feature of this model is the close association between the membrane based HCO_3^- pumps and CA within the chloroplast. This ensures that the $\delta^{13}C_a$ fixed by Rubisco has an isotopic composition close to that of HCO_3^- and therefore theoretically giving the observed value of $\epsilon_{P/a}$.

The conclusions based on the application of empirical models can be criticised for the assumption that $CO_{2(aq)}$ is the sole source of inorganic carbon. However, although the source of inorganic carbon is not known (*i.e.* $CO_{2(aq)}$ or HCO_3^-) the observed relationship between $\delta^{13}C_{POC}$ and $[CO_{2(aq)}]$ suggests that this is probably a fair assumption. The validity of this assumption is further enforced by the results of this study which indicate that changes on $\delta^{13}C_{POC}$ can either be dependent or independent of the $[CO_{2(aq)}]$, which would suggest different sources of inorganic carbon are being utilised by the cell.

In addition, the ability of the simple physiological models used here (see section 6.6) to correctly predict the potentially complex kinetic isotope effects within the boundary layer around the cell and within the cell itself can again be criticised. The effect of these kinetic isotope affects on the isotopic composition of the CO_2 fixed by Rubisco is difficult to quantify and may ultimately require the development of a sophisticated numerical model to kinetically describe the ΣCO_2 system in and around a cell before a complete solution is achieved.

Chapter 8: Conclusions

The aims of this thesis were twofold: (i) to determine the equilibrium fractionation factors associated with the stable isotopes of carbon between $CO_{2(aq)}$ and HCO_3^- and HCO_3^- and CO_3^{2-} in sea water and (ii) to investigate the relationship between the isotopic composition of phytoplankton and their photosynthetic source of inorganic carbon, $CO_{2(aq)}$ or HCO_3^-, in relation to the mechanism of inorganic carbon acquisition.

With respect to the first aim, many marine studies have been conducted which use the fractionation factors $\alpha_{b/a}$ and $\alpha_{c/b}$, determined in media with a low ionic strength, to calculate the isotopic composition of $CO_{2(aq)}$, HCO_3^- and CO_3^{2-} in sea water (*e.g.* Rau *et al.*, 1992, Francois *et al.*, 1993). However, basic thermodynamic reasoning suggested this application may not be correct due to the effects of the complex ionic media found in sea water on the isotope specific equilibrium constants. If the ionic effects on the isotope specific equilibrium constants were not proportional, the equilibrium fractionation factors would be dependent on the ionic strength and composition of the medium and more specifically, in the case of marine studies, on the salinity of the sea water. The application of a simple empirical relationship to predict the effect of complex ionic media on an equilibrium constant suggested that the fractionation factors are not influenced by the ionic strength of sea water. However, this is only a simple and general empirical model and as a result it does not necessarily preclude the possibility of ionic fractionation effects that maybe more rigorously investigated by applying the ionic solution theory or by direct experimental investigation.

Limited experimental evidence (Thode *et al.*, 1965 and Zhang *et al.*, 1995) suggests that the equilibrium distribution of ^{12}C and ^{13}C between the various species of dissolved inorganic carbon maybe effected by the ions present within the medium. The experiments of Thode *et al.* (1965) appear to show that the distribution of ^{12}C and ^{13}C within the ΣCO_2 pool is affected by both the strength and composition of the ionic medium. In particular they noted a large isotope effect associated with the presence of Mg^{2+} ions. It was suggested, by Thode *et al.* (1965), that this effect could be explained by the enrichment of ^{13}C in the $MgCO_3$ complexes so decreasing the degree of isotopic fractionation between

HCO_3^- and CO_3^{2-}. This is of particular relevance to sea water because of the importance of $MgCO_3$ complexes which form ~75% of the total CO_3^{2-} pool. Further indirect evidence for the modification of $\alpha_{c/b}$ in sea water was given by Zhang *et al.* (1995) who found that the measured isotopic enrichment between $CO_{2(g)}$ and the ΣCO_2 pool in sea water differed from the enrichment predicted by the application of fractionation factors determined in solutions of low ionic strength. It was concluded that the observed difference was probably attributable to a decrease in $\alpha_{c/b}$ due to the formation of $MgCO_3$ complexes although $\alpha_{c/b}$ was not directly determined in sea water.

The results of the experiments conducted here appear to indicate that the isotopic fractionation between $CO_{2(aq)}$ and HCO_3^- in sea water (S=34) is not significantly different from the values measured in solutions of low ionic strength at the same temperature. However, the isotopic fractionation between HCO_3^- and CO_3^{2-} in sea water appeared to be increased (ϵ_{c-b}=-14‰) relative to the previously determined theoretical (-0.4‰, Thode *et al.*, 1965) and experimental (-2.5‰, Zhang *et al.*, 1995) determined values for solutions of low ionic strength. The direction of change of this isotope effect is opposite to the effect predicted for a sea water medium by the results of Thode *et al.* (1965) and Zhang *et al.* (1995).

A series of experimental runs were also conducted in solutions of low ionic strength and over a wider range of pHs to confirm the values of $\alpha_{b/a}$ and $\alpha_{c/b}$ determined during previous studies. However, although the calculated value of $\alpha_{b/a}$ was in agreement with previous studies and the sea water experiments presented here, $\alpha_{c/b}$ was considerably larger than earlier studies and was concluded to be in error. The erroneous nature of this result must cast doubt on the validity of the experimental design and in particular the possibility that isotopic equilibrium between the two phases was not always achieved at all pHs. Nevertheless as there did not appear to be any particular reason why pH should greatly effect the time taken to reach isotopic equilibrium within the experimental system the values of $\alpha_{b/a}$ and $\alpha_{c/b}$ determined in sea water at 5°C and 20°C were cautiously accepted and the measured values of $\alpha_{c/b}$ were applied throughout the rest of this study. As the values of $\alpha_{b/a}$ determined during this study did not appear to be significantly affected by the salinity of the medium, the more comprehensive results of Mook *et al.* (1974) have been used.

The experimental design of the study presented here allowed the fractionation factors $\alpha_{b/a}$ and $\alpha_{c/b}$ to be determined simultaneously by conducting different experimental runs at the same temperature, but different pHs, and iteratively fitting the results so the calculated values of $\alpha_{b/a}$ and $\alpha_{c/b}$ showed no pH dependence. The design of the experimental apparatus also permitted the gaseous and aqueous phases to be completely isolated from each other which allowed the two phases to be separately sampled without disturbing the equilibrium conditions. Previous experiments (*e.g.* Mook *et al.*, 1974, Zhang *et al.*, 1995) have either frozen the aqueous phase to allow the gaseous phase to be sampled separately or just tried to remove the gaseous phase as quickly as possible to prevent isotopic exchange. The various design features implemented in this study were introduced in an attempt to improve on the design of previous experiments and allow the experiments to be conducted under more 'natural' conditions (*i.e.* atmospheric pressures).

However, given the disagreement between the values of $\alpha_{c/b}$ presented here and in previous studies, there is an obvious need for the experiments to be repeated. As their does not seem to be any reason to suggest the experimental design is at fault the most likely cause of the error is probably due to the relative lack of precision associated with the $\delta^{13}C_{\Sigma CO2}$ determination. Therefore, if the experiments were to be repeated it would be necessary to run replicate $\delta^{13}C_{\Sigma CO2}$ samples at the end of each experiment. It is suggested at least three samples need to be run to increase the accuracy of the $\delta^{13}C_{\Sigma CO2}$ result for each experimental run. It would also be prudent to confirm that the rate at which isotopic equilibrium was achieved between the gaseous and aqueous phases in the experiment system was not effect ed by the pH.

It has been found (Rau, 1994) that both the spatial and temporal variations in the marine $\delta^{13}C_{POC}$ signal can be largely explained (90%) by changes in the $[CO_{2(aq)}]$. The general explanation for this observation has relied on the assumption that marine phytoplankton derive their photosynthetic inorganic carbon requirement by the passive diffusion of $CO_{2(aq)}$. As a result, when the $[CO_{2(aq)}]$ decreases, the degree of isotopic fractionation between $CO_{2(aq)}$ and the photosynthetic product lessens. However, it has been demonstrated that certain species of phytoplankton posses the ability to utilise HCO_3^-, probably via a CCM to actively transport HCO_3^- across the external cell wall. As a result, it has been suggested that the observed changes in the oceanic $\delta^{13}C_{POC}$ signal in relation to

the $[CO_{2(aq)}]$ maybe more correctly explained by the increased use of HCO_3^- as the $[CO_{2(aq)}]$ decreases (Raven and Johnston, 1991). Despite this interpretation, models, based on the assumption of exclusive $CO_{2(aq)}$ usage, have continued to be applied to interpret observed changes in the $\delta^{13}C_{POC}$ in relation to the $[CO_{2(aq)}]$. In an attempt to increase the degree of physiological correctness some models have also accounted for the isotopic composition of $CO_{2(aq)}$ and the level of the photosynthetic demand in relation to the external $[CO_{2(aq)}]$.

In an attempt to reconcile these two contradictory theories concerning the acquisition of inorganic carbon (*i.e.* $CO_{2(aq)}$ or HCO_3^- uptake) detailed measurements were carried out during phytoplankton blooms in a mesocosm and in the Menai Strait to try and obtain a well constrained data set. The results were then subsequently interpreted in terms of either $CO_{2(aq)}$ or HCO_3^- usage.

The results of the mesocosm experiment appeared to indicate the $\delta^{13}C_{POC}$ signal could be well explained by the simple empirical model of Rau (1994) relating the $\delta^{13}C_{POC}$ signal to changes in the $[CO_{2(aq)}]$. In fact, due to the low $[CO_{2(aq)}]$ experienced during the mesocosm experiment the data presented here represents an extension of the existing data set. The results also indicated that as the $[CO_{2(aq)}]$ approached zero the isotopic composition of the phytoplankton approached the isotopic composition of the $CO_{2(aq)}$. The results were further interpreted by applying the model modified by Francois *et al.* (1993). The interpretation of the mesocosm results based on this model appeared to indicate that the rate of phytoplankton growth, during the bloom, was carbon limited. Further evidence from the ^{14}C productivity measurements appeared to confirm this interpretation.

An attempt has also been made to interpret the mesocosm results by applying the model suggested by Hayes (1993) which assumed the phytoplankton are exclusive users of HCO_3^-. This approach suggested the 'leakiness' of the cell decreased from 0.67 to 0.39 during the course of the bloom. This degree of 'leakiness' is broadly consistent with the results obtained from phytoplankton culture experiments in which the algae were assumed to be using a CCM (Sharkey and Berry, 1985). Unlike the passive diffusion of $CO_{2(aq)}$, the active uptake of HCO_3^- requires energy to operate the membrane-based pumps. The increased energetic costs associated with the uptake of HCO_3^- would be expected to be offset by some ecological advantage afforded by the use of this uptake mechanism. One

possible advantage is that a high rate of inorganic carbon acquisition could be maintained under conditions where the $[CO_{2(aq)}]$ was low. Under these conditions, phytoplankton which were only able to utilise $CO_{2(aq)}$ maybe at a competitive disadvantage as their maximum rate of growth would be largely dependent on the $[CO_{2(aq)}]$ in the external medium. The chlorophyll specific productivity results obtained during the mesocosm experiment appear to indicate that the carbon uptake rate decreased by 90% from day 0 to day 3. By day 3 the nutrients (nitrate, silicate and phosphate) had not yet been exhausted and the $[CO_{2(aq)}]$ had decreased by ~50% suggesting that the growth rate of the phytoplankton was not nutrient limited. As the growth rate of phytoplankton with the ability to use HCO_3^- would have been expected to remain high the observed decrease would suggest that the phytoplankton within the enclosure could only utilise $CO_{2(aq)}$.

In order to study temporal changes in the isotopic composition of phytoplankton in the Menai Strait it was necessary to correct the $\delta^{13}C_{POC}$ for the effect of refractory organic matter to obtain $\delta^{13}C_P$. The corrected results indicated that the response of the $\delta^{13}C_P$ signal, in relation to the $[CO_{2(aq)}]$, appeared to vary between the two blooms studied. During the initial spring bloom, which was dominated by diatoms, the observed changes in the $\delta^{13}C_P$ could be well explained by changes in the $[CO_{2(aq)}]$ and was generally consistent with previously published empirical models. However, the $\delta^{13}C_P$ during the second bloom, which was dominated by *Phaeocystis* appeared to remain constant despite large changes in the $[CO_{2(aq)}]$. The most basic interpretation of this data would indicate that the isotopic composition of *Phaeocystis* is not dependent on the $[CO_{2(aq)}]$ suggesting that *Phaeocystis* may acquire its inorganic carbon from the HCO_3^- pool via a CCM. However, the observed isotopic enrichment between $CO_{2(aq)}$ and the phytoplankton during this period is considerably larger than the value determined in culture experiments in which the phytoplankton used a CCM. As a result a hypothetical model to describe the uptake of inorganic carbon by *Phaeocystis* has been proposed. The main aim of the model was to try and account for the unusually large value of $\epsilon_{POC/a}$. It was suggested that this could be accounted for by a close association between a HCO_3^- pump and carbonic anhydrase on the chloroplast membrane so all of the HCO_3^- pumped into the chloroplast is completely converted to $CO_{2(aq)}$. This would ensure the isotopic composition on the $CO_{2(aq)}$ is the same as the HCO_3^- entering the chloroplast.

The conclusions drawn from both the mesocosm and Menai Strait studies have been derived by interpreting the results in the context of several empirical and physiological models which have been proposed to account for the $^{12}C/^{13}C$ ratios observed in phytoplankton. However, it is apparent that no one of the models can account for the observed changes in the $\delta^{13}C_{POC}$ of phytoplankton.

In order to resolve this problem, it is probably necessary to conduct a series of well constrained field and laboratory culture studies. The results of these studies could then be used in conjunction with a kinetic model to describe the ΣCO_2 system and the distribution of ^{12}C and ^{13}C within, and around a phytoplankton cell. An approach such as this is necessary to try and fully understand the chemical and physiological processes which occur during the uptake and fixation of inorganic carbon. Once a detailed understanding is obtained it will then be possible to use simplified models to interpret the oceanic $\delta^{13}C_{POC}$ signal in terms of the spatial and temporal variations in the acquisition of carbon by phytoplankton. In addition, paleo-oceanographic applications (*i.e.* Rau, 1994, Jasper and Hayes, 1994) could be further applied with confidence if detailed modelling indicates that the empirical relationship between $\delta^{13}C_{POC}$ and the $[CO_{2(aq)}]$, which has been found in today's oceans, is largely dependent on the $[CO_{2(aq)}]$ and not subject evolutionary and/or environmental changes.

Probably, the most interesting result of the various studies presented in this thesis is the observation that the $\delta^{13}C_{POC}$ of the *Phaeocystis* dominated bloom in the Menai Strait (*see CHAPTER* 7) is independent of the $[CO_{2(aq)}]$. Although it has been concluded that this is indicative of HCO_3^- uptake it is necessary to conduct further studies to confirm this conclusion.

Therefore, in summary, the results presented in this thesis suggest that:

i. The isotopic fractionation between $CO_{2(aq)}$ and HCO_3^- is not affected significantly by the ionic medium of sea water and as a result the values of $\alpha_{b/a}$ determined by Mook *et al.* (1974) can be used.

ii. The isotopic fractionation between HCO_3^- and CO_3^{2-} is affected by ionic medium of sea water and results in the preferential enrichment of ^{12}C in the

CO_3^{2-} pool relative to the values estimated and determined in solutions of low ionic strength.

iii. Changes in the $\delta^{13}C_{POC}$ observed during the mesocosm experiment and during the spring diatom bloom in the Menai Strait were consistent with previously derived relationships relating the isotopic composition of phytoplankton to the $[CO_{2(aq)}]$. As a result it was concluded that $CO_{2(aq)}$ was the most likely source of inorganic carbon. Furthermore, the application of the Francois *et al.* (1993) model appeared to indicate that the growth rate of the phytoplankton, during the bloom, may have been carbon limited.

iv. The observed decoupling of the $\delta^{13}C_{POC}/[CO_{2(aq)}]$ relationship during the *Phaeocystis* bloom implied that the uptake of inorganic carbon by *Phaeocystis* was not dependent on the $[CO_{2(aq)}]$ and as a result it was suggested that *Phaeocystis* may obtain its inorganic carbon requirement from the HCO_3^- pool via a CCM which maybe exclusive to *Phaeocystis*.

Appendices

Appendix 1: A Description of the Methodology Used to Determine the Isotopic Composition of ΣCO_2 in Sea Water

Introduction

The most commonly employed technique to determined the $\delta^{13}C_{\Sigma CO2}$ of sea water is based on the acidification of a sea water sample and the subsequent collection and cryogenic distillation of the $CO_{2(g)}$ released (*e.g.* McCorkle, 1987). This technique relies on the acidification of a sample to displace the equilibrium between the various species of ΣCO_2 so all of the ΣCO_2 exists as $CO_{2(aq)}$ which is then stripped from the sample in a N_2 gas flow. The methods employed during the sampling, sample storage and stripping of the sample are described in this appendix.

A fundamental problem associated with this technique is the absence of any standard reference material. Therefore when establishing the technique a series of replicate samples were made which were used as internal reference standards. Isotope effects may occur during the extraction of $CO_{2(g)}$ from the sample and as a result the isotopic composition of the collected $CO_{2(g)}$ may be dependent on the extraction efficiency of the procedure. If the yield is ~100 % isotope effects during the extraction of ΣCO_2 will not be observed. Investigations indicate that an extraction efficiency of ~99 % is achieved during this procedure and the isotopic composition of the extract should closely represent the $\delta^{13}C_{\Sigma CO2}$ of the sample. The precision of the method is ±0.05 ‰.

Sampling

i. Take a water sample using a discrete water sampler (*e.g.* Go-Flow bottle). Other methods of sampling may be used but caution must be exercised to avoid excessive turbulence which will enhance the rate of exchange of CO_2 between the sample and the atmosphere and cause alteration of the isotopic composition of the sample.

ii. A portion of the sea water sample is transferred to a 250 cm^3 borosilicate glass bottle with a ground glass stopper. The sample transfer is performed using a length of Nalgene tubing. The tip of the sample transfer tube should be placed at the

bottom of the bottle and the sea water allowed to flow gently into the bottle, caution should be exercised to avoid the formation of bubbles. The bottle should be allowed to fill and overflow with about twice the volume of the bottle before removing the tube. The air space in the bottle should then be adjusted so it occupies ~1 % of the bottle volume when the stopper is replaced. To prevent alteration of the $\delta^{13}C_{\Sigma CO2}$ by biological activity saturated mercuric chloride solution is added. The recommended amount of mercuric chloride is 50 µl per 250 cm^3 bottle (Dickson and Goyet, 1991), although during this study 250 µl per 250 cm^3 was added due to the high density of phytoplankton during the mesocosm study.

iii. The sample may then be stored until it can be transferred to an ampoule for permanent storage (see below). During this study samples were not stored in this manner for longer than two.

Sample Storage

Samples for the analysis of the $\delta^{13}C_{\Sigma CO2}$ can be stored for long periods in heat sealed borosilicate glass ampoules. No study has been conducted to investigate the effect of long term storage on the $\delta^{13}C_{\Sigma CO2}$ of the sample.

iv. Take the required number of borosilicate glass ampoules (10 cm^3) and number each ampoule uniquely using a diamond tipped glass pencil.

ii. Weigh the ampoule using a precision balance (±0.001 g.) and record the weight.

iii. The ampoules are now ready to be filled.

iv. Take an ampoule and flush it with N_2 . This can be achieved by attaching a blunt needle to the N_2 supply. The tip of the blunt needle should reach the bottom of the ampoule. Allow the ampoule to flush with N_2 for ~1 to 2 minutes. The N_2 supply should be turned on in advance of use to ensure that the system is fully flushed through with N_2 (any $CO_{2(g)}$ is removed by passing the N_2 through Carbososb). The flow of N_2 should be ~1 dm^3 per minute and can be checked by placing the tip of the needle into a beaker of water - the bubbling rate should be moderate.

v. Take a clean, all plastic, graduated 30 cm^3 syringe with a large diameter blunt needle attached. The needle should be long enough so it can reach the base of the ampoule.

vi. Take the 250 cm^3 bottle containing the sample, remove the stopper and gently draw some sample into the syringe (~10 cm^3) avoiding the formation of air bubbles. Remove the syringe from the bottle, invert and expel nearly all of the contents. The purpose of this procedure is to remove the air space and air bubbles that maybe present within the syringe, if all of the sample is expelled the air space with in the syringe will not be removed. This procedure may be repeated several times to ensure the syringe is thoroughly flushed. Then fill the syringe with ~30 cm^3 of sample, again expel nearly all of the sample and refill. This flushing procedure is basically designed to ensure that the $\delta^{13}C_{\Sigma CO2}$ of the sea water sample within the syringe is the same as the $\delta^{13}C_{\Sigma CO2}$ of the sample within the bottle.

vii. Remove the blunt needle from the syringe and attach a 25 mm Swinex filter holder containing a 0.4 µm nuclepore filter then refit the needle to the outlet of the filter holder.

viii. Remove the flushing needle from the ampoule and place it in the next ampoule to be filled.

ix. Expel ~10 cm^3 of sample through the filter into a beaker, this is to expel air and flush the filter holder.

x. Place the tip of the blunt needle of the syringe into the ampoule so it reaches the bottom of the ampoule and expel ~10 cm^3 of sample into the ampoule.

xi. Quickly seal the ampoule by heating the middle of the ampoule neck using a heat gun. The portion of the ampoule tip removed during sealing should be retained.

xii. Weigh the sample and the tip of the ampoule together. This will allow the weight of the sample to be calculated and therefore enable the $[\Sigma CO_2]$ ($\mu mol.kg^{-1}$) to be calculated by manometrically determining the amount of $CO_{2(g)}$ collected per sample.

xiii. The sample may now be stored.

ΣCO_2 Extraction Procedure

The extraction procedure described below relies on the acidification of the sea water sample and the subsequent stripping on the $CO_{2(aq)}$ by a stream of CO_2 free N_2. For the procedure, a stripper, into which the ampoule is placed, is attached to the vacuum line (*FIGURE* A1.1).

Before starting, check the pressure of the vacuum line and ensure taps 5 and 17 are closed. The left portion of the line (*i.e.* to the left of taps 5 and 17) should be at high vacuum ($< 0 \times 10^{-4}$ torr). Then attach a collection bottle (used to transfer the extracted $CO_{2(g)}$ to the mass spectrometer) to the line at the position indicted and evacuate it ($< 0 \times 10^{-4}$ torr). If many samples are run it is impractical to evacuate the right hand portion of the line (not including the stripper) to the same degree between samples (due to the presence of small quantities of water) and therefore this portion of the line is only evacuated to $\sim 8 \times 10^{-3}$ torr. When these pressures have been achieved the line is ready for use. To reduce the amount of water leaving the stripper, water at ~0°C is circulated around the condenser from a reservoir containing ice and water. This should be prepared before the running of samples commences.

i. Place the stripper vertically in a clamp attached to a laboratory retort stand.

ii. Add ~ 1 cm^3 standard phosphoric acid through the top of the stripper so the frit is covered.

iii. Unscrew the top side tap of the stripper so that its tip is flush with the inside wall of the stripper and ensure that the lower side tap is screwed in fully.

iv. Take the ampoule containing the sample and place it in the stripper so the tip is uppermost. The base of the ampoule should rest on the lower side tap.

v. Adjust the upper side tap so that its tip is in contact with the ampoule.

vi. Replace the upper portion of the stripper and attach the outlet of the stripper to the vacuum line and attach the inlet of the stripper to the flexible vacuum tubing which is connected to the CO_2 free N_2 supply using an Ultra-Torr fittings.

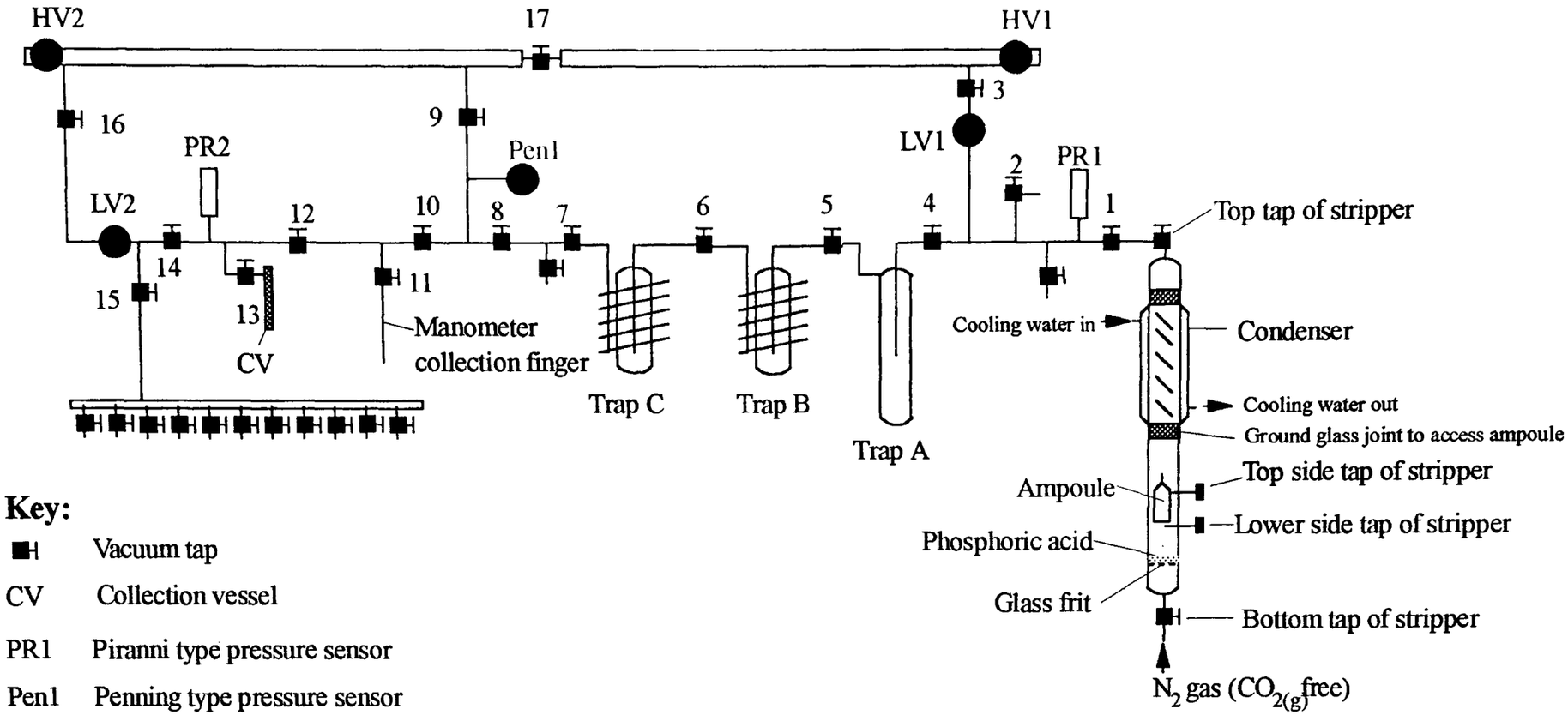

Key:

■H	Vacuum tap
CV	Collection vessel
PR1	Piranni type pressure sensor
Pen1	Penning type pressure sensor
LV1	Low (roughing) vacuum pump
HV1	High vacuum pump

FIGURE A1.1. The vacuum line used during the stripping and collection of CO_2 from a $\delta^{13}C_{\Sigma CO2}$ sample

vii. Open the top tap of the stripper so the N_2 can flow out to the atmosphere, open the bottom tap of the stripper and open the pin valve so that the phosphoric acid above the frit bubbles vigorously. The configuration of the taps should allow the N_2 to flow through the stripper and out through the top tap to flush the system.

viii. The system should be flushed for >10 minutes to ensure any CO_2 in the phosphoric acid or within the system is removed.

ix. Whilst the system is flushing the $N_{2(l)}$ / ethanol slush traps (× 1)and $N_{2(l)}$ traps (× 2) should be prepared. The temperature of the slush traps should be ~ -90 to -95°C, the temperature can be checked using a temperature probe.

x. After the stripper has been flushed close the nitrogen regulator, the top tap of the stripper, taps 4 and 13 and isolate the right hand portion of the line from HV1 by closing the tap to HV1.

xi. Open tap 1 and the tap to the roughing pump (LV1) to evacuate the stripper. The pressure on the pirani gauge (PIR1) will rapidly drop but eventually the rate of pressure decrease will slow and the boiling of the phosphoric acid decrease. The pressure at which this occurs is ~2×10^0 torr.

xii. When the stripper has been sufficiently evacuated close the bottom tap on the stripper, continue to pump for a short time, then close the tap on the top of the stripper and then the tap to LV1 when the pressure falls to ~2×10^{-2} torr. Turn on the pump to pump the cooling water around the stripper.

xiii. Turn the top side tap of the stripper so that the ampoule breaks and unscrew the lower side tap so the smashed ampoule falls into the phosphoric acid.

xiv. Open the top tap on the stripper and then tap 4 so the stripper is open to the ethanol / $N_{2(l)}$ trap (trap A) and allow any water to freeze for 2 minutes. The top tap of the stripper should only be partly opened as this reduces the rate of gas flow and improves the efficiency of the condenser.

xv. Whilst the water is freezing close taps 7 and 6 and place the Dewars containing $N_{2(l)}$ around the spiral traps (traps B and C).

xvi. Open tap 5 and then tap 6 so the sample is admitted to the two spiral traps and allow to freeze for 5 minutes.

xvii. Open the bottom tap of the stripper and open the pin valve so a slow flow of $N_{2(g)}$ bubbles through the acidified sample (stripping). The stripping should continue for ~10 minutes after which the pressure reading on PIR1 should be ~1 × 10^3 torr. After which the bottom tap of the stripper and the pin valve should be closed.

xviii. Close taps 9, 11, 13 and 16 and isolate the high vacuum pump by closing the tap to HV2.

xix. Open tap 7 and then the tap to LV2. The tap should not be opened fully as pumping should be slow so that the pressure on PIR1 only falls slowly. When a pressure of ~0 × 10^0 torr is reached the sample in the stripper will bubble more vigorously. At this point close the top tap of the stripper and after a short period (~30 seconds) close tap 1 followed by tap 5. The pressure in the line can now be monitored on PIR2. When the pressure reaches ~9 × 10^{-2} torr close tap 5. When the correct pressure is reached (*i.e.* ~2×10^{-2} torr) close the tap to LV2 and open taps 9 and 16 and open the tap to HV2 and continue pumping until <0 × 10^{-4} torr and then close tap 7.

xx. Remove all of the Dewars.

xxi. Heat the spiral traps with a hot air gun and then replace the water trap on trap C (-90 to -95°C) and leave in place for 8 minutes. The temperature of the ethanol / $N_{2(l)}$ water trap may need to be readjusted by the addition of $N_{2(l)}$.

xxii. Open the tap to the manometer and allow the pressure to drop to 0 × 10^{-4} torr and then close the tap again and record the manometer reading. Close taps 9, 13 and 14.

xxiii. Place a small Dewar containing liquid nitrogen around the collection finger of the manometer and open tap 7 so that $CO_{2(g)}$ from the sample freezes into the manometer for 8 minutes.

xxiv. Close tap 8 and open taps 9 and 14 to pump away incondensable gas, when the pressure reaches $<0 \times 10^{-4}$ torr close the tap to the manometer and remove the Dewar containing $N_{2(l)}$ and replace with a beaker containing water at room temperature.

xxv. The manometer pressure will rise as CO_2 frozen in the manometer sublimes. When the pressure reading on the manometer stabilises record the pressure. This can then be used to calculate the $[\Sigma CO_2]$ in the sample using the sample weight recorded when the ampoule was sealed.

xxvi. Whilst the manometer is stabilising tap 13 can be opened to ensure that the sample collection bottle is fully evacuated.

xxvii. Close tap 13 and place a small Dewar containing $N_{2(l)}$ around the collection bottle.

xxviii. Close taps 10 and 14 and open the tap to the manometer and then tap 13 to allow the sample to freeze into the collection bottle for 2 minutes.

xxix. After 2 minutes close the sample bottle and tap 13 and remove from the vacuum line. The sample is now ready for mass spectrometric determination.

Appendix 2: A Description of the Methodology Used to Determine the Isotopic Composition of Particulate Organic Carbon

Introduction

Variations in the natural abundance of ^{12}C and ^{13}C in organic samples can be determined using a high precision, double beam, triple collecting mass spectrometer. Before mass spectrometric determination can proceed the organic sample must be converted to $CO_{2(g)}$ and purified. The method employed during this study is based on sealed tube, off line Dumas combustion technique and the sections below describe the procedures employed during sampling, sample storage, sample preparation and analysis of POC.

Sampling

i. Precombust the required number of 47 mm GF/F filters at 500°C for three hours. The filters can be stored by wrapping in precombusted (500°C.) aluminium foil.

ii. Take water sample and transfer it to a container suitable to transport the sample to the site of filtration.

iii. Pour the required amount of sample (~1 dm^3) into a measuring cylinder.

iv. Record the volume of sample to be filtered. (note the volume filtered depends on the concentration of suspended matter it is therefore best to judge the amount of sample required by the colour of the filter. If too much sample is filtered the filter will block and cells may become ruptured).

v. Filter the water through a precombusted GF/F filter as soon as possible. (note: ensure that the filtering apparatus is clean and has not been used for isotope tracer studies as this may contaminate the sample).

vi. Ensure that the sample in the measuring cylinder is continually mixed whilst filtering.

vii. Rinse the measuring cylinder and filter with prefiltered sea water to ensure all of the POC has been collected, washing should be kept to a minimum.

viii. Place filter paper in a clean petri - slide and label.

ix. Place sample in freezer (-20°C.). The samples may be stored in this manner indefinitely.

Sample Preparation

In order to determine the ratio of ^{12}C and ^{13}C in POC the organic matter must first be converted to $CO_{2(g)}$ by combustion. This section describes the methodologies employed to prepare samples for combustion.

Apparatus and Consumables

i. Precombusted (910°C.) quartz (ID. = 10 mm) outer tubes
ii Precombusted (910°C.) quartz (O.D. = 9 mm) inner tubes
iii. Precombusted (500°C.) aluminium foil
iv. Precombusted (500°C.) strips silver foil
v. Granulated elemental copper
vi. Granulated copper oxide, precombusted (910°C.)
vii. Clean scalpel
viii. One quarter of a precombusted GF/F filter per sample
ix. Clean tube stand for outer quartz tubes
x. Tippex
xi. Two pairs of clean tweezers
xii. Two clean spatulas, large and small
xiii. Two clean thistle funnels, long and short stem
xiv. Clean tube stand for inner tubes
xv. Disposable gloves

Preparation of Reagents and Consumables

i. Precombust aluminium foil and silver strips at 500°C. for three hours.
ii. Precombust copper oxide at 910°C. for 18 hours.
iii. Make quartz outer tubes; ID. = 10 mm, length = 250 mm, test for leaks and precombust at 910°C. for three hours.
iv. Make quartz inner tubes; O.D. = 9 mm, length = 110 mm, precombust at 910°C. for three hours.

Sample Preparation

i. Remove required samples from freezer.

ii. Punch out the filtered area using an appropriately sized clean, hole punch.

iii. Place samples in an air tight plastic box with a petri dish containing a small amount of concentrated HCl. Acidify the samples over night to remove any $CaCO_3$.

iv Place samples in drying oven (40 - 50°C.) until dry (~4 - 6 hours).

iv. The samples may now be stored in a desiccator until required.

v. Place large outer tubes in a clean rack and cover with precombusted aluminium foil to prevent contamination with airborne particles.

vi. Using Tipex, write the sample number on the outside of the large sample tube.

vii. Place inner tube in tube stand and cover with precombusted aluminium foil. (caution - do not touch the inner tube with hands, tweezers must be used, wear gloves).

viii. Take sample filter and cut into ~8 strips using tweezers and scalpel. The strips should be sufficiently narrow to allow them to fall to the bottom of the quartz inner tube.

viii. Using tweezers, place the strips of filter paper and a silver strip into the small inner tube.

ix. Weigh out ~0.5 g and ~1.0 g of copper and copper oxide respectively onto a sheet of precombusted aluminium foil

x. Pour the copper and copper oxide into the inner tube using a short, clean thistle funnel.

xi. Take one quarter of a precombusted GF/F filter, fold, and place in the end of the small inner tube to act as a plug.

xii. Place inner tube upside down in large outer tube, without touching the inner tube.

xiii. Pull a constriction in the large outer tube, about 170 mm from the base of the tube by heating with a gas torch. The constriction should be ~50 mm in length, this will allow the sample to be easily sealed in the correct place.

xiv. Place sample on vacuum line and evacuate over night until the pressure is $<0 \times 10^{-4}$ torr.

xv. Seal sample ready for combustion.

Standard preparation

i. Place required number of outer quartz tubes in rack and cover with precombusted aluminium foil.

ii. Weigh out 2 mg of alanine on precombusted aluminium foil, and record the weight (~±0.1 mg).

iii. Add, to the same piece of aluminium foil 0.5 g of elemental copper and 1 g of precombusted copper oxide.

iv. Pour the weighed material directly into the quartz outer tube using a long stem thistle funnel.

v. Continue as described in the previous section, parts xiv - xvi.

Sample Extraction

i. Combust the evacuated and sealed samples. The combustion will involve heating the samples to 910°C. for three hours. The muffle furnace is then programmed to cool slowly, this aids the conversion of NO_x to N_2, and therefore forms a "cleaner" sample. Combustion can be performed a few days prior to sample extraction. Combustion may produce some compounds which may react with, and therefore modify the isotopic composition of the $CO_{2(g)}$. It is not advisable to combust samples unless they will be used within a few days.

ii. Score the sample tubes at the appropriate height so when placed in the cracker tube the scored portion of sample is level with the tap barrel that will be used to crack open the sample.

iii. Place the sample tube in the cracker tube and attach to vacuum line.

iv. Evacuate line so that the pressure $<6.8 \times 10^{-5}$ torr.

v. When the vacuum is sufficient isolate the traps and switch the traps to cool with no $N_{2(l)}$ for 5 minutes.

vi. Add three cups of $N_{2(l)}$ to each trap and set the trap temperature to ~ -80°C. When the temperature approaches the right temperature reset temperature controllers to -90°C.

vii. When the correct temperature has been achieved isolate the sample from the rest of the line by closing tap A and crack sample open.

viii. Open tap to trap (tap B) so sample is allowed to freeze into the traps for 10 minutes.

ix. After 10 minutes close tap D and open tap C.

x. Add $N_{2(l)}$ to the beaker around the collection bottle and allow the sample to freeze for 10 minutes.

xi. Shut tap C, open D and pump away the non-condensable gas and then close the collection bottle and remove $N_{2(l)}$ and remove from line, the sample is now ready to be run on the mass spectrometer.

Appendix3 The Spectrophotometric Determination Of pH In Sea Water

A3.1 Introduction

As our understanding of the chemical nature of sea water improved, it has become increasingly apparent that the measurement of oceanic pH, using potentiometric techniques, was hindered by both conceptual (*e.g.* Sillén, 1966 and Dickson, 1993a) and methodological problems (UNESCO, 1987). Therefore, despite its position as a master variable (Sillén, 1966), reflecting the thermodynamic state of all the various acid/base systems present in sea water, the pH of sea water became an infrequently determined parameter.

One of the main problems associated with the potentiometric determination of sea water pH was the relative lack of precision (>0.02 pH units, UNESCO, 1987) associated with the use of glass electrodes, especially when compared with the precision of other techniques used to define the ΣCO_2 system in the marine environment (*i.e.* fCO_2 and $[\Sigma CO_2]$). However, recent work on both the conceptual problems of defining the pH of sea water (Dickson, 1993) and methodological problems associated with its measurement have improved both the precision and accuracy of sea water pH determinations. A major methodological improvement was achieved by the re-introduction of pH indicators (Cooper, 1933) used in conjunction with high performance spectrophotometers (Robert-Baldo *et al*, 1985). This has improved the precision with which pH can be determined by at least an order of magnitude (Byrne and Breland, 1989 and Clayton and Byrne, 1993). The development of accurate pH buffers specifically for use in the marine environment (Dickson, 1993) has allowed the increase in precision to be mirrored by an increase in accuracy. Recent investigations now suggest that total alkalinity (TA) can be determined more precisely using spectrophotometric pH determination and $\Sigma CO_{2(aq)}$ measurements than by direct potentiometric determinations (Byrne, pers.. comm.).

The subsequent sections in this appendix outline the theory and methods used to accurately standardise two pH indicators, cresol red and *m*-cresol purple, and the protocol adopted during the sampling and measurement of pH samples.

A3.2 Theory

The spectrophotometric determination of pH is mainly based on the use of sulfonephthalein indicators which can be used to determine pH over the entire pH range of 0-13 (*e.g.* Vogel, 1989, p265). All of these sulfonephthalein compounds act as diprotic acids which partially disassociate to form H_2I, HI^- and I^{2-} on addition to a solution (where I^{2-} represents the unprotonated form of the indicator):

$$I^{2-}+H^+ \Leftrightarrow HI^- \qquad \textbf{Eqn. A3.1}$$

$$HI^-+H^+ \Leftrightarrow H_2I \qquad \textbf{Eqn. A3.2}$$

The relative concentrations of the different species of indicator (H_2I, HI^- and I^{2-}) will be dependent on the equilibrium constants, K_x and K_y, of the indicator and the pH of the solution:

$$K_x = \frac{[HI^-]}{[H^+][I^{2-}]} \qquad \textbf{Eqn. A3.3}$$

$$K_y = \frac{[H_2I]}{[HI^-][H^+]} \qquad \textbf{Eqn. A3.4}$$

Each indicator species (H_2I, HI^- and I^{2-}) forms a different, highly coloured dye, with a distinct absorption spectra, and it is the existence of these differently coloured, pH dependent species which make these ideal compounds with which to spectrophotometrically determine pH.

The total concentration of indicator, $[I_T]$, in a solution can therefore be written for all conditions as (Clayton and Byrne, 1993):

$$[I_T] = [I^{2-}]+[HI^-]+[H_2I] \qquad \textbf{Eqn. A3.5}$$

and the measured absorbance (A) at a particular wavelength (λ) is given by:

$$_\lambda A=(_\lambda\beta_I[I^{2-}]+_\lambda\beta_{HI}[HI^-]+_\lambda\beta_{H_2I}[H_2I]).l \qquad \textbf{Eqn. A3.6}$$

where $_\lambda\beta_z$ is the molar absorbtivity at wavelength λ, and l is the path length in cm. The molar absorbtivity is defined as the absorption due to an indicator species z when the concentration, [z] = 1 mol/l and the path length , l = 1 cm. (Vogel, 1989, p650). The total concentration of the indicator can be expressed in terms of K_x and K_y where:

$$[I_T]=[I^{2-}](1+K_x[H^+]+K_xK_y[H^+]^2) \qquad \textbf{Eqn. A3.7}$$

and similarly, expressing the absorbance in terms of K_x and K_y:

$$\frac{_\lambda A}{l} =[I^{2-}].(_\lambda\beta_I+_\lambda\beta_{HI}.K_x.[H^+]+_\lambda\beta_{H_2I}.K_x.K_y.[H^+]^2) \qquad \textbf{Eqn. A3.8}$$

The specific absorption coefficient, ${}_\lambda a$, (${}_\lambda a = {}_\lambda A / l.[I_T]$), can be calculated by dividing equation A3.8 by equation A3.7:

$$\lambda a = \frac{\lambda . A}{l.[I_T]} = \frac{\lambda\beta_I + \lambda\beta_{HI}.K_x.[H^+] + \lambda\beta_{H_2I}.K_x.K_y.[H^+]^2}{1 + K_x.[H^+] + K_x.K_y.[H^+]^2} \qquad \textbf{Eqn. A3.9}$$

The $\log K_x$ and $\log K_y$ values for all sulfonephthalein indicators are separated by more than a factor of 10^6 (King and Kester, 1989) and therefore the concentration of H_2I for all sulfonephthalein indicators only becomes important at low pH's ($\log K_y < 2$). It has therefore been standard practice to treat sulfonephthalein indicators as monoprotic acids within the pH range encountered in the marine environment and hence disregard the effects of K_y and H_2I (King and Kester, 1989).

Ideally, the pH of the sample should be approximately the same as the $\log K_x$ value of the indicator and the exact value of $\log K_x$ varies depending on the indicator type. The pH range over which a particular indicator can be used is approximately; $pH_{max} < pK_x + 1$ and $pH_{min} > pK_x - 1$. However, recent recommendations (Clayton and Byrne, 1993) suggest $pH_{max} \sim pK_x$ and $pH_{min} > pK_x - 1$ for maximum precision.

Therefore by disregarding the affects of H_2I, and hence K_y equation A3.9 can be simplified to the following form:

$$\lambda a = \frac{\lambda\beta_I + \lambda\beta_{HI}.K_x[H^+]}{1 + K_x.[H^+]} \qquad \textbf{Eqn. A3.10}$$

This equation can then be rearranged and written in terms of pH, assuming $pH = -\log[H^+]$ and $[H_2I] \sim 0$:

$$pH = \log K_x + \log\left(\frac{\psi - e_1}{e_2 - \psi.e_3}\right) \qquad \textbf{Eqn. A3.11}$$

Where, $\psi = {}_2A/{}_1A$ and $e_1 = {}_2\beta_{HI}/{}_1\beta_{HI}$, $e_2 = {}_2\beta_I/{}_1\beta_{HI}$ and $e_3 = {}_1\beta_I/{}_1\beta_{HI}$. (${}_1A$ is the measured absorbance at ~430 nm and ${}_2A$ is the measured absorbance at ~570 nm, depending on the indicator used).

A3.3 Calibration of Sulfonephthalein Indicators

A3.3.1 Introduction

The standardisation of a particular type of indicator involves the determination of the various parameters in equation A3.11 (K_x, e_1, e_2 and e_3). The choice of indicator depends on the pH range in which it will be used. The two indicators used during this study, cresol red (pK=7.8) and *m*-cresol purple (pK=8.0) have been employed by previous workers (Byrne and Breland, 1989, and Clayton and Byrne, 1993 respectively).

As this study utilises a fundamentally different type of spectrophotometer (see section A3.3.2) it was thought necessary to redetermine molar absorbtivity values and $\log K_x$.

Variations in temperature and salinity as well as the pH scale used will alter the apparent value of K_x. It is therefore necessary to determine this variation and this can be achieved by using an accurately calibrated buffer solution. The following sections outline the methods employed to calibrate the two indicator types used during this study.

A3.3.2 Materials and Apparatus

The pH measurements were carried out using a Hewlett-Packard diode array spectrophotometer (model: HP 8452). This type of instrument permits the absorbance to be measured simultaneously at several wavelengths. However, unlike instruments employed on previous studies, which were high precision double beam spectrophotometers (*e.g.* Clayton and Byrne, 1993),the selected wavelengths can only be whole, even wavelengths (*i.e.* 260, 262, 264,.....) with a wavelength band width of 2 nm.

The additions of indicator were made from indicator stock solutions which were prepared by dissolving the appropriate amount of the sodium salt (NaI) of each indicator in distilled water (250 ml). The concentration of the stock solutions was 2×10^{-3} M. The sodium salts of the indicators are readily soluble in water, unlike the acidic forms (H_2I) which are rendered water-soluble by adding sufficient NaOH to neutralise the sulphonic acid group (Vogel, 1989, p267). The indicator solutions were kept refrigerated in an air tight bottle while not in use.

The affect of temperature and salinity on K_x can be determined using an accurately calibrated pH buffer. This study uses a recently published recipe (Dickson, 1993) for a tris sea water buffer which has been calibrated on the total hydrogen ion concentration scale. The sea water buffer was prepared and stored as recommended (Dickson, 1993). The salinity of the prepared sea water buffer was 35.

All measurements were carried out in a cylindrical 10 cm glass spectrophotometer cell, the volume of which was ~30 ml. Temperature determinations were made using a digital thermometer (Comark) in conjunction with a thermocouple (±0.1°C).

A3.3.3 Determination of the Wavelengths of Maximum and Minimum Absorption

The molar absorption coefficients of the different indicator species are normally determined at the wavelength of maximum absorption and therefore the wavelength of maximum absorption must first be found. This was achieved by adding aliquots of indicator to acidic (pH ~ 5) and basic (pH ~ 11) solutions and then performing an absorbance scan over the range 400 - 750 nm. The absorbance maxima of the two forms of the indicator were readily

apparent as peaks. The results indicated absorbance maxima at 434 ($_1\lambda$=HI^-) and 572 nm ($_2\lambda$=I^{2-}) for cresol red and 436 ($_1\lambda$=HI^-) and 578 nm ($_2\lambda$=I^{2-}) for *m*-cresol purple.

Shifts in the absorbance baseline during the measurement of a sample may lead to errors. This was corrected for by simultaneously measuring the absorbance of a sample at a wavelength where the absorbance of the indicator is negligible ($_3\lambda$) and at the wavelengths of maximum absorbance, $_1\lambda$ and $_2\lambda$ (Byrne and Breland, 1989). The measured absorbencies at $_1\lambda$ and $_2\lambda$ were then corrected for baseline shifts by the addition, if negative, or the subtraction, if positive of the measured absorbance at $_3\lambda$. The wavelength of minimum absorption was found to be 730 nm for both cresol red (Byrne and Breland) and *m*-cresol purple.

A3.3.4 Determination of the Molar Absorption Coefficients

The molar absorbtion coefficient is defined as the measured absorbance by an indicator species when it's concentration is equal to one mole over a path length of 1 cm. The molar absorbtion coefficient is normally measured at the wavelength of maximum absorption which applies to that particular indicator species(H_2I, HI^- and I^{2-}). However, as the absorbance spectra associated with each particular form of indicator overlap it is necessary to measure the molar absorbtion coefficient for each form of the indicator at each wavelength (*i.e.* $_1\beta_{HI}$, $_2\beta_{HI}$, $_1\beta_I$ and $_2\beta_I$).

In order to ensure that all of the indicator is present as one form, the pH of the solution can be adjusted to maximise its concentration. The pH at which the concentration of a particular indicator species approaches the concentration of the total indicator species (*i.e.* $[I_T]$=$[H_2I]$, $[HI^-]$ or $[I^{2-}]$) can be calculated using equations A3.3 and A3.4 and approximate values for K_x and K_y. It can be shown that >99% of the indicator will exist in the form HI^- when pH = pK_x - 3 and in the form I^{2-} when pH = pK_x + 3 (King and Kester, 1989). The contribution of H_2 I to the measured absorbance at $_1\lambda$ when [HI] ~ $[I_T]$ (pH = pK_x - 3) is less than 0.1% and was therefore not included in the calibration procedure (Byrne *et al*, 1988, and Byrne and Breland, 1989). However, a recent high precision work (+/-0.0004 pH units) by Clayton and Byrne (1993) hasincluded the contribution of H_2I to the absorbance measured during their standardisation procedure.

The molar absorption coefficients for HI^- and I^{2-} were determined at both wavelengths ($_1\lambda$ and $_2\lambda$) in a 0.72M NaCl solution. The pH of this solution was adjusted to the desired strength by the addition of $1x10^{-3}$M HCl and 1M NaOH solutions prepared using

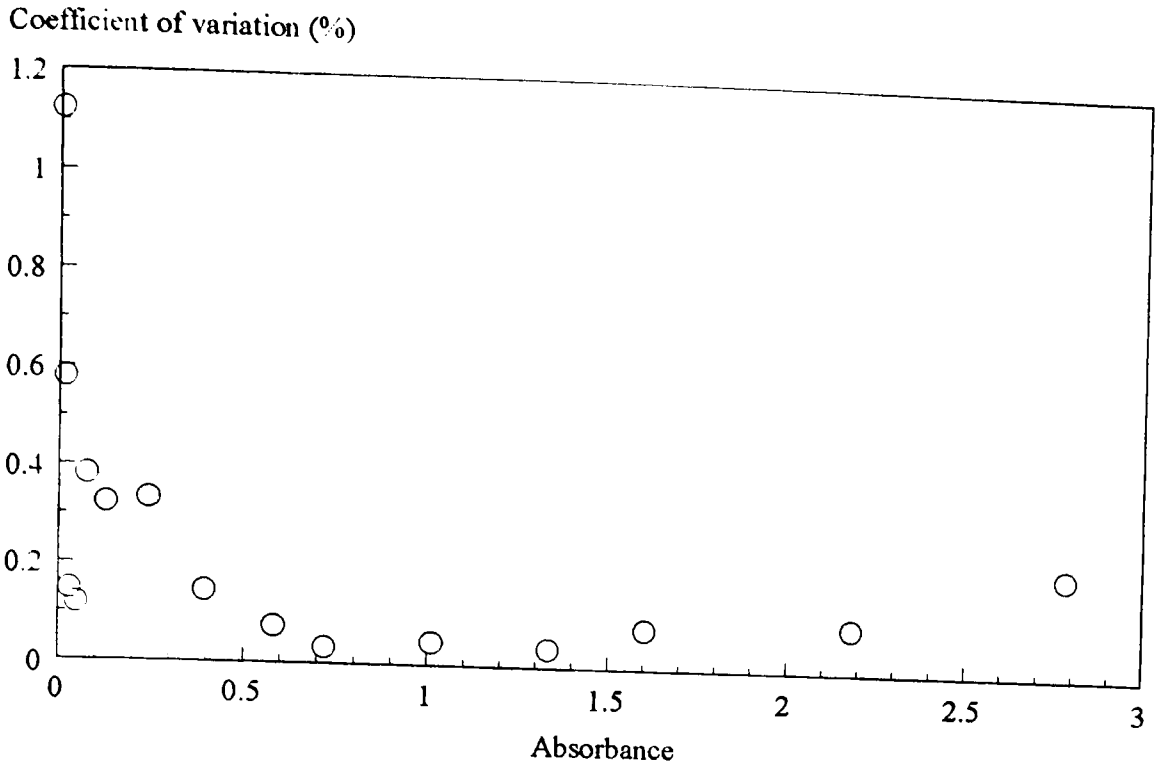

FIGURE 1. Variations in the coefficient of variation with absorbance on a diode array spectrophotometer (coefficient of variation (%) = (standard deviation/mean)×100). The standard deviation and mean absorbencies were calculated from replicate (n=10) measurements at each absorbance. The results indicate that the precision is maximal in the range 0.5-2.0 absorbance units.

standardised solutions (Convol®). The appropriate quantity of indicator was then added and the absorbance determined. In order to maximise the precision it is necessary to adjust the concentration of the indicator so the measured absorbance falls within the range of maximum precision on the spectrophotometer (~0.5-2.0 absorbance units) (Fig. 1). However, due to the large difference in absorbance between the two wavelengths it is not possible for both absorbencies to be determined simultaneously on the same solution without loss of precision. For example, if the measured absorbance of HI at ${}_1\lambda$ was 2, the measured absorbance at ${}_2\lambda$ would be ~0.01, well below the range of optimum precision. Therefore the molar absorption coefficient were determined in solutions containing different concentration of the indicator to maximise precision. The molar absorption coefficients and e_x values (equation A3.11) actually determined are shown in Table 1 along with previously published values.

A3.3.5 Determination of the Dissociation Constant, K_x

The dissociation constants for sulfonephthalein indicators are well known for non-ionic media. The ionic strength as well as the type and concentration of the individual ionic constituents will influence the apparent value of the dissociation constant and therefore, due to the complex ionic nature of sea water it is simplest to measure K_x using a constant ionic

TABLE 1. Molar Absorption Coefficients, e_x and $logK_x$ values measured during this study for cresol red and *m*-cresol purple. Published values are shown for reference. The published values of $logK_x$ for cresol red were determined in a buffer of unknown type (Byrne and Breland, 1989). The log K_x values measured during this study were determined at 20.2°C. The results determined during this study are given along with the measured standard deviation (σ_{n-1})

	Cresol Red (This study)	***m*-cresol purple** (This study)	**Cresol Red** (Byrne and Breland, 1989)	***m*-cresol purple** (Clayton and Byrne, 1993)
$_1\beta_I$	1724±3	2093±3	-	-
$_1\beta_{HI}$	21543±8	15915±7	-	-
$_2\beta_I$	61053±12	354515±28	-	-
$_2\beta_{HI}$	109±1	142±2	-	-
e_1	$5.092x10^{-3}$±$4x10^{-5}$	0.0090±$1x10^{-4}$	$2.86x10^{-3}$	0.0069
e_2	2.834±0.001	2.169±0.002	2.7985	2.222
e_3	0.0800±$1x10^{-4}$	0.1315±$2x10^{-4}$	0.0903	0.133
$logK_x$	7.7966±$9x10^{-4}$	8.0402±$7x10^{-4}$	7.8164	8.0768

medium approach. This is most easily achieved using a sea water buffer whose pH has been accurately determined on a constant ionic medium scale (see section A3.3.2).

From equation A3.11 it is apparent that if the values of e_x are known and ψ is measured in a solution of known pH the value of $logK_x$ can be calculated. Recent work (Dickson, 1993) has suggested sea water pH should be measured on the total hydrogen ion concentration scale ($[H^+]_{free}+[HSO_4^-]$) using a constant ionic medium approach. The recipe suggested by Dickson (1993) to make a sea water buffer (tris) with an accurately determined pH consistent with this approach was used to determine $logK_x$ during this study.

The value of $logK_x$ was determined by the addition of the appropriate indicator (50 µl) to a sample of sea water buffer in the 10cm cell and measuring the absorbencies, A_1 and A_2 and the temperature. The pH of the buffer could then be calculated and hence $logK_x$.

The determined values of the molar absorption coefficients and $logK_x$ were then further refined (Clayton and Byrne, 1993) by entering these values, along with the measured absorbences into equation A3.10. The calculated and measured specific absorbtivities were then compared and the molar absorption coefficients and adjusted so $_\lambda\beta_{z\ calculated}=_\lambda\beta_{z\ measured}$. This was repeated for both wavelengths. Refined molar absorption coefficients values were input into equation A3.11 and the value of $logK_x$ recalculated. This process was repeated

Figure 2a

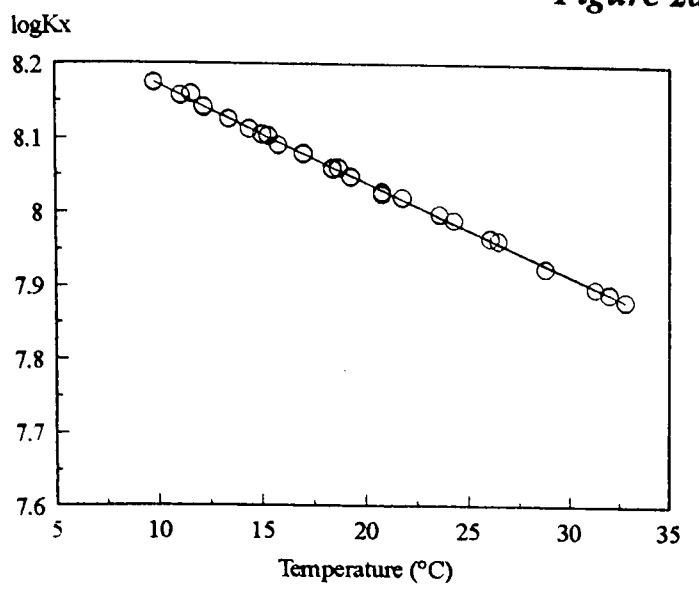

Figure 2b

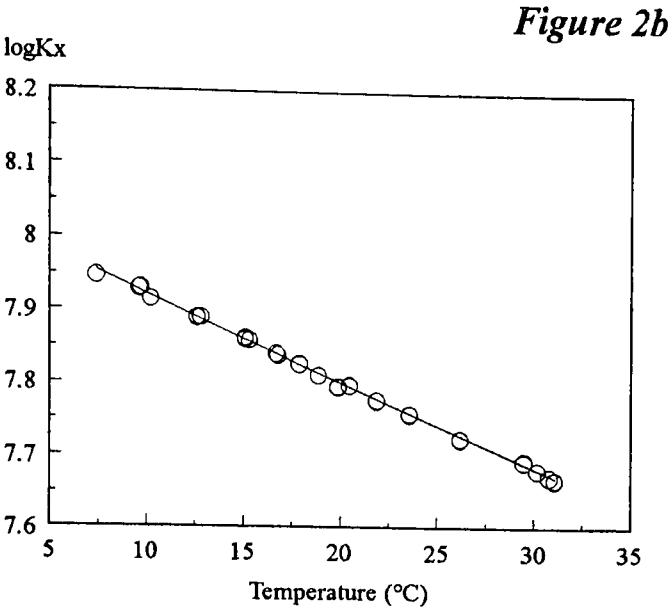

FIGURE 2. The variation of $logK_x$ with temperature (°C) , for cresol red (a) and *m*-cresol purple (b). The lines on both diagrams represent the best fit linear (solid line) and non-linear (dashed line) of the measured data. Relevant statistical information is given Table 2.

TABLE 2. The affect of temperature on $logK_x$ for cresol red and *m*-cresol purple. The experimentally derived results (see Figure 2) were fitted to linear (Table 2A) and second order polynomial (Table 2B) expressions of the form indicated .The calculated coefficients and statistical parameters have been given.

Table 2a $logK_x=a+b.t$	**a**	**b**	**Standard error of a**	**Standard error of b**	**R^2**	**RSS**	**n**
Cresol red	8.039	-0.01194	0.003	$8x10^{-5}$	0.998	$4.6x10^{-4}$	36
***m*-cresol purple**	8.296	-0.01275	0.003	$7x10^{-5}$	0.998	$6.57x10^{-4}$	49

Table 2b $logK_x=a+b.t+c.t^2$	**a**	**b**	**c**	**Standard error of a**	**Standard error of b**	**Standard error of c**	**R^2**	**RSS**	**n**
Cresol red	8.047	-0.0127	$1.953x10^{-5}$	$5x10^{-3}$	$5x10^{-4}$	$1.2x10^{-5}$	0.999	$4.17x10^{-4}$	36
***m*-cresol purple**	8.309	-0.0141	$3.177x10^{-5}$	$4.5x10^{-3}$	$4.5x10^{-4}$	$1.1x10^{-5}$	0.999	$4.77x10^{-4}$	49

until subsequent iterations were constant. The final values obtained for both of the indicator types used are shown in Table 1 along with previously published values for comparison.

A3.3.6 The Affect of Temperature on the Equilibrium Constant, K_x

The equilibrium constant K_x will vary with temperature and as the pH measurements will be carried out in a non-thermostated cell it is necessary to determine this effect. This can be achieved by using the sea water buffer and measuring changes in $_1A$ and $_2A$ with

temperature. As the pH of the buffer solution is accurately known in relation to temperature the value of $logK_x$ can be calculated using eqn. A3.11.

The 10 cm cell was filled with buffer and a 50µl aliquot of indicator was added using a micro-pipette. The cell was then cooled to <10°C in a water bath, prior to placing it in the spectrophotometer. The absorbencies, A_1 and A_2, and the temperature were recorded. The cell was then removed from the spectrophotometer and allowed to warm slightly, the measurements were then repeated. Both of the indicators were calibrated over the temperature range ~10-30°C.

The calculated values of $logK_x$ were plot against temperature and fitted to linear and non-linear expressions (Figure 2). The calculated constants, coefficients and statistical parameters relating to the fitted lines are given in Table 2. The calculated values of the residual sum of squares (RSS) and r^2 for both indicators indicate that the variation of $logK_x$ with temperature is best described by a second order polynomial expression.

A3.3.7 Determination of the Affect of Salinity on the Equilibrium Constant, K_x

The value of the equilibrium constant, K_x, is effected by salinity as well as temperature. Again the effect of salinity on the value of $logK_x$ can be measured using the prepared sea water buffer. However, the tris sea water buffer recipe used during this study has only been calibrated for use between salinity's of 30 and 40 (Dickson, 1993). Furthermore, the salinity of the prepared buffer was only 35 and therefore the affect of salinity on $logK_x$ was only studied over the salinity range 30-35.

Initial experiments were carried out by diluting aliquots of existing buffer (S=35) to make up solutions of the following salinity's; 30, 31, 33 and 34. When the measurements were performed it became apparent that the calculated values of $logK_x$ showed a poor and scattered relationship with respect to salinity. This was attributed to the relatively small effect that salinity has on the altering the value of $logK_x$, especially in relation to the relatively large effect of temperature. Therefore as the temperature of the cell was not thermostatically controlled, each buffer, and therefore each measurement was made at a slightly different temperature. This slight temperature difference between samples probably caused most of the scatter.

In order to overcome this problem, measurements were subsequently made by placing the buffer (S=35) in a large (250 ml) open topped cell to which the appropriate quantity of

Figure 3a

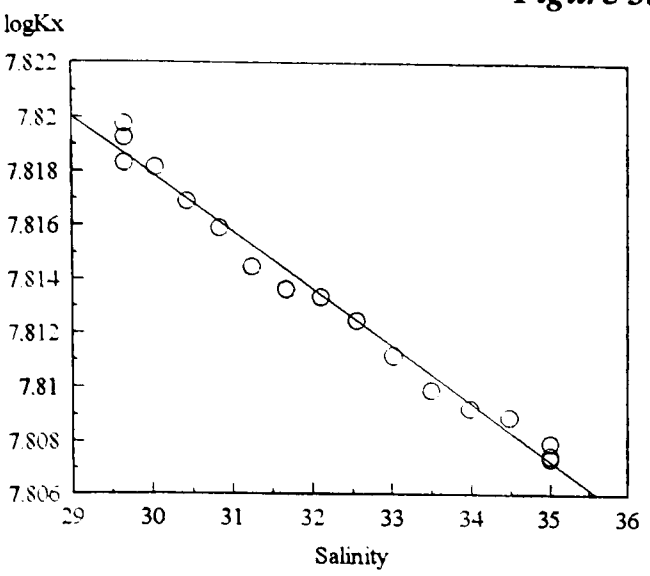

Figure 3b

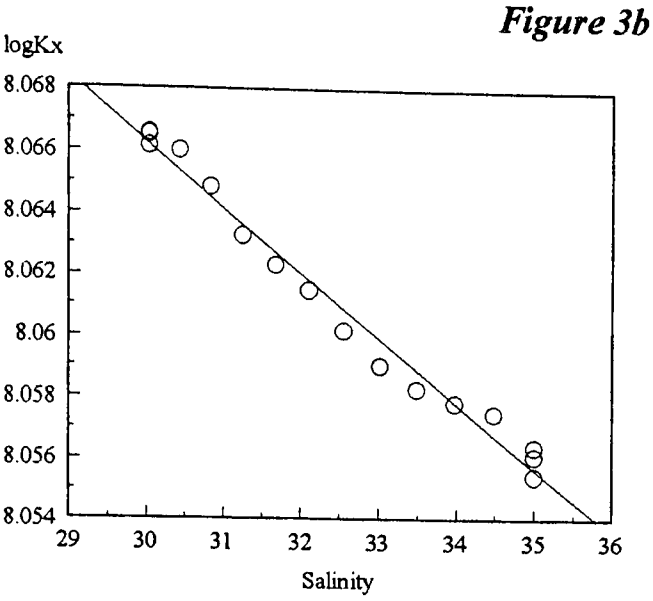

FIGURE 3. Variations in the measured value of $logK_x$ with salinity for cresol red (a) and *m*-cresol purple (b). The lines in both graphs represent the best linear fit calculated by minimising the residual sum of squares. Statistical information relating to the linear regression are shown in Table 3.

TABLE 3. Variations in the value of $logK_x$ with salinity were described by a linear equation (see Figure 3). The calculated coefficients and statistical parameters relating linear regressions for cresol red and *m*-cresol purple are given below.

$logK_x$= a+b×salinity	a	b	Standard error of a	Standard error of b	R^2	RSS	n
Cresol red	7.8073	0.00213	$5x10^{-4}$	$7x10^{-5}$	0.986	$6x10^{-5}$	17
***m*-cresol purple**	8.0557	0.00212	$5x10^{-4}$	$7x10^{-5}$	0.983	$4x10^{-6}$	16

indictor was added ($[I_T]$~$5x10^{-6}$ for *m*-cresol purple and ~$3.5x10^{-6}$ for cresol red). The effect of salinity on $logK_x$ was then determined by adding small quantities of water (Milli-Q, CO_2 free) to the cell by means of a burette. After each addition of water, the contents of the cell were stirred and the temperature and absorbencies measured.

It was again apparent from the experimental results that small changes in temperature (<0.1°C) affected the calculated values of $logK_x$. For example, the temperature drifted slowly during one experiment by 0.3°C, and as the maximum resolution of the thermometer was 0.1°C, this steady drift was recorded as two jumps in temperature. When the data was initially processed and plotted, the points at which the recorded temperature jumped by 0.1°C were obvious by jumps in the calculated value of $logK_x$. Therefore, in order to reduce the effect of this problem the measured temperature data was fitted to a linear expression to linearly describe the temperature drift and eliminate jumps. This linear description of the temperature variation during the experiment was then used to calculate $logK_x$. This improved the quality of data and the results are shown in Figure 3. A linear expression was

fitted to the experimental data and the relevent statistical parameters are summarised in Table 3.

The calculated slope is similar for both indicators (Table 3). Previous studies have indicated variations in slope between indicator types (Byrne and Breland, 1989, Clayton and Byrne, 1993). However, due to the chemical similarity between sulfonephthalein indicators, variations in the apparent dissociation constant with changes in the ionic strength may be expected to be similar.

A3.3.8 Summary of Calibration Results

From the data obtained, and given in Table 1, eqn. A3.11 can be rewritten for cresol red and *m*-cresol purple as determined using a diode array spectrophotometer and the artificial sea water buffer recipe given by Dickson (1993) on the total hydrogen ion concentration scale:

$$\text{Cresol red: } pH = \log K_x + \log\left(\frac{\psi + 5.092\times10^{-3}}{2.834 - (\psi \times 0.0800)}\right) \qquad \textbf{Eqn. A3.12}$$

$$m\text{-Cresol purple: } pH = \log K_x + \log\left(\frac{\psi + 0.0090}{2.169 - \psi \times 0.1315}\right) \qquad \textbf{Eqn. A3.13}$$

In order to calculate the equilibrium constant, $\log K_x$, in relation to temperature and salinity, the following expressions can be written using the results given in Tables 2 and 3:

Cresol red:

$$\log K_x = 8.047 + (-0.0127\times t) + (1.95\times10^{-5}\times t^2) + (0.00213 \times (35 - S)) \qquad \textbf{Eqn. A3.14}$$

m-Cresol purple:

$$\log K_x = 8.309 + (-0.0141\times t) + (3.177\times10^{-5}\times t^2) + (0.00212 \times (35 - S) \qquad \textbf{Eqn. A3.15}$$

where t is the temperature in °C and S is the salinity. Therefore by combining eqns A3.12 and A3.14, and A3.13 and A3.15 the pH of a sea water sample can be calculated on the total hydrogen ion concentration scale if the temperature and salinity have been determined.

A3.4 The Experimental Determination of Sea Water pH

A3.4.1 The Sampling, Storage and Measurement of Sea Water pH Samples

The pH of sea water is primarily controlled by the buffering effect of the ΣCO_2 system. As the acidity of sea water is mainly due to the action of carbonic acid, the loss or addition of CO_2 from a sample will alter the pH. Therefore in order to take a representative sea water sample for any measurement concerning the ΣCO_2 system caution must be exercised to prevent changes in the $[\Sigma CO_2]$.

Samples for the determination of pH were taken during a temporal study of the Menai Strait (see Chapter 6) and during experiments conducted to determine the carbon isotope enrichment factor between $CO_{2(aq)}$ and HCO_3^- (see chapter 4). The subsequent text outlines the sampling and measurement protocol adopted for each study.

Sea water samples from the Menai Strait were taken using a hand operated plastic bilge pump fitted with plastic hoses. The end of the effluent hose was placed at the bottom of a 10 dm^3 plastic aspirator. The plastic aspirator was rinsed twice using pumped water and then allowed to fill slowly, to prevent excessive turbulence. The sample was allowed to overflow by at least a full volume before the sample transfer tube was withdrawn. The aspirator was then covered by a black plastic bag and returned to the laboratory.

A Nalgene tube was then fitted to the tap of the aspirator and the other end of the tube was placed in the 10 cm spectrophotometer cell. The cell was then allowed to fill slowly, again to reduce excessive turbulence. The cell was allowed to overflow by at least a full volume before the tube was removed and the stoppers replaced ensuring no air bubbles were present. The cell was then dried and transferred to the spectrophotometer.

The experiments conducted to determine the isotopic enrichment factor between $CO_{2(aq)}$ and HCO_3^- were carried using the apparatus described in Chapter 4. Samples were taken at the end of each experiment by siphoning water from the aqueous reaction vessel using Nalgene tubing. The effluent end of the siphon tube was placed in the 10 cm spectrophotometer cell and the cell filled as described above.

The wavelengths at which the absorbencies were determined ($_1\lambda$, $_2\lambda$ and $_3\lambda$) appropriate to the specific indicator were selected and blank measurements were made. A known quantity of indicator was then added (100 - 150 µl) using a micropipette. The cell was then shaken to ensure the indicator and sample were totally mixed and then returned to the sample compartment of the spectrophotometer and the absorbance measurements repeated. The temperature of the sample was also taken.

The temperature and salinity of the sample can then be used to calculate $\log K_x$ using eqns A3.14 and A3.15 for cresol red and *m*-cresol purple respectively. The measured absorbencies (ψ), along with the calculated values of $\log K_x$ can be input into the appropriate equations (A3.12 for cresol red and A3.13 for *m*-cresol purple) to calculate the pH of the sample.

Figure 4a

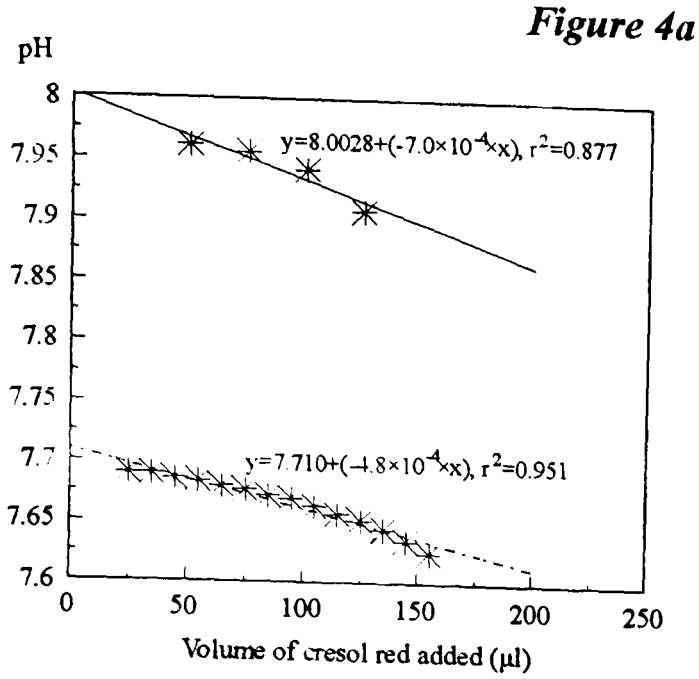

Figure 4b

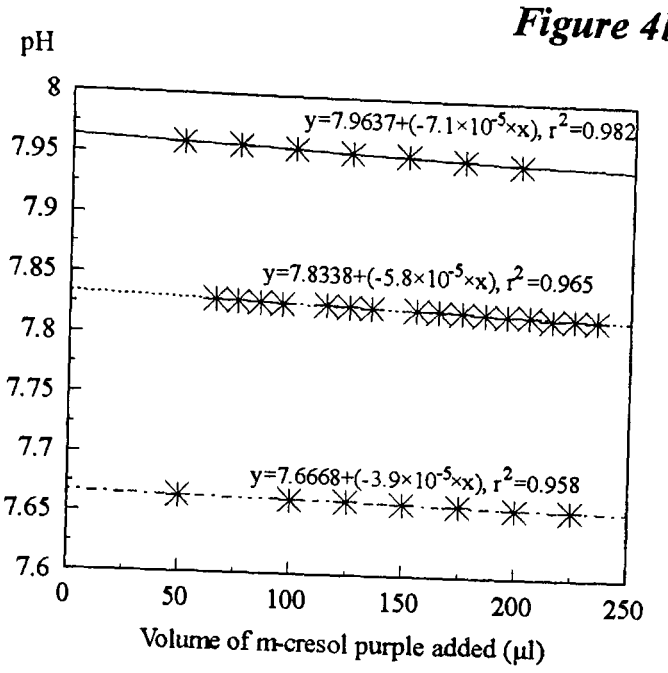

FIGURE 4. Variations in the pH of a sample due to the addition of cresol red (a) and *m*-cresol purple (b). Linear regressions were performed on the experimental results and the calculated equations are given and plotted above along with the calculated r^2 values.

A3.4.2 Assessing the Affect of Indicator Additions on the pH of a Sample

An addition of indicator to a sea water sample will alter the pH of the sample. The magnitude of this effect will be primarily determined by the pH difference between the sample and the indicator. In order to accuratley calculate the pH of the sample this effect must be quantified. Clayton and Byrne (1993) corrected for the indicator affect by adding two aliquots of indicator to a sample and calculating the shift in ψ. A series of such measurements were conducted for each batch of indicator and by assuming the effect of successive indicator additions was linear a volume dependent correction factor could be calculated.

The approach adopted during this study was slightly different to the approach described by Clayton and Byrne (1993). All pH measurements were made from the same indicator stock solutions which were kept for over a year. Periodic measurements were made to determine the pH shift associated with the addition of each indicator and to check if this effect varied with time. The measurements were made by adding successive, small (10 - 50µl) amounts of cresol red or *m*-cresol purple to a sea water sample. After each addition of indicator the absorbencies were determined at the appropriate wavelengths and the temperature of the sample was recorded. The affect of the indicator was then determined by calculating the pH of the sample after each addition of indictor and correcting for any temperature drift. A linear expression was then fit to the data to describe the pH change associated with the addition of cresol red or *m*-cresol purple. The results are graphically

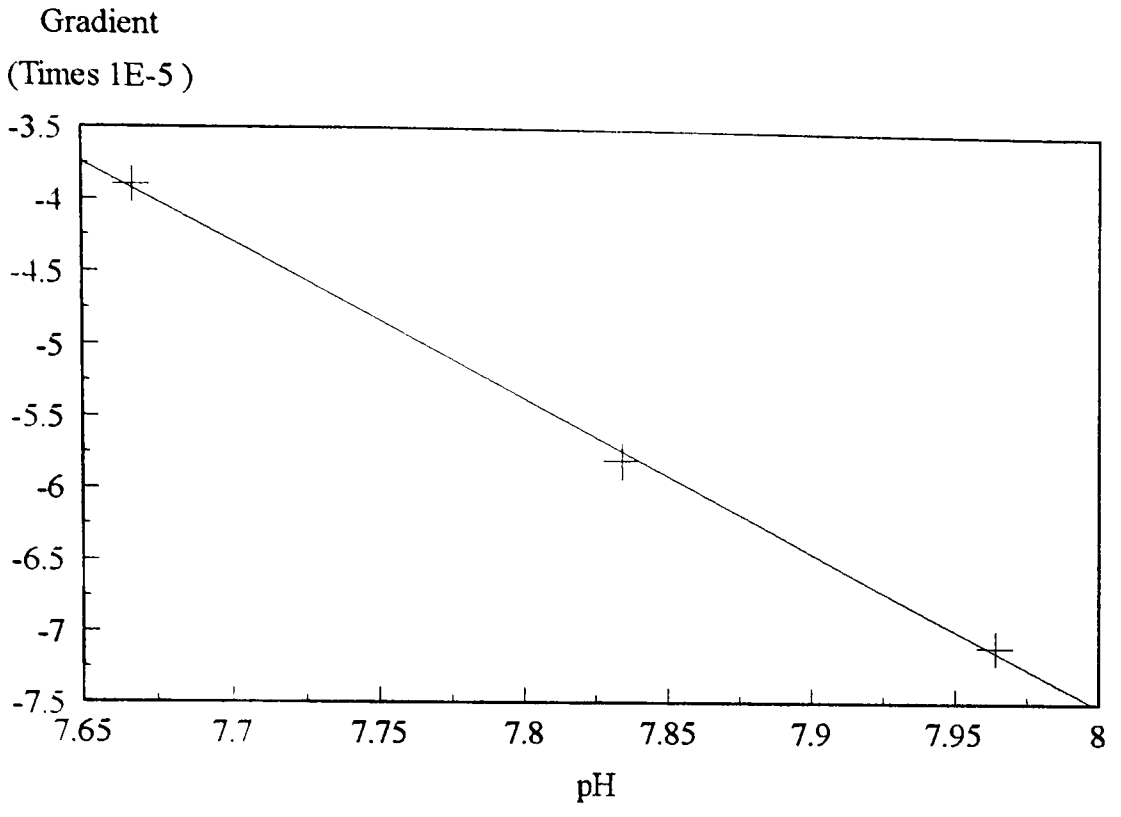

FIGURE 5. The experimentally measured affect of *m*-cresol purple on the pH of a sample was calculated (see Figure 4) using a linear regression. The results indicated that the calculated slope of the pH change maybe dependent on the pH of the sample and not due to variations in the pH of the indicator with time. The above graph plots the calculated slopes against the pH of the sample. It would appear that the pH change due to the addition of *m-cresol* purple is dependent on the pH of the sample.

shown in figures 4a and 4b along with the calculated linear expression. From the results presented in Figure 4 it is apparent that:

- *i* The pH shift due to the addition of cresol red was poorly described by a linear expression.
- *ii* The pH shift due to the addition of *m*-cresol purple is well described by a linear expression.
- *iii* The slope of the pH change, due to the addition of indicator varied with time and / or pH.

Due to the non-linearity of the pH shift associated with the addition of cresol red, *m*-cresol purple was used in preference for experimental pH determinations.

The slope of the pH shift associated with addition of *m*-cresol purple appeared to differ between successive determinations (see Fig. 4b). This variation may have been due to changes in the pH of the indicator stock solution with time and / or due to differences in the pH of the samples used. A plot of the calculated slopes against pH (see Fig. 5) for *m*-cresol purple indicate a close relationship between the pH of the sample and the calculated slope. This suggests that any changes in the calculated slope were not due changes in the pH of the indicator, but due to the differing pH of the samples. This view is further supported by the

TABLE 4. The precision and accuracy with which pH can be measured was determined experimentally by measuring replicate sea water samples with cresol red and *m*-cresol purple at the same temperature and calculating the pH using the equations given in section A3.3.8

	Number of replicates	Number of measurements per replicate	Temperature (°C)	Salinity (‰)	pH_{TOTAL}
Cresol red	4	4	18.3	35.37	7.586±0.001
m-cresol purple	3	4	18.3	35.37	7.591±0.002

fact that the changes in the calculated slopes do not vary consistently with time if listed chronologically (*i.e.*-7.1×10^{-5}, -3.9×10^{-5} and -5.8×10^{-5}). Changes in the pH of the indicator stock solution (*e.g.* due to the influx of CO_2) would be expected to produce systematic changes in the calculated slope with time.

It is therefore apparent that both the pH of the sample and the volume and pH of the indicator are important factors affecting the measured pH of a sample. It would also appear that the form (*i.e.* linear or non-linear) of the volume dependent pH shift may be dependent on the indicator type.

A3.4.3 The Calculation of in situ pH

The pH determinations were carried out in an non-thermostated cell. Therefore the pH measurements were not carried out at the *in situ* temperature. The pH of a sample will be affected by temperature changes and therefore the *in situ* pH must be calculated.

The *in situ* pH can only be calculated if a temperature independent parameter of the carbonate system is known *(i.e.* TA or $[\Sigma CO_2]$, if expressed on a gravimetric, µeq/Kg-soln, as opposed to a volumetric, µeq/l, scale).

During this study, samples were also taken to determine the $[\Sigma CO_2]$. Therefore using the measured values of $[\Sigma CO_2]$ and pH the TA could be calculated, and then using the calculated TA value the pH at the *in situ* temperature could be calculated.

A3.5 Discussion

The spectrophotometric determination of sea water pH has proved to be both precise and robust. Measurements conducted to asses the precision and accuracy of the technique (see Table 4) indicate that spectrophotometric methods, as opposed to potentiometric methods, can improve the precision of sea water pH determinations by at least an order of magnitude. The internal accuracy of the standardisation procedure was assessed by comparing the pH

measured on duplicate samples using each indicator. The results (see Table 4) indicate that the measured pH differed slightly (0.005 pH units) depending on the indicator used.

It is more difficult to asses the absolute accuracy of the technique. The accuracy of the method primarily relies on the accuracy of the pH buffer used to calibrate cresol red and *m*-cresol purple. Although the sea water buffer was prepared as prescribed (Dickson, 1993) it was not possible to check the pH of the buffer used against one prepared by Dr A. Dickson. This may therefore be a possible source of error.

References

References

Abelson, P. H. and Hoering, T. C., **1961**. Carbon isotope fractionation in formation of amino acids by photosynthetic organisms. Proc. US Nat Acad. Sci., 47, 623.

Arnelle, D. and O'Leary, M. H., **1992**. Binding of carbon dioxide to phosphoenolpyruvate carboxykinase deduced from carbon kietic isotope effects. *Biochemistry*, **31**, 4363 - 4368.

Atkins, P. W., **1994**. Physical Chemistry, fifth addition. Oxford Universiy Press, Oxford.

Bacastow, R. B. and Maier - Reimer, E., **1991**. *Global Biogeochemical Cycles*, **5**, 71 - 85.

Badger, M. R., **1987**. The CO_2 - concentrating mechanism in aquatic photoautotrophs. In: The Biochemistry of plants (Hatch, M. D. And Boardman, N. K., eds.), Academic Press, San Diego, 219 - 274.

Beardall, J., **1985**. Occurrence and importance of HCO_3^- utilisation in microscopic algae. *In*: Inorganic Carbon Uptake by Aquatic Photosynthetic Organisms (Lucas, W. J. and Berry, J. A. *eds.*), 83-96. *American Society of Plant Physiologists*, Maryland.

Beardall, J., **1989**. Photosynthesis and photorespiration in marine phytoplankton. *Aquatic Botany*, **34**, 105 - 130.

Beardall, J., MuKerji, D., Glover, H. E. and Morris, I., **1976**. The path of carbon in photosynthesis by marine phytoplankton. *Journal of Phycoclogy*,**12**, 409-417.

Beardall, J. and Raven, J. A., **1981** Transport of inorganic carbon and the 'CO_2 concentrating mechanism' in *Chlorella emersonii* (Chlorophyceae).*Journal of Phycology*, **17**, 134-141.

Beardall, J., Griffiths, H. and Raven, J. A., **1982**. Carbon isotope discrimination and the carbon concentrating mechanism in *Chlorella emersonii*. *Journal of Experimental Botany*, **33**, 739 - 737.

Berger, W. H., Smetacek, V. S. and Wefer, G. (Eds), **1989**. Productivity of the Oceans, Present and Past, Wiley - Interscience, Chichester.

Bigeleisen, J., **1965**. Chemistry of isotopes. *Science*, **147**, 463- 471.

Bigeleisen, J. and Mayer, M. G., **1947**. Calculation of equlibrium constants for isotopic exchange reactions. *The Journal of Chemical Physics*, **15 (5)**, 261- 267.

Bigeleisen, J., Lee, M. W. and Mandel, F., **1973**. Equlibrium isotope effects. *Annual Review of Physical Chemistry*, **24**, 407- 440.

Blight, S. P., Bentley, T. B., Lefevre, D., Robinson, C., Rodrigues, R., Rowlands, J. and Williams, P. J. LeB., **1995.** The phasing of autotrophic and heterotrophic plankton metabolism in a temperate coastal ecosystem. *Marine Ecology Progress Series*, **128**, 61-75.

Bowes, G., **1985**. Pathways of CO_2 fixation by aquatic organisms. *In*: Inorganic Carbon Uptake by Aquatic Photosynthetic Organisms (Lucas, W. J. and Berry, J. A. *eds.*), 187-210. American Society of Plant Physiologists, Maryland.

Broecker, W. S. and Oversby, V. M., **1971.** Chemical equilibria in the earth. McGaw - Hill, New York, 150 -170.

Buch, K., Harvey, H. W., Wattenberg, H. and Gripenberg, S., **1932.** Über das kohlensäuresystem in meerwasser. Rapp. Cons. Explor. Mer, **79**, 1 -70.

Burnet, W. C. and Schafer, O. A., **1980.** Effect of ocean dumping on $^{13}C/^{12}C$ ratios in marine sediments from the New York Bight. Estuarine and Coastal Marine Science, **11**, 605 - 611.

Burns, B. and Beardall, J., **1987.** Utilisation of inorganic carbon by marine microalgae. *Journal of Experimental Marine Biology and Ecology*, **107**, 75 - 86.

Byrne, R. H., and Breland, J. A., **1989**. High precision multiwavelength pH determinations in sea water using cresol red. *Deep-Sea Research*, **36 (5)**, 803- 810

Clayton, T. D. and Byrne, R. H., **1993.** Spectrophotometric sea water measurements: total hydrogen ion concentration scale calibration of *m*-cresol purple and at-sea results. *Deep - Sea Research*, **40 (10)**, 2115 - 2129.

Coffin, R. B., Cifuentes, L. A. and Elderidge, P. M., **1994.** The use of stable carbon isotopes to study microbiological processes in estuaries. In: Stable Isotopes in Ecology and Environmental Science (Lajtha, K. And Michener, R. H., eds). Blackwell Scientific Publications, London, 222 - 240.

Conway, N. M., Kennicut II, M. C. and Van Dover, C. L., **1994.** Stable isotopes in the study of marine chemosynthetic - based ecosystems. In: Stable Isotopes in Ecology and Environmental Science (Lajtha, K. And Michener, R. H., eds). Blackwell Scientific Publications, London, 158 - 186.

Cooper, L. N. M., **1933.** Chemical constituents of biological importance in the English Channel, November 1930 to January 1932. Part 2. Hydrogen ion concentration, excess base carbon dioxide and oxygen. *Journal of the Marine Biological Association of the UK*, **18**, 729 - 753.

Craig, H., **1953.** The geochemistry of stable isotopes. *Geochimica et Cosmochimica Acta*, **3**, 53 - 92.

Dalziel, K., **1953.** An apparatus for the spectrokinetic study of rapid reactions. The kinetics of carbonic acid dehydration. *Biochemical Journal*, **55**, 86 - 90.

Degens, E. T., Guillard, R. R. L., Sackett, W. M. and Hellebust, J. A., **1968b**. Metabolic fractionation of carbon isotopes in marine plankton- I. temperature and respiration experiments. *Deep-Sea Research*, **15**, 1-9.

Deines, P., Langmuir, D. and Harmon, R. S., **1974**. Stable carbon isotope ratios and the existance of a gas phase in the evolution of carbonate ground waters. *Geochimica et Cosmochimica Acta*, **38**, 1147- 1164.

Denbigh, K., **1981.** The principles of chemical equilibrium. Cambridge University Press, Cambridge.

Descolas-Gros, C. and Fontugne, M., R., **1985**. Carbon fixation in marine phytoplankton: carboxylase activities and stable carbon-isotope ratios; physiological and paleoclimatological aspects. *Marine Biology*, **87**, 1-6.

Descolas-Gros, C. and Fontugne, M., R., **1988**. Carboxylase activities and carbon isotope ratios of Mediterranean phytoplankton. Oceanologica Acta, Special Issue, 245 - 250.

Descolas-Gros, C. and Fontugne, M., **1990.** Stable isotope fractionation by marine phytoplankton during photosynthesis. *Plant Cell and Environment,* **13,** 207-218.

Deuser, W. G. and Degens, E. T., **1967**. Carbon isotope fractionation in the system CO_2 (gas)- CO_2 (aqueous)- HCO_3^- (aqueous). *Nature*, **215**, 1033- 1035.

Dickson, A. G., **1984**. pH scales and proton transfer reactions in saline media such as sea water. *Geochimica et Cosmochimica Acta*, **48**, 2299-2308.

Dickson, A. G., **1993**. pH buffers for sea water media based on the total hydrogen ion concentration scale. *Deep- Sea Research*, **40 (1)**, 107- 118.

Dickson, A. G. and Riley, J. P., **1979**. The estimation of acid dissociation constants in sea water media from potentiometric titrations with strong base. I. The ionic product of water- K_W. *Marine Chemistry*, 7, 89- 99.

Dixon, G. K., Brownlee, C. and Merrett, M. J., **1989.** Measurement of internal pH in the coccolithophore *Emiliania huxleyi* 2', 7'-bis-(2-carboxyethyl)-5 (and-6) carboxyfluorescein acetoxymethylester and digital imaging microscopy. *Planta*, **178**, 443-449.

DOE, **1991**. Handbook of methods for the analysis of the various parameters of the carbon dioxide system in sea water; version 1. A. G. Dickson and Goyet, C. eds. ORNL/CDIAC-74.

Ducklow, H. W., Kirchman, D. L., Quinby, H. L., Carlson, C. A. and Dam, H. G., **1993.** Stocks and dynamics of bacterioplankton carbon during the spring bloom in the eastern North Atlantic Ocean. Deep - Sea Research II, **40 (1/2)**, 245 - 263.

Ehleringer, J. R. and Rundel, P. W., **1988**. Stable isotopes; history, units and instrumentation. *In*: Stable Isotopes in Ecological Research (Rundel, P. W., Ehleringer, J. R. and Nagy, K. A., *eds.*), 1- 15. Springer- Verlag New York Incorporated.

Falkowski, P., G., **1991.** Species variability in the fractionation of ^{13}C and ^{12}C by marine phytoplankton. *Journal of Plankton Research*, **13**, 21-28.

Farquhar, G. D., O'Leary, M. H. and Berry, J. A., **1982**. On the relationships between carbon isotope discrimination and the intercellular carbon dioxide in leaves. *Australian Journal of Plant Physiology*, **9**, 121- 137

Farquhar, G. D., Ehleringer, J. R., and Hubick, K. T., **1989.** Carbon isotope discrimination and photosynthesis. *Annual Review of Plant Physiology and Plant Molecular Biology*, **40**, 505 - 537.

Fogel, M. L., Cifuentes, L. A., Velinsky, D. J. and Sharp, J. H., **1992.** Relationship of carbon availability in estuarine phytoplankton to isotopic compostion. *Marine Ecology Progress Series*, **82**, 291 - 300.

Fontugne, M. R. and Duplessy, J., -C., **1981**. Organic carbon isotopic fractionation by marine phytoplankton in the temperature range -1 to 31°C. *Oceanoloica Acta*, **4 (1)**, 85-89.

Francois, R., Altabet, M. A., Goericke, R., McCorkle, D. C., Brunet, C., and Poison, A., **1993.** Changes in $\delta^{13}C$ of surface water particulate organic matter accross the sutropical convergence in the SW Indian Ocean. *Global Biogeochemical Cycles*, 7 **(3)**, 627 - 644.

Fritz, P. and Fontes, J. Ch., **1980**. Introduction. *In*: Handbook on Environmental

Geochemistry (Fritz, P. and Fontes, J. Ch., *eds.*), 1- 19. Elsevier Scientific Publishing Company.

Frost, A. A. and Pearson, R. G., **1953.** Kinetics and mechanism. John Wiley and Sons, Inc., New York.

Fuhrmann, R. and Zirino, A., **1988.** High resolution determination of the pH of sea water with a flow-through system. *Deep-Sea Research*, **35**, 197-208.

Gavis, J. and Ferguson, J. P., **1975**. Kinetic of carbon dioxide uptake by phytoplankton at high pH. *Limnology and Oceanography*, **20(2)**, 211-221.

Gibbons, B. H. and Edsall, J. T., **1963.** Rate of hydration of carbon dioxide and dehydration of carbonic acid at 25°C. *Journal of Biological Chemistry*, **238**, 3502 - 3507.

Goericke, R., Montoya, J. P. and Fry, B., **1994.** Physiology of isotopic fractionation in algae and cyanobacteria. In: Stable Isotopes in Ecology and Environmental Science (Lajtha, K. And Michener, R. H. Eds.), Blackwell Scientific Publications, London., 187 - 221.

Goericke, R. and Fry, B., **1994.** Variations of marine plankton $\delta^{13}C$ with latitude, temperature and dissolved CO_2 in the world ocean. Global Biogeochemical Cycles, **8 (1)**, 85 - 90.

Goyet, C. and Poisson, A., **1989**. New determination of carbonic acid dissociation constants in seawater as a function of temperature and salinity. *Deep- Sea Research*, **30 (11)**, 1635-1654.

Hanson, I., **1973.** A new set of acidity constants for carbonic acid and boric acid in sea water. *Deep - Sea Research*, **20**, 461 - 478.

Harvey, J. G., **1968.** The flow of water through the Menai Strait. *Geophysical Journal of the Royal Astrological Society*, **15**, 517 - 528.

Hayes, J. M., **1993**. Factors controlling ^{13}C contents of sedimentary organic compounds: Principles and evidence. *Marine Geology*, **113**, 111-125.

Hayes, J. M., Popp, B. N., Takigiku, R. and Johnson, M. W., **1989**. An isotopic study of biogeochemical relationships between carbonates and organic carbon in the Greenhorn Formation. *Geochimica et Cosmochimica Acta*, **53**, 2961-2972.

Jasper, J. P. and Hayes, J. M., **1994.** Reconstruction of paleoceanic PCO_2 levels from carbon isotopic compostion of sedimentary biogenic components. In: Carbon Cycling in the Glacial Ocean: Constraints in the Ocean's Role in Global Change (Zahn, R. Ed.), NATO ASI Series, Vol. I 17, Spriger - Verlag Berlin Heidelberg. 307 - 321.

Jespersen, A. and Kristoffersen, K., **1987**. Measurements of chlorophyll-a from phytoplankton using ethanol as extraction solvent. *Arch. Hydrobiol.*, **109 (3)**, 445- 454.

Johnson, K. S., **1982**. Carbon dioxide hydration and dehydration kinetics in seawater. *Limnology and Oceanography*, **27 (5)**, 849- 855.

Keeling, C. D. and Whorf, T. P., **1991.** In: Trends '91(Boden, T. A., Sepanski, R. J. and Stoss, F. W. Eds.). Oakridge National Laboratory, Oakridge. 12 - 15.

Kerby, N. W. and Raven, J. A., **1985.** Transport and fixation of inorganic carbon by marine algae. *Advances in Botanical Research*, **11**, 71-403.

King, D. W. and Kester, D. R., **1989.** Determination of sea water pH from 1.5 to 8.5 using colorimetric indicators. *Marine Chemistry*, **26**, 5 - 20.

Kiørboe, T., **1993.** Turbulence, phytoplankton cell size and the structure of pelagic food webs. In: Advances in Marine Biology (Blaxter, J.. H. S. And Southward, A. J. Eds.), 29, 1 - 72.

Kopczyńska, E. E., Goeyens, L., Semeneh, M., Dehairs, F., **1995**. Phytoplankton composition and cell carbon distribution in Prydz Bay, Anarctica: relation to organic particulate matter and its $\delta^{13}C_{POC}$ values. *Journal of Plankton Research*, **17 (4)**, 685-707.

Laidler, K. J., **1965.** Chemical Kinetics. McGraw - Hill, New York.

Laws, E. A., Popp., B. N., Bidigare, R. R., Kennicutt, M. C. and MacKo, S. A., **1995.** Dependence of phytoplankton carbon isotopic compostion on growth rate and $[CO_{2(aq)}]$: theoretical considerations and experimental results. *Geochimica et Cosmochimica Acta*, **59 (6)**, 1131 - 1138.

Lesniak, P. M. and Sakai, H., **1989.** Carbon isotope fractionation between dissolved carbonate (CO_3^{2-}) and $CO_{2(g)}$ at 25°C and 40°C. *Earth and Planetary Science Letters*, **95**, 297 - 301.

Lyman, J., **1956.** Buffer mechanism of sea water. Thesis, University of California at Los Angeles, 196pp.

Mariotti, A., German, J. C., Hubert, P., Kaiser, P., Letolle, R., Tardieux, A. and Tardieux, P., **1981.** Experimental determination of nitrogen kinetic isotope fractionaion: some priciples; illustration for the purpose of denitrification nitrification processes. *Plant and Soil*, **62**, 413 - 430.

Marlier, J. F. and O'Leary, M. H., **1984.** Carbon kinetic isotope effects on the hydration of carbon dioxide and the dehydration of bicarbonate ion. *Journal of the American Chemical Society*, **106**, 5054 - 5057.

McCabe, B., ms., **1985.** The dynamics of ^{13}C in several New Zealand lakes. PhD thesis, University of Waikato, 278p.

McCorkle, D. C., **1987.** Stable isotopes in deep sea pore waters: Modern chemistry and paleoceanographic implications. PhD dissertation, University of Washington.

McCorkle, D. C., Emerson, S. R. and Quay, P. D., **1985**. Stable carbon isotopes in marine porewaters. *Earth and Planetary Science Letters*, **74**, 13- 26.

Mehrbach, C., Culberson, C. H., Hawley, J. E., and Pytkowocz, R. M., **1973**. Measurement of the apparent dissociation constants of carbonic acid in seawater at atmospheric pressure. *Limnology and Oceanography*, **18 (6)**, 897- 907.

Miller, I. D., **1985.** Nutrient distribution in relation to the thermohaline discontinuity in the North - East Irish Sea. PhD thesis, University of Wales.

Millero, F. J., Byrne, R. H., Wanninkhof, R., Feely, R., Clayton, T., Murphy, P., and Lamb., M. F., **1993**. The internal consistency of CO_2 measurements in the equatorial Pacific. *Marine Chemistry*, **44**, 269-280.

Mook, W. G., Bommerson, J. C. and Staverman, W. H., **1974**. Carbon isotope fractionation

between dissolved bicarbonate and gaseous carbon dioxide. *Earth and Planetary Science Letters*, **22**, 169- 176.

Najjar, R. G., Sarmiento, J. L. and Toggweiler, J. R., **1992.** *Global Biogeochemical Cycles*, **67**, 45 - 76.

O'Leary, M. H., **1981**. Carbon isotope fractionation in plants. *Phytochemistry*, **20** (4), 553-567.

O'Leary, N. J. P., **1984**. Measurement of the isotope fractionation associated with diffusion of carbon dioxide in aqueous solution. *Journal of Physical Chemistry*, **88**, 823-825

O'Leary, M. H., Madhaven, S. and Paneth, P., **1992.** Physical and chemical basis of carbon isotope fractionation in plants. *Plant, Cell and Environement*, **15**, 1099 -1104.

Owens, N. J. P., **1987**. Natural variations in ^{15}N in the marine environment. *Advances in Marine Biology*, **24**, 389-451.

Packard, T. T., Garfield, P. C. and Martinez, R., **1983.** Respiration and respiratory enzyme activity in aerobic and anaerobic cultures of marine denitrifying bacteria, *Pseudoonas. Deep - Sea Research*, **30**, 227 - 244.

Paneth, P. and O'Leary, M. H., **1985.** Carbon isotope effects on dehydration of bicarbonate ion catalysed by carbonic anhydrase. *Biochemistry*, **24**, 5143 - 5147.

Parsons, T. R., Takahashi, M. and Hargrave, B., **1984a.** Biological Oceanographic Processes, Pergammon Press, Oxford.

Parsons, T. R., Maita, Y. and Lalli, C. M., **1984b**, A manual of chemical and biological methods for sea water analysis. Pergamon Press, Oxford.

Pinsent, B. R., Pearson, L. and Roughton, F. J. W., **1956.** The kinetics of combination of carbon dioxide with hydroxide ions. *Transactions of the Faraday Society*, **47**, 263 - 269.

Popp, B. N., Takigiku, R., Hayes, J. M., Louda, J. W. and Baker, E. W., **1989.** The post - paleozoic chronology and mechanism of ^{13}C depletion in primary marine organic matter. *American Journal of Science*, **289**, 436 - 454.

Rau, **1994.** Variations in sedimentary organic $\delta^{13}C$ as a proxy for past changes in ocean and atmospheric CO_2 concentrations. In: Carbon Cycling in the Glacial Ocean: Constraints in the Ocean's Role in Global Change (Zahn, R. Ed.), NATO ASI Series, Vol. I 17, Spriger - Verlag Berlin Heidelberg. 307 - 321.

Rau, G. H., Takahashi, T., Des Marais, D. J. and David, J., **1989**. Latitudinal variations in plankton ^{13}C: implications for CO_2 and productivity in past oceans. *Nature*, **341**, 516-518.

Rau, G. H., Sullivan, C. W. and Gordon, L. I., **1991a**. $\delta^{13}C$ and $\delta^{15}N$ variations in Weddell Sea particulate organic matter. *Marine Chemistry*, **35**, 355-369.

Rau, G.H., Takahashi,T., Des Marais,D.J., and Sullivan,C.W.,**1991b**. Particulate organic matter $\delta^{13}C$ variations across the Drake Passage. *Journal of Geophysical Research*, **96 (15)**,131-15,135.

Rau, G. H., Takahashi, T., Des Marais, D. J., Repeta, D. J. and Martin J. H., **1992**. The relationship between $\delta^{13}C$ of organic matter and $[CO_2(aq)]$ in ocean surface water; Data from JGOFS site in the northeast Atlantic Ocean and a model. *Geochimica et*

Cosmochimica Acta, **56**, 1413-1419.

Raven, J. A, **1991**. Implications of inorganic carbon utilisation: ecology, evolution and geochemistry. *Canadian Journal of Botany*, **69**, 908- 924.

Raven, J. A. and Johnston, A. M., **1991**. Mechanisms of inorganic carbon acquisition in marine phytoplankton and the implications for the use of other resources. *Limnology and Oceanography*, **36 (8)**, 1701-1714.

Raymont, J. E. G., **1980.** Plankton and Productivity in the Oceans. Pergammon Press, Oxford.

Reid, A. F. and Urey, H. C., **1943.** The use of the exchange between carbon dioxide, carbonic acid, bicarbonate ion and water for isotopic concentration. *Journal of Chemical Physics*, **11**, 403-412.

Riebesell, V., Wolf-Gladrow, D. A. and Smetacek, V., **1993**. Carbon dioxide limitation of marine phytoplankton growth rates. *Nature*, **361**, 249- 251.

Robert-Baldo, G. L., Morris, M. J. and Byrne, R. H., **1985**. Spectrophotometric determinations of sea water pH using phenol-red. *Analytical Chemistry*, **57**, 2564- 2567.

Robinson, C. and Williams, P. J. LeB., **1991.** Development and assesment of an analytical system for the accurate and continual measurement of total dissolved inorganic carbon. *Marine Chemistry*, **34**, 157 - 175.

Roeske, C. A. and O'Leary, M. H., **1984.** Carbon isotope effects on the enzyme - catalysed carboxylation of ribulose bisphosphate. *Biochemistry*, **23**, 6275 - 6284.

Roy, R. N., Roy, L. N., Vogel, K. M., Porter - Moore, C., Pearson, T., Good, C. E., Millero, F J., Campbell, D. M., **1993.**,The dissociation constants of carbonic acid in sea water at salinities 5 to 45 and temperatures 0 to 45°C. *Maine Chemistry*, **44**, 249 - 267.

Sarmiento, J. L. and Siegenthaler, U., **1992.** New production and the global carbon cycle. In: Primary Productivity and Biogeochemical Cycles in the Sea (Falkowski, P. G. And Woodhead, A. D.), Environmental Science Research, **43**, Plenum Press, New York.

Sharkey, T. D. and Berry, J. A., **1985**. Carbon isotope freactionation of algae as influenced by inducible CO_2 concentrating mechanism. *In*: Inorganic Carbon Uptake by Aquatic Photosynthetic Organisms (Lucas, W. J. and Berry, J. A. *eds.*),389-401. American Society of Plant Physiologists, Maryland.

Siegenthaler, U. and Joos, F., **1992.** Use of a simple model for studying ocean tracer distributions and global carbon cycle. *Tellus*, **44B**, 186 - 207.

Siegenthaler, U. and Sarmiento, J. L., **1993.** Atmospheric carbon dioxide and the ocean. *Nature*, **365**, 119 - **125.**

Sillen, L. G., **1966**. Master variables and activity scales. *In*: Equilibrium concepts in natural water systems (Gould R. F. *ed*).American Chemical Society, Washington D. C., Advances in Chemistry Series **67**, American Chemical Society.

Sirs, J. A., **1958a**. Electrometric stopped flow measurements of rapid reactions in solution. Part 1. Conductivity measurements. *Transaction of the Faraday Society*, **54**, 201 - 206.

Sirs, J. A., **1958b**. Electrometric stopped flow measurements of rapid reactions in solution.

Part 2. Glass electrode pH measurements. *Transaction of the Faraday Society*, *54*, 207 - 212.

Sillén, L. G., **1967**. Master variables and activity scales. *In*: equilibrium concepts in natural water systems (Stumm, W. ed.). American Chemical Society, Washigton D. C., Advances in Chemistry series, **67**, 45-56.

Skirrow,G., **1974**. The dissolved gasses - Carbon dioxide. *In*: Chemical Oceanography (Riley, J. P. and Skirrow, G. *eds*), **2**, 1- 181. Academic Press, London.

Small, L. F., Donaghay, P. L. and Pytkowicz, R. M., **1977.** Effects of enhaced CO_2 levels on growth characteristics of two marine phytoplankton species. In: The Fate of Fossil Fuel CO_2 in the Oceans (Anderson, N. R. And Malahoff, A. Eds.), Marine Science, Vol. 6., Plenum Press, New York.

Stumm , W. and Morgan, J. J., **1981.** Aquatic chemistry, an introduction emphasising chemical equilibria in natural waters, John Wiley and Sons, Chichester.

Tan, F. C., and Strain, P. M., **1979.** Organic carbon isotope ratios in recent sediments in the St Lawrence Estuary and the Gulf of St Lawrence. *Estuarine and Coastal Marine Science*, **8**, 213 - 225.

Tan, F. C. and Strain, P. M., **1983.** Sources, sinks and distribution of organic carbon in the St. Lawerence Estuary, Canada. *Geochimica et Cosmochimica Acta*, **47**, 125 - 132.

Tans, P. P., Fung, I. Y. and Takahasshi, T., **1990.** Observational constraints on the global atmospheric CO_2 budget. *Science*, **247**, 1431 - 1438.

Thielman, J., Tolbert, N. E., Goyal, A. and Senger, H., **1990.** Two systems for concentrating CO_2 and bicarbonate during photosynthesis by *Scenedesmus*. *Plant Physiology*, **92**, 622 - 629.

Thode, H. G., Shima, M., Rees, C. E. and Krishnamurty, K. V., **1965**. Carbon-13 isotope effects in systems containing carbon dioxide, carbonate and metal ions. *Canadian Jornal of Chemistry*, **43**, 582- 595.

Turner, J. V., **1982.** Kinetic fractionation of carbon - 13 during calcium carbonate precipitation. *Geochimica et Cosmochimica Acta*, **46**, 1183 - 1191.

UNESCO, **1987.** Thermodynamics of the carbon dioxide system in sea water. Report by the carbon dioxide sub-panel of the joint panel on oceanographic tables and standards. UNESCO technical papers in marine science, 51.

Vogel, A. I., **1989.** Vogel's textbook of quantitative chemical analysis, fifth edition (revised by Jeffery, G. H., Bassett, J., Mendjam, J., and Denney, R. C.). Longman Scietific and Technical, Harlow, England.

Vogel, J. C., **1960.** Isotope separation factors of carbon in the equilibrium system CO_2 - HCO_3^- - CO_3^{2-}. Summer course on Nucl. Geol., Varenna, 216.

Vogel, J. C., Grootes, P. M. and Mook, W. G., **1970**. Isotopic fractionation between gaseous and dissolved carbon dioxide. *Z. Physik*, **230**, 225- 238.

Volk, T. and Hoffert, M. I., **1985.** Ocean carbon pumps: Analysis of relative strengths and efficiencies in ocean - driven atmospheric CO_2 changes, In: The carbon cycle and

atmospheric CO_2: Natural Variations Archean to Present (Sundquist, E. And Broecker, W. S. eds.), Geophysical Monographs 32, American Geophysical Union.

Wainwright, S. C. and Fry, B., **1994**. Seasonal variations of the stable isotopic compositions of coastal marine plankton from Woods Hole, Massachusetts and Georges Bank. *Estuaries*, **17 (3)**, 552-560.

Weiss, R. F., **1974.** Carbon dioxide in water and sea water: the solubility of a non - ideal gas. *Marine Chemistry*, **2**, 203 - 215.

Wendt, I., **1968.** Fractionation of carbon isotopes and its temperature dependance in the system CO_2- gas- CO_2 in solution and HCO_3^-- CO_2 in solution. *Earth and Planetary Science Letters*, **4**, 64 - 68.

Zhang, J., Quay, P. D. and Wilbur, D. O., **1995.** Carbon isotope fractionation during gas - water exchange and dissolution of CO_2. *Geochimica et Cosmochimica Acta*, **59 (1)**, 107 - 114.